Joint PhD degree in Environmental Technology

Docteur de l'Université Paris-Est
Spécialité: Science et Technique de l'Environnement

Dottore di Ricerca in Tecnologie Ambientali

Degree of Doctor in Environmental Technology

Thesis for the degree of Doctor of Philosophy in Environmental Technology

Tesi di Dottorato – Thèse – PhD thesis – Väitöskirja

Suchanya Wongrod

Biochars from solid digestates as sorbing materials for metal(loid)s removal from water

23/05/2019, Tampere

In front of the PhD evaluation committee

Prof. Silvia Fiore	Reviewer
Prof. Marie-Odile Simonnot	Reviewer
Prof. Florence Pannier	Reviewer
Prof. Eric D. van Hullebusch	Promotor
Prof. Piet N.L. Lens	Co-promotor
Prof. Giovanni Esposito	Co-promotor
Asst. Prof. Aino-Maija Lakaniemi	Co-promotor
Prof. Gilles Guibaud	Chair

Marie Sklodowska-Curie European Joint Doctorate, Advanced Biological Waste-to-Energy Technologies

Evaluation committee

Chair

Prof. Gilles Guibaud
PEIRENE Équipe Développement d'indicateurs ou prévision de la qualité des eaux
URA IRSTEA
Université de Limoges
Limoges, France

Reviewers/Examiners

Prof. Silvia Fiore
Department of Environment, Land and Infrastructures Engineering
Politecnico di Torino
Italy

Prof. Marie-Odile Simonnot
Laboratoire Réactions et Génie des Procédés
Université de Lorraine - CNRS (UMR 7274)
France

Prof. Florence Pannier
Laboratoire de Chimie Analytique Bio-Inorganique et Environnement
Université de Pau et des Pays de l'Adour - CNRS (UMR 5254)
France

Thesis Promotor

Prof. Eric D. van Hullebusch
Laboratoire Géomatériaux et Environnement
Université Paris-Est
Marne-la-Vallée, France

Thesis Co-Promotors

Prof. Piet N.L. Lens
Department of Environmental Engineering and Water Technology
IHE Delft Institute for Water Education
Delft, The Netherlands

Prof. Giovanni Esposito
Department of Civil and Mechanical Engineering
University of Cassino and Southern Lazio
Cassino, Italy

Asst. Prof. Aino-Maija Lakaniemi
Faculty of Engineering and Natural Sciences
Tampere University
Tampere, Finland

Supervisory team

Thesis Supervisor

Prof. Eric D. van Hullebusch
Laboratoire Géomatériaux et Environnement
Université Paris-Est
Marne-la-Vallée, France

Thesis Co-Supervisors

Prof. Gilles Guibaud
PEIRENE Équipe Développement d′indicateurs ou prévision de la qualité des eaux
URA IRSTEA
Université de Limoges
Limoges, France

Prof. Piet N.L. Lens
Department of Environmental Engineering and Water Technology
IHE Delft Institute for Water Education
Delft, The Netherlands

Thesis Instructors

Dr. Stéphane Simon
PEIRENE Équipe Développement d′indicateurs ou prévision de la qualité des eaux
URA IRSTEA
Université de Limoges
Limoges, France

Dr. Yoan Pechaud
Laboratoire Géomatériaux et Environnement
Université Paris-Est
Marne-la-Vallée, France

Dr. David Huguenot
Laboratoire Géomatériaux et Environnement
Université Paris-Est
Marne-la-Vallée, France

This research was conducted in the framework of the Marie Sklodowska-Curie European Joint Doctorate (EJD) in Advanced Biological Waste-to-Energy Technologies (ABWET) and supported by from Horizon 2020 under grant agreement no. 643071.

Abstract

Sewage sludge digestate (SSD) and the organic fraction of municipal solid waste digestate (OFMSWD) are currently considered as alternative feedstocks for biochar production due to the high amount of the organic solid waste remaining at the end of the treatment. The pyrolysis of solid digestate is known as an alternative to promote the recycling of organic wastes and generate added-value bio-products (*e.g.* biochar). Generally, the digestate biochar has a much lower sorption capacity for metal(loid)s compared to activated carbons. Therefore, chemical treatment is considered as a potential option to improve the biochar surface properties and thus inducing a better sorption ability for metal(loid)s on the biochar surface.

In this present work, the SSD and OFMSWD derived biochars were treated with 2 M KOH or 10% H_2O_2 followed by batch washing or batch and subsequent column washings with ultrapure water. The physicochemical properties including the pH of point of zero charge (pH_{PZC}), the Brunauer-Emmett-Teller surface area (S_{BET}) and cation exchange capacity (CEC) were determined for all the biochars in order to link their improved surface properties to the enhanced sorption ability for metal(loid)s. All the biochars were then used to study the influence of chemical treatment and biochar washing procedure on the sorption behavior of Pb(II), Cd(II) and As(III, V) through the batch sorption kinetics and isotherms. Moreover, the As redox state distribution (*i.e.* As(III) and As(V)) during the As(III) sorption onto the biochar surface and in liquid solution was determined by using solid-liquid extraction followed by liquid chromatographic analysis.

Results showed increases of the pH_{PZC}, S_{BET} and CEC after chemical treatment of the biochar, in accordance with the enhanced sorption ability for Pb(II), Cd(II) and As(V). For instance, the maximum sorption capacity (Q_m) was increased from 1.6 µmol g^{-1} (As(V)) and 15.4 µmol g^{-1} (Cd(II)) on the raw SSD biochar to 8.1 µmol g^{-1} (As(V)) and 306.1 µmol g^{-1} (Cd(II)) after the H_2O_2 and KOH treatment, respectively (at initial pH 5.0). Similarly, the Q_m of Pb(II) was also increased from 31.4 µmol g^{-1} (raw SSD biochar) to 121.9 µmol g^{-1} on the H_2O_2 modified SSD biochar. However, the sorption capacity for Pb(II) was not determined after KOH treatment due to the failing of the Langmuir isotherm model to fit the experimental data. This indicates that insufficient washing of the KOH-modified SSD biochar can hinder the Pb(II) sorption due to the release dissolved organic compounds from this biochar that may interact with Pb^{2+} and thereby forming Pb-ligand complexes in the solution. In addition, the As redox distribution

showed a large oxidation (70%) of As(III) to As(V) in KOH-modified SSD biochar with batch washing, while As(III) was partially oxidized (7%) in the KOH-modified SSD biochar with batch and subsequent column washings. This highlights an important role of washing procedure for sorption of metal(loid)s, particularly for Pb(II) and As(V).

The As extraction followed by liquid chromatographic analysis was successfully established to quantitatively recover and preserve As(III) oxidation with the use of ascorbic acid. During the sorption kinetics, As(III) may be stable or partially oxidized depending on the biochar treatment. In addition, the oxidation of As(III) was strongly induced by the biochar material and to a lesser extent by the release of dissolved compounds from the biochar.

In summary, digestate biochars with the chemical treatment followed by a proper biochar washing procedure can be successfully used as potential sorbents to enhance the Pb(II), Cd(II) and As(III, V) sorption capacity. Moreover, the determination of As redox distribution on the biochars and in liquid phase during the sorption process can be achieved through the As extraction and chromatographic analysis, providing a better understanding of the transformation between As(III) and As(V) in the biochar-liquid sorption system.

Tiivistelmä

Jätevesilietteen (SSD) ja kiinteän jätteen lietteen orgaaninen osuuden (OFMSWD) katsotaan tällä hetkellä olevan vaihtoehtoisia raaka-aineita biocharin tuotantoon käsittelyn jälkeisen korkean jäljelle jääneen kiinteän orgaanisen jätteen määränsä ansiosta. Kiinteän lietteen pyrolyysi tunnetaan vaihtoehtoisena menetelmänä, jolla edistetään orgaanisten jätteiden kierrätystä ja tuotetaan lisäarvoa tuottavia biotuotteita (esim. biochar). Yleisesti biochar on paljon alhaisempi sorptiokapasiteetti metalloid teihin verrattuna aktiivihiiliin. Siksi kemiallisen käsittelyn katsotaan olevan vaihtoehto biocharin pinnan ominaisuuksien parantamiseen ja täten paremman metall(oid)ien sorptiokyvyn indusointiin biocharin pinnalla.

Tässä työssä, SSD ja OFMSWD pohjaiset biochar it käsiteltiin 2 M KOH:lla tai 10% H_2O_2:lla jonka jälkeen ne eräpestiin tai eräpestiin ja kolonnipestiin ultrapuhtaalla vedell'. Fysikokemialliset ominaisuudet mukaanlukien isoelektrisen pisteen pH:n (pH_{PZC}), Brunauer-Emmet-Tellerin pinta-alan (S_{BET}) ja kationinvaihtokapasiteetin (CEC) määriteltiin kaikille biochareille, tavoitteena liittää niiden paremmat pintaominaisuudet metall(oid)ien lisääntyneeseen sorptiokykyyn. Kaikkia biochareja käytettiin sen jälkeen kemiallisen käsittelyn ja biochar pesun vaikutuksen tutkimiseen Pb(II):n, Cd(II):n ja As(III, V):n sorptiokäyttäytymiseen eräsoprptiokinetiikan ja isotermian avulla. Lisäksi, As redox-tila jakauma (As(III) ja As(V)) As(III):n sorption aikana biochar pintaan ja neste yhdisteeseen määriteltiin käyttämällä kiinteä-nesteuuttoa ja sen jälkeistä nesteen kromatograafista analyysia.

Tulokset osoittivat pH_{PZC}:n, S_{BET}:n ja CEC:n lisääntymisen biocharin kemiallisen käsittelyn jälkeen Pb(II):n, Cd(II):n ja As(V):n tehostetun sorptiokyvyn mukaisesti. Esimerkiksi maksimaalinen sorptiokapasiteetti (Q_m) kasvoi 1,6 umol g^{-1}:stä (As(V)) ja 15,4 umol g^{-1}:stä (Cd(II)) raakaa SSD-biocharista arvoon 8,1 umol g^{-1} (As(V)) ja 306,1 µmol g^{-1} (Cd(II)) H_2O_2:n ja KOH-käsittelyn jälkeen (alussa pH 5,0). Samoin Pb(II):n Qm:ää lisättiin 31,4 µmol g^{-1}:stä (raakaa SSD-biocharia) 121,9 µmol g^{-1}:een H_2O_2-modifioidulla SSD-biocharilla. Pb(II):n sorptiokapasiteettia ei kuitenkaan määritetty KOH-käsittelyn jälkeen, koska Langmuir-isotermimallia ei saatu sopimaan kokeellisiin tuloksiin. Tämä osoittaa, että KOH-modifioidun SSD-biocharin riittämätön pesu voi haitata Pb(II)-sorptiota, joka johtuu liuenneista orgaanisista yhdisteistä, jotka voivat olla vuorovaikutuksessa Pb^{2+}:n kanssa ja siten muodostaa Pb-ligandikomplekseja liuoksessa. Lisäksi As redox -jakauma osoitti suurta hapetusta (70%) As(III):sta

As(V):hen KOH-modifioidussa SSD-biocharissa eräpesulla, kun taas As(III) hapetettiin osittain (7%) KOH-modifioitu SSD-biochar, jossa on erä- ja myöhemmät kolonnipestiin. Tämä korostaa pesumenettelyn tärkeää merkitystä metall(oid)in sorptiolle, erityisesti Pb(II):lle ja As(V):lle.

As-uutto ja sen jälkeinen nestekromatografinen analyysi suoritettiin onnistuneesti As(III):n hapettumisen kvantitatiivisen palautumisen ja säilyttämisen saavuttamiseksi askorbiinihapon avulla. Sorptiokinetiikan aikana As(III) voi olla stabiili tai osittain hapettunut biochar käsittelystä riippuen. Lisäksi biochar materiaali indusoi voimakkaan As(III):n hapettumisen ja vähäisemmän hapettumisen liuenneiden yhdisteiden vapautumisella biocharista.

Yhteenvetona voidaan todeta, että liete biocharit, joilla on kemiallinen käsittely ja oikeanlainen biochar pesumenettely, voidaan käyttää onnistuneesti sorbentteina Pb(II), Cd(II) ja As(III, V) sorptiokyvyn parantamiseksi. Lisäksi As redox-jakauma biocharilla ja nestemäisissä liuoksissa sorption aikana voidaan saavuttaa As-uutolla ja kromatografisella analyysillä, mikä antaa paremman käsityksen As(III):n ja As(V):n välisestä transformaatiosta biochar-neste-sorptiossa systeemissä.

Sommario

I digestati dai fanghi di depurazione (SSD) e dalla frazione organica dei rifiuti solidi urbani (OFMSWD) sono attualmente considerati materie prime alternative per la produzione di biochar in seguito all'elevata quantità di rifiuti solidi organici che rimangono alla fine del trattamento. La pirolisi del digestato solido è nota come alternativa per promuovere il riciclaggio di rifiuti organici e genera bio-prodotti a valore aggiunto (ad esempio biochar). In generale, il biochar da digestato ha una capacità di adsorbimento molto inferiore per metal(loid)i rispetto ai carboni attivati. Pertanto, il trattamento chimico è considerato come opzione per migliorare le proprietà superficiali del biochar e quindi indurre una migliore capacità di adsorbimento per metal(loid)i sulla superficie del biochar.

Nel presente studio, biochar derivati da SSD e OFMSWD sono trattati con una soluzione 2 M KOH o 10% H_2O_2, e in seguito lavati in batch o lavati in batch e successivamente in colonne con acqua ultra pura. Le proprietà fisico-chimiche del biochar tra cui il punto di carica zero (pH_{PZC}), l'area superficiale di Brunauer-Emmett-Teller (S_{BET}) e la capacità di scambio cationico (CEC) sono determinati al fine di associare le loro proprietà superficiali migliorate con la capacità di adsorbimento per i metal(loid)i. In seguito, il biochar è usato per studiare le conseguenze del trattamento chimico e delle procedure di lavaggio sul comportamento di adsorbimento di Pb(II), Cd(II) e As(III, V) mediante le cinetiche di adsorbimento e isoterme in batch. Inoltre, la distribuzione dello stato di ossidazione di As (cioè As(III) e As(V)) durante l'esperimento di assorbimento di As(III) sulla superficie del biochar e nella fase liquida è stata determinata utilizzando l'estrazione solido-liquido seguita da un' analisi cromatografica.

I risultati hanno mostrato un aumento di pH_{PZC}, S_{BET} e CEC dopo il trattamento chimico del biochar, in accordo con l'aumentata capacità di adsorbimento per Pb(II), Cd(II) e As(V). Ad esempio, la capacità massima di adsorbimento (Q_m) è aumentata da 1,6 µmol g^{-1} (As(V)) e 15,4 µmol g^{-1} (Cd(II)) sul biochar SSD grezzo a 8,1 µmol g^{-1} (As(V)) e 306.1 µmol g^{-1} (Cd(II)) dopo il trattamento con H_2O_2 e KOH, rispettivamente (a pH iniziale 5.0). Allo stesso modo, il Q_m di Pb(II) è aumentato da 31,4 µmol g^{-1} (biochar grezzo SSD) a 121,9 µmol g^{-1} sul biochar SSD modificato con H_2O_2. Tuttavia, la capacità di adsorbimento di Pb(II) in seguito al trattamento con KOH non è stata determinata a causa del fallito modello di isoterma Langmuir per spiegare i dati sperimentali.

Ciò indica che un lavaggio insufficiente del biochar SSD modificato con KOH può ostacolare l'adsorbimento di Pb(II) dovuto ai composti organici disciolti da questo biochar che possono interagire con Pb^{2+} e quindi formare complessi di Pb-legante nella soluzione. Inoltre, la distribuzione dello stato redox di As ha mostrato un'ampia ossidazione (70%) di As(III) a As(V) nel biochar SSD modificato con KOH e con lavaggio in batch, mentre As(III) è stato parzialmente ossidato (7%) nel biochar SSD modificato con KOH e con lavaggio in batch e successivo lavaggio in colonna. Ciò evidenzia un ruolo importante della procedura di lavaggio per l'adsorbimento di metal(loid)i, in particolare per Pb(II) e As(V).

L'estrazione di As, seguita da un'analisi cromatografica liquida, è stata considerata di successo per recuperare quantitativamente e preservare l'ossidazione di As(III) con l'uso di acido ascorbico. Durante la cinetica di adsorbimento, As(III) può essere stabile o parzialmente ossidato a seconda del trattamento del biochar. Inoltre, l'ossidazione di As(III) è stata fortemente indotta dal materiale da cui deriva il biochar e in misura minore dal rilascio di composti disciolti dal biochar.

In sintesi, il biochar prodotto dal digestato, trattato chimicamente e lavato con una corretta procedura può essere utilizzato con successo come potenziale assorbente di Pb(II), Cd(II) e As(III, V). Inoltre, la distribuzione dello stato di ossidazione di As sul biochar e le fasi liquide durante esperimenti di adsorbimento può essere verificata mediante l'estrazione di As e l'analisi cromatografica, che forniscono evidenza delle trasformazioni tra As(III) e As(V) nel sistema di adsorbimento biochar-fase liquida.

Résumé

Les digestats des boues d'épuration (SSD) et les digestats de la fraction organique des déchets ménagers (OFMSWD) ont été récemment considérés comme des sources potentielles pour la production de biochars en raison des quantités grandissantes de digestats solides restant à la fin de la digestion anaérobie. La pyrolyse des digestats solides est connue comme une technique pour promouvoir le recyclage des déchets organiques et générer des bio-produits à valeur ajoutée (*i.e.* biochar). En outre, en raison d'une capacité de sorption des métal(loïde)s des biochars moins bonnes par rapport aux charbon actifs traditionnels, la modification chimique des biochars bruts est considérée comme une alternative pour améliorer les propriétés de surface des biochars et induire ainsi une meilleure capacité de sorption des métal(loïde)s.

Dans ce travail, les biochars SSD et OFMSWD ont été traités avec 2 M de KOH ou 10% de H_2O_2, suivis d'un lavage en batch seul ou batch combiné avec un lavage en colonne à l'aide d'eau ultrapure. Les analyses des propriétés de biochar, le pH du point de charge nulle (pH_{PZC}), la surface spécifique de Brunauer-Emmett-Teller (S_{BET}) et la capacité d'échange cationique (CEC) ont été effectuées sur les biochars bruts et modifiés afin de relier leurs propriétés de surface au comportement de sorption vis-à-vis des métal(loïde)s. Tous les biochars ont ensuite été utilisés pour étudier l'influence du traitement chimique et de la procédure de lavage des biochars sur le comportement de sorption du Pb(II), Cd(II) et As(III, V) à travers l'étude de la cinétique et des isothermes de sorption. De plus, l'évolution de l'état redox As (*i.e.* As(III) et As(V)) pendant la sorption de l'As(III) sur la surface du biochar et en solution liquide a été déterminée par extraction solide-liquide suivie d'une analyse en chromatographie liquide.

Les résultats ont montré des augmentations de pH_{PZC}, S_{BET} et CEC après traitement chimique du biochar, concomitant avec l'augmentation de la capacité de sorption pour le Pb(II), le Cd(II) et l'As(V). Par exemple, la capacité de sorption maximale (Q_m) a été augmentée de 1,6 µmol g^{-1} (As(V)) à 15,4 µmol g^{-1} (Cd(II)) sur le biochar de SSD brut à 8,1 µmol g^{-1} (As(V)) et 306,1 µmol g^{-1} (Cd(II)) après le traitements au H_2O_2 et KOH, respectivement (au pH initial de 5,0). De même, la valeur de Q_m du Pb(II) a augmenté de 31,4 µmol g^{-1} (biochar de SSD) à 121,9 µmol g^{-1} sur le biochar modifié par H_2O_2. Néanmoins, la capacité de sorption du biochar SSD modifié par KOH n'a pas été déterminée en raison de l'impossibilité de modéliser les données expérimentales avec le modèle de l'isotherme de Langmuir. Cela indique qu'un lavage insuffisant du biochar

SSD modifié par KOH peut inhiber la sorption de Pb(II) en raison de la libération de composés organiques dissous de ce biochar pouvant interagir avec Pb^{2+} et ainsi former des complexes Pb-ligand dans la solution. En outre, l'étude de la distribution de l'état redox de l'arsenic a montré une oxydation importante (70%) de As (III) en As (V) dans le biochar SSD traité au KOH avec lavage par batch, tandis que l'As(III) a été partiellement oxydé (7%) dans le biochar SSD traité au KOH avec un lavage en colonne. Ceci met en évidence le rôle important de la procédure de lavage sur l'efficacité de la sorption des métal(loïde)s, en particulier pour le Pb (II) et l'As (V).

L'extraction de l'arsenic fixé par les biochars suivie d'une analyse par chromatographie en phase liquide a été établie avec succès pour récupérer quantitativement et préserver l'oxydation de l'As(III) à l'aide d'acide ascorbique. Au cours de la cinétique de sorption, As (III) peut être stable ou partiellement oxydé en fonction du traitement chimique subit par les biochars. Il a été montré que l'oxydation de As(III) était fortement induite par le biochar et, dans une moindre mesure, par des composés dissous libérés par les biochars.

En résumé, les biochars de digestat modifiés par traitement chimique suivi d'une procédure de lavage appropriée du biochar peuvent être utilisés avec succès comme sorbants de Pb(II), Cd(II) et As(III, V). En outre, l'évolution de la distribution redox de l'arsenic dans les biochars et les solutions liquides à l'aide de l'extraction de liquide solide et de l'analyse chromatographique a été déterminée. Cela permet de mieux comprendre la transformation entre As(III) et As(V) lors la sorption de l'arsenic sur les biochars.

Samenvatting

Zuiveringsslib digestaat (SSD) en de organische fractie van stedelijk vast afval digestaat (OFMSWD) worden momenteel beschouwd als alternatieve grondstoffen voor de productie van biochar vanwege de hoge hoeveelheid organisch vast afval die overblijft aan het einde van de behandeling. De pyrolyse van vast digestaat staat bekend als een alternatief om de recycling van organisch afval te bevorderen en bioproducten met toegevoegde waarde (bv. biochar) te genereren. Over het algemeen heeft de biochar van digestaat een veel lagere sorptiecapaciteit voor metalen in vergelijking met actieve kool. Daarom wordt chemische behandeling beschouwd als een mogelijke optie om de eigenschappen van het biocharoppervlak te verbeteren en zo een betere sorptiecapaciteit voor metalen op het biocharoppervlak te bewerkstelligen.

In dit werk werden de SSD en OFMSWD afgeleide biochars behandeld met 2 M KOH of 10% H_2O_2, gevolgd door batchwassing of batchwassing gevolgd door kolomwassing met ultrapuur water. De fysisch-chemische eigenschappen, waaronder de pH van het punt van nul lading (pH_{PZC}), de Brunauer-Emmett-Teller oppervlakte (S_{BET}) en kation exchange capacity (CEC) werden bepaald voor alle biochars om hun verbeterde oppervlakte-eigenschappen te koppelen aan de verbeterde sorptiecapaciteit voor metalen. Alle biochars werden vervolgens gebruikt om de invloed van chemische behandeling en de wasprocedure op het sorptiegedrag van Pb(II), Cd(II) en As(III, V) te bestuderen door de batch sorptiekinetiek en isothermen. Bovendien werd de As redox-statusverdeling (d.w.z. As(III) en As(V)) tijdens de As(III) sorptie op het oppervlak van de biochar en in vloeibare oplossing bepaald met behulp van vaste-vloeistofextractie gevolgd door vloeistofchromatografische analyse.

De resultaten toonden stijgingen van de pH_{PZC}, S_{BET} en CEC na chemische behandeling van de biochar, in overeenstemming met de verbeterde sorptiecapaciteit voor Pb(II), Cd(II) en As(V). Zo werd bijvoorbeeld de maximale sorptiecapaciteit (Q_m) verhoogd van 1,6 µmol g^{-1} (As(V)) en 15,4 µmol g^{-1} (Cd(II)) op de ruwe SSD-biochar tot 8,1 µmol g^{-1} (As(V)) en 306,1 µmol g^{-1} (Cd(II)) na, respectievelijk, de H_2O_2- en KOH- behandeling (bij initiële pH 5,0). Ook de Q_m van Pb(II) werd verhoogd van 31,4 µmol g^{-1} (ruwe SSD-biochar) tot 121,4 µmol g^{-1} op de H_2O_2 gemodificeerde SSD-biochar. De sorptiecapaciteit voor Pb(II) werd echter niet bepaald na de KOH-behandeling als gevolg van het falen van het Langmuir isotherm model om de experimentele gegevens te fitten. Dit wijst erop dat onvoldoende wassen van de KOH-gemodificeerde SSD-biochar de Pb(II)-sorptie kan belemmeren als gevolg van het vrijkomen van opgeloste

organische verbindingen uit deze biochar die kunnen reageren met Pb^{2+} en zo Pb-ligand complexen in de oplossing kunnen vormen. Bovendien vertoonde de As redox distributie een significante oxidatie (70%) van As(III) tot As(V) in KOH-gemodificeerde SSD-biochar met batchwassing, terwijl As(III) gedeeltelijk werd geoxideerd (7%) in de KOH-gemodificeerde SSD-biochar met batch en daaropvolgend kolomwassingen. Dit benadrukt de belangrijke rol van de wasprocedure voor de sorptie van metalen, in het bijzonder voor Pb(II) en As(V).

De As-extractie gevolgd door vloeistofchromatografische analyse werd met succes vastgesteld om de As(III)-oxidatie met behulp van ascorbinezuur kwantitatief te herstellen en te behouden. Tijdens de sorptiekinetiek kan As(III) stabiel of gedeeltelijk geoxideerd zijn, afhankelijk van de biocharbehandeling. Bovendien werd de oxidatie van As(III) sterk geïnduceerd door het biochar materiaal en in mindere mate door het vrijkomen van opgeloste verbindingen uit de biochar.

Samenvattend kan digestaat met chemische behandeling, gevolgd door een goede biocharwasprocedure met, succes worden gebruikt als potentieel sorbens om de Pb(II), Cd(II) en As(III, V) sorptiecapaciteit te verbeteren. Bovendien kan de As redox-verdeling tussen de biochars en in oplossing tijdens de sorptie worden gemeten door As-extractie en chromatografische analyse, waardoor een beter inzicht wordt verkregen in de transformatie tussen As(III) en As(V) in het sorptiesysteem voor biochar-vloeistofsorptie.

Preface

This dissertation summarizes the research work performed at University of Paris-Est (France), University of Limoges (France) and IHE Delft Institute for Water Education (the Netherlands). All the experimental works were financially supported by the Marie Skłodowska-Curie European Joint Doctorate (EJD) Advanced Biological Waste-to-Energy Technologies (ABWET) programme under the European Union Horizon 2020 framework (grant agreement no. 643071).

I would like to thank my promotor, Prof. Eric D. van Hullebusch, for his guidance through my research works and for his supervision during four years of my PhD. Special thanks to my co-supervisor, Prof. Gilles Guibaud and my instructor, Dr. Stéphane Simon for their generous guidance, supports and valuable comments on my results and thoroughly the manuscripts. I am thankful to my co-promotors, Prof. Piet Lens and Asst. Prof. Aino-Maija Lakaniemi, and my instructors, Dr. Yoan Pechaud and Dr. David Huguenot for their valuable suggestions on my research works and the manuscripts. I also thank Prof. Silvia Fiore from Politecnico di Torino, Prof. Marie-Odile Simonnot from Université de Lorraine and Prof. Florence Pannier from Université de Pau et des Pays de l'Adour for reviewing my thesis.

All my friends I met during four years of my PhD, especially Andreina Laera, Anna Gienlik, Ramita Khanongnuch and Wannapawn Watsuntorn, and friends from Limoges, Diệp, Noël, Eloi, Sylvain, Robin and Anne-Lise are acknowledged for the amazing time spent together.

I offer my grateful thanks to my family, especially my father for the great support and motivation throughout the tough time during my PhD life abroad.

March 2019
Suchanya Wongrod

Contents

List of Symbols and Abbreviations

BET	Brunauer-Emmett-Teller
$BMSW^{bat}$	Biochar derived from organic fraction of municipal solid waste digestate with batch washing
$BMSW\text{-}H_2O_2{}^{bat}$	Hydrogen peroxide modified biochar from organic fraction of municipal solid waste digestate with batch washing
$BMSW\text{-}KOH^{bat}$	Potassium hydroxide modified biochar from organic fraction of municipal solid waste digestate with batch washing
BSS^{bat}	Biochar derived from sewage sludge digestate with batch washing
BSS	Biochar derived from sewage sludge digestate with batch and subsequent continuous column washing
$BSS\text{-}H_2O_2{}^{bat}$	Hydrogen peroxide modified biochar from sewage sludge digestate with batch washing
$BSS\text{-}H_2O_2$	Hydrogen peroxide modified biochar from sewage sludge digestate with batch and subsequent continuous column washing
$BSS\text{-}KOH^{bat}$	Potassium hydroxide modified biochar from sewage sludge digestate with batch washing
BSS-KOH	Potassium hydroxide modified biochar from sewage sludge digestate with batch and subsequent continuous column washing
CA	Cellulose acetate
CEC	Cation exchange capacity
DMA	Dimethylarsinic acid
DOC	Dissolved organic compounds
EC	Electrical conductivity
FTIR	Fourier transform infrared spectroscopy
GF-AAS	Graphite furnace atomic absorption spectrometry
ICP-OES	Inductively coupled plasma optical emission spectroscopy
LC-AFS	Liquid chromatography coupled to atomic fluorescence spectrometry
MMA	Monomethylarsonic acid
MP-AES	Microwave plasma atomic emission spectroscopy
OFMSW	Organic fraction of municipal solid waste
OFMSWD	Organic fraction of municipal solid waste digestate
PFO	The pseudo-first-order kinetic model
PSO	The pseudo-second-order kinetic model
pH_{PZC}	pH of point of zero charge
RDC	Release of dissolved compounds
S_{BET}	Brunauer-Emmett-Teller specific surface area
SSD	Sewage sludge digestate
XRD	X-ray diffraction

List of Publications

I. Wongrod, S., Simon, S., Guibaud, G., Lens, P.N.L., Pechaud, Y., Huguenot, D., van Hullebusch, E.D. (2018). Lead sorption by biochar produced from digestates: Consequences of chemical modification and washing. Journal of Environmental Management 219: 277–284.

II. Wongrod, S., Simon, S., van Hullebusch, E.D., Lens, P.N.L., Guibaud, G. (2018). Changes of sewage sludge digestate-derived biochar properties after chemical treatments and influence on As(III and V) and Cd(II) sorption. International Biodeterioration & Biodegradation 135: 96–102.

III. Wongrod, S., Simon, S., van Hullebusch, E.D., Lens, P.N.L., Guibaud, G. (2019). Assessing arsenic redox state evolution in solution and solid phase during As(III) sorption onto chemically-treated sewage sludge biochars. Bioresource Technology 275: 232–238.

Author's Contribution

Paper I: Suchanya Wongrod planned and performed the experiments on biochar characterization and metal analysis and wrote the manuscript. Gilles Guibaud is the corresponding author. Gilles Guibaud and Stéphane Simon helped in data evaluation and revising the manuscript. Eric van Hullebusch, Piet Lens, Yoan Pechaud and David Huguenot contributed to the planning of the experiments as well as the manuscript revision.

Paper II: Suchanya Wongrod performed the experiments, characterized the biochar properties, metal(loid)s analysis, data interpretation and wrote the manuscript. Stéphane Simon helped in arsenic speciation analysis, data evaluation and is the corresponding author. Gilles Guibaud and Stéphane Simon contributed to the planning of experimental work and commented on the manuscript. Eric van Hullebusch and Piet Lens helped in revising the manuscript.

Paper III: Suchanya Wongrod performed the extraction, acid digestion and sorption experiments, data interpretation and wrote the manuscript. Stéphane Simon helped in arsenic speciation analysis, data interpretation and is the corresponding author. Gilles Guibaud and Stéphane Simon participated in planning the experiments and revising the manuscript. Eric van Hullebusch and Piet Lens contributed thoroughly to the revision of the manuscript.

1 Introduction

Metal(loid)s like arsenic (As), lead (Pb) and cadmium (Cd) are toxic and carcinogenic elements that mainly originate from anthropogenic activities such as discharges of wastewater from industries, agricultural use of pesticides and mining. Urban rivers are found to be increasingly contaminated with several metal(loid)s, particularly As, Cd and Pb (Islam et al., 2015). The metal(loid) pollutants often generate concerns over their potential effects on human health and the environment. Singh et al. (2015) reported that about 150 million people are affected by As poisoning in drinking water worldwide. To date, the use of certain metal(loid)s such as As-containing compounds has been banned due to a severe impact to health hazards. However, since the As, Cd and Pb are non-biodegradable and persistent, they tend to remain for a long time in the environmental cycle. Hence, the reduction of the As, Cd and Pb toxicity in water bodies becomes necessary.

To decrease the toxicity of As, Cd, and Pb in polluted water, the understanding of chemistry of each element is very important. The toxicity of the As, Cd, and Pb depends significantly on the chemical species of each specific element. Arsenic, as a metalloid, mainly exists in four oxidation states: arsenate (As(V)), arsenite (As(III)), arsenic (As(0)), and arsine (As(-III)). Among these species, arsenite (As(III)) and arsenate (As(V)) are known as the most toxic forms of As (Hughes et al., 2011), whereas metals like Cd and Pb mostly occur in divalent ion forms (*i.e.* Cd(II) and Pb(II)) in the environment.

Because of the acute toxicities of As(III, V), Cd(II) and Pb(II), many treatment approaches such as chemical precipitation, oxidation, coagulation and flocculation, ion exchange, phytoremediation, membrane separation and adsorption have been used to reduce the concentrations of these pollutants in water (Inyang et al., 2016; Jadhav et al., 2015; Jain and Singh, 2012; Singh et al., 2015). Sorption is considered as a cost efficient and simple treatment technique and biochar has recently been used as a

potential sorbing material for metal(loid)s due to a great abundance of various biowaste feedstocks used for the production of biochar (Ding et al., 2016; Ofomaja et al., 2014; Peng et al., 2018; Wang et al., 2016; Zhou et al., 2017).

Currently, by-product organic waste digestates generated after the organic waste and wastewater treatment plants (*e.g.* sewage sludge digestate and the organic fraction of municipal solid waste digestate) are considered as an opportunity to produce low-cost and effective biochars for metal(loid)s removal from water/wastewater. Pyrolysis (300–650 °C) is the most favorable thermal process that helps to improve the digestate properties as well as adding more value to the biochar products. The obtained biochars usually contain increased surface functional groups and suitable physical and chemical properties, and thereby attracting more metal(loid)s to sorb onto these sorbents (Kambo and Dutta, 2015). Nevertheless, certain raw biochars, particularly from the sewage sludge digestate, exhibit low adsorption capacities toward metal(loid)s, the biochar modification is required to enhance the sorption ability of such inorganic pollutants.

Biochar modification techniques such as physical and chemical treatments are considered as alternatives for improvement of the biochar properties. Physical treatment *via* steam activation provides new porosities and increases surface area (S_{BET}) on the biochar. A significant increase of the S_{BET} was observed on a willow biochar (*i.e.* from 11.4 to 840 m^2 g^{-1}) with steam activation (Kołtowski et al., 2017). However, the steam activation has a high operation cost due to its operation at high temperature (>800 °C) (Wang and Liu, 2018). Chemical modification of biochar is alternatively considered as a low-cost approach since no heat is used during the treatment. Biochar exposed to acidic, oxidative or alkaline solutions (*e.g.* H_2O_2 and KOH) induces the oxidation of biochar surface and thus more surface functional groups, particularly carboxyl and hydroxyl groups, are potentially generated onto the biochar surface (Sizmur et al., 2017; Xue et al., 2012). Such improved properties from chemical treatments could facilitate more sorption for metal(loid)s onto the biochar (Jin et al., 2014; Petrovic et al., 2016; Regmi et al., 2012). However, certain chemicals such as KOH have the ability to dissolve organic compounds from biochar (Lin et al., 2012; Liou & Wu, 2009; Liu et al., 2012). These dissolved organic compounds (DOC) could interfere with the metal sorption onto biochar by forming soluble metal-ligand complexes (Mancinelli et al., 2017). Therefore, the implementation of a biochar washing procedure after chemical treatment is required.

Generally, after the biochar chemical modification, several batch washings with ultrapure water until the pH becomes stable are performed on the biochar (Huang et al., 2017; Regmi et al., 2012; Wu et al., 2017) without any concern on the releasing

compounds (*e.g.* DOC, PO_4^{3-}, CO_3^{2-}) from the modified biochar. A continuous washing of biochar by using a column reactor is considered as another option to eliminate all the releasable compounds from the biochar. It is recommended that the proper washing procedures after biochar treatment should be implemented in order to obtain a cleaned-biochar prior to its use as a potential sorbent for metal(loid)s.

This thesis focuses on the biochar production from organic waste digestates (*i.e.* sewage sludge digestate and the organic fraction of municipal solid waste digestate) and its application as a sorbing material for As(III, V), Cd(II) and Pb(II) removal from aqueous solutions. The chemical modification by using H_2O_2 and KOH and washing procedures were applied on the biochars in order to obtain the chemically-modified biochars with improved surface properties. This study is also the first to report proper biochar washing procedures after the chemical treatment. The physical, chemical and structural properties of raw and chemically-modified biochars are also analyzed in detail. The sorption kinetics and isotherms for As(III, V), Cd(II) and Pb(II) were performed in batch systems to investigate the sorption mechanisms and sorption behaviors during sorption process. Furthermore, the assessment of As redox species evolution during the As(III) sorption by biochars was performed. This study is also the first to highlight the role of biochar towards the As redox modifications.

2 Theoretical background

2.1 Metal(loid)s pollution in environment

Metals and metalloids water contamination are of high concern due to their persistence and toxicity towards aquatic organisms and human beings even at low concentrations. Metals like lead (Pb) and cadmium (Cd) are considered as toxic and carcinogenic elements in Europe (Tóth et al., 2016), which dominantly prevail in divalent ions, *i.e.* Pb(II) and Cd(II). The pollution sources of these metal elements mostly originate from smelters, mining, agricultural activities and wastewater discharges from industries. As a consequence, the contamination of Cd(II) and Pb(II) could pose severe threats to the aquatic environment. The Pb(II) poisoning of children has been heavily found in Haina (Dominican Republic), as a result from a car battery recycling factory (Kaul et al., 1999). Islam et al. (2015) reported a Cd(II) and Pb(II) contamination in an urban river in Bangladesh regarding the exceeded limits of such elements in this river, while the sediments were moderately to heavily contaminated with Cd(II), Pb(II) and arsenic (As).

Arsenic (As) is known as a metalloid which features both metal and nonmetal properties. Arsenic occurs naturally in the environment and its pollution was mostly caused from the mobilization under natural conditions. Nevertheless, anthropogenic activities such as mining, ore smelting and use of arsenic in industry and agriculture are other possible sources of As contamination in water. In the past century, arsenic has been used in pesticides, paint pigment, wood preservatives and constituents for products (Hughes et al., 2011). However, the use of arsenic-containing compounds has been restricted today due to their significant impact towards health hazards. Singh et al. (2015) reported that more than 150 million peoples are globally threatened by As contamination in drinking water and about 70% was in Asia, particularly in Bangladesh, China and India. Bangladesh was found to be exposed the largest As poisoning in groundwater in the world history (Argos et al., 2010). Based on the World Health Organization (WHO)

guidelines, the provisional concentration limit of As in drinking water is 10 μg L^{-1}. Nevertheless, the As concentrations in surface water and drinking water vary from 1–5000 μg L^{-1} depending on the sources of arsenic pollution (Singh et al., 2015). Kim et al. (2002) reported heavy As contamination at the levels of 12–828 μmol g^{-1} in mine tailings in Korea which acts as a main source of As contamination in groundwater.

To reduce the concentration of As in polluted water, understandings of As chemistry and toxicity are of great importance. Arsenic toxicity is directly linked to its chemical speciation (particularly the redox state), which mainly exists in four oxidation states: arsenate (As(V)), arsenite (As(III)), arsenic (As(0)), and arsine (As(-III)) and the pH is an important parameter to control the solubility of arsenic in water. Among four species of As, the As(V) is the most stable form in aerobic water, while As(III) is predominant in reduced redox condition (Singh et al., 2015). Arsenic generally presents in various chemical forms which classifies into two types: organic and inorganic forms. The organic species of As such as monomethylarsonic acid (MMA) and dimethylarsinic acid (DMA) show intermediate toxicity, while the inorganic forms of As (*i.e.* As(III) and As(V)) are the most toxic ones that humans are exposed in the environment (Hughes et al., 2011).

Due to the acute toxicity of As(III, V), Cd(II) and Pb(II), numerous treatments such as chemical precipitation, oxidation, coagulation and flocculation, ion exchange, phytoremediation, membrane separation and adsorption have been dedicated to decrease their concentrations in contaminated water and effluent (Inyang et al., 2016; Jadhav et al., 2015; Jain and Singh, 2012; Singh et al., 2015). Among these techniques, sorption is known as a cost effective and simple treatment (Ding et al., 2016; Ofomaja et al., 2014; Peng et al., 2018; Wang et al., 2016; Zhou et al., 2017). To date, biochar has been increasingly used as a potential sorbing material in sorption treatment. Sorption of As(III, V), Cd(II) and Pb(II) by biochars produced from agricultural residues (*e.g.* pine wood, rice husk and switchgrass) has been intensively reported (Liu and Zhang, 2009; Regmi et al., 2012; Wang et al., 2015b). Nevertheless, by-product organic digestates obtained from organic wastes and/or wastewater treatment plants are currently considered as promising and abundant materials to produce low-cost and effective biochars for treating metal(loid)s in polluted water.

2.2 Biochar production from organic waste digestate

Over the last decade, biogas production by anaerobic digestion (AD) has been considered as a main source of renewable energy which has been essentially developed all over Europe with the commissioning of about 13,000 biogas facilities

(Plana and Noche, 2016). During the AD process, biogas is produced as a main product, and the remaining organic waste (*i.e.* digestate) as a by-product. Due to a significant growth of the biogas sector in Europe, the digestate quantity has substantially faced an important increase. The production capacities of digestate can be approximately 20 m^3 per year or about 10 tons per year at an averagely biogas plant capacity of 500 kW (Plana and Noche, 2016). Consequently, the European Union (EU) has made progress on the development of digestate management in many countries; however, further essential implementation is still going on.

Currently, the agricultural utilization of digestate is one of the most applicable options in the EU. Nevertheless, the reuse of digestate in agriculture has faced technical problems due to insufficient management to have a well valorization system for digestate. In addition, a much higher loading capacity of digestate than its application on land (*i.e.* 1–2 times per year) hinders the digestate utilization in the fields (Alvarenga et al., 2015; Fytili and Zabaniotou, 2008). Landfilling is another alternative for the digestate treatment which accounts for 35–45% in Europe (Plana and Noche, 2016). However, this technique will be phased out by the EU legislation due to high metal contents in certain types of digestates, particularly from pig manure. The digested pig manure usually contains high Cu and Zn concentrations that may significantly cause an environmental risk to soils (Nkoa, 2014; Zhang et al., 2016).

Today, pyrolysis of organic waste digestates (*e.g.* the organic fraction of municipal solid waste and sewage sludge digestates) has created a substantial interest by scientific community, particularly in Europe. This technology is considered as an environmentally sustainable approach due to its abilities to recycle the organic waste digestate, reduce the digestate quantity and generate added value bio-products such as biochar. The digestate-derived biochar can be further used as a potential sorbent towards metal(loid)s in polluted water.

2.2.1 Organic fraction of municipal solid waste digestate

The organic fraction of municipal solid waste digestate (OFMSWD) is the by-product sludge remaining after the organic fraction of municipal solid waste anaerobic treatment. The organic fraction of municipal solid waste (OFMSW) mainly composes of organic portion which accounts for 30–40% in Europe (Cesaro et al., 2019). The OFMSW is usually qualified by high moisture content and biodegradability regarding a large content of organic waste, food waste and leftovers from residences, restaurants, factories and markets (Peng and Pivato, 2017). After the AD of the OFMSW, biogas and digestate

are generated. The by-product digestate varies in compositions depending on the source, collection time and system (Alibardi and Cossu, 2015). Based on the characteristics of the OFMSWD, it may cause adverse impacts and pose risks in the environment due to odors, volatile organic compounds (VOCs) and groundwater contamination by leachate (Cesaro et al., 2019).

The OFMSWD is usually enriched in Cu and Zn (Pituello et al., 2014), which is likely to concentrate during the AD process (Tampio et al., 2016). A direct application of this organic waste in the field may be a concern due to the presence of metals as well as organic micropollutants at relatively high concentration in this waste digestate. Therefore, management options for the digestate are proposed to stabilize this waste digestate *via* several technologies such as thermal processes (*e.g.* pyrolysis and gasification) (Garlapalli et al., 2016). Pyrolysis is considered as an alternative approach to eliminate the VOCs and recover material and/or energy from digestates including the OFMSWD as well as the one from anaerobic wastewater treatment plant (*i.e.* sewage sludge digestate).

2.2.2 Sewage sludge digestate

Sewage sludge digestate (SSD) is an organic by-product generated after the anaerobic wastewater treatment. The SSD is rich in Cu, Cr, Pb and Zn (Pituello et al., 2014) as well as Fe and P (Yuan et al., 2015) due to the addition of $FeCl_3$ for phosphate precipitation during the wastewater treatment. Moreover, the SSD is also rich in mineral fractions, depending on the diversity and complexity of each sewage sludge (Zielińska et al., 2015). High ash contents were found in sewage sludge (59%) due to the dominant mineral fractions such as SiO_2, $CaSO_4 \cdot 2H_2O$ and $CaCO_3$ contained in this waste (Zielińska et al., 2015). Like the OFMSW digestate, the SSD contains relatively high metal contents, thus thermal treatments remain as attractive alternatives to retain metals in the added-value solid biochar product.

2.2.3 Biochar production technologies

Thermal treatment technologies (*e.g.* pyrolysis, hydrothermal carbonization and gasification) are known to improve the quality of digestate by adding value to the bioenergy products (*i.e.* syngas, bio-oil and biochar). Thermal treatments are normally operated at temperature ranging from 300 to 1000 °C (Inyang et al., 2016; Novotny et al., 2015). Figure 2.1 shows the overall biochar production *via* several technologies including slow and fast pyrolysis, gasification, and hydrothermal processes. Under slow pyrolysis, biochar is produced under low heating rates (10–30 °C min^{-1}) and long

residence times (5 min–12 h) at temperatures ranging from 300 to 650 °C (Figure 2.1). In general, higher temperatures result in lower biochar yields due to partial degradation of lignin and cellulose (Kambo and Dutta, 2015). The biochar production *via* slow pyrolysis provides high biochar yields (25–35%) and oxygen-containing surface functional groups such as hydroxyl and carboxyl (Kambo and Dutta, 2015). Such functions may favor the sorption capacity towards metal(loid)s. Fast pyrolysis has been used mainly to produce biofuels (bio-oil) as main products, with biochar and syngas as by-products. Under fast pyrolysis, the process performs at 400–700 °C with a very high heating rate (~1000 °C s^{-1}) and short residence times (< min) (Figure 2.1). High bio-oil yields (75%) and low biochar yields (10–15%) are often observed in fast pyrolysis (Mohan et al., 2014). Due to lower biochar yields and higher operation costs from fast pyrolysis, slow pyrolysis is recognized as a more favorable process for biochar production. The slow pyrolysis usually converts biomass (*e.g.* digestate) into a C-rich biochar with suitable physicochemical properties on biochar surface.

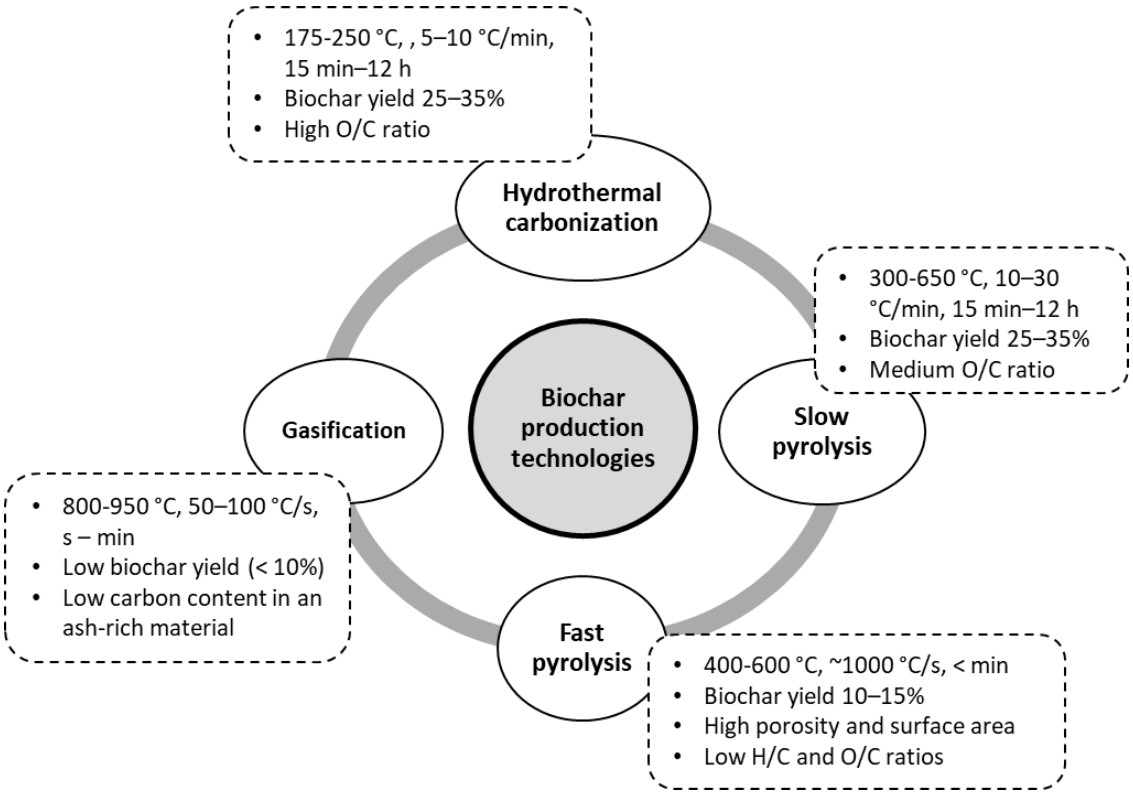

Figure 2.1: Overview of biochar production technologies (data was obtained and modified from Kambo and Dutta (2015); Novotny et al. (2015); Sohi et al. (2010)).

Pre-treatments of digestate as a feedstock, *e.g.* sieving to small particle size (<2 mm) and drying (65–80 °C) to reduce the moisture to less than 10% are required to obtain

homogenous biochar (Pituello et al., 2014). Similar to biomass, the digestate is mainly comprised of cellulose, hemicellulose, lignin, protein and fatty acids (Pituello et al., 2014). The transformation of digestate takes place along increasing temperature. Thermal decomposition of digestate occurred at temperature between 250 and 350 °C (Pituello et al., 2014). Hemicellulose started to decompose at temperatures from 200 to 260 °C, whereas cellulose and lignin degradation occurred at temperatures of 240–350 °C and 280–500 °C, respectively (Novotny et al., 2015). The biochar physicochemical properties are substantially affected by the production temperature. Zielińska et al. (2015) found that the pH values of sewage sludge biochars continuously increased along higher temperature in which the biochar becomes more alkaline at temperature beyond 500 °C. During pyrolysis, the organic matter from digestate also undergoes structural modifications such as the conversion of aliphatic forms to aromatic compounds (Zama et al., 2017), provide more stability (*e.g.* aromaticity) of biochar structures.

Table 2.1 shows the comparison of biochar sorption capacities for Pb(II) produced at different pyrolysis temperatures. From Table 2.1, the peanut shell biochar has the highest maximum sorption capacity (Q_m) (254.8 µmol g^{-1}) for Pb(II), while the lowest Q_m was found on biochar from rice husk (8.6 µmol g^{-1}) (at initial pH 5.0). The biochar from pine wood also showed a low sorption for Pb(II) (18.8 µmol g^{-1}), while much higher Pb(II) sorption abilities were found on biochars from dairy waste digestate, sugar beet digestate and medicine residue (196.9–248.0 µmol g^{-1}) (Table 2.1). Due to low sorption capacities of certain biochars, they are not completely suitable as sorbing materials. Therefore, pre- or post- treatments of biochars such as physical and chemical activations (Sizmur et al., 2017) to improve the sorption efficiency for metal(loid)s become necessary.

Table 2.1: Comparison of maximum sorption capacities for Pb(II) by biochars produced from different organic waste materials.

Biochar material	Pyrolysis temperature	Q_m (µmol g^{-1})	Experimental conditions: initial pH, biochar dosage	Reference
Pine wood	300	18.8	pH 5.0, 4 g L^{-1}	Liu & Zhang (2009)
Rice husk	300	8.6	pH 5.0, 4 g L^{-1}	Liu & Zhang (2009)
Peanut shell	350	254.8	pH 5.0, 4 g L^{-1}	Wang et al. (2015)
Whole sugar beet digestate	600	196.9	pH 5.0, 2 g L^{-1}	Inyang et al. (2012)
Dairy waste digestate	600	248.0	pH 5.0, 2 g L^{-1}	Inyang et al. (2012)
Medicine material residues	350	222.5	pH 5.0, 4 g L^{-1}	Wang et al. (2015)

2.2.4 Physicochemical properties of biochar

Physicochemical properties such as C, H, O, N, mineral content, specific surface area and structural properties are also developed on the biochar surface (Pituello et al., 2014; Yuan et al., 2015; Zielińska et al., 2015). Due to such improved properties of biochar, it has abilities to retain nutrients, reduce carbon dioxide emission in soil and remove several contaminants both in water and soil (Ahmad et al., 2014; Inyang et al., 2016; Novotny et al., 2015). Biochar generally contains both negative and positive surface charges, depending on the pH.

The pH of point of zero charge (pH_{PZC}) is the pH at which the biochar is net neutral or contains equal numbers of positive and negative charges on its surface. At the pH condition below the pH_{PZC}, the biochar exhibits net positive charges, while it is net negatively-charged at the pH condition beyond the pH_{PZC}. Changing of the pH condition will alter the surface charges of biochar and thus it will strongly affect the possibility of electrostatic interaction. Therefore, the pH is required to be optimized in order to improve the sorption of metal(loid)s onto the biochar. At circumneutral pH, where negatively-charged biochars are predominant, they have been used for sorption of

metals like lead (Pb), zinc (Zn) and cadmium (Cd) from polluted water (Ding et al., 2016; Ho et al., 2017; Park et al., 2017).

Electrical conductivity (EC) and cation exchange capacity (CEC) are also known as important parameters for the biochar. The EC is a measure of dissolved ionic species present in the solutions, which is often measured in term of the capacity to transmit electrical current. Since the electrical current is transported by the ions in the solutions, the EC increases as the solutions contain more dissolved ionic species. Therefore, the EC is considered as a key parameter for the biochar application towards metal(loid) sorption from the aqueous solutions. The CEC is a measure of the biochar ability to exchange cationic elements (*e.g.* Ca^{2+}, Mg^{2+}, K^{+} and Na^{+}) on its surface with metal ions in the solutions. Therefore, the CEC parameter can be an indicator to show the possibility of positively-charged metal ions (*e.g.* Pb^{2+} and Cd^{2+}) to sorb onto the biochar surface *via* cation exchange mechanism.

2.3 Modification and washing of biochar

Table 2.2 compares the sorption abilities for As(III), As(V) and Cd(II) by biochars obtained from different origin of feedstocks. From Table 2.2, the highest sorption ability for As(V) was found on a carbonaceous nanofiber with the Q_m of 670 µmol g^{-1}, in a comparable range with a magnetic carbonaceous tea waste (507 µmol g^{-1}) (both at initial pH 5.0). In addition, biochar from paper mill sludge was able to efficiently sorb both As(V) and Cd(II) with the Q_m of 303 and 369 µmol g^{-1}, respectively (Table 2.2). However, biochar produced from rice straw showed relatively low Q_m for both As(III) and As(V), *i.e.* 5.9 µmol g^{-1} and 7.3 µmol g^{-1}, respectively (Table 2.2). Due to low sorption abilities of certain biochars, biochar modification is considered as an effective approach to increase the sorption efficiency for metal(loid)s in water.

Biochar modification technologies such as physical and chemical activation have recently been used to improve properties of biochar. Physical activation generally provides high-temperature steam to clean biochar pore sites and create new porosities, which consequently increases surface area (S_{BET}) on the biochar. Lima et al. (2010) found an increase of the S_{BET} of biochar produced from broiler litter, from 4.6 to 136 m^2 g^{-1} after steam activation. A significantly higher S_{BET} on a steam activated willow-derived biochar, from 11.4 to 840 m^2 g^{-1}, was also reported (Kołtowski et al., 2017). Nevertheless, the steam activation is often operated at high temperature (>800 °C), resulting in a high operation cost, particularly for a large scale operation (Wang and Liu, 2018).

Chemical treatment of biochar is the most common and low-cost technique as no heat is required during the operation. Acidic or alkaline treatments induce an oxidation of biochar, which consequently creates more oxygen-containing functional groups on the biochar surface (Sizmur et al., 2017; Xue et al., 2012). The S_{BET} also increases after exposing the biochar to chemical solutions (*e.g.* H_2O_2 and KOH) (Jin et al., 2014; Wang and Liu, 2018). Acidic treatment (*e.g.* H_2O_2 as an oxidant) helps to remove mineral fractions from biochar, thus inducing a more hydrophilic property of the biochar (Shen et al., 2008). An increase of surface functional groups, particularly carboxyl, was also observed on the biochar treated with H_2O_2 (Xue et al., 2012). Similarly, alkaline treatment also produces more surface functional groups (*e.g.* hydroxyl and carboxyl), but increases basicity in the biochar material (Huang et al., 2017; Jin et al., 2014; Petrovic et al., 2016). Such improved properties from both H_2O_2 and KOH treatments induce more sorption for metal(loid)s like As(III), As(V), Cu(II), Cd(II) and Pb(II) onto the modified biochars (Jin et al., 2014; Petrovic et al., 2016; Regmi et al., 2012).

Due to a chemical property of KOH to dissolve ash and condense organic matter (*e.g.* lignin and cellulose) in the modified biochar (Lin et al., 2012; Liou & Wu, 2009; Liu et al., 2012), a release of dissolved organic compounds (DOC) and mineral ash from the modified biochar can be observed. The release of DOC from biochar could interact with metal ions such as Cd(II), Cu(II) and Pb(II), and thereby affecting the mobility of such elements through the formation of soluble metal-ligand complexes (Mancinelli et al., 2017). Since this DOC interferes the sorption of metals onto the biochar, the elimination of such released compounds from biochar becomes necessary. To date, a concern to implement a proper biochar washing procedure after chemical treatment is scarce and requires more attention by scientists.

In general, after the chemical treatment of biochar, several batch washings of biochar with ultrapure water until the pH becomes stable are usually performed (Huang et al., 2017; Regmi et al., 2012; Wu et al., 2017). Nevertheless, these batch washings are often conducted without a concern on the release of organic or inorganic compounds (*e.g.* DOC, PO_4^{3-}, CO_3^{2-}, Ca^{2+} and Mg^{2+}) from the biochar. Currently, a continuous column washing of biochar is proposed as an alternative to control the elimination of the releasable compounds and thereby obtain a complete-washed biochar. The selection of biochar washing procedure should be studied with a caution, especially considering the test on biochar ability to release organic and inorganic compounds, particularly after chemical treatment. The properly washed biochar can be further used as a potential sorbent to remove metal(loid)s from water, without any interference of dissolved compounds during sorption treatment.

Table 2.2: Comparison of the sorption performance of As(III), As(V) and Cd(II) by different types of biochars.

Biochar	Element	Q_m (μmol g^{-1})	Concentration ranges (μM)	Solution pH	Reference
Rice straw biochar	As(III)	5.9	13–667	-	Wu et al. (2017)
Pine wood biochar	As(III)	16	0–18	3.5	Mohan et al. (2007)
Oak wood biochar	As(III)	78	0–18	3.5	Mohan et al. (2007)
Rice straw biochar	As(V)	7.3	13–667	-	Wu et al. (2017)
Fe(II)-loaded activated carbon	As(V)	27	7–113	3.0	Özge et al. (2013)
Red mud-modified biochar from rice straw	As(V)	79	13–667	-	Wu et al. (2017)
Paper mill sludge biochar	As(V)	303	280–2529	6.5	Yoon et al. (2017)
Magnetic carbonaceous tea waste	As(V)	507	10–1335	5.0	Wen et al. (2017)
Carbonaceous nanofiber	As(V)	670	100–900	5.0	Cheng et al. (2016)
Paper mill sludge biochar	Cd(II)	369	187–2506	6.5	Yoon et al. (2017)
H_2O_2-treated yak manure biochar	Cd(II)	419	10–1779	-	Wang and Liu (2018)
Graphene oxide nanosheet	Cd(II)	945	40–450	6.0	Zhao et al. (2011)

2.4 Application of biochar for metal(loid)s removal from water

Recently, the application of biochar for metal(loid)s removal from polluted water has received attention by many researchers. Biochar is recognized as an effective sorbing material to immobilize both metals and oxyanions (such as As) due to a great abundance of feedstocks as well as suitable physicochemical properties regarding the biochar's sorption ability. Studies on the sorption of metal(loid)s by biochars are

important to tackle water pollutants and understand the sorption mechanisms in order to determine the sorption behaviors of every inorganic element.

2.4.1 Sorption of metal(loid)s by raw and modified biochars

To assess the sorption of metal(loid)s by biochar in aqueous solutions, a set of batch experiments on adsorption kinetics and isotherms is often conducted. The adsorption kinetics are performed to obtain the time required for each metal(loid) to reach equilibrium state. Generally, metal sorption by the biochar reaches the equilibrium within 24 h, while a longer time may be required for other pollutants (such as organic pollutants). After obtaining the equilibrium time, the sorption isotherms are further conducted to predict the sorption mechanisms and the maximum adsorption capacity (Q_m) of biochar obtained from the Langmuir isotherm equation (see section 4.3.2 in chapter 4).

Figure 2.2 shows the main sorption mechanisms involved in metal(loid)s sorption by the biochars including cation exchange, surface complexation, surface precipitation and physical adsorption. Among these mechanisms, cation exchange of metals with Ca^{2+} and Mg^{2+} is considered as one of the main contributor for the sorption of positively-charged metals (*e.g.* Pb^{2+} and Cd^{2+}) by biochars (Figure 2.2), which accounts for 40–52% (Li et al., 2017). Cation exchange can be also occurred with K^+ and Na^+ to a lesser extent (<8.5%) (Li et al., 2017), which is also reported by Lu et al. (2012). Furthermore, the surface complexation between metals and surface functional groups of biochars (such as carboxyl and hydroxyl groups) also plays an important role, contributing for about 40% of metal removal (Li et al., 2017). In addition, surface precipitation may also occur as the sludge-based biochars usually contain a high amount of phosphate (PO_4^{3-}) and carbonate (CO_3^{2-}) on the biochar surface (Figure 2.2). A high specific surface area of biochar could favor a physical sorption of metal(loid)s onto the biochars (Agrafioti et al., 2014). The relative importance of these sorption mechanisms depends on the origin of biochar feedstocks.

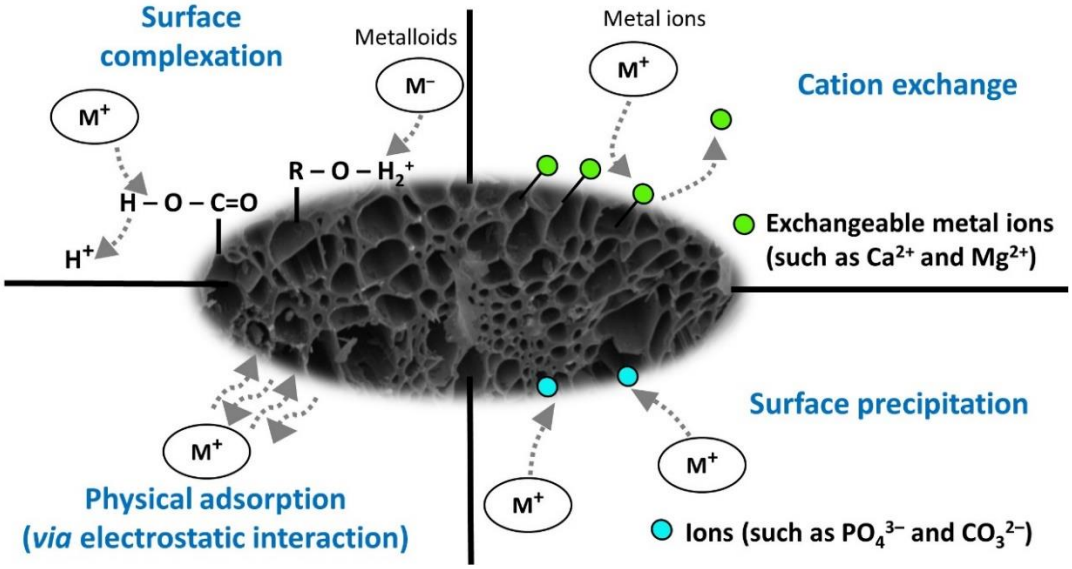

Figure 2.2: Interaction of biochar with metal(loid) pollutants during the sorption mechanism.

From the literature, sorption of Pb(II) by activated carbons (Cechinel et al., 2014), agricultural waste-derived biochars (*e.g.* pine wood or rice husk) (Liu & Zhang, 2009), natural zeolite and kaolinite clay (Andrejkovicova et al., 2016; Jiang et al., 2009) have also been intensively reported. The higher metal(loid)s sorption capacities are probably due to favorable physicochemical properties (*e.g.* surface charges) of such biochars (Liu & Zhang, 2009; Zielińska et al., 2015). As previously discussed, the sorption abilities for Cd(II) by carbonaceous materials are also high, compared to the digestate-based biochar (Table 2.2). However, even if low sorption abilities for As(V) and Cd(II) by the SSD digestate biochar were observed (Table 2.2), the modification of this biochar induces increases of the sorption toward these pollutants. For instance, the Cd(II) sorption capacity (at initial pH 5.0) of the SSD biochar was enhanced from 15.4 µmol g^{-1} (raw biochar) to 218.7 and 306.0 µmol g^{-1}, respectively, on the H_2O_2 and KOH modified biochars (Wongrod et al., 2018b). Jin et al. (2014) found an enhanced As(V) sorption (at initial pH 6.0) by municipal organic waste-derived biochar after alkaline treatment, *i.e.* from 325.6 to 412.4 µmol g^{-1}. The Q_m for Pb(II) was also increased from 368.7 µmol g^{-1} (raw manure biochar) to 818.0 µmol g^{-1} on the H_2O_2-modified biochar (Wang and Liu, 2018). The findings from literature affirm that the chemically-modified biochars are efficient to physically or chemically sorb both metals and metalloids. Nevertheless, due to many existing chemical species of some oxyanions, particularly As in water (as described in section 2.1), the investigation of arsenic redox transformation during biochar-As sorption treatment should be considered. This is to tackle the arsenic species evolution in water bodies as well as in the solid phase biochar

since the arsenic has different affinity toward different biochar types, and therefore the sorption behaviors of biochars can be altered through the interaction with different As species.

2.4.2 Arsenic redox distribution in biochars

Arsenic contamination in surface water and groundwater has become a major concern to affect human health worldwide, particularly in Asia (Singh et al., 2015). Human exposure to As even at low concentrations poses a severe threat to human health (Argos et al., 2010). Of all As species, arsenite (As(III)) and arsenate (As(V)) are noted as the most toxic forms in the environment. The sorption is known as a simple and potential treatment technique to immobilize As from water. Therefore, the assessment of As redox species distribution during the As sorption by biochar becomes interesting since there is no information on the role of biochar toward the As redox modification.

The transformation between As(III) and As(V) is naturally occurs both in soil and water, depending on the surrounding environmental conditions (*e.g.* pH and redox potential). Since As(III) is more mobile and weakly bound to solid material, the As(III) is far more toxic than As(V) (Manning et al., 2002). Therefore, the biochar can be used to induce the oxidation of As(III) to As(V), and as a result reducing the As toxicity in polluted water. Chemical redox speciation of As is of great importance to quantify and tackle As(III) and As(V) species both on solid phase of biochar and in liquid exposition solutions during the sorption between As species and the biochar.

Generally, arsenic speciation in solid-phase biochar can be accessed *via* X-ray absorption near edge structure (XANES) spectroscopy (Niazi et al., 2018a, 2018b). Nevertheless, due to a relatively high operation cost and a less accessibility to synchrotron facilities, the use of this equipment is often limited to few researchers. Hence, there is a need to implement a technology for the analysis of As redox species on solid-phase samples that can be easily accessed by the scientific community. Solid-liquid extraction is considered as a conventional technique that can be efficiently used to recover As from the solid material. Solid-liquid extraction followed by separation techniques (*e.g.* liquid chromatography (LC)) coupled to spectrometric detection techniques (*e.g.* atomic fluorescence spectroscopy (AFS) and inductively coupled plasma mass spectrometry (ICP-MS)) is currently considered as an effective technique for determination of the As speciation on the solid-phase biochar after the sorption process. The use of these coupling techniques can provide a useful information on the As redox distribution in both liquid solutions and on the biochar surface.

3 Aims of the present work

Due to a great availability of digestates, the valorization of these waste streams is considered as an alternative option to eliminate the toxic volatile organic compounds (VOCs) from the digestates and obtain added-value biochar product. The biochar can be further used as a medium in sorption process, particularly for metal(loid) removal.

The aim of this research work was to develop biochars derived from by-product organic waste digestates as sorbents for metal(loid)s removal from water. To improve their sorption capacity, chemical treatments and biochar washing procedure were investigated. The specific objectives of this study are summarized as follows:

- Determine the changes of physicochemical properties of biochars produced from sewage sludge digestate (SSD) and the organic fraction of municipal solid waste digestate (OFMSWD) before and after chemical treatments (Papers I, II and III).
- Investigate the effect of chemical treatments and washing procedures of biochars on the enhancement of Pb(II), Cd(II) and As(III and V) sorption capacity (Papers I, II and III).
- Observe the As(III) and As(V) redox state distribution in the solid biochars and in solutions during arsenic sorption by using conventional chromatographic analysis instead of solid-phase analysis (Papers II and III).

4 Material and methods

4.1 Biochar preparation

4.1.1 Raw biochar preparation

Two organic waste digestates were used as feedstocks for biochar production and then studied as sorbents for metal(loid)s removal from water (Papers I, II and III). Dewatered sewage sludge digestate (SSD) was collected in the storage tank after dewatering and drying processes from a domestic wastewater treatment plant (WWTP) located in Limoges, France. The SSD was further dried and then submitted to slow pyrolysis at industrial scale (Biogreen® technology) at 350 °C for 15 min (Table 4.1). These production conditions were selected based on previous studies by Pituello et al. (2014) and Yuan et al. (2015).

Table 4.1: Overview of the pyrolysis conditions (temperature and residence time) applied to solid digestate samples for biochar production (OFMSWD: organic fraction of municipal solid waste digestate and SSD: sewage sludge digestate).

Samples	Temperature (°C)	Residence time (min)	Paper
OFMSWD	400	60	I
SSD	350	15	I, II, III

The organic fraction of municipal solid waste digestate (OFMSWD) was obtained from a solid waste treatment plant located in France. As illustrated by Figure 4.1, the OFMSWD was dried at 65 °C for 24 h to reduce the initial moisture content to less than 10% and sieved into a particle size of 2 mm to remove impurities such as plastic bags, needles and glasses from the samples before pyrolysis (Paper I). The biochar was

then produced under slow pyrolysis at lab scale using porcelain crucibles with lid-covers (Haldenwanger 79 MF, Germany) in a muffle furnace.

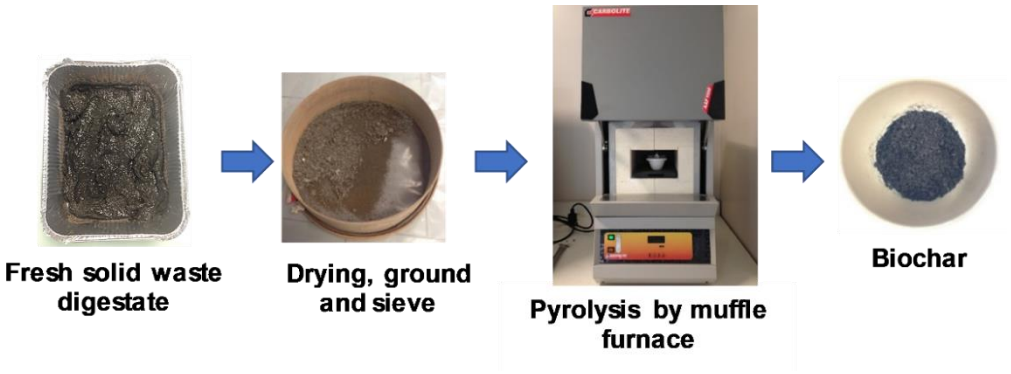

Figure 4.1: Scheme of biochar production from organic fraction of municipal solid waste digestate (OFMSWD) under slow pyrolysis at lab scale.

To find the optimal conditions for biochar production, the OFMSWD was pyrolyzed at different temperatures: 200, 300, 350, 400, 450 and 500 °C, at a residence time of 1 h and a heating rate of 15 °C min^{-1} (Figure 4.2). Results showed a partial conversion of the OFMSWD to the biochar at temperatures of 200–350 °C due to a remaining of organic matter (brown color) in the crucible. In addition, the presence of ash content at temperatures beyond 400 °C was observed, according to remained-oxygen in the muffle that may induce the combustion reaction (Figure 4.2). Therefore, pyrolysis at 400°C for 1 h was at the optimal conditions regarding a complete conversion of organic matter into biochar.

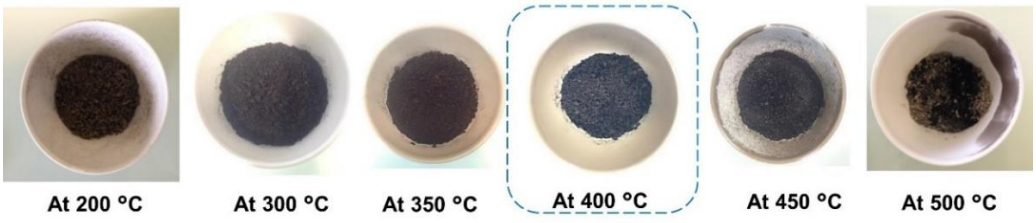

Figure 4.2: Biochar production from organic fraction of municipal solid waste digestate (OFMSWD) at different pyrolysis temperatures (residence time of 1 h and a heating rate of 15 °C min^{-1}).

4.1.2 Chemical treatment and washing of biochar

As discussed in chapter 2, post-treatments after biochar production are required to enhance the biochar sorption capacity for metal(loid)s. Both the SSD and OFMSWD biochars were thus chemically-treated with either a 10% H_2O_2 solution (*i.e.* 100 g biochar per 1 L of a 10% H_2O_2 solution) (modified from Xue et al., 2012) or a 2 M KOH solution (100 g biochar per 2.5 L of a 2 M KOH solution) (modified from Jin et al., 2014) with continuous stirring at 25 °C for 2 h. To eliminate releasable ions (*e.g.* PO_4^{3-}, HCO_3^-/CO_3^{2-}, Ca^{2+} and Mg^{2+}) and organic compounds from the biochar after the chemical treatments, the biochars were then washed with ultrapure water. Two different approaches were tested: (1) a batch washing and (2) the same batch washing followed by a continuous column washing. The overview of two different washing procedure after biochar treatments is illustrated in Figure 4.3.

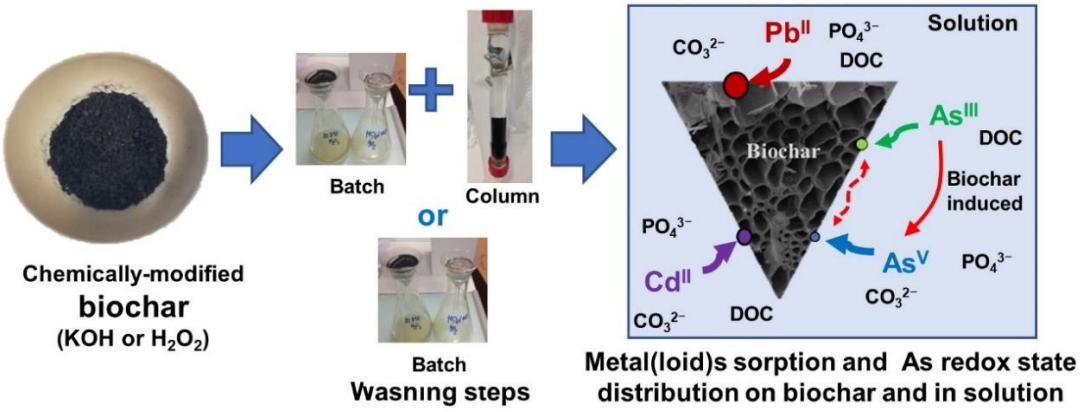

Figure 4.3: Overview of chemical treatments and washing procedure of biochar for metal(loid)s sorption and arsenic redox state distribution on biochar and in solution experiments (Papers I, II and III).

For the batch washing, 2 g of biochar were washed with 200 mL of ultrapure water at 20 (± 2) °C. The batch washing was performed in triplicate in a row until the pH became stable (Jin et al., 2014; Wu et al., 2017; Xue et al., 2012). For the column washing, a part of the batch-washed biochar was submitted to a subsequent continuous washing using ultrapure water in a glass column (2.8 cm in diameter and 42.5 cm in height). Glass beads (2.0 mm in diameter) were filled at the bottom of the glass column to maintain the flow distribution. Peristaltic pumps (Ismatec Reglo Analog, Model No. ISM827, Ismatec SA Company, Switzerland) were used to control the up-flow velocity (0.77 ± 0.01 cm min^{-1}) with a hydraulic retention time of 6 h. The pH, electrical conductivity (EC), the concentrations of PO_4^{3-}, HCO_3^-/CO_3^{2-} and dissolved organic

carbon (DOC) were measured to follow the progress of washing (Paper I). The column washing was considered completed once these parameters reached threshold values, *i.e.* stable pH, similar EC between inflowing and outflowing rinsing water solutions, and low concentrations (<1 mg L^{-1}) of PO_4^{3-}, HCO_3^-/CO_3^{2-} and DOC at the outflowing rinsing water solutions. Once the biochar washing procedure were accomplished, the biochars were dried in an oven at 50 °C for 24 h and kept in a desiccator for further use.

The batch and column-washed biochars were consecutively studied (Figure 4.3) to investigate the influence of the washing procedure on sorption capacity for Pb(II), Cd(II) and As(III, V) as well as its influence on the conversion of redox-sensitive elements (in solution and on the solid phase) during As(III) sorption (Table 4.2). The raw OFMSWD biochar and its H_2O_2 and KOH modified biochars with batch washing are labeled as BMSW^{bat}, BMSW-$H_2O_2^{bat}$ and BMSW-KOH^{bat}, respectively. The SSD biochars and its H_2O_2 and KOH modified biochars with batch washing are denoted as BSS^{bat}, BSS-$H_2O_2^{bat}$ and BSS-KOH^{bat}, respectively. The H_2O_2 and KOH modified SSD biochars with batch and subsequent column washings are labeled as BSS-H_2O_2 and BSS-KOH, respectively. All information concerning chemical treatments, washing procedure and sample labelling are reported in Table 4.2.

Table 4.2: Overview of chemical treatments and washing procedure of biochar to study the sorption ability for Pb(II), Cd(II) and As(III, V) and the influence on its redox state distribution in solution and on the biochar during As(III) sorption.

Sample	Chemical treatment/ washing procedure	Label	Metal(loid) element	Paper
BMSW	unmodified / batch	BMSW^{bat}	Pb(II)	I
	H_2O_2 / batch	BMSW-$H_2O_2^{bat}$		
	KOH / batch	BMSW-KOH^{bat}		
BSS	unmodified / batch	BSS^{bat}	Pb(II)	I
	H_2O_2 / batch	BSS-$H_2O_2^{bat}$		
	H_2O_2 / batch+column	BSS-H_2O_2		
	KOH / batch	BSS-KOH^{bat}		
	KOH / batch+column	BSS-KOH		
BSS	unmodified / batch	BSS^{bat}	Cd(II) and As(III, V)	II, III
	unmodified / batch+column	BSS		
	H_2O_2 / batch	BSS-$H_2O_2^{bat}$		
	H_2O_2 / batch+column	BSS-H_2O_2		
	KOH / batch	BSS-KOH^{bat}		
	KOH / batch+column	BSS-KOH		

4.2 Biochar characterization

4.2.1 Overview of the biochar characterization

Chemical, physical and structural analyses were performed on feedstocks, raw and modified biochars to determine the changes of properties occurring at each modification step, *i.e.* pyrolysis and chemical treatments. The pH and EC of material suspension in water as well as the pH of point of zero charge (pH_{PZC}), the total metal(loid) contents and the cation exchange capacity (CEC) of raw and modified biochars were determined. The Brunauer-Emmett-Teller (BET) N_2 sorption, X-ray diffraction (XRD) and Fourier transform infrared spectroscopy (FTIR) were applied to, respectively, determine specific surface area, crystalline structure and surface functional groups of the raw and modified biochars (Papers I and II). In addition, arsenic redox distribution in liquid solution and solid phase of biochars were also determined using liquid chromatography coupled to atomic fluorescence spectrometry (LC-AFS). All analytical methods and instruments used in all experiments are shown in Table 4.3 and detailed in the following subchapters.

Table 4.3: Analytical methods and instruments used for biochar characterization in Papers I-III.

Parameter	Analytical methods and instruments	Paper
pH	pH-meter LPH 330T, Tacussel, France	I, II, III
pH of point of zero charge (pH_{PZC})	Zetametry by the zeta potential at different pH ranges	II, III
Zeta potential	Zetasizier Nanoseries (Nano-ZS), Malvern, UK	II, III
Electrical conductivity (EC)	CDM 210 conductivity-meter, Radiometer, Denmark	I, II
Dissolved organic carbon (DOC)	AFNOR standard method (NF EN 1484 Juillet 1997; AFNOR, 1997a), TOC Analyzer (multi N/C® 2100S, Analytikjena, Germany)	I
Phosphate (PO_4^{3-})	AFNOR colorimetric method (NF EN 1189 Janvier 1997; AFNOR, 1997b), Vis spectrophotometer (DR1900, Hach, France) at λ 700 nm	I, II
(Bi)carbonate (HCO_3^-/CO_3^{2-})	ARNOR titrimetric method (NF EN ISO 9963-1 Février 1996; AFNOR, 1996) using 10^{-3} M HCl as a titrant and phenolphthalein and mixed bromocresol green-methyl red as indicators.	I
Cation exchange capacity (CEC)	Cobalt hexamine trichloride method (Aran et al., 2008), Präzisions-pH-meter E510, Metrohm AG, Switzerland and spectrometer	II, III

Table 4.3: Analytical methods and instruments used for biochar characterization in Papers I-III.

Parameter	Analytical methods and instruments	Paper
Specific surface area	Brunauer-Emmett-Teller (BET) N_2 sorption method at 77 K (3Flex, Micromeritics, USA)	II, III
Crystalline structure	X-ray diffraction (XRD), a powder diffractometer (AXS D8, Bruker, Germany)	I, II
Surface functional groups	Fourier transform infrared spectroscopy (FTIR), Shimadzu IRAffinity-1 Spectrometer with a deuterated-triglycine sulfate (DTGS) detector	I, II
Total metals (*i.e.* Al, Ca, Cd, Cr, Cu, K, Ni, Pb, Mg, Mn, Na, Fe and Zn)	Acid digestion (EPA Method 3050B; EPA, 1996), inductively coupled plasma optical emission spectroscopy (ICP-OES) (Optima 8300, PerkinElmer, France) or microwave plasma atomic emission spectroscopy (MP-AES) (Agilent 4100, Agilent Technologies Inc., USA)	I, II
Total As	Graphite furnace atomic absorption spectrometry (GF-AAS) (240Z, Agilent Technologies, USA)	II, III
Arsenic speciation	Liquid chromatography coupled to atomic fluorescence spectrometry (LC-AFS) with hydride generation (HG) (PS Analytical Millennium Excalibur, PS Analytical, UK)	II, III

4.2.2 Chemical analysis

To measure the pH of the raw feedstocks, the raw and chemically-modified biochars, a suspension of solid sample in deionized water (1 g: 20 mL) was stirred continuously for 5 min and let to settle for 15 min, then the sample suspension was measured using a pH-meter (LPH 330T, Tacussel, France). The electrical conductivity (EC) of all biochars were measured using a conductivity-meter (CDM 210, Radiometer, Denmark).

The pH of point of zero charge (pH_{PZC}) of raw and modified biochars was determined from zetametry by determining the zeta potential at different pH ranges (Mahmood et al., 2011). Firstly, 40 mL of background electrolyte solution (0.01 M $NaNO_3$) containing 0.2 g of biochar were equilibrated with continuous magnetic stirring at 20 (± 2) °C for 40 min. The pH of the mixture was adjusted in the range of 2.0–10.0 by using HNO_3 (0.1, 0.5 and 1 M) and NaOH (0.1, 0.5 and 1 M). After 40 min of stirring, the pH was measured and corrected until each solution reached a stable targeted pH. The suspension was then filtered with a 0.45 µm cellulose acetate (CA) syringe filter before

determining the zeta potential (Zetasizier Nanoseries (Nano-ZS), Malvern, UK). This filtration was performed to prevent the settlement of biochar particles in the measurement cell of the zetameter and to avoid the clogging of the device by big particles. We hypothesize that all biochar particles display the same behavior, neglecting a particle size effect. The pH_{PZC} values of biochars were determined from the different zeta potential along the pH ranges (2.0–10.0).

For the determination of the biochar cation exchange capacity (CEC), 2 g of biochar sample (dry weight) were mixed with 40 mL of 0.05 N cobalt hexamine trichloride ($[Co(NH_3)_6]Cl_3$) solution (99% *w/w*, Sigma-Aldrich) in polypropylene tubes (Aran et al., 2008). The suspensions were shaken for 1 h to allow the sorption of cobalt (Co) on solid phase of biochars using an orbital shaker (KS 501 digital, IKA^{TM}, USA) at 60 rpm, then centrifuged at 7000 g for 10 min (Rotina 420, Hettich, Germany). The supernatant was filtered through Whatman polyethersulfone (PES) syringe filters (0.2 µm). The pH (Präzisions-pH-meter E510, Metrohm AG, Switzerland) and absorbency at 472 nm (UV–vis spectrophotometer, Lambda 365, PerkinElmer, USA) of each sample were measured immediately. All experiments were performed in triplicate and the results are reported as mean values. The CEC (meq 100 g^{-1} or $cmol^{+}$ kg^{-1}) can be calculated from differences of absorbencies between initial $[Co(NH_3)_6]Cl_3$ solution and remaining Co in residual solution using Eq. (1) (Aran et al., 2008):

$$CEC = \left[\frac{Abs_{Co} - Abs_{sample}}{Abs_{Co}}\right] \times 50 \times \frac{V}{m} \times 100 \qquad \text{(Eq. 1)},$$

where Abs_{Co} and Abs_{sample} refer to the absorbency (at 472 nm) of 0.05 N $[Co(NH_3)_6]Cl_3$ and of sample (supernatant after filtration), respectively. *V* and *m* correspond to solution volume in liter and biochar dry mass in gram, respectively.

Total metal contents including Al, Ca, Cd, Cr, Cu, K, Ni, Pb, Mg, Mn, Na, Fe and Zn in raw feedstocks and biochars were determined by inductively coupled plasma optical emission spectroscopy (ICP-OES) (Optima 8300, PerkinElmer, France) after acid digestion performed according to the Standard Method 3050B (EPA, 1996) by using H_2O_2 (30% *w/w*, Sigma-Aldrich), concentrated HCl (37% *w/w*, Merck) and HNO_3 (65% *w/w*, Merck). The digestion was performed using a heating block at 95 (± 5) °C. The digested solutions were filtered using a Whatman grade 1 qualitative filter paper and metal(loid) elements.

During the continuous column washing of the raw and chemically-modified biochars, liquid samples were collected at the outlet of the column along the time to measure pH, EC, DOC, PO_4^{3-} and HCO_3^-/CO_3^{2-}. DOC was measured following the AFNOR French standard method (NF EN 1484 Juillet 1997; AFNOR, 1997a). A colorimetric method (NF EN 1189 Janvier 1997; AFNOR, 1997b) was applied to measure PO_4^{3-} with a spectrophotometer at λ 700 nm using AFNOR standard method. For HCO_3^-/CO_3^{2-} analysis, a titrimetric method from AFNOR (NF EN ISO 9963-1 Février 1996; AFNOR, 1996) was performed using HCl (10^{-3} M) as a titrant and phenolphthalein and mixed bromocresol green-methyl red as indicators. The total releasable amounts of Ca^{2+} and Mg^{2+} were measured using microwave plasma atomic emission spectroscopy (MP-AES), respectively, at λ 422.673 nm and λ 285.213 nm.

4.2.3 Physical and structural analyses

Brunauer-Emmett-Teller specific surface area (S_{BET}) of all biochar samples were measured using the N_2 sorption method at 77 K. Before measurement, the biochars were dried at 105 °C for 5 h (Memmert, France).

X-ray diffraction (XRD) was employed to identify the crystalline structures of the raw feedstocks, the raw and modified biochars. The samples were grounded to less than 100 µm particle size and were characterized using a powder diffractometer (AXS D8, Bruker, Germany) with Cu Kα radiation at 1.54 Å wavelength over the 2θ range from 10° to 32°, for 10 seconds per step, at 40 kV voltage and 40 mA current with a Solx (Si-Li) detector. The crystalline compounds present in biochar were identified using the X'Pert HighScore software for data analysis with the reference from the International Center for Diffraction Data (ICDD).

Fourier transform infrared spectroscopy (FTIR) was used to identify the functional groups present on biochar surfaces. Each sample was mixed with KBr in a ratio of 1 mg sample (particle size 100 µm) per 200 mg KBr and the pellet was prepared by compression under vacuum (Jouraiphy et al., 2005). The analysis was performed using a Shimadzu IRAffinity-1 Spectrometer with a deuterated-triglycine sulfate detector. The scanning was performed from 4000 to 800 cm^{-1} wavenumber at a resolution of 16 cm^{-1}.

4.3 Batch sorption experiments

Sorption kinetics and isotherms were performed to, respectively, determine the time required to reach sorption equilibrium and the maximum sorption capacity of biochars. Three sorption kinetic models (*i.e.* pseudo-first-order (PFO), pseudo-second-order (PSO) and intraparticle diffusion) and two sorption isotherm models (*i.e.* Langmuir and Freundlich) were used to describe the experimental data as well as the sorption processes (Zhao et al., 2015a).

All batch sorption experiments for As(III), As(V), Cd(II) and Pb(II) were separately performed at an initial pH value of 5.0 (± 0.2), adjusted using HNO_3 or NaOH (Papers I, II and III). The stock solutions of As(III), As(V), Cd(II) and Pb(II) were prepared separately from $AsNaO_2$, $Na_2HAsO_4.7H_2O$, $Cd(NO_3)_2$ and $Pb(NO_3)_2$. The solid/liquid ratio was set to 4 g of biochar per 1 L of metal(loid) solution and the resulting suspensions were shaken at 20 (± 2) °C using an orbital shaker (KS 501 digital, IKATM, USA) at 180 rpm. The equilibrium time for sorption tests, determined from sorption kinetic studies, was 24 h. All sorption experiments were conducted in duplicate (Papers I and III) and triplicate (Paper III), and the mean values are reported followed by standard deviation. Additional analyses were conducted if a variation over 10% was observed.

After sorption equilibrium time was reached, the solid phase of biochar was separated from the solution by filtration through Whatman polyethersulfone (PES) syringe filters (0.2 µm). The remaining Cd and Pb concentrations in solution were determined by microwave plasma atomic emission spectroscopy (MP-AES) at λ 228.8 nm and 405.781 nm, respectively (Paper I). The As concentration in the solution was measured using graphite furnace atomic absorption spectrometry (GF-AAS) at λ 193.7 nm.

4.3.1 Sorption kinetics

The study of sorption kinetics for metal(loid)s removal from aqueous solutions is important, providing the information about the reaction pathways and the mechanism of the sorption processes. Sorption kinetics are normally used to describe the uptake rate of pollutants (*e.g.* metal(loid)s) sorbed by adsorbents (*e.g.* biochar) at different contact times. Therefore, it is significant to know the kinetic rate for metal(loid)s removal from aqueous solutions until the equilibrium state is reached. In general, three types of kinetic models: the pseudo-first-order (PFO), pseudo-second-order (PSO) and intraparticle diffusion are usually used to explain the experimental data.

The PFO kinetic model was first introduced around the 19th century by Lagergren (1898). However, the kinetic studies became more popular when Ho and McKay (1999) have rearranged the PFO equation into a linearized form and proposed the PSO kinetic model to better describe the correlation of the experimental data. The intraparticle diffusion kinetic model was used to determine the sorption mechanisms such as the degree of boundary layer like film diffusion and mass transfer between liquid-solid interface (Nethaji et al., 2013; Z. Zhao et al., 2015). The following equations are illustrated as followed:

Pseudo-first-order:

$$\log(Q_e - Q_t) = \log Q_e - \frac{k_1 t}{2.303} \quad \text{(Eq. 2)},$$

Pseudo-second-order:

$$\frac{t}{Q_t} = \frac{1}{k_2 Q_e^2} + \frac{t}{Q_e} \quad \text{(Eq. 3)},$$

Intraparticle diffusion:

$$Q_t = k_i t^{1/2} + C \quad \text{(Eq. 4)},$$

where Q_t and Q_e are sorption capacity (µmol g^{-1}) at time t (h) and at equilibrium, k_1 (h^{-1}), k_2 ($g(\mu mol\ h)^{-1}$) and k_i (µmol ($g\ h^{1/2})^{-1}$) are the rate constants for the PFO, PSO and intraparticle diffusion kinetic models, respectively (Liu and Zhang, 2009; Z. Zhao et al., 2015). *C* is the intraparticle diffusion constant related to the boundary layer diffusion. All sorption kinetic parameters and corresponding uncertainties were obtained by non-linear regression using Statistica software (v6.1, StatSoft).

4.3.2 Sorption isotherms

Sorption isotherms are generally used to determine the adsorption capacity of metal(loid)s onto biochars at different metal(loid) concentrations in bulk solutions under the equilibrium condition. Several isotherm models have been used to describe the experimental data such as the Langmuir, Freundlich, Temkin, and Dubinin-Radushkevich models. Langmuir and Freundlich, the two most common isotherm models, were used to study the sorption behaviors and predict the removal efficiency for metal(loid)s. The following equations are expressed as follows:

Langmuir model:

$$\frac{C_e}{Q_e} = \frac{1}{K_L Q_m} + \frac{C_e}{Q_m} \quad \text{(Eq. 5)},$$

Freundlich model:

$$\ln Q_e = \ln K_F + \frac{1}{n} \ln C_e \quad \text{(Eq. 6)},$$

where C_e is the equilibrium solution concentration (μM), Q_e and Q_m are the adsorption capacity at equilibrium and the maximum adsorption capacity (μmol g^{-1}), respectively. K_L and K_F are the sorption constants for the Langmuir and Freundlich isotherm models, respectively, and n is the Freundlich constant which indicates the favorability of sorption.

4.4 Arsenic analysis during sorption tests

During sorption for As, the redox reaction between As(III) and As(V) can be possibly occurred. Therefore, the study on arsenic redox state evolution during sorption for As(III) by biochars was further performed in aqueous solutions under batch experiments (Paper III). Total As and As species (*i.e.* As(III) and As(V)) were individually quantified in both liquid solutions and on the solid-phase of biochars during and/or after the sorption process. The detailed information for As analysis is described in the following subchapters.

4.4.1 Arsenic analysis in solution and deduction of sorbed arsenic

Total As was analyzed using GF-AAS (240Z, Agilent Technologies, USA) at λ 193.7 nm. The redox distribution of As species was determined by LC-AFS with hydride generation (HG) (PS Analytical Millennium Excalibur, PS Analytical, UK) with conditions detailed by Wan et al. (2014). Arsenic redox evolution in solutions obtained from solid-liquid extraction was analyzed within 5 h after recovering the samples in order to avoid the oxidation of As(III) to As(V).

After sorption experiments, the amount of total As sorbed onto the biochar ($Q_{sol.}$, in μmol) was calculated from the difference between the initial and final concentrations of As (C_i and C_f, in μmol L^{-1}) and multiple with the total volume of the solution (V, in L) according to Eq. (7):

$$Q_{sol.} = (C_i - C_f) \times V \quad \text{(Eq. 7)},$$

The sorption capacity of biochar (in µmol g^{-1}) for As can be further obtained by dividing the $Q_{sol.}$ with the mass of biochar (on dry weight).

4.4.2 Extraction of As(III) and As(V) from biochar

Since there is no soft extraction procedure for As from biochar available in the literature, an extraction procedure was designed (Paper III) based on previous studies reported by Thomas et al. (1997), Montperrus et al. (2002) and Zhang et al. (2015). The extraction was performed by 0.3 M phosphoric acid (H_3PO_4, 85% *w/w*, Carlo ERBA). Ascorbic acid (0.5 M) (99.5% *w/w*, Fluka) was added to avoid the As oxidation in the solution during the extraction steps (Xu et al., 2015).

After sorption tests, biochars were quickly rinsed with ultrapure water in order to eliminate the excessive As solution from the biochar. The biochar (0.15 g) was then transferred into a Teflon tube with 25 mL of the extracting solution and heated at 80 °C for 20 min using a microwave device (Multiwave GO, Anton Paar, France). Then, the extracted solutions were recovered by centrifugation (Multifuge X3 FR, Thermo Fisher Scientific) at 3400 rpm for 20 min. The supernatant was collected and filtrated through a 0.2 µm PES syringe filters, then transferred to a 50 mL gauged flask completed with ultrapure water before analysis by LC-AFS. All extractions were performed in triplicate.

4.4.3 Biochar acid digestion for total arsenic measurements

After sorption experiments, the biochar (about 0.15 g) was rinsed 3 times with ultrapure water and transferred into a digestion tube. 6 mL of concentrated nitric acid (HNO_3, 69.5% *w/w*, Panreac ITW) were added then 6 mL of hydrogen peroxide (H_2O_2, 30% *w/w*, Carlo ERBA) were slowly added into the tube to avoid fast reaction due to the strong oxidizing property of this chemical. The digestion tube was left for 12 h to avoid over-pressure during microwave-assisted digestion regarding the high initial release of CO_2 from samples. 3 mL of concentrated hydrochloric acid (HCl, 37% *w/w*, VWR) were then added to the tube and the microwave-assisted digestion was performed at 180 °C for 4 h in 4 cycles (1 h per 1 cycle) to ensure a complete digestion of biochar material. The digested solutions were recovered and diluted with ultrapure water to a constant volume of 50 mL. The filtration of samples was performed using 0.2 µm PES syringe filters prior to total As analysis by GF-AAS at λ 193.7 nm.

4.5 Statistical analysis

The physicochemical properties of biochar and sorption experiments for metal(loid)s were performed in triplicate and the values are reported as means followed by standard deviation unless otherwise stated. Constants for sorption kinetic and isotherm parameters were stimulated by the non-linear regression using Statistica software (v6.1, StatSoft). Statistical analysis of the experimental data was performed by the t-test with two-tailed distribution at a statistical significance level of $P \leq 0.01$ for data comparison.

5 Result and discussion

5.1 Characterization of digestates and biochars

5.1.1 Evolution of chemical and physical properties during pyrolysis

Table 5.1 shows the properties of the organic fraction of municipal solid waste digestate (OFMSWD) and its derived biochar (BMSW), and of the sewage sludge digestate (SSD) and the SSD-derived biochar (BSS) obtained after pyrolysis. Comparison of two digestates, a higher pH value was found on the OFMSWD (8.0 ± 0.1) compared to the SSD (6.0 ± 0.1). This is in accordance to higher alkali metal elements (*e.g.* Ca, Mg, Na and K) contained in the OFMSWD than in the SSD (Table 5.1). However, metals such as Cu, Mn and Zn were mainly found in both solid digestates.

Pyrolysis also induced changes of pH values between digestates (raw feedstocks) and biochars. For both the OFMSWD and SSD, higher pH values were observed for biochars, *i.e.* from 8.0 (± 0.1) for OFMSWD to 8.9 (± 0.1) for BMSW and from 6.0 (± 0.1) for SSD to 6.5 (± 0.1) for BSS. The increases of pH can be due to the concentration of inorganic elements/compounds in the biochars according to the separation of alkali metal salts from the organic matrix (Shinogi and Kanri, 2003; Zielińska et al., 2015).

During pyrolysis, metals were retained in the biochars, while As (metalloid) was partly volatilized at the temperature below 400 °C. The As transformation during thermal treatment was also observed by Duan et al. (2017). Consequently, higher metal contents were found in both the BMSW and BSS than in the digestates, whereas a lower As content was found in the BSS (0.63 ± 0.02 µmol g^{-1}) compared to the SSD (1.05 ± 0.04 µmol g^{-1}) (Table 5.1). These findings were in correlation to the study from Pituello et al. (2014). Due to a strong uncertainty of As value for the BSS and no As information for both the OFMSWD and BMSW, more caution should be concerned when using these samples. It was also noticed that a 4–fold higher Ca content was found in the BMSW compared to the BSS (Table 5.1). This could induce the cation exchange between Ca^{2+} and metal ions and thus more metal sorption can be expected on the BMSW. Nevertheless, both the BMSW and BSS display the presences of Al, Fe and Mn (Table 5.1) that could be partially in metal oxide forms such as Al_2O_3, Fe_2O_3 and MnO. Therefore, this could promote the metal ions to sorb onto the biochars (Agrafioti et al., 2014; Wang et al., 2015a).

Table 5.1: Properties of the organic fraction of municipal solid waste digestate (OFMSWD), its derived biochar (BMSW), and sewage sludge digestate (SSD) and its derived biochar (BSS) before and after pyrolysis.

Parameters	OFMSWD	BMSW	SSD	BSS
Pyrolysis conditions	-	400 °C, 1 h	-	350 °C, 15 min
pH in water	8.0 ± 0.1[a]	8.9 ± 0.1	6.0 ± 0.1	6.5 ± 0.1
Biochar yield (%wt)	na[b]	74 ± 1	na	na
Ash (%wt)	52 ± 1	68 ± 1	na	na
Moisture content (%wt)	81 ± 1[c]	na	na	na
Al (µmol g^{-1})	667 ± 37	519 ± 37	408 ± 37	519 ± 37
As (µmol g^{-1})[b]	dl[d]	dl	1.05 ± 0.04	0.63 ± 0.02
Ca (µmol g^{-1})	2.22 ± 0.05	2.87 ± 0.03	0.50 ± 0.03	0.75 ± 0.03
Cd (µmol g^{-1})	dl	dl	dl	0.08 ± 0.01
Cr (µmol g^{-1})	1.81 ± 0.02	1.92 ± 0.04	0.81 ± 0.02	0.92 ± 0.02
Cu (µmol g^{-1})	4.11 ± 0.11	6.86 ± 0.08	6.14 ± 0.16	9.71 ± 0.11
Fe (µmol g^{-1})	197 ± 18	287 ± 18	1182 ± 18	1182 ± 18
K (µmol g^{-1})	818 ± 26	563 ± 26	102 ± 26	102 ± 26
Mg (µmol g^{-1})	127 ± 18	182 ± 18	91 ± 18	146 ± 18
Mn (µmol g^{-1})	5.88 ± 0.06	7.59 ± 0.06	8.68 ± 0.13	14.02 ± 0.15
Na (µmol g^{-1})	1392 ± 44	1392 ± 44	174 ± 44	217 ± 44
Ni (µmol g^{-1})	0.73 ± 0.09	0.65 ± 0.05	0.43 ± 0.02	0.70 ± 0.02
Pb (µmol g^{-1})	0.49 ± 0.03	0.63 ± 0.06	0.39 ± 0.05	0.41 ± 0.02
Zn (µmol g^{-1})	10.60 ± 0.20	13.58 ± 0.19	11.56 ± 0.16	15.56 ± 0.20

[a] Values reported as means (n=3) followed by standard deviation.

[b] na refers to not available.

[c] Values reported on dry basis.

[d] dl refers to below detection limit (*i.e.* 50 µg L^{-1} for As and 5 µg L^{-1} for Cd).

Figures 5.1(a) and 5.1(b) show the change of XRD spectra between feedstocks and biochars after pyrolysis of the OFMSWD and SSD, respectively. XRD analysis showed that OFMSWD contained the crystalline structures of quartz (SiO_2) and calcite ($CaCO_3$) (Figure 5.1(a)). Similar trends were also found in its derived biochar with slight shifts on the XRD spectra. On the other hand, only SiO_2 was detected in SSD and BSS (Figure 5.1(b)). The results showed no significant differences of XRD spectra between the digestates and the biochars. This indicates that the pyrolysis only induced the insignificant modification of surface properties of biochars. Nevertheless, the presence of $CaCO_3$ on the biochar, in this case on the BMSW, may contribute to more sorption of metal elements (Al-Degs et al., 2006; Jiang et al., 2009).

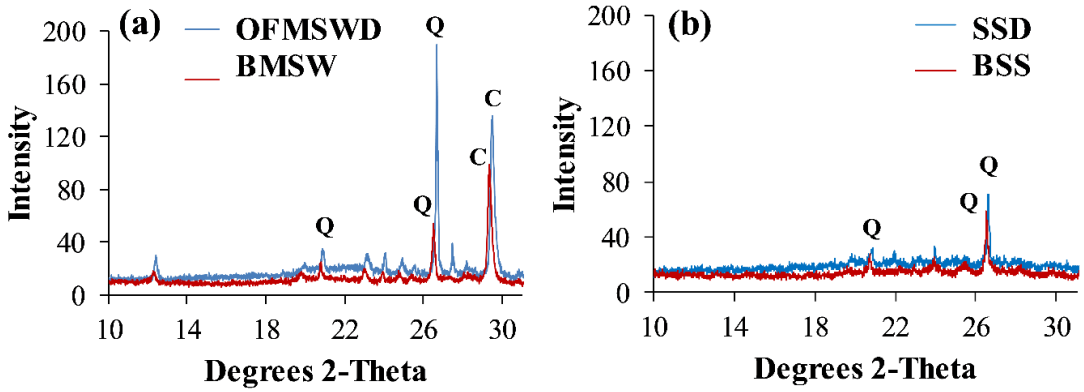

Figure 5.1: XRD spectra of the organic fraction of municipal solid waste digestate (OFMSWD) and its derived biochar produced at 400 °C (BMSW) (a) and sewage sludge digestate (SSD) and its derived biochar produced at 350 °C(BSS) (b) (Q and C refer to quartz (SiO_2) and calcite ($CaCO_3$), respectively).

Figures 5.2(a) and 5.2(b) illustrate, respectively, the changes of FTIR spectra of the OFMSWD and its derived biochar (BMSW), and the SSD and its biochar (BMSW) obtained before and after pyrolysis. From Figure 5.2(a) and 5(b), the FTIR spectra showed that both the OFMSWD and SSD contained the absorbance peaks of hydroxyl (–OH) groups (3425 cm^{-1}), $–CH_3$ stretching of aliphatic groups (2924 cm^{-1}), and C–C skeleton and C–O stretching (1033 cm^{-1}). Similar surface functional groups were also detected on their derived biochars. Nevertheless, a strong intensity of $–CH_2$ scissoring (1427 cm^{-1}) was only found in the OFMSWD and its biochar (BMSW), whereas C=C stretching vibrations (1600 cm^{-1}) was only detected in the SSD and BSS. Such surface groups presented on the biochars can take part in the sorption interaction for metal(loid)s (Chen et al., 2011; Pituello et al., 2014). Results from FTIR spectra indicated that the pyrolysis only induced small variations between the digestates and biochars, particularly at temperature below 400 °C. The results also demonstrated the differences in surface functional groups between BMSW and BSS corresponding to different feedstock type and pyrolysis temperature.

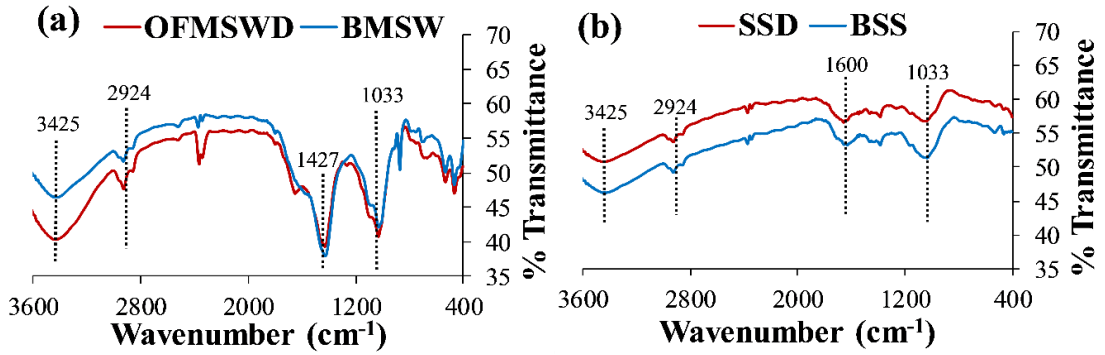

Figure 5.2: FTIR spectra of the organic fraction of municipal solid waste digestate (OFMSWD) and its derived biochar produced at 400 °C (BMSW) (a) and sewage sludge digestate (SSD) and its derived biochar produced at 350 °C(BSS) (b).

5.1.2 Influence of chemical treatment on biochar properties

To understand the effect of chemical treatment on biochar properties, the sewage sludge digestate-derived biochar (BSS) was selected to study its physicochemical properties before and after chemical treatment. Table 5.2 shows the corresponding properties of the raw BSS and its chemically-modified biochars.

Table 5.2: Chemical and physical properties of sewage sludge digestate-derived biochar and its chemically-modified biochars (Papers I, II and III).

Biochar	Total As (µmol g^{-1})	pH in water	pH_{pzc}	ZP[a] at pH 5 (mV)	Electrical conductivity (µS cm^{-1})	S_{BET}[b] (m^2 g^{-1})	CEC[c] ($cmol^+$ kg^{-1})
BSS	0.63 ± 0.02	6.4 ± 0.1	2.7	-9.8	4.0 ± 0.1	0.4 ± 0.1	2.0 ± 0.1
BSS-H_2O_2	0.39 ± 0.02	6.5 ± 0.1	2.9	-16.5	4.1 ± 0.3	5.7 ± 0.1	2.9 ± 0.1
BSS-KOH	0.17 ± 0.02	8.4 ± 0.1	3.4	-8.1	6.2 ± 0.5	7.9 ± 0.1	13.4 ± 0.1
BSS-KOH[bat]	0.31 ± 0.03	10.0 ± 0.1	2.9	-17.1	324.0 ± 2.4	3.0 ± 0.1	20.8 ± 0.1

[a] ZP refers to zeta potential.

[b] S_{BET} refers to Brunauer-Emmett-Teller surface area of biochar.

[c] CEC refers to cation exchange capacity of biochar.

Note: all values reported are mean of triplicate followed by standard deviation, except pH_{PZC} and zeta potential.

Chemical treatment had an effect on the pH changes of the biochars. Similar pH values were found for both the BSS (6.4 ± 0.1) and its H_2O_2-modified biochar (6.5 ± 0.1), whereas the value was strongly increased for KOH-modified biochar with batch and

subsequently continuous column washings (8.4 ± 0.1). The increase of pH is likely due to the property of KOH to increase the hydroxyl (–OH) groups as well as the basicity on the modified biochar (Fan et al., 2016; Li et al., 2014).

The electrical conductivities (EC) of the raw and modified biochar suspensions remained in similar ranges, except for KOH-modified biochar with batch washing (BSS-KOH^{bat}). A much higher EC of the BSS-KOH^{bat} among other biochars can be due to the ability of KOH to modify the biochar surface by dissolving inorganic elements/compounds from the biochar (Lin et al., 2012; Liou and Wu, 2009; Liu et al., 2012). Therefore, a release of inorganic ions (*e.g.* phosphate and carbonate) from this KOH-modified biochar contributes to its high EC value (Paper I).

Figure 5.3 shows the evolution of the zeta potential along the pH ranges for raw and modified biochars from SSD. The pH of point of zero charge (pH_{PZC}), determining the pH at which the net charge on the biochar surface is zero, was obtained from this curve. The corresponding values of the zeta potential at pH 5 and pH_{PZC} are presented in Table 5.2. Results showed similar pH_{PZC} values for both BSS (~2.7) and BSS-H_2O_2 (~2.9), whereas a slightly higher pH_{PZC} was observed for BSS-KOH (~3.4). Nevertheless, due to small variations of pH_{PZC} (2.7–3.4) among all biochars, they are not prone to strongly modify the pH on the sorption for metal(loid)s, except if the experiments are performed at pH below 5. From the literature, the pH_{PZC} of biochar has been rarely reported and the information on the variability of biochar with different chemical treatments is limited. However, our pH_{PZC} results are in consistent with biochars from a straw residue (~1.9) (Qiu et al., 2009) and paper mill sludges (4.0–6.0) (Guo et al., 2018). In addition, the negative values of zeta potential at pH 5 (Table 5.2) indicated that the raw and modified biochars were net negatively charged, for instance -16.5 mV and -17.1 mV for the BSS-H_2O_2 and BSS-KOH^{bat}, respectively.

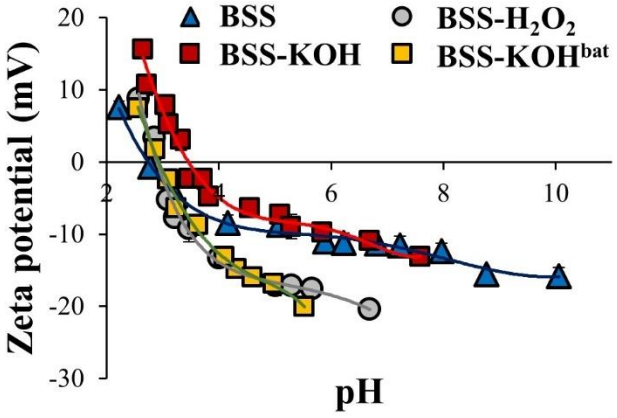

Figure 5.3: Evolution of the zeta potential as a function of the pH values.

The cation exchange capacity (CEC) of all biochars are given in Table 5.2. Results showed a slight increase of CEC after H_2O_2 treatment of biochar, *i.e.* from 1.9 (± 0.1) $cmol^+ kg^{-1}$ (BSS) to 2.9 (± 0.1) $cmol^+ kg^{-1}$ (BSS-H_2O_2), whereas a 6-fold increase of CEC was observed on the BSS-KOH. A significantly higher CEC in the KOH-modified biochar may result from the chemical property of KOH to modify the surface of biochar, as previously discussed. Therefore, more possibility of exchangeable cations (*e.g.* Na^+, K^+, Mg^{2+} and Ca^{2+}) associated on the biochar to exchange with metal elements like Pb(II) and Cd(II). However, the CEC values found (Table 5.2) were still far lower than those reported for wood biochar (45.7 $cmol^+ kg^{-1}$) and straw-derived biochar (483.4 $cmol^+ kg^{-1}$) (Ding et al., 2016; Jiang et al., 2014).

The S_{BET} of all biochars were also improved (7–20 times) after the chemical treatments, *e.g.* from 0.4 (± 0.1) $m^2 g^{-1}$ for raw biochar to 5.7 (± 0.1) $m^2 g^{-1}$ for BSS-H_2O_2 and 7.9 (± 0.1) $m^2 g^{-1}$ for BSS-KOH (Table 5.2). The increase of S_{BET} implies that H_2O_2 and KOH induced higher porosities on the modified biochars. Our results are consistent with those reported for sewage sludge biochars (4.0–14.3 $m^2 g^{-1}$) (Agrafioti et al., 2013; Yuan et al., 2015) and pineapple-peel-derived biochars (0.7–2.1 $m^2 g^{-1}$) (Wang et al., 2016). However, our S_{BET} values are still far lower than those reported for activated carbons (1215.0–1316.0 $m^2 g^{-1}$) (Gong et al., 2015).

The total As content in raw and chemically-modified SSD biochars was analyzed and the values are reported in Table 5.2. Significant decreases of the As content were found after treating the raw biochar with KOH or H_2O_2, for example from 0.63 (± 0.02) µmol g^{-1} for BSS to 0.39 (± 0.02) µmol g^{-1} for BSS-H_2O_2 and 0.17 (± 0.02) µmol g^{-1} for BSS-

KOH (Paper III). The reduction of As in the modified biochars can be due to the ability of KOH and H_2O_2 to modify the solid phase of the raw biochar. As a result, As could be released from biochar matrix during the chemical treatments.

In summary, the increase of CEC and S_{BET} values after biochar treatments highlights that the chemically-modified biochars, particularly with KOH provided higher exchangeable cations and active pore sites on their surfaces. Therefore, the sorption of metals such as Pb(II) and Cd(II) may be enhanced by the modified biochar (*e.g. via* complexation) (Mohan et al., 2014) (Paper II). The global negative charge of biochars (from zeta potential) also indicate a better potential for modified biochars to sorb cationic metal ions but this may hinder the sorption ability for oxyanions such as As. In the case of BSS-KOH, the higher values of zeta potential (*i.e.* the lower negative charge) may allow a better sorption capacity towards As compared to other biochars.

5.1.3 Effect of biochar washing after chemical treatment

As discussed in chapter 4 (section 4.1.2), the SSD biochars were washed with ultrapure water in two approaches: (1) a triple batch washing in a row until the pH became stable and (2) the same batch washing followed by continuous column washing. During the column washing, the pH, EC, PO_4^{3-}, HCO_3^-/CO_3^{2-} and DOC were measured over time until completion to ensure the elimination of all these releasable compounds (Paper I).

Figures 5.4(a) and 5.4(b) represent the evolutions of pH and EC over time during a continuous column washing of BSS-KOH^{bat} and BSS-$H_2O_2^{bat}$, respectively. The pH values of BSS-KOH^{bat} decreased steadily after 23 h of washing and became stable at pH 8.4 (± 0.1) after 64 h whereas for the H_2O_2-modifed biochar, it remained almost stable at 6.5 (± 0.1). Similarly, dramatic decreases of EC occurred throughout the manipulations on both modified biochars, which is consistent with the decreasing trends of the PO_4^{3-}, HCO_3^-/CO_3^{2-} and DOC (Figure 5.4(c-d)).

Figures 5.4(c) and 5.4(d) show the release of PO_4^{3-}, HCO_3^-, CO_3^{2-} and DOC from the BSS-KOH^{bat} and BSS-$H_2O_2^{bat}$, respectively, over time during column washing. The concentrations of PO_4^{3-}, CO_3^{2-}, HCO_3^- and DOC continuously decreased along the washing time (Figure 5.4(c, d)). These reductions are in correlation to the decline of conductivity (Figure 5.4(a, b)). For example, the high concentrations of PO_4^{3-} (55 mg L^{-1}), CO_3^{2-} (99 mg L^{-1}) and HCO_3^- (1418 mg L^{-1}) released from KOH-modified biochar were related to the high conductivity (391 µS cm^{-1}) at the initial washing period (Figure 5.4(a, c)). The released compounds were continuously declined along the lower

conductivities, indicating that these two profiles were correlated (Figure 5.4(a, c)). The similar trends were also observed for the BSS-$H_2O_2^{bat}$; however, with much lower concentrations of the PO_4^{3-}, CO_3^{2-}, HCO_3^- and DOC (Figure 5.4(b, d)).

Comparison between KOH and H_2O_2 treatments, the biochar washings demonstrated that the KOH-modified biochar released much higher DOC, PO_4^{3-} and HCO_3^-/CO_3^{2-} than the H_2O_2 biochar. This is according to different abilities of KOH and H_2O_2 to modify the solid phase of biochar (Paper I). In addition, the column washing was considered complete when stable pH values, similar EC of inlet/outlet solutions (*i.e.* 3–6 µS cm^{-1}) and low concentrations (<1 mg L^{-1}) of PO_4^{3-}, HCO_3^-/CO_3^{2-} and DOC were observed, *i.e.* beyond 72 h for the KOH-modified SSD biochar (BSS-KOH^{bat}) and 22 h for the H_2O_2-modified biochar (BSS-$H_2O_2^{bat}$).

From the previously published data (Huang et al., 2017; Regmi et al., 2012; Wu et al., 2017), pH stabilization was normally used as a key parameter for biochar batch washing. However, our findings highlight that it was not sufficient to eliminate the dissolved organic matter and releasable ions from biochar (Paper I). A direct control of the release of PO_4^{3-} and HCO_3^-/CO_3^{2-} from the biochar is of importance because these releasable ions can hinder the sorption for metal(loid)s onto the biochars. Therefore, the conductivity is proposed as a more accurate indicator rather than the pH (Paper I). The continuous washing of biochars and the conductivity monitoring were further applied in Papers II and III.

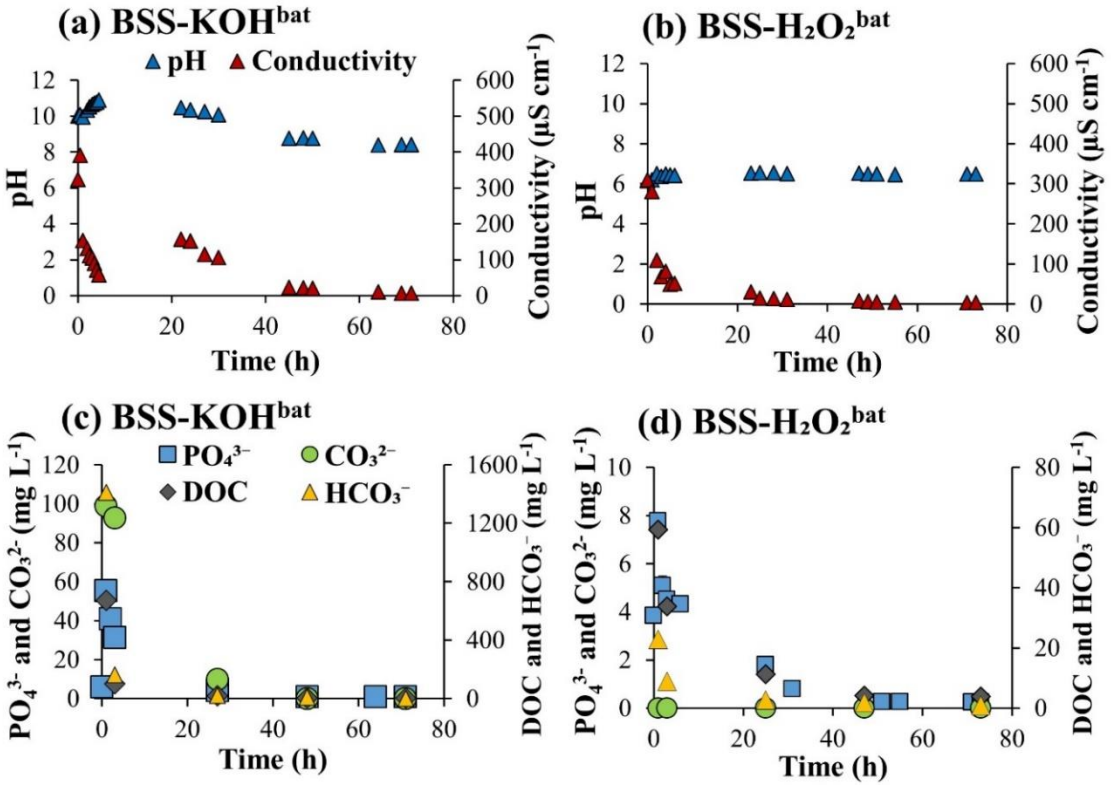

Figure 5.4: Evolution of pH and conductivity during continuous washing of BSS-KOH^{bat} (a) and BSS-H_2O_2^{bat} (b), and concentration profile of released phosphate, (bi)carbonate and dissolved organic carbon (DOC) for BSS-KOH^{bat} (c) and BSS-H_2O_2^{bat} (d) (Paper I).

Due to the potential release of organic and inorganic elements/compounds from the KOH-modified biochars, they were further selected to study the influence of biochar washing procedures on the physicochemical properties of biochars (Paper II). The observations on the changes between the observed biochar properties in previous subchapters (5.1.1 and 5.1.2) and the ones found during biochar washing procedures were parallelly established.

The pH, EC, S_{BET} and CEC, total As content of the KOH-modified biochars with batch and continuous washings are given in Table 5.2. The results showed that the uncomplete batch washing after biochar treatment influenced the change of biochar properties. The pH of KOH biochar was decreased after a subsequent column washing, *i.e.* from 10.0 (± 0.1) for BSS-KOH^{bat} to 8.4 (± 0.1) for BSS-KOH. This is consistent with a dramatic decrease of EC value by 50-time in the BSS-KOH (6.2 ± 0.5 µS cm^{-1}), compared to the BSS-KOH^{bat} (324 ± 2 µS cm^{-1}) (Table 5.2). These differences are likely due to the releasable ions (*e.g.* PO_4^{3-}, HCO_3^-/CO_3^{2-}, Ca^{2+} and Mg^{2+}) from the BSS-KOH^{bat} that significantly altered both the pH and EC values (Papers I and II). These

findings are also supported by Yuan et al. (2015), as the authors reported a high EC value (7750 µS cm^{-1}) in the sewage sludge biochar with no washing with ultrapure water after pyrolysis.

A decrease of CEC was observed for the BSS-KOH, compared to the BSS-KOH^{bat}, *i.e.* from 20.8 (± 0.1) $cmol^{+}$ kg^{-1} (BSS-KOH^{bat}) to 13.4 (± 0.1) $cmol^{+}$ kg^{-1} (BSS-KOH). Similarly, the total As were also reduced after the KOH biochar was subsequently washed in a column reactor. In this case, from 0.31 (± 0.03) µmol g^{-1} (BSS-KOH^{bat}) to 0.17 (± 0.02) µmol g^{-1} (BSS-KOH). However, a higher S_{BET} was found on the BSS-KOH compared to BSS-KOH^{bat} (Table 5.2). The reduction of CEC and total As content but increase in S_{BET} could be explained by the elimination of releasable compounds (*e.g.* DOC, PO_4^{3-} and HCO_3^{-}/CO_3^{2-}) from the biochars. Hence, lower risk of As toxicity and more available active pore sites, while lower exchangeable cations on the BSS-KOH.

These findings highlight that the pH, EC, S_{BET}, CEC, and total As content were strongly influenced by the biochar washing procedure. Therefore, the careful washing procedure after biochar chemical treatment is recommended to avoid interferences during sorption for metal(loid)s.

5.2 Sorption kinetics for Pb(II), Cd(II) and As(III, V) by biochars

The study on sorption is highly important to provide insights regarding the sorption reactions and the sorption mechanisms. It also helps to predict the rate for metal(loid) removal from aqueous solutions and the sorption capacity of a sorbent (*e.g.* biochar) towards metal(loid) elements. In this study, the sorption experiments were performed to determine the influence of chemical treatments and biochar washing procedures on the sorption capacities of biochars for Pb(II), Cd(II) and As(III, V) (Papers I and II). The sorption kinetics were firstly conducted to obtain the time required for Pb(II), Cd(II) and As(III, V) to reach equilibrium state. After that, the sorption isotherms were performed to predict the maximum sorption capacity of biochar for each metal(loid) element. The link between the biochar properties and the sorption ability of biochar towards Pb(II), Cd(II) and As(III, V) are discussed in detail in the following subsections.

5.2.1 Effect of chemical treatments of biochars on Pb(II), Cd(II) and As(V)

Figure 5.5 shows the influence of contact time on the Pb(II) sorption by raw biochars (*i.e.* $BMSW^{bat}$ and BSS^{bat}) from the organic fraction of municipal solid waste digestate (OFMSWD) and sewage sludge digestate (SSD) and their H_2O_2 or KOH modified

biochars (BMSW-$H_2O_2^{bat}$, BMSW-KOH^{bat}, BSS-$H_2O_2^{bat}$ and BSS-KOH^{bat}) submitted to batch washing. The pseudo-first-order (PFO) and pseudo-second-order (PSO) kinetic models were used to describe the kinetic data for Pb(II) (Paper I). Table 5.3 shows the corresponding parameters obtained from fittings of the PFO and PSO models with the Pb(II) kinetic data by raw and chemically-modified biochars. The constants obtained (Table 5.3) show that the Pb(II) sorption kinetics were strongly fitted to the PSO model with high coefficients of correlation (R^2>0.99) for all the raw and modified biochars. This suggests that simple chemical reactions between Pb(II) and biochars were literally taken place (Nethaji et al., 2013). Due to the best-fit of the Pb(II) kinetic data to the PSO model, the intraparticle diffusion kinetic model does not apply for Pb(II).

$BMSW^{bat}$ and BSS^{bat} showed different Pb(II) sorption kinetics as the sorption equilibrium was achieved within 2 h for the $BMSW^{bat}$, while it was beyond 5 h for the BSS^{bat} (Figure 5.5). In addition, a rapid Pb(II) sorption at initial state followed by a slow reaction until reaching an equilibrium were observed on the $BMSW^{bat}$, while a slower Pb(II) sorption reaction throughout the kinetic time was found on the BSS^{bat} (Figure 5.5). These different behaviors were due to variations of biochar properties among different origins of digestate feedstocks. A stronger intensity of O–containing functional groups (1033 cm^{-1}) in the OFMSWD than SSD was observed (Figure 5.2). Such property could promote a faster Pb(II) kinetic removal rate due to more possibility of Pb ions to bind onto the O-containing functional groups of biochar (Bogusz et al., 2017). Furthermore, a much higher cationic element content such as Ca, K, Mg and Na were found on the $BMSW^{bat}$, compared to the BSS^{bat} (Table 5.1). This could induce the cation exchange interaction with Pb(II) and thus enhancing the sorption ability onto the $BMSW^{bat}$ (Paper I). These results are in agreement with a previous study of Zhang et al. (2017) on the use of celery biochars with high alkaline mineral contents to remove metals from water.

Considering the effect of biochar chemical treatments with KOH or H_2O_2, the kinetic rates for Pb(II) sorption were different on the chemically-modified biochars (Paper I). Results showed that the KOH induced faster Pb(II) sorption kinetic rates by both BSS-KOH^{bat} and BMSW-KOH^{bat} compared to their raw biochars (Figure 5.5). In this case, the equilibrium times for the KOH-modified biochars were achieved within 2 h. Similarly, a previous study from Regmi et al. (2012) showed an enhanced kinetic removal rate for metal by a switchgrass biochar with the KOH treatment. Nevertheless, the biochar treated with H_2O_2 may induce or hinder the Pb(II) sorption kinetics, depending on the biochar feedstock types. For instance, an equilibrium time for Pb(II) removal rate was slower on the BSS-$H_2O_2^{bat}$ (beyond 7 h) than on the BSS^{bat} (5 h). However, an improved equilibrium time for Pb(II) was observed on the BMSW-$H_2O_2^{bat}$ (within 1 h) compared to its raw biochar (2 h) (Figure 5.5). In addition, the BMSW-$H_2O_2^{bat}$ showed the highest

PSO sorption kinetic rate (k_2) among all biochars (Table 5.3). This suggests that Pb^{2+} ions strongly interact with external surface sites of the biochar and consequently forming the outer-sphere complexes of Pb(II) onto its surface (Wang et al., 2015a).

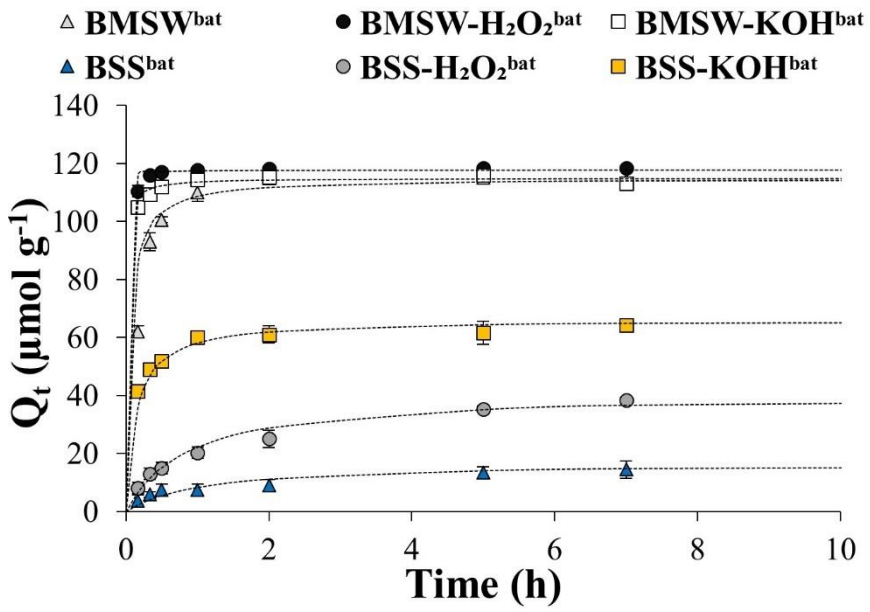

Figure 5.5: Adsorption kinetics for Pb(II) by $BMSW^{bat}$, $BMSW\text{-}H_2O_2{}^{bat}$, $BMSW\text{-}KOH^{bat}$, BSS^{bat}, $BSS\text{-}H_2O_2{}^{bat}$ and $BSS\text{-}KOH^{bat}$ at different contact times fitted with the pseudo-second-order kinetic model (initial pH=5, initial concentration: 482.6 µmol L^{-1} (100 mg L^{-1})) (Paper I).

Table 5.3: Constants for the pseudo-first-order (PFO) and pseudo-second-order (PSO) kinetic model fittings for Pb(II) sorption by different types of biochars (Paper I).

Biochar	**Pb(II)**						
		PFO			PSO		
	$Q_{e,exp}$[a] (µmol g^{-1})	Q_e (µmol g^{-1})	k_1 (h^{-1})	R^2	Q_e (µmol g^{-1})	k_2 (g(µmol h)$^{-1}$)	R^2
BSS^{bat}	16.4	16.4	0.500	0.327	16.7	0.080	0.996
$BSS\text{-}H_2O_2{}^{bat}$	39.6	39.6	0.581	0.786	41.1	0.029	0.999
$BSS\text{-}KOH^{bat}$	66.2	66.1	1.764	na[b]	66.6	0.073	0.999
$BMSW^{bat}$	114.5	114.7	4.443	0.980	116.2	0.027	0.999
$BMSW\text{-}H_2O_2{}^{bat}$	118.2	118.4	10.177	0.856	119.0	0.047	1.000
$BMSW\text{-}KOH^{bat}$	114.9	116.0	7.766	0.780	116.2	0.046	1.000

[a] $Q_{e,exp}$ and Q_e refer to equilibrium adsorption capacity obtained from the experiments and from model fittings, respectively.

[b] na refers to not available due to no satisfactory fit by the model.

$BMSW^{bat}$, $BMSW\text{-}H_2O_2{}^{bat}$ and $BMSW\text{-}KOH^{bat}$ refer to raw biochar from the organic fraction of municipal solid waste digestate, and its H_2O_2 and KOH modified biochars with batch washing, respectively. BSS^{bat}, $BSS\text{-}H_2O_2{}^{bat}$ and $BSS\text{-}KOH^{bat}$ refer to raw biochar from sewage sludge digestate, and its H_2O_2 and KOH modified biochars with batch washing, respectively.

The improvement of equilibrium time on the chemically-modified biochars was directly linked to the alteration of biochar properties after the chemical treatment. Due to the ability of chemical reagents, particularly KOH, to modify the biochar properties such as increase/decrease pH on the biochar surface, dissolve inorganic compounds and condense organic matter from the biochar (Fan et al., 2016; Li et al., 2014). Consequently, this could promote the faster Pb(II) kinetic removal rates on the chemically-modified biochars. Nevertheless, the source of feedstocks should also be considered since this study found a slightly slower Pb(II) sorption rate on the H_2O_2-modified biochar from SSD, compared to its raw SSD biochar.

Due to a potential release of organic/inorganic compounds from biochars observed in section 5.1.3, the batch and subsequent continuous washings were further applied to raw SSD biochar and its chemically-modified biochars. These manipulations were performed to eliminate the released compounds from the biochars in order to provide suitable biochars for Cd(II) and As(III, V) removal from aqueous solutions (Paper II). The batch and subsequent column washings of the raw SSD biochar and its H_2O_2 and KOH modified biochars are noted as BSS, BSS-H_2O_2 and BSS-KOH, respectively.

Similar to Pb(II), the PFO and PSO kinetic models were used to stimulate the experimental data for Cd(II) and As(III, V) by all biochars (Paper II). The intraparticle diffusion kinetic model was additionally applied for the Cd(II) and As(III, V) in order to obtain more information on the sorption mechanisms (Zhao et al., 2015). Figure 5.6 shows the Cd(II) sorption by BSS, BSS-H_2O_2 and BSS-KOH as a function of contact time with the PSO kinetic model-fittings. All the corresponding kinetic constants of the PFO, PSO and intraparticle diffusion kinetic models are given in Table 5.4.

Results showed that the experimental data for Cd(II) sorption was best described by the PSO model (Paper II). Similar to Pb(II), faster PSO kinetic rates for the Cd(II) sorption were found on both the KOH and H_2O_2 modified biochars, compared to its raw biochar (BSS) (Figure 5.6). For instance, the BSS reached equilibrium after 10 h, while less than 5 h for the chemically-modified biochars (Figure 5.6). The enhancement of the Cd(II) sorption kinetic rates onto the chemically-modified biochars is likely due to the ability of chemicals (such as KOH or H_2O_2) to modify the biochar properties as previously discussed in a subparagraph for Pb(II) sorption kinetics. In addition, based on the intraparticle diffusion model-fitting parameters in Table 5.4, the *C* constants are not equal to zero, literally suggesting that there were some degrees of boundary layer and the rate limiting step was not only controlled by the intraparticle diffusion. Other mechanisms such as film diffusion and external mass transfer may take part in the sorption processes (Nethaji et al., 2013). In addition, the sorption kinetics for metals

can be controlled by the particle sizes of biochars, and thus the kinetics may be limited by the diffusion of metals in the biochars (Rees et al., 2013).

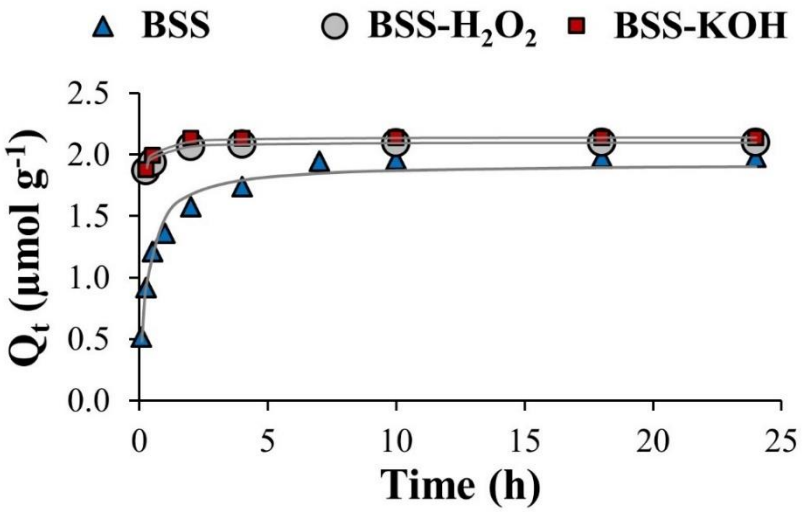

Figure 5.6: Effect of chemical treatment on sorption kinetics for Cd(II) by the raw and chemically-modified sewage sludge biochars fitted with the pseudo-second-order kinetic model (initial pH=5, initial concentration: 10 µmol L^{-1}) (Paper II).

Table 5.4: Constants for the pseudo-first-order (PFO), pseudo-second-order (PSO) and intraparticle diffusion kinetic models of Cd(II) sorption by raw biochar from sewage sludge digestate and its chemically-modified biochars (Paper II).

Biochar	Cd(II)								
	PFO			PSO			Intraparticle diffusion		
	k_1 (h^{-1})	Q_e (µmol g^{-1})	R^2	k_2 (g(µmol $h)^{-1}$)	Q_e (µmol g^{-1})	R^2	k_i (µmol (g $h^{1/2})^{-1}$)	C	R^2
BSS	0.184	0.94	0.923	1.724 ± 0.204	1.93 ± 0.04	0.983	0.269 ± 0.039	0.956 ± 0.101	0.852
BSS-H_2O_2	0.400	0.14	0.881	12.251 ± 0.803	2.09 ± 0.01	0.985	0.042 ± 0.010	1.932 ± 0.029	0.787
BSS-KOH	1.217	0.19	0.763	12.907 ± 0.479	2.14 ± 0.01	0.993	0.041 ± 0.013	1.973 ± 0.036	0.699

BSS, BSS-H_2O_2 and BSS-KOH refer to raw biochar from sewage sludge digestate, and its H_2O_2 and KOH modified biochars with batch and subsequent column washings.
All sorption kinetic constants and uncertainties for Cd(II) were obtained by non-linear regression using Statistica software (v6.1, StatSoft).

Apart from metals like Pb(II) and Cd(II), the effect of biochar chemical treatment on the sorption kinetics for metalloids such as arsenic (As) was further studied. This

manipulation was performed to observe if the chemical treatment of biochar induces similar sorption behaviors for As, compared to those for Pb(II) and Cd(II).

Figure 5.7 shows the influence of chemical treatment on the sorption kinetics for As(V) by the raw, H_2O_2 and KOH modified biochars submitted to batch and subsequent column washings (*i.e.* BSS, BSS-H_2O_2 and BSS-KOH, respectively). No data on As(III) sorption was shown due to a very low or absence of sorption by the BSS and BSS-H_2O_2. The PFO, PSO and intraparticle diffusion models were used to describe the experimental data and the corresponding values are reported in Table 5.5.

Comparison of the raw and modified biochars showed that the As(V) sorption kinetic rates (k_2) of the BSS (0.630 ± 0.098) and BSS-H_2O_2 (0.619 ± 0.092) were similar (Table 5.5), reaching the equilibrium time after 10 h (Figure 5.7). However, unlike the Pb(II) and Cd(II), a much slower kinetic rate for As(V) sorption by the KOH modified biochar (BSS-KOH) than by the raw biochar was observed with the equilibrium time being reached beyond 24 h (Figure 5.7). Nevertheless, Wang et al. (2015a) also showed the slower As(V) sorption kinetic rate by biochar with chemical treatment, compared to its raw pine wood biochar. The slow rate for As(V) sorption by the KOH biochar could be due to the formation of inner layer complexes *via* surface complexation between the hydroxyl groups on the biochar surface and the arsenic species (Velazquez-Peña et al., 2019). This statement was also supported by previous studies (Catalano et al., 2008; Wang et al., 2015b).

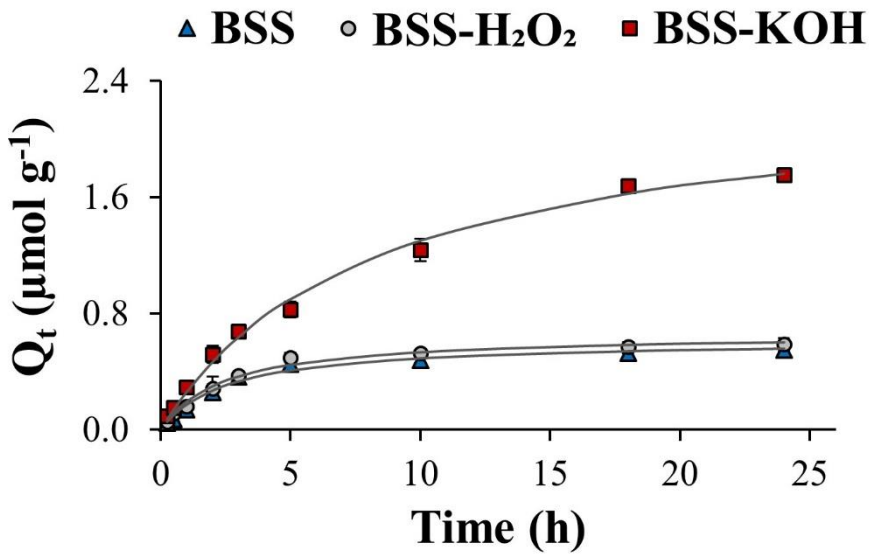

Figure 5.7: Effect of chemical treatment on sorption kinetics for As(V) by the raw and chemically-modified sewage sludge biochars fitted with the pseudo-second-order kinetic model (initial pH=5, initial concentration: 10 µmol L^{-1}) (Paper II).

Table 5.5: Constants for the pseudo-first-order (PFO), pseudo-second-order (PSO) and intraparticle diffusion kinetic models of As(V) sorption by raw biochar from sewage sludge digestate and its chemically-modified biochars (Paper II).

Biochar	As(V)								
	PFO			PSO			Intraparticle diffusion		
	k_1 (h^{-1})	Q_e (µmol g^{-1})	R^2	k_2 (g(µmol $h)^{-1}$)	Q_e (µmol g^{-1})	R^2	k_i (µmol (g $h^{1/2})^{-1}$)	C	R^2
BSS	0.167	0.40	0.918	0.630 ± 0.098	0.62 ± 0.03	0.985	0.115 ± 0.013	0.065 ± 0.035	0.910
BSS-H_2O_2	0.188	0.44	0.948	0.619 ± 0.092	0.66 ± 0.03	0.985	0.121 ± 0.014	0.083 ± 0.036	0.913
BSS-KOH	0.165	1.84	0.969	0.052 ± 0.006	2.35 ± 0.09	0.995	0.396 ± 0.012	-0.074 ± 0.030	0.993

BSS, BSS-H_2O_2 and BSS-KOH refer to raw biochar from sewage sludge digestate, and its H_2O_2 and KOH modified biochars with batch and subsequent column washings, respectively.
All sorption kinetic constants and uncertainties for As(V) were obtained by non-linear regression using Statistica software (v6.1, StatSoft).

In summary, the sorption kinetics for Pb(II), Cd(II) and As(V) onto all biochars exhibited the best-fit by the PSO model (Papers I and II), theoretically suggesting that the sorption between these metal(loid)s and biochars mainly occurred *via* simple chemical reactions (Nethaji et al., 2013). Moreover, the BSS-KOH showed the fastest kinetic rate for Pb(II) and Cd(II) sorption among other biochars, while the slowest rate was observed for As(V) sorption. This slower rate of the As(V) sorption onto the BSS-KOH could be described by its high k_i rate constant (Table 5.5), suggesting that the intraparticle diffusion mainly involved in the sorption mechanism of As(V). These findings also indicate that the KOH biochars only accelerated the sorption kinetics for metals, while more time was required for As(V) to reach the equilibrium state by this biochar.

5.2.2 Effect of biochar washings on Cd(II) and As(III, V)

Due to the chemical treatment of biochar, particularly with KOH, that induced a strong release of organic and inorganic compounds from the biochar into solutions (see section 5.1.3), it was therefore decided to focus on the effect of biochar washing procedures after KOH treatment on the sorption for metal(loid) elements. To observe if the biochar washing procedures affect the metal(loid)s sorption, the KOH-modified biochar from SSD with batch washing was additionally submitted to a continuous column washing (see section 4.1.2). After these manipulations, the KOH-modified biochars with a batch washing (*i.e.* BSS-KOH^{bat}) versus batch and subsequent column

washings (*i.e.* BSS-KOH) were further compared on the sorption for Cd(II) and As(III, V) (Paper II).

Figures 5.8(a), 5.8(b) and 5.8(c) compare the effect of biochar washing procedures (*i.e.* batch versus batch and subsequent column washings) after KOH treatment for Cd(II), As(III) and As(V) sorption kinetics, respectively. The model-fitting constants are also given in Table 5.6. The PSO kinetic model showed the best-fit to explain the experimental data for Cd(II), As(III) and As(V) sorption by all the KOH modified biochars from SSD (R^2>0.96) (Table 5.6).

From Figures 5.8(a) and 5.8(b), the sorption kinetic rates for Cd(II) and As(III) were insignificantly affected by the washing steps after the KOH treatment. In comparison with the batch washed BSS-KOH^{bat}, the batch and additional column washed BSS-KOH showed a faster kinetic rate for Cd(II), with the PSO rate constant (k_2) of 12.907 (± 0.479) g(µmol h)$^{-1}$, compared to 6.298 (± 0.338) g(µmol h)$^{-1}$ for the BSS-KOH^{bat} (Table 5.6, Paper II). A similar observation was found for As(III), but with a slight increase of the k_2 values, *i.e.* from 0.205 (± 0.042) g(µmol h)$^{-1}$ to 0.378 (± 0.067) g(µmol h)$^{-1}$ with the addition of continuous column washing (Table 5.6, Paper II). The enhanced sorption kinetic rates for Cd(II) and As(III) can be linked to the increment of surface area of the KOH biochar with additional column washing. In this case, the surface area was increased from 3.0 (± 0.1) m^2 g^{-1} for the BSS-KOH^{bat} to 7.9 (± 0.1) m^2 g^{-1} for the BSS-KOH (Table 5.2). The higher surface pore sites on the biochar can induce more sorption for Cd(II) and As(III) (Bogusz et al., 2017; Wu et al., 2017), and thus improving the kinetic reaction rates.

In contrast, a significant alteration of the sorption kinetics for As(V) was observed on the KOH modified biochars with different biochar washing steps (Figure 5.8(c)). Compared to the BSS-KOH^{bat}, the sorption kinetics for As(V) were much slower on the BSS-KOH with a 3-time decrease of the k_2 value (Figure 5.8(c) and Table 5.6). This is probably due to the sorption conditions at initial pH 5.0 as As(III) remains in neutral form whereas As(V) is anionic. As a result, a significantly higher variation of As(V) sorption kinetics by the KOH biochars was found, compared to the As(III). This is likely due to the competition between the release of DOC and PO_4^{3-} from the BSS-KOH^{bat} (section 5.1.3) and the As(V) oxyanion, while no interference of such releasable compounds from the BSS-KOH.

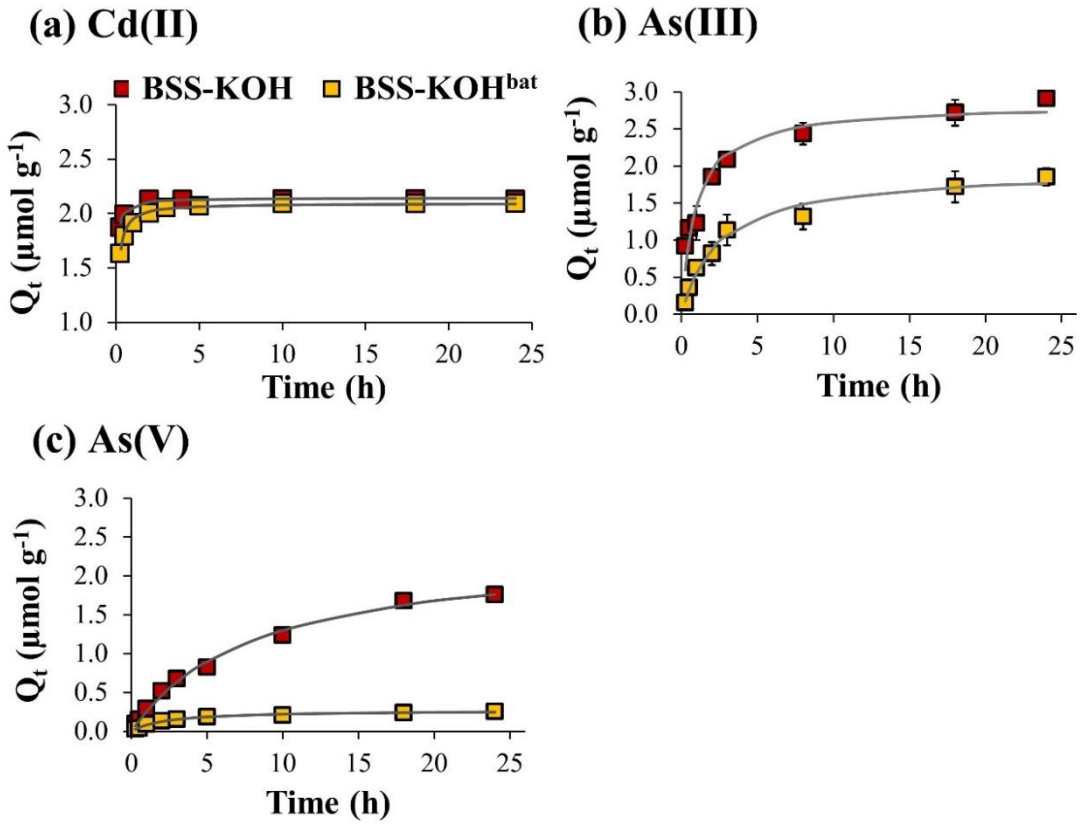

Figure 5.8: Influence of biochar washing of KOH-modified biochars on sorption kinetics for Cd(II) (a), As(III) (b) and As(V) (c) fitted with the pseudo-second-order kinetic model (initial pH=5, initial concentration: 10 µmol L^{-1}) (Paper II).

Table 5.6: Constants for the pseudo-first-order (PFO), pseudo-second-order (PSO) and intraparticle diffusion kinetic models of Cd(II), As(III) and As(V) sorption by KOH-modified biochars from sewage sludge digestate with different biochar washing procedures (Paper II).

Biochar	**Cd(II)**								
	PFO			PSO			Intraparticle diffusion		
	k_1 (h^{-1})	Q_e (µmol g^{-1})	R^2	k_2 (g(µmol $h)^{-1}$)	Q_e (µmol g^{-1})	R^2	k_i ((µmol (g $h^{1/2})^{-1}$)	C	R^2
BSS-KOH^{bat}	0.652	0.38	0.942	6.298 ± 0.338	2.09 ± 0.10	0.987	0.077 ± 0.018	1.799 ± 0.046	0.749
BSS-KOH	1.217	0.19	0.763	12.907 ± 0.479	2.14 ± 0.01	0.993	0.041 ± 0.013	1.973 ± 0.036	0.699
Biochar	**As(III)**								
	PFO			PSO			Intraparticle diffusion		
	k_1 (h^{-1})	Q_e (µmol g^{-1})	R^2	k_2 (g(µmol $h)^{-1}$)	Q_e (µmol g^{-1})	R^2	k_i ((µmol (g $h^{1/2})^{-1}$)	C	R^2
BSS-KOH^{bat}	0.134	1.44	0.967	0.205 ± 0.042	1.94 ± 0.10	0.975	0.358 ± 0.033	0.219 ± 0.086	0.948
BSS-KOH	0.128	1.62	0.934	0.378 ± 0.067	2.83 ± 0.11	0.961	0.429 ± 0.044	0.981 ± 0.113	0.938
Biochar	**As(V)**								
	PFO			PSO			Intraparticle diffusion		
	k_1 (h^{-1})	Q_e (µmol g^{-1})	R^2	k_2 (g(µmol $h)^{-1}$)	Q_e (µmol g^{-1})	R^2	k_i ((µmol (g $h^{1/2})^{-1}$)	C	R^2
BSS-KOH^{bat}	0.139	0.19	0.954	1.599 ± 0.340	0.27 ± 0.02	0.969	0.050 ± 0.006	0.036 ± 0.015	0.919
BSS-KOH	0.165	1.84	0.969	0.052 ± 0.006	2.35 ± 0.09	0.995	0.396 ± 0.012	-0.074 ± 0.030	0.993

BSS-KOH^{bat} refers to KOH modified biochar from sewage sludge digestate (SSD) with batch washing.

BSS-KOH refers to KOH modified biochar from SSD with batch and subsequent column washings.

All sorption kinetic constants and uncertainties for Cd(II) and As(V) were obtained by non-linear regression using Statistica software (v6.1, StatSoft).

Furthermore, the different behaviors among two KOH biochars could be linked to the variations of their properties (*e.g.* zeta potential and surface area) before and after subsequent column washing (Table 5.2). Even if both the KOH biochars were net negatively charged on their surfaces at pH 5.0 (*i.e.* initial pH of sorption conditions); however, the BSS-KOH had an improved surface area and a 2-time higher zeta potential (*i.e.* lower negative charges), compared to the BSS-KOH^{bat} (Table 5.2). Such improved properties of the BSS-KOH could induce more As(V) sorption onto this biochar and thus require more time to reach equilibrium state than the BSS-KOH^{bat}. In addition, the kinetic data obtained from model-fittings can be used to explain the different sorption behaviors among the KOH biochars. From Table 5.6, the kinetic data showed that the As(V) sorption by the BSS-KOH was well described by both the PSO and intraparticle diffusion kinetic models (R^2>0.99). This suggests that the intraparticle diffusion and/or chemical sorption could be the rate controlling step for the BSS-KOH. Consequently, the As(V) could transfer through diffusion and sorbed on the pore sites of the BSS-KOH and/or *via* chemical interaction between the functional groups of the BSS-KOH and the As(V) species. However, for the BSS-KOH^{bat}, the PSO model was best fitted to describe the As(V) sorption (R^2>0.96), indicating that chemical interaction between the As(V) species and the BSS-KOH^{bat} was mainly occurred (Table 5.6).

These findings showed that the biochar washing procedures (batch versus batch and subsequent column washings) slightly affected the sorption kinetics for Cd(II) and As(III) by the KOH modified biochars. However, a much slower sorption of As(V) was observed on the KOH biochar with the additional column washing. This could be described by the changes of biochar properties, particularly surface area and zeta potential, before and after the additional column washing step. In addition, this slower rate of the As(V) by the BSS-KOH can be linked to the best-fit of the kinetic data to both the PSO and intraparticle diffusion model. This indicates that not only a simple chemical reaction but also the intraparticle diffusion model were occurred during the As(V) sorption by the BSS-KOH. Nevertheless, the chemical sorption were considered as the main mechanism for Cd(II) and As(III) sorption by the KOH biochars, in line with the PSO model assumption.

5.3 Sorption isotherms for Pb(II), Cd(II) and As(III, V) by biochars

The sorption isotherms for Pb(II), Cd(II) and As(III, V) by the different raw and chemically-modified biochars were studied to investigate the influence of biochar

chemical treatments on the maximum sorption capacity (Q_m) for these elements (Papers I and II). Due to various oxidation states of metalloids such as arsenic, the study on the evaluation of arsenic speciation during sorption experiments was also studied (Paper III).

5.3.1 Effect of chemical treatments of biochars on Pb(II), Cd(II) and As(V)

The sorption isotherms for Pb(II) by raw biochars from SSD and OFMSWD (*i.e.* BSS^{bat} and $BMSW^{bat}$) and their H_2O_2 or KOH modified biochars (with batch washing after chemical treatments) were carried out in batch experiments (Paper I). Due to the potential release of organic/inorganic compounds from biochars after chemical treatments as previously reported in section 5.1.3, all biochars were submitted to batch and subsequent continuous column washings to eliminate the releasable ions. After that, the raw and chemically-modified biochars from SSD (with batch and subsequent column washings) were selected to study the influence of biochar chemical treatments on the Cd(II) and As(V) sorption isotherms (Paper II). The sorption experiments for these metal(loid)s were performed at an initial pH of 5.0 and at equilibrium conditions (agitation at 180 rpm for 24 h). For all the sorption tests, two isotherm models, namely Langmuir and Freundlich, were chosen to stimulate the sorption behavior of each metal(loid) element.

Langmuir model showed the best fit to describe the sorption for Pb(II), Cd(II) and As(V) by all biochars (except the Pb(II) sorption by $BSS\text{-}KOH^{bat}$ due to non-fitting). This literally suggests the possibility of monolayer sorption of metal(loid)s on the homogeneous biochar surface (Zhao et al., 2015b). For this reason, the sorption capacity and sorption affinity of the biochar towards Pb(II), Cd(II) and As(V) were attained by the maximum sorption capacity (Q_m) and Langmuir constant (K_L) obtained from Langmuir isotherms. More information on the sorption isotherms for Pb(II), Cd(II) and As(V) were described in detail in the following subparagraphs.

Figures 5.9(a) and 5.9(b) represent the Pb(II) sorption as a function of equilibrium Pb(II) concentrations by batch washed $BMSW^{bat}$, $BMSW\text{-}H_2O_2{}^{bat}$ and $BMSW\text{-}KOH^{bat}$ (5.9(a)) and by BSS^{bat}, $BSS\text{-}H_2O_2{}^{bat}$ and $BSS\text{-}KOH^{bat}$ (with zooms of C_e at low concentration ranges) (5.9(b)), respectively. The constant parameters of model-fittings for Langmuir and Freundlich isotherms for Pb(II) are reported in Table 5.7.

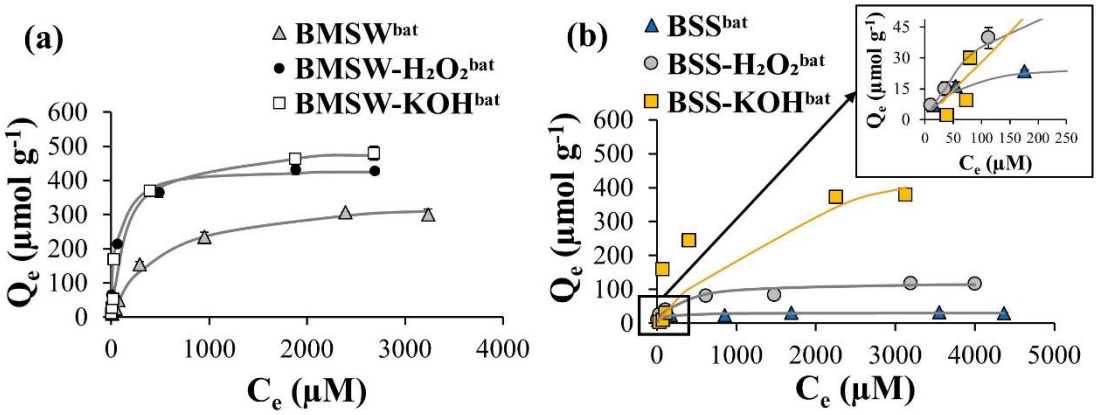

Figure 5.9: Sorption isotherms for Pb(II) by BMSW^{bat}, BMSW-H_2O_2^{bat} and BMSW-KOH^{bat} (a) and by BSS^{bat}, BSS-H_2O_2^{bat} and BSS-KOH^{bat} with zooms of C_e at low concentration ranges (b) as a function of equilibrium Pb(II) concentrations (initial pH=5, 24 h, initial concentration: 0–5000 µM, Langmuir model-fittings except BSS-KOH^{bat} due to non-fitting) (Paper I).

Table 5.7: Constants for Langmuir and Freundlich isotherm model-fittings of Pb(II) sorption by raw and chemically-modified digestate biochars with batch washing (Paper I).

Biochar	Pb(II)					
	Langmuir			Freundlich		
	K_L (L µmol^{-1})	Q_m (µmol g^{-1})	R^2	K_F ((µmol g^{-1})(L µmol^{-1})$^{1/n}$)	n	R^2
BMSW^{bat}	0.002	357.1	0.993	2.557	1.585	0.940
BMSW-H_2O_2^{bat}	0.016	434.7	0.997	25.557	2.555	0.896
BMSW-KOH^{bat}	0.006	500.0	0.998	10.240	1.875	0.860
BSS^{bat}	0.014	31.4	0.994	7.802	5.647	0.782
BSS-H_2O_2^{bat}	0.004	121.9	0.984	5.610	2.623	0.956
BSS-KOH^{bat}	0.001	714.2	0.294	1.991	1.472	0.566

BMSW^{bat}, BMSW-H_2O_2^{bat} and BMSW-KOH^{bat} refer to raw biochar from the OFMSWD, and its H_2O_2 and KOH modified biochars with batch washing, respectively.
BSS^{bat}, BSS-H_2O_2^{bat}, and BSS-KOH^{bat} refer to raw biochar from SSD, and its H_2O_2 and KOH modified biochars with batch washing, respectively.

Comparing the Q_m between raw digestate biochars, an 11-time higher Q_m of BMSW^{bat} than that of BSS^{bat} was reported (Table 5.7). However, the BSS^{bat} had a larger K_L value, compared to BMSW^{bat} (Table 5.7), indicating a higher affinity of the BSS^{bat} towards Pb(II) than the BMSW^{bat}. These findings highlight that the Pb(II) sorption by biochar was significantly affected by the sources of biochar feedstocks. The differences of Pb(II) sorption capacities among the raw biochars can be linked to the biochar physicochemical properties. From Figure 5.2 and Table 5.1, a stronger intensity of O-containing functional groups and a 4-time higher Ca content in the OFMSWD than in the SSD were observed. As a result, more possibility of Pb ions to sorb onto the BMSW^{bat} *via* the chemical sorption and/or cation exchange mechanisms may take place

(Li et al., 2017). A previous study of Cataldo et al. (2016) also reported the cation exchange between Pb(II) and Ca-modified biochar.

Figures 5.10(a) and 5.10(b) show, respectively, the Cd(II) and As(V) sorption isotherms by batch and subsequent column washed BSS, BSS-H_2O_2 and BSS-KOH (Paper II). The constant values corresponding to Langmuir and Freundlich sorption models are given in Table 5.8.

From Table 5.7 and Table 5.8, the evolutions of the Langmuir parameters (Q_m and K_L values) of the biochars towards Pb(II), Cd(II) and As(V) were observed after biochar chemical treatments. The higher K_L values for Pb(II) by the modified OFMSWD biochars than its raw biochar were observed, while the modified SSD biochars showed a lower K_L value for Pb(II) after chemical treatment (except the BSS-KOH^{bat} due to non-fitting) (Table 5.7, Paper I). Similar to Pb(II), the K_L values for Cd(II) were also lower on the modified SSD biochars with batch and subsequent column washings (BSS-H_2O_2 and BSS-KOH), compared to the raw biochar (BSS) (Table 5.8). However, for As(V), the well-fitting of the Langmuir model for its sorption was found with no significant evolutions of K_L values after chemical treatments (Table 5.8). These findings indicated that the chemical treatments induced a higher sorption affinity for Pb(II) on the modified biochars from OFMSWD (Paper I). However, the chemically-modified biochars from SSD showed a lower affinity towards Pb(II) and Cd(II), while the chemical treatments did not modify the affinity of the biochars for As(V) species (Papers I and II).

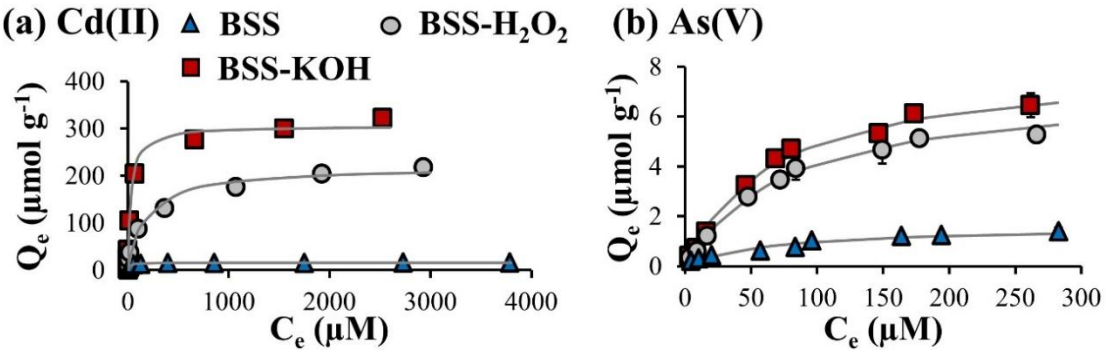

Figure 5.10: Effect of chemical treatment and biochar washing on sorption isotherms for Cd(II) (a) and As(V) (b) by the raw and chemically-modified sewage sludge digestate biochars (initial pH=5, 24 h, Langmuir model fitting) (Paper II).

Table 5.8: Constants for the Langmuir and Freundlich isotherm models for Cd(II) and As(V) sorption by raw and chemically-modified biochars from sewage sludge digestate (Paper II).

Biochar	Cd(II)					
	Langmuir			Freundlich		
	K_L (L µmol^{-1})	Q_m (µmol g^{-1})	R^2	K_F ((µmol g^{-1})(L µmol^{-1})$^{1/n}$)	n	R^2
BSS	0.061 ± 0.009	15.49 ± 0.32	0.992	3.163	4.336	0.796
BSS-H_2O_2	0.005 ± 0.001	218.73 ± 6.91	0.990	5.893	2.008	0.942
BSS-KOH	0.032 ± 0.004	306.09 ± 6.07	0.994	23.460	2.570	0.933
Biochar	As(V)					
	Langmuir			Freundlich		
	K_L (L µmol^{-1})	Q_m (µmol g^{-1})	R^2	K_F ((µmol g^{-1})(L µmol^{-1})$^{1/n}$)	n	R^2
BSS	0.015 ± 0.006	1.60 ± 0.23	0.958	0.112	2.185	0.986
BSS-H_2O_2	0.012 ± 0.003	7.22 ± 0.67	0.989	0.156	1.456	0.966
BSS-KOH	0.014 ± 0.003	8.11 ± 0.53	0.994	0.196	1.473	0.967

BSS, BSS-H_2O_2, and BSS-KOH refer to raw biochar from sewage sludge digestate, and its H_2O_2 and KOH modified biochars, respectively, with batch and subsequent column washings.
All sorption kinetic constants and uncertainties for Cd(II) and As(V) were obtained by non-linear regression using Statistica software (v6.1, StatSoft).

The enhancement of the Q_m values for Pb(II) sorption was observed on the biochars after the chemical treatments (Figure 5.9(a, b)). For the OFMSWD based biochars, it was increased from 357.1 µmol g^{-1} (raw biochar) to 434.7 µmolg g^{-1} and 500.0 µmol g^{-1} for BMSW-$H_2O_2^{bat}$ and BMSW-KOH^{bat}, respectively (Table 5.7). Similarly, for the SSD based biochars, the Q_m values for Pb(II) were improved, from 31.4 µmol g^{-1} (BSS^{bat}) to 121.9 µmol g^{-1} (BSS-$H_2O_2^{bat}$) (Table 5.7). Nevertheless, for the BSS-KOH^{bat}, due to unexpected low Pb(II) sorption abilities at low equilibrium Pb(II) concentrations (C_e) (0–200 µM) (Figure 5.9(b)), Langmuir model was failed to explain the sorption behavior of this biochar. Therefore, no Q_m value of the BSS-KOH^{bat} was reported (Table 5.7). The alteration of Pb(II) sorption could be described by a potential release of DOC from the BSS-KOH^{bat} (as previously discussed in section 5.1.3), which could possibly form soluble ligand complexes with Pb(II) and thus hinders the Pb(II) sorption onto the biochar, particularly at the low Pb(II) concentrations (<200 µM) (Paper I).

Similar to Pb(II), the sorption capacities for Cd(II) and As(V) were also enhanced on the modified SSD biochars (submitted to batch and additional column washings) (Figure 5.10(a, b)). From Table 5.8, the Q_m values for Cd(II) and As(V) were improved, respectively, by 15–20 times and by 4–5 times after the H_2O_2 or KOH treatments. The enhancement of sorption abilities for Pb(II), Cd(II) and As(V) by the chemically-modified SSD biochars can be directly linked to the improved biochar physicochemical properties

after chemical treatments (Table 5.2). The higher surface areas of the chemically-modified SSD biochars, compared to its raw biochar (Table 5.2), are in agreement with their higher sorption capacities towards Pb(II), Cd(II) and As(III, V). These results are consistent with previous published data (Ding et al., 2016; Wu et al., 2017), who reported that the surface area plays an important role in the sorption of metal(loid)s by biochars. Moreover, increases of cation exchange capacities of the SSD biochars after the chemical treatments (Table 5.2) may induce more sorption of positively-charged metals like Pb(II) and Cd(II). Furthermore, a slight increase of pH_{pzc} on the chemically-modified SSD biochars, compared to the raw biochar, leads to the more positive charges on their surfaces (Table 5.2), and thus enhancing the sorption for anionic As(V) (at pH = 5.0).

Overall, these findings suggest that the biochar treatments with KOH or H_2O_2 could modify the biochar properties and thus induce more Pb(II) sorption on the modified biochars (Paper I). Nevertheless, a caution on the use of KOH for biochar treatment should be highly concerned to eliminate the releasable compounds from the biochar, and thereby preventing an alteration of the Pb(II) sorption on the isotherm curve.

5.3.2 Effect of biochar washing approaches on Pb(II), Cd(II) and As(III, V)

In this section, the comparisons of the sorption isotherms for Pb(II) by the batch washed BSS-KOH^{bat} and BSS-$H_2O_2^{bat}$ versus batch and additional column washed BSS-KOH and BSS-H_2O_2 were performed (Paper I). This is to observe if the biochar washing steps after the KOH or H_2O_2 treatments affect the sorption behavior and sorption capacity towards Pb(II). After that, the KOH-modified biochars were selected to further study the influence of biochar washing steps on the sorption isotherms for Cd(II) and As(III, V) (Papers II). As previously mentioned in section 5.3.1, the Langmuir and Freundlich isotherm models were used to describe the sorption behavior for Pb(II), Cd(II) and As(III, V).

For Pb(II), Figure 5.11(a) represents its sorption isotherms on the KOH and H_2O_2 modified SSD biochars fitted with the Langmuir model. Figures 5.11(b) and 5.11(c) compare the biochar washing procedures: batch versus batch and subsequent continuous column washings of the KOH and H_2O_2 modified biochars, respectively, on the Pb(II) sorption isotherms at low C_e of Pb(II). Figures 5.11(d) and 5.11(e) show the comparisons of the Pb(II) sorption isotherms between the H_2O_2 and KOH modified biochars submitted to batch washing and batch and subsequent column washings, respectively. For Cd(II), As(III) and As(V), the experimental data fitted with the Langmuir

model is shown in Figure 5.12(a), 5.12(b) and 5.12(c), respectively. All the constants of Langmuir and Freundlich isotherm models for these metal(loid)s are given in Tables 5.9 and 5.10.

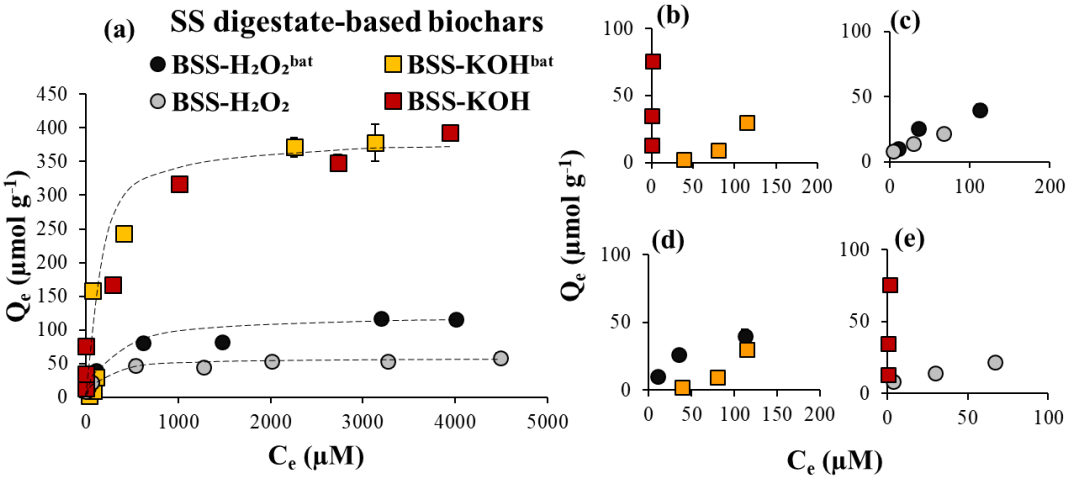

Figure 5.11: Comparison of the Pb(II) sorption isotherms on sewage sludge digestate-based biochars with different washing modes fitted with the Langmuir model (except BSS-KOH^{bat} due to non-fitting) (a). Figure (b) to (e) are zooms of C_e at low concentration ranges (<200 µM); batch-washed BSS-KOH^{bat} versus continuous washed BSS-KOH (b), BSS-H_2O_2^{bat} versus BSS-H_2O_2 (c), and with different chemical treatments; BSS-KOH^{bat} versus BSS-H_2O_2^{bat} (d), and BSS-KOH versus BSS-H_2O_2 (e) (Paper I).

Table 5.9: Effect of biochar washing procedures (batch versus batch and subsequent continuous washings) on the Pb(II) sorption by chemically-modified biochars from sewage sludge digestate fitted with Langmuir and Freundlich isotherm models (Paper I).

Biochar	Pb(II)					
	Langmuir			Freundlich		
	K_L (L µmol^{-1})	Q_m (µmol g^{-1})	R^2	K_F (µmol g^{-1})(L µmol^{-1})$^{1/n}$	n	R^2
BSS-H_2O_2^{bat}	0.004	121.9	0.984	5.610	2.623	0.956
BSS-H_2O_2	0.007	58.1	0.994	6.030	3.527	0.967
BSS-KOH^{bat}	0.001	714.2	0.294	1.991	1.472	0.566
BSS-KOH	0.007	386.6	0.987	38.00	3.462	0.926

^{bat} refers to biochar washing in batch system with ultrapure water (triplicate in a row).

BSS-H_2O_2^{bat} and BSS-KOH^{bat} refer to H_2O_2 and KOH modified biochars from sewage sludge digestate (SSD), respectively, with batch washing.

BSS-H_2O_2, and BSS-KOH refer to H_2O_2 and KOH modified biochars from SSD, respectively, with batch and subsequent column washings.

From Table 5.9 and Table 5.10, the sorption data for Pb(II), Cd(II) and As(III, V) was well fitted with the Langmuir model (R^2>0.96) for all the modified SSD biochars with both the batch washing and batch and subsequent column washings, except the Pb(II) sorption by the BSS-KOH^{bat}. Nevertheless, the Langmuir model was able to describe the Pb(II) sorption on this KOH-modified biochar with the additional column washing (BSS-KOH) (Table 5.9). This is likely due to the elimination of DOC from the KOH biochar after the subsequent column washing (Figure 5.4(c), section 5.1.3). However, unlike the Pb(II), the release of the DOC from the BSS-KOH^{bat} did not modify the Cd(II) sorption due to its well-fitting of the Langmuir model (Table 5.10) (section 5.1.3). This could be explained by a much higher K_L value of the biochar towards Cd(II) (*e.g.* 0.032 L µmol^{-1} for BSS-KOH) than Pb(II)) (*e.g.* 0.007 L µmol^{-1} for BSS-KOH) (Tables 5.9 and 5.10). Consequently, a higher affinity of the biochar for Cd(II) than Pb(II) and/or a weaker reaction between Cd ions and the DOC in solutions could be occurred (Papers I and II).

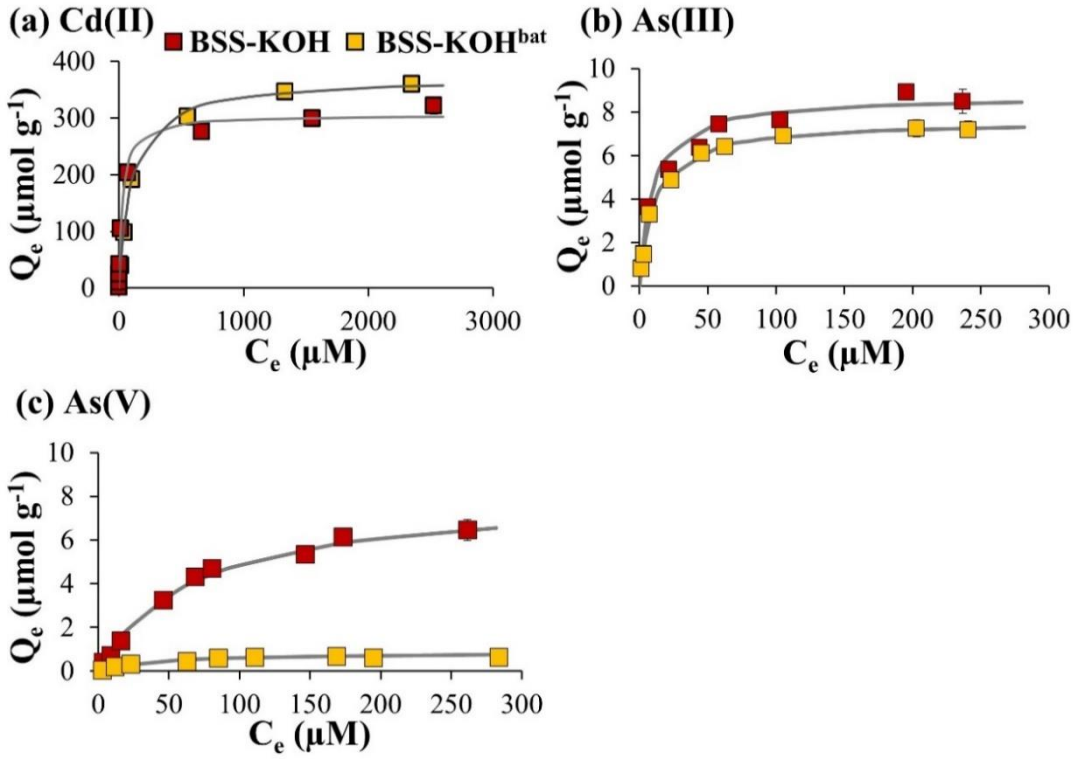

Figure 5.12: Influence of biochar washings of KOH-modified sewage sludge digestate biochars on sorption isotherms for Cd(II) (a), As(III) (b) and As(V) (c) (initial pH=5, 24 h, Langmuir model fitting) (Paper II).

From the Langmuir parameters (Table 5.9), the higher K_L values for Pb(II) were observed on the modified biochars with the additional column washing step, for instance, from 0.004 L µmol^{-1} for the BSS-$H_2O_2^{bat}$ to 0.007 L µmol^{-1} for the BSS-H_2O_2. Similarly, for Cd(II), the K_L value of KOH-modified SSD biochars was also increased after the subsequent washing of biochar (Table 5.10). This suggests that the additional biochar washing step induced a higher sorption affinity of the chemically-modified towards Pb(II) and Cd(II). In contrast, for As(III, V), no significant differences of the K_L values were found on the KOH biochars with different biochar washing steps (Table 5.10). This implies that no evolution in the affinity for As species towards the KOH-modified SSD biochars (Paper II). However, the lower K_L value of As(V) than As(III) indicates that the As(V) species had less affinity for both the BSS-KOH and BSS-KOH^{bat}, compared to the As(III) (Paper II).

Table 5.10: Constants for the Langmuir and Freundlich isotherm models for Cd(II), As(III) and As(V) sorption by KOH-modified biochars from sewage sludge digestate with different biochar washing steps (Paper II).

Biochar	**Cd(II)**					
	Langmuir			Freundlich		
	K_L (L µmol^{-1})	Q_m (µmol g^{-1})	R^2	K_F ((µmol g^{-1})(L µmol^{-1})$^{1/n}$)	n	R^2
BSS-KOH^{bat}	0.009 ± 0.001	372.49 ± 6.71	0.996	9.013	1.849	0.882
BSS-KOH	0.032 ± 0.004	306.09 ± 6.07	0.994	23.460	2.570	0.933
Biochar	**As(III)**					
	Langmuir			Freundlich		
	K_L (L µmol^{-1})	Q_m (µmol g^{-1})	R^2	K_F ((µmol g^{-1})(L µmol^{-1})$^{1/n}$)	n	R^2
BSS-KOH^{bat}	0.088 ± 0.007	7.60 ± 0.12	0.996	1.007	2.420	0.880
BSS-KOH	0.103 ± 0.018	8.74 ± 0.33	0.976	1.059	2.299	0.884
Biochar	**As(V)**					
	Langmuir			Freundlich		
	K_L (L µmol^{-1})	Q_m (µmol g^{-1})	R^2	K_F ((µmol g^{-1})(L µmol^{-1})$^{1/n}$)	n	R^2
BSS-KOH^{bat}	0.024 ± 0.008	0.85 ± 0.09	0.965	0.044	1.867	0.906
BSS-KOH	0.014 ± 0.003	8.11 ± 0.53	0.994	0.196	1.473	0.967

BSS-KOH^{bat} refers to KOH modified biochar from sewage sludge digestate (SSD) with batch washing.
BSS-KOH refers to KOH modified biochar from SSD with batch and subsequent column washings.
All sorption kinetic constants and uncertainties for Cd(II) and As(V) were obtained by non-linear regression using Statistica software (v6.1, StatSoft).

Considering the effect of biochar washings on the modified SSD biochars, no significant variations of the Pb(II) sorption were found on the H_2O_2-modified biochar with additional column washing at low C_e of Pb(II) (<200 µM, Figure 5.11(c)). This is likely due to a

small release of DOC from the H_2O_2 biochars to alter the Pb(II) sorption (Figure 5.4(d), section 5.1.3). However, the Pb(II) sorption capacities were significantly enhanced on the KOH biochar with additional biochar washing (BSS-KOH) at low C_e of Pb(II) (<200 µM, Figure 5.11(b)). Nevertheless, no evolution of the Pb(II) sorption was observed among the KOH biochars with different washing steps at high C_e of Pb(II) (1000–5000 µM, Figure 5.11(a)). Compared to Pb(II), a slightly lower Cd(II) sorption ability was observed on the KOH biochar with the subsequent column washing (Figure 5.12(a)) as the Q_m value was decreased from 372 ± 7 µmol g^{-1} (BSS-KOH^{bat}) to 306 ± 7 µmol g^{-1} for the BSS-KOH (Table 5.10). These findings suggest that the continuous column washing induced an improvement of the Pb(II) sorption capacity on the KOH-modified biochar at low equilibrium Pb(II) concentrations (<200 µM). However, the sorption for Pb(II) and Cd(II) was not significantly affected by the biochar washing steps, particularly at the high equilibrium concentrations (Papers I and II).

In contrast, a slight improvement of As(III) sorption capacity was observed on the KOH biochar with the subsequent column washing (BSS-KOH), while this biochar had a 10-fold higher As(V) sorption, compared to the batch washed BSS-KOH^{bat} (Figure 5.12(b, c)). The strong difference of the sorption capacity for As(V) can be due to a strong release of PO_4^{3-} from the BSS-KOH^{bat} (Paper I) that may significantly compete with As(V) and thus hinder the As(V) sorption onto this biochar. It has been previously reported that the presence of PO_4^{3-} in solutions could facilitate the mobility of As(V) from the sorbents (Neupane et al., 2014). Due to a potential release of DOC and PO_4^{3-} from the BSS-KOH^{bat} as previously observed in section 5.1.3, this could strongly affect the mobilization of As(V) rather than As(III) (Kim et al., 2018) since the DOC and PO_4^{3-} are also negatively-charged compounds. Han et al. (2011) and Manning et al. (2002) also reported that the presences of DOC and PO_4^{3-} in water could compete with oxyanions of As(V) under oxidizing and aerobic conditions, while As(III) is neutral at pH below 9.2. Furthermore, during the As(III) sorption, the arsenic redox distribution showed that about 70% of As(III) was oxidized to As(V) in the BSS-KOH^{bat}, while a partial oxidation (7%) was found in the BSS-KOH (Paper II).

In summary, this section highlights that the proper biochar washing steps after the chemical treatments are required to eliminate biochar leachable compounds that may alter the sorption for metal(loid)s. From this study (Paper I), the complete washing by using a column reactor was necessary for the alkali modified biochars towards the Pb(II) and As(V) sorption. In addition, during this study, a variation of As species repartition, *i.e.* oxidation of As(III) into As(V), was observed with the KOH-modified SSD biochars. Therefore, an investigation on the redox distribution of arsenic between As(III) and As(V) during the sorption has been further investigated (Paper III).

5.4 The redox distribution of arsenic in the biochar-solution system

The KOH-modified SSD biochars were selected to further understand the influence of chemical modifications on the behavior of arsenic redox distribution in the biochar-solution system. Speciation analyses were performed during the As(III) sorption experiments by chromatography couple to atomic spectrometry (Paper III) which, in contrast to solid-phase techniques such as XANES, required to transfer arsenic from the biochar to a liquid phase. Thus, first of all, an extraction procedure for As(III) and As(V) in the solid biochars was tested and validated. After that, the influence of chemical treatments and washing procedures of biochars on the inorganic arsenic redox distribution during As(III) sorption was investigated (Paper III).

5.4.1 Extraction procedure for arsenic redox evolution in biochars

Before analysis, the validation of an extraction procedure for biochars is necessary to allow a quantitative recovery of total As and As species without any conversions between As(III) and As(V). In this study, the BSS-KOH^{bat} was selected regarding its ability to oxidize As(III) (Papers II and III).

The addition of ascorbic acid in the extraction solution for As(III) stabilization was assessed by applying the extraction method to biochars with/without spiking with a known amount of As(III) just before starting the extraction procedure. Results showed that all spiked As(III) was recovered by this extraction procedure (Paper III). The results also suggest that when using only 0.3 M H_3PO_4, the spiked As(III) was significantly oxidized to As(V) (Paper III). Indeed, the addition of 0.167 µmol of As(III) to the biochar before performing the extraction step resulted in the increases of 0.117 (± 0.009) µmol and 0.047 (± 0.004) µmol for As(III) and As(V), respectively (Paper III). Therefore, about 29% conversion of spiked As(III) to As(V) was observed. Nevertheless, no As(III) oxidation was found during the extraction with H_3PO_4 and ascorbic acid. The differences of As(III) amounts between before and after spiking was 0.168 (± 0.009) µmol, matching with the As(III) added (0.167 µmol). Thus, the addition of ascorbic acid is essential to preserve As(III) stability during the extraction.

Moreover, the extraction yields of As sorption by the biochars were estimated after the sorption experiment for As(III) by recovering the biochars after the sorption and then submitting them to acid digestion and extraction (Paper III). Table 5.11 shows the comparison of total amount of sorbed arsenic determined after acid digestion or

extraction procedure. Results showed that the total sorbed-As by the raw and H_2O_2 modified biochars were too low to be correctly quantified and thus no calculation of the extraction yields was performed (Table 5.11). For the BSS-KOH^{bat}, the total sorbed-As was quantitatively recovered by the extraction, whereas for BSS-KOH about one fourth could not be extracted with these extraction conditions. The differences of the extraction efficiency may result from different sorption interactions of As from one biochar to the other. Nevertheless, the majority of As was extracted from the biochars and the identification of As species in the extracted solutions still gave an overview of the main As speciation and sorption by the biochars.

Table 5.11: Comparison of total amount of sorbed arsenic determined after acid digestion or extraction procedure (Paper III).

Biochar	Total arsenic (µmol)		Recovery from extraction (%)
	Extraction	Acid digestion	
BSS	0.002 ± 0.004	0.013 ± 0.013	nq[a]
BSS-H_2O_2	0.040 ± 0.013	0.080 ± 0.013	nq
BSS-KOH	0.934 ± 0.040	1.241 ± 0.040	75 ± 4
BSS-KOH^{bat}	0.840 ± 0.053	0.800 ± 0.040	105 ± 9

[a] nq refers to not quantified due to very low values detected by liquid chromatography coupled to atomic fluorescence spectroscopy (LC-AFS) with hydride generation (HG) and/or graphite furnace atomic absorption spectrometry (GF-AAS).

5.4.2 Determination of As(III) and As(V) sorbed by biochars

During the As(III) sorption, the biochar samples were exposed in the solutions with an initial As(III) amount of 1.949 µmol. At the end of experiments, each biochar was recovered then separately submitted to acid digestion and to extraction for the determination of the total sorbed As and for the assessment of the redox evolution of sorbed As, respectively. The exposition solution was also analyzed to determine the remaining As amount and to assess the distribution between As(III) and As(V). The comparison of the As(III), As(V) and total As quantities in the exposition solutions and sorbed-As onto the biochars after the acid digestion and extraction procedure is reported in Table 5.12 and more details are described in the following subsections.

5.4.2.1 Evolutions of As(III) and As(V) species in liquid phase solutions

From Table 5.12, no significant differences of the total As between the initial and the final exposition solutions of BSS and BSS-H_2O_2 were observed, implying that no As was sorbed by these biochars. Nevertheless, the As concentrations from the final

exposition solutions of both the BSS-KOH and BSS-KOH^{bat} were 2–3 times decreased, compared to the initial As(III) concentration (Table 5.12). The deduced As concentrations showed that the arsenic was able to sorb onto both the BSS-KOH and BSS-KOH^{bat} with the sorption efficiencies of 67% and 50%, respectively (from the calculations in liquid phase solutions).

Comparison of the arsenic redox distribution in the final exposition solutions showed that almost no As(III) was oxidized to As(V) for both BSS and BSS-H_2O_2 (Table 5.12). For the KOH-modified SSD biochars, the assessment of redox distribution only concerned the unsorbed As. In the case of the BSS-KOH, no significant oxidation of As(III) was found, while about 28% of the remaining As was oxidized to As(V) for the BSS-KOH^{bat}. These results are in agreement with the findings from Paper II with a large oxidation (70%) of As(III) in BSS-KOH^{bat} and a partial oxidation (7%) in BSS-KOH during As(III) sorption.

To elucidate if the oxidation was induced by the released compounds from the biochar into the solution or by only the biochar, a control was conducted by replacing the biochar with the release of dissolved compound (RDC) solutions from BSS-KOH^{bat} (Paper III). Figures 5.13(a) and 5.13(b) demonstrate a remaining of arsenic during the As(III) sorption, respectively, onto the BSS-KOH^{bat} and with only the release of dissolved compounds (RDC) from the BSS-KOH^{bat} (a control) as a function of time. During the sorption kinetics of As(III) on the BSS-KOH^{bat}, results showed gradual decreases of As(III), according to reductions of total As over time (Figure 5.13(a)). However, from Figure 5.13(b), no complexation between arsenic and RDC was observed due to almost stable amounts of As(III), As(V) and total As along the time. Considering the As speciation demonstrated a slight oxidation of As(III) in the RDC solutions (9% of the final dissolved arsenic was As(V)) (Figure 5.13(b)), while up to 43% of the final dissolved arsenic was oxidized in the presence of the biochar (Figure 5.13(a)). These findings highlight that the biochar material mainly induced the oxidation of As(III) to As(V) and to a lesser extent by the RDC releasing from the biochar, while no transformation of As(V) to As(III) was found in solutions during the As(III) sorption (Paper III).

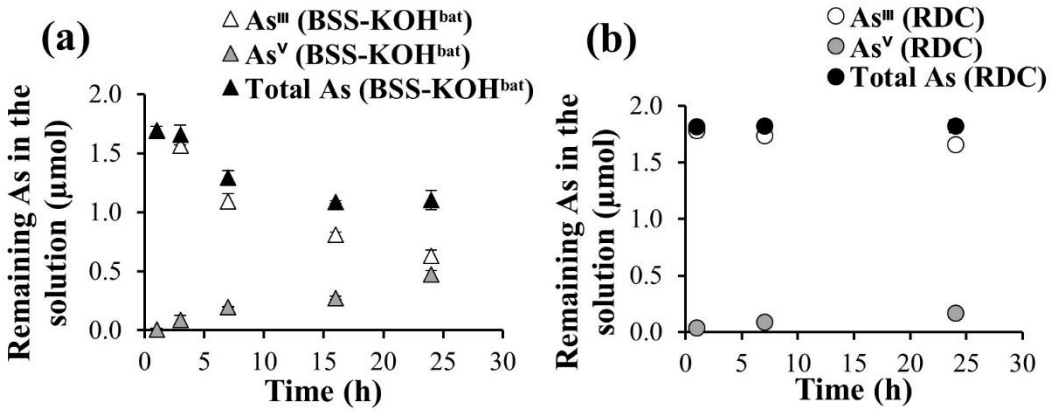

Figure 5.13: Arsenic redox distribution in solutions during sorption kinetics for As(III) by BSS-KOH^{bat} (a) and for control with only released dissolved compounds (RDC) from BSS-KOH^{bat} (b) (Paper III).

5.4.2.2 Evolutions of As(III) and As(V) species in solid phase of biochars

Considering the As species from extraction of biochars after the sorption, similar distributions between As(III) and As(V) were observed for both the BSS-KOH and BSS-KOH^{bat} (Table 5.12). The majority of arsenic was sorbed as As(III) (90–92%), while only 8–10% was sorbed as As(V) onto the KOH-modified SSD biochars (Table 5.12). The KOH-modified SSD biochars favored the sorption for As(III) rather than for As(V), in agreement with a previous finding (Paper II) on the comparison of the sorption between As(III) and As(V) by these biochars.

Among all the SSD based biochars, the BSS-KOH^{bat} showed a higher oxidation of As(III) to As(V) than other biochars in the final solution (Table 5.12). This is probably due to the ability of this biochar to release the DOC into solution (section 5.1.3). Since the DOC could act as electron acceptors, more oxidation of As(III) to As(V) can be found during the As(III) sorption. A previous study (Dong et al., 2014) also reported that the presence of dissolved organic matter induced more As(III) oxidation.

For the BSS-KOH, the redox distribution of sorbed As was quite similar to the one observed in the final solution (Table 5.12). However, for the BSS-KOH^{bat}, the As species distribution in the exposition solution and on the biochar were different: only 8% of the sorbed As was As(V) (from extraction), while As(V) species represent 28% of As in the final solution. This could be due to the As(V) reduction on the biochar during the sorption process, as also observed by Niazi et al. (2018a, 2018b) who studied the As speciation on wood and leaf derived biochars by using the solid phase XANES technique. In the case for the H_2O_2 modified biochar, the low sorbed As by this biochar resulted in a low

accuracy of the As redox distribution and thus should be taken with caution. The percentage of As(V) sorbed onto the BSS-H_2O_2 (24%) was higher than in the exposition solution (4%) (Table 5.12), suggesting that the As(III) could potentially oxidized to As(V) on the biochar during the sorption.

The results showed that the percentage of As(V) was not the same between the final solutions and the extracted biochars, except for the BSS-KOH. This is likely due to the low sorption ability of both the BSS and BSS-H_2O_2 for As, which lead to a low accuracy of the As distributions. Nevertheless, for the BSS-KOH, similar distributions of As(V) between the final solution and the extracted biochar can be linked to a complete washing of this biochar to eliminate all the releasable compounds that may disturb the sorption process (section 5.1.3).

The findings also suggest that the biochars could act as electron donors and/or electron acceptors. The reduction of As(V) to As(III) on biochars could be corresponding to the presence of biochar functions such as phenolic or alcoholic (–OH) and carboxyl (–COOH) groups on the biochar surface (Papers I and II). These functional groups could act as electron donors and thus inducing the reduction of As(V) (Choppala et al., 2016). Nevertheless, the oxidation of As(III) to As(V) on the biochar can also occur with the presence of redox active species (*e.g.* FeO(OH)) on the biochar (Niazi et al., 2018a, 2018b). Based on the biochar properties (Table 5.1), the SSD biochar contained iron (Fe) (~1182 µmol g^{-1}) and manganese (Mn) (~14 µmol g^{-1}) that could be partially in metal oxide forms. As a result, these metal oxides could promote the redox transformation of As(III) to As(V) on the biochar (Gude et al., 2017; Han et al., 2011; Manning et al., 2002; Vithanage et al., 2017).

Table 5.12: Comparison of As speciation and total As in exposition solutions and sorbed onto biochars (initial As(III) amount in exposition solution: 1.949 µmol) (Paper III).

Biochar	Exposition solution				Sorbed As onto biochar				
	Initial	Final			Acid digestion		Extraction		
	As(III)	As(III)+As(V)	As(III)	As(V)	Total As	Sorption yield	As(III)+As(V)	As(III)	As(V)
	(µmol)	(µmol)	(%)	(%)	(µmol)	(%)	(µmol)	(%)	(%)
BSS	1.949	1.935 ± 0.027	99	1	0.013 ± 0.013	<1	0.002 ± 0.004	na	na
BSS-H_2O_2	1.949	1.908 ± 0.040	96	4	0.080 ± 0.013	4	0.040 ± 0.013	76	24
BSS-KOH	1.949	0.640 ± 0.040	98	2	1.241 ± 0.040	64	0.934 ± 0.040	90	10
BSS-KOH^{bat}	1.949	0.961 ± 0.067	72	28	0.800 ± 0.040	41	0.840 ± 0.053	92	8

na refers to not available due a value close to limit of quantification.

6 Conclusions

This research work illustrates the capability of biochars produced from sewage sludge digestate (SSD) and the organic fraction of municipal solid waste digestate (OFMSWD) towards metals (*i.e.* Pb(II) and Cd(II)) and metalloids (*i.e.* As(III, V)) removal from water through the batch sorption kinetic and isotherm studies (Papers I and II). The chemical treatments (KOH or H_2O_2) followed by the biochar washing procedures (batch washing *versus* batch and subsequent column washings) were implemented for the first time in this study to improve the sorption performance for Pb(II), Cd(II) and As(III, V) on the chemically-modified digestate biochars (Papers I and II). In addition, the redox state distribution of As species (*i.e.* As(III) and As(V)) during the As(III) sorption on the solid phase of biochar and in liquid solutions was successfully monitored for the first time in this study (Paper III). The important findings of this thesis are critically summarized as follows:

Significant evolutions of the pH value, electrical conductivity, surface area, cation exchange capacity, and total As content were found after submitting the raw biochars to different chemical treatments and biochar washing procedures (batch washing versus batch and subsequent column washings) (Papers I and II). The additional continuous column washing was able to significantly eliminate the DOC and PO_4^{3-} from modified the biochar, particularly with the KOH treatment.

All the sorption kinetic data for Pb(II), Cd(II) and As(V) on the raw and chemically-modified biochars was best described by the pseudo-second-order (PSO) kinetic model, literally suggesting that the simple chemical sorption was considered as the rate controlling mechanism for these elements by the biochar (Papers I and II). The KOH or H_2O_2 treatments strongly induced faster kinetic rates for cationic metals, *i.e.* Pb(II) and Cd(II), on the modified biochars due to their higher PSO rate constants (k_2), compared to the raw biochars both from SSD and OFMSWD (Papers I and II). The improved

sorption kinetics for Pb(II) and Cd(II) were linked to the higher surface area and cation exchange capacity of the modified biochar after the chemical treatments. Nevertheless, a slower sorption rate for As(V) oxyanions was observed after treating the SSD biochar with KOH (*i.e.* BSS-KOH), while no variation was found between the raw and H_2O_2-modified SSD biochars (*i.e.* BSS and BSS-H_2O_2, respectively) (Paper II). Different biochar washing procedures after the KOH treatment also induced the changes of the sorption kinetics towards Pb(II), Cd(II) and As(III, V). Compared to the KOH-modified SSD biochar with batch washing (BSS-KOH^{bat}), a batch and subsequent column washings of this biochar (BSS-KOH) induced faster sorption rates for both Cd(II) and As(III). However, the additional washing of the KOH biochar showed a slower sorption rate towards As(V) species (Paper II). This highlights that both the chemical treatments (KOH or H_2O_2) and the additional continuous column washing procedures induced faster sorption rates of the modified biochars towards Pb(II), Cd(II) and As(III). However, the KOH modification followed by the column washing procedures induced a slower sorption rate for As(V) on the modified biochar. This is likely due to the well-fittings of the As(V) sorption data with both the PSO and intraparticle diffusion kinetic models, highlighting that the chemisorption and/or the intraparticle diffusion were considered as the rate controlling mechanisms during the sorption for the As(V) species on this biochar (Paper II).

The chemical treatments of biochars significantly affected the sorption isotherms for Pb(II) (Paper I), As(III, V) and Cd(II) (Paper II). The results showed the well-fittings of the Langmuir isotherm model with the Pb(II), Cd(II) and As(III, V) sorption for all the raw and chemically-modified biochars, except the Pb(II) sorption by the batch washed BSS-KOH^{bat} due to non-fitting (Papers I and II). Due to a potential release of the DOC from the BSS-KOH^{bat} into solutions, these compounds could subsequently form soluble-ligand-complexes with Pb ions and thus altered the Pb(II) sorption behavior, particularly at low equilibrium Pb(II) concentrations (<200 µM). Nevertheless, the Pb(II) sorption was able to follow the Langmuir model on the KOH modified SSD biochar with a subsequent column washing (BSS-KOH) (Paper I). The sorption for As(V) was also significantly influenced by the improper washing of the KOH-modified biochar (BSS-KOH^{bat}). Due to the ability of this biochar to release PO_4^{3-} into solutions, these releasable ions could compete with As(V) oxyanions and thus hinder the As(V) sorption on the biochar. Therefore, the additional continuous column washing after the biochar chemical treatment, particularly for the KOH, is highly recommended to prevent interferences during the sorption for these metal(loid)s.

The maximum sorption ability (Q_m) for Pb(II), Cd(II) was significantly increased on the modified biochars after the chemical treatments (Papers I and II). The enhanced Q_m of

the chemically-modified biochars towards Pb(II), Cd(II) is probably due to the improved biochar properties, especially the cation exchange capacity, specific surface area and, to a less extent on the point of zero charge of biochar (Papers I and II). Nevertheless, the lower K_L Langmuir constant values for Pb(II), Cd(II) were observed after the chemical treatments, indicating a lower sorption affinity for Pb(II) and Cd(II) on the modified SSD biochars. However, the chemical treatments did not modify the As(V) sorption affinity on the modified biochars. The additional biochar washing procedure induced a higher sorption affinity for Pb(II) and Cd(II) but a slightly lower affinity for As species both As(III) and As(V) on the modified biochars.

Arsenic as As(III) was found to be stable or partially oxidized to As(V) with time during the As(III) sorption experiments, depending on the biochar chemical treatments implemented (KOH or H_2O_2) (Paper III). In addition, a higher oxidation of As(III) to As(V) was observed in the KOH-modified biochar rinsed by a batch washing (Paper III). This oxidation was mainly induced by the biochar components and to a lesser extent by the release of DOC from the biochar (Paper III). The As speciation in the solid phase of different biochars was successfully accomplished by extraction with phosphoric and ascorbic acids followed by chromatographic analysis using liquid chromatography coupled to atomic fluorescence spectroscopy (LC-AFS) (Paper III). Moreover, ascorbic acid plays an important role in preserving As(III) oxidation during the biochar extraction. The results on the solid-liquid extraction showed that As was mainly sorbed as As(III) (76–92%) by the raw and chemically-modified biochars (Paper III). However, the redox transformation between As(III) and As(V) in the solutions demonstrated that the reduction and/or oxidation may take place, according to different biochar treatments (Paper III). The occurrence of As redox transformation both in the liquid solution and on the biochar was successfully achieved in this study (Paper III). Thus, this allows a direct comparison of arsenic in solid and liquid phases and provide more insights on how to further assess the fate of As in aquatic environments.

7 Future perspectives

This thesis showed the improved sorption capacities of the chemically-modified biochars from organic waste digestates for Pb(II), Cd(II) and As(III, V) in single element sorption system. Therefore, further study on the competitive sorption of metal(loid)s by the biochar can be accomplished to stimulate the real sorption behaviors in the environments. In addition, the information about the sorption mechanisms (*i.e.* surface complexation, ion exchange and precipitation) involved during the sorption for metal(loid)s should be further conducted to highlight the sorption interactions between the biochar and metal(loid)s in the multi-element sorption system. Moreover, the competitive effect of each elements/compounds present in water (*e.g.* DOC, PO_4^{3-} and CO_3^{2-}) as well as the evolution of pH value can be the aim of future work.

In this study, the chemical treatments (*i.e.* KOH or H_2O_2) followed by the continuous washing procedures of the biochar required a long operation time for the biochar preparations (*e.g.* about 1 week for a column washing step) and a huge amount of water usage to eliminate the releasable compounds from the modified biochars after the chemical treatments. Therefore, alternative modification techniques of the biochar such as coating with carbonaceous materials (*e.g.* graphene oxide and carbon nanotubes) may help to provide more oxygen-containing functional groups on the biochar surface.

In this thesis, the sorption kinetic and isotherm studies of the Pb(II), Cd(II) and As(III, V) had been performed only in batch experiments, which operated in a short time period (24 h). Therefore, the sorption of these metal(loid)s in a continuous system by using a continuous column reactor should be further conducted to test the stability of the biochar for metal(loid) elements in a long-term as well as to quantify the life-time of biochar before reaching a saturation stage.

References

AFNOR (1997a) Qualité de l'eau. Tome 2. Lignes directrices pour le dosage du carbone organique total (TOC) et carbone organique dissous (COD). Norme EN 1484., 6th ed. France.

AFNOR (1997b) Qualité de l'eau. Tome 3. Dosage du phosphore. Dosage spectrométrique à l'acide du molybdate d'ammonium. Norme EN 1189, 6th ed. France.

AFNOR (1996) Qualité de l'eau. Tome 2. Détermination de l'alcalinité. NF EN ISO 9963-1., 6th ed. France.

Agrafioti E, Bouras G, Kalderis D, Diamadopoulos E (2013) Biochar production by sewage sludge pyrolysis. J Anal Appl Pyrolysis 101:72–78.

Agrafioti E, Kalderis D, Diamadopoulos E (2014) Arsenic and chromium removal from water using biochars derived from rice husk, organic solid wastes and sewage sludge. J Environ Manage 133:309–314.

Ahmad M, Rajapaksha AU, Lim JE, Zhang M, Bolan N, Mohan D, Vithanage M, Lee SS, Ok YS (2014) Biochar as a sorbent for contaminant management in soil and water: A review. Chemosphere 99:19–23.

Al-Degs YS, El-Barghouthi MI, Issa AA, Khraisheh, MA, Walker, GM (2006) Sorption of Zn(II), Pb(II), and Co(II) using natural sorbents: Equilibrium and kinetic studies. Water Res 40:2645–2658.

Alibardi L, Cossu R (2015) Composition variability of the organic fraction of municipal solid waste and effects on hydrogen and methane production potentials. Waste Manag 36:147–155.

Alvarenga P, Mourinha C, Farto M, Santos T, Palma P, Sengo J, Morais MC, Cunha-Queda C (2015) Sewage sludge, compost and other representative organic wastes as agricultural soil amendments: Benefits versus limiting factors. Waste Manag 40:44–52.

Andrejkovicova S, Sudagar A, Rocha J, Patinha C, Hajjaji W, da Silva EF, Velosa A, Rocha F (2016) The effect of natural zeolite on microstructure, mechanical and heavy metals adsorption properties of metakaolin based geopolymers. Appl Clay Sci 126:141–152.

Aran D, Maul A, Masfaraud JF (2008) A spectrophotometric measurement of soil cation exchange capacity based on cobaltihexamine chloride absorbance. Comptes Rendus Geosci 340:865–871.

Argos M, Kalra T, Rathouz PJ, Chen Y, Pierce B, Parvez F, Islam T, Ahmed A, Rakibuz-Zaman M, Hasan R, Sarwar G, Slavkovich V, van Geen A, Graziano J, Ahsan H (2010) Arsenic exposure from drinking water, and all-cause and chronic-disease mortalities in Bangladesh (HEALS): A prospective cohort study. Lancet 376:252–258.

Bogusz A, Nowak K, Stefaniuk M, Dobrowolski R, Oleszczuk P (2017) Synthesis of biochar from residues after biogas production with respect to cadmium and nickel removal from wastewater. J Environ Manage 201:268–276.

Catalano JG, Park C, Fenter P, Zhang Z (2008) Simultaneous inner- and outer-sphere arsenate adsorption on corundum and hematite. Geochim Cosmochim Acta 72:1986–2004.

Cataldo S, Gianguzza A, Milea D, Muratore N, Pettignano A (2016) Pb(II) adsorption by a novel activated carbon – alginate composite material. A kinetic and equilibrium study. Int J Biol Macromol 92:769–778.

Cechinel MAP, Ulson de Souza SMAG, Ulson de Souza AA (2014) Study of lead(II) adsorption onto activated carbon originating from cow bone. J Clean Prod 65:342–349.

Cesaro A, Conte A, Belgiorno V, Siciliano A, Guida M (2019) The evolution of compost stability and maturity during the full-scale treatment of the organic fraction of municipal solid waste. J Environ Manage 232:64–270.

Chen X, Chen G, Chen L, Chen Y, Lehmann J, McBride, MB, Hay AG (2011) Adsorption of copper and zinc by biochars produced from pyrolysis of hardwood and corn straw in aqueous solution. Bioresour Technol 102:8877–8884.

Cheng W, Ding C, Wang X, Wu Z, Sun Y, Yu S, Hayat T, Wang X (2016) Competitive sorption of As(V) and Cr(VI) on carbonaceous nanofibers. Chem Eng J 293:311–318.

Choppala G, Bolan N, Kunhikrishnan A, Bush R (2016) Differential effect of biochar upon reduction-induced mobility and bioavailability of arsenate and chromate. Chemosphere 144:374–381.

Ding Z, Hu X, Wan Y, Wang S, Gao B (2016) Removal of lead, copper, cadmium, zinc, and nickel from aqueous solutions by alkali-modified biochar: Batch and column tests. J Ind Eng Chem 33:239–245.

Dong X, Ma LQ, Gress J, Harris W, Li Y (2014) Enhanced Cr(VI) reduction and As(III) oxidation in ice phase: Important role of dissolved organic matter from biochar. J Hazard Mater 267:62–70.

Duan L, Li X, Jiang Y, Lei M, Dong Z, Longhurst P (2017) Arsenic transformation behaviour during thermal decomposition of *P. vittata*, an arsenic hyperaccumulator. J Anal Appl Pyrolysis 124:584–591.

EPA (1996) Method 3050B: Acid digestion of sediments, sludges, and soils. EPA SW846-3050.

Fan S, Tang J, Wang Y, Li H, Zhang H, Tang J, Wang Z, Li X (2016) Biochar prepared from co-pyrolysis of municipal sewage sludge and tea waste for the adsorption of methylene blue from aqueous solutions: Kinetics, isotherm, thermodynamic and mechanism. J Mol Liq 220:432–441.

Fytili D, Zabaniotou A (2008) Utilization of sewage sludge in EU application of old and new methods: A review. Renew Sustain Energy Rev 12:116–140.

Garlapalli RK, Wirth B, Reza MT (2016) Pyrolysis of hydrochar from digestate: Effect of hydrothermal carbonization and pyrolysis temperatures on pyrochar formation. Bioresour Technol 220:168–174.

Gong XJ, Li WG, Zhang DY, Fan WB, Zhang XR (2015) Adsorption of arsenic from micro-polluted water by an innovative coal-based mesoporous activated carbon in the presence of co-existing ions. Int Biodeterior Biodegrad 102:256–264.

Gude JCJ, Rietveld LC, van Halem D (2017) As(III) oxidation by MnO_2 during groundwater treatment. Water Res 111:41–51.

Guo K, Gao B, Yue Q, Xu X, Li R, Shen X (2018) Characterization and performance of a novel lignin-based flocculant for the treatment of dye wastewater. Int Biodeterior Biodegrad 133:99–107.

Han X, Li YL, Gu JD (2011) Oxidation of As(III) by MnO_2 in the absence and presence of Fe(II) under acidic conditions. Geochim Cosmochim Acta 75:368–379.

Ho SH, Chen Y, Yang Z, Nagarajan D, Chang JS, Ren N (2017) High-efficiency removal of lead from wastewater by biochar derived from anaerobic digestion sludge. Bioresour Technol 246:142–149.

Ho YS, McKay G (1999) Pseudo-second order model for sorption processes. Process Biochem 34:451–465.

Huang H, Tang J, Gao K, He R, Zhao H, Werner D (2017) Characterization of KOH modified biochars from different pyrolysis temperatures and enhanced adsorption of antibiotics. RSC Adv 7:14640–14648.

Hughes MF, Beck BD, Chen Y, Lewis AS, Thomas DJ (2011) Arsenic exposure and toxicology: A historical perspective. Toxicol Sci 123:305–332.

Inyang M, Gao B, Yao Y, Xue Y, Zimmerman AR, Pullammanappallil P, Cao X (2012) Removal of heavy metals from aqueous solution by biochars derived from anaerobically digested biomass. Bioresour Technol 110:50–56.

Inyang MI, Gao B, Yao Y, Xue Y, Zimmerman A, Mosa A, Pullammanappallil P, Ok YS, Cao X (2016) A review of biochar as a low-cost adsorbent for aqueous heavy metal removal. Crit Rev Environ Sci Technol 4:406–433.

Islam S, Ahmed K, Raknuzzaman M (2015) Heavy metal pollution in surface water and sediment: A preliminary assessment of an urban river in a developing country. Ecol Indic 48:282–291.

Jadhav SV, Bringas E, Yadav GD, Rathod VK, Ortiz I, Marathe KV (2015) Arsenic and fluoride contaminated groundwaters: A review of current technologies for contaminants removal. J Environ Manage 162:306–325.

Jain CK, Singh RD (2012) Technological options for the removal of arsenic with special reference to South East Asia. J Environ Manage 107:1–18.

Jiang M, Wang Q, Jin X, Chen Z (2009) Removal of Pb(II) from aqueous solution using modified and unmodified kaolinite clay. J Hazard Mater 170:332–339.

Jiang T, Xu R, Gu T, Jiang J (2014) Effect of crop-straw derived biochars on Pb(II) adsorption in two variable charge soils. J Integr Agric 13:507–516.

Jin H, Capareda S, Chang Z, Gao J, Xu Y, Zhang J (2014) Biochar pyrolytically produced from municipal solid wastes for aqueous As(V) removal: Adsorption property and its improvement with KOH activation. Bioresour Technol 169:622–629.

Jouraiphy A, Amir S, Gharous ME, Revel JC, Hafidi M (2005) Chemical and spectroscopic analysis of organic matter transformation during composting of sewage sludge and green plant waste. Int Biodeterior Biodegrad 56:101–108.

Kambo HS, Dutta A (2015) A comparative review of biochar and hydrochar in terms of production, physico-chemical properties and applications. Renew Sustain Energy Rev 45:359–378.

Kaul B, Sandhu RS, Depratt C, Reyes F (1999) Follow-up screening of lead-poisoned children near an auto battery recycling plant, Haina, Dominican Republic. Environ Health Perspect 107:917–920.

Kim HB, Kim SH, Jeon EK, Kim D, Tsang DCW, Alessi DS, Kwon EE, Baek K (2018) Effect of dissolved organic carbon from sludge, rice straw and spent coffee ground biochar on the mobility of arsenic in soil. Sci Total Environ 636:1241–1248.

Kim MJ, Ahn KH, Jung Y (2002) Distribution of inorganic arsenic species in mine tailings of abandoned mines from Korea. Chemosphere 49:307–312.

Kołtowski M, Charmas B, Skubiszewska-Zięba J, Oleszczuk P (2017) Effect of biochar activation by different methods on toxicity of soil contaminated by industrial activity. Ecotoxicol Environ Saf 136:119–125.

Lagergren SY (1898) Zur theorie der sogenannten adsorption gelöster stoffe. K Sven Vetenskapsakad Handl 24:1–39.

Li H, Dong X, Silva EBD, Oliveira LMD, Chen Y, Ma LQ (2017) Mechanisms of metal sorption by biochars: Biochar characteristics and modifications. Chemosphere 178:466–478.

Li J, Li Y, Wu Y, Zheng M (2014) A comparison of biochars from lignin, cellulose and wood as the sorbent to an aromatic pollutant. J Hazard Mater 280:450–457.

Lima IM, Boateng AA, Klasson KT (2010) Physicochemical and adsorptive properties of fast-pyrolysis bio-chars and their steam activated counterparts. J Chem Technol Biotechnol 85:1515–1521.

Lin Y, Munroe P, Joseph S, Henderson R, Ziolkowski A (2012) Water extractable organic carbon in untreated and chemical treated biochars. Chemosphere 87:151–157.

Liou TH, Wu SJ (2009) Characteristics of microporous/mesoporous carbons prepared from rice husk under base- and acid-treated conditions. J Hazard Mater 171:693–703.

Liu P, Liu WJ, Jiang H, Chen JJ, Li WW, Yu HQ (2012) Modification of bio-char derived from fast pyrolysis of biomass and its application in removal of tetracycline from aqueous solution. Bioresour Technol 121:235–240.

Liu Z, Zhang FS (2009) Removal of lead from water using biochars prepared from hydrothermal liquefaction of biomass. J Hazard Mater 167:933–939.

Lu H, Zhang W, Yang Y, Huang X, Wang S, Qiu R (2012) Relative distribution of Pb^{2+} sorption mechanisms by sludge-derived biochar. Water Res 46:854–862.

Mahmood T, Saddique MT, Naeem A, Westerho P, Mustafa S (2011) Comparison of different methods for the point of zero charge determination of NiO. Ind Eng Chem Res 50:10017–10023.

Mancinelli E, Baltrėnaitė E, Baltrėnas P, Marčiulaitienė E, Limane B, Bartkevic V (2017) Dissolved organic carbon content and leachability of biomass waste biochar for trace metal (Cd, Cu and Pb) speciation modelling. J Environ Eng Landsc Manag 25:354–366.

Manning BA, Fendorf SE, Bostick B, Suarez DL (2002) Arsenic(III) oxidation and arsenic(V) adsorption reactions on synthetic birnessite. Environ Sci Technol 36:976–981.

Mohan D, Pittman CU, Bricka M, Smith F, Yancey B, Mohammad J, Steele PH, Alexandre-Franco MF, Gómez-Serrano V, Gong H (2007) Sorption of arsenic, cadmium, and lead by chars produced from fast pyrolysis of wood and bark during bio-oil production. J Colloid Interface Sci 310:57–73.

Mohan D, Sarswat A, Ok YS, Pittman CU (2014) Organic and inorganic contaminants removal from water with biochar, a renewable, low cost and sustainable adsorbent – A critical review. Bioresour Technol 160:191–202.

Montperrus M, Bohari Y, Bueno M, Astruc A, Astruc M (2002) Comparison of extraction procedures for arsenic speciation in environmental solid reference materials by high-performance liquid chromatography-hydride generation-atomic fluorescence spectroscopy. Appl Organomet Chem 16:347–354.

Nethaji S, Sivasamy A, Mandal AB (2013) Adsorption isotherms, kinetics and mechanism for the adsorption of cationic and anionic dyes onto carbonaceous particles prepared from *Juglans regia* shell biomass. Int J Environ Sci Technol 10:231–242.

Neupane G, Donahoe RJ, Arai Y (2014) Kinetics of competitive adsorption/desorption of arsenate and phosphate at the ferrihydrite-water interface. Chem Geol 368:31–38.

Niazi NK, Bibi I, Shahid M, Ok YS, Burton ED, Wang H, Shaheen SM, Rinklebe J, Lüttge A (2018a) Arsenic removal by perilla leaf biochar in aqueous solutions and groundwater: An integrated spectroscopic and microscopic examination. Environ Pollut 232:31–41.

Niazi NK, Bibi I, Shahid M, Ok YS, Shaheen SM, Rinklebe J, Wang H, Murtaza B, Islam E, Nawaz MF, Lüttge A (2018b) Arsenic removal by Japanese oak wood biochar in aqueous solutions and well water: Investigating arsenic fate using integrated spectroscopic and microscopic techniques. Sci Total Environ 621:1642–1651.

Nkoa R (2014) Agricultural benefits and environmental risks of soil fertilization with anaerobic digestates: A review. Agron Sustain Dev 34:473–492.

Novotny EH, Maia CMBDF, Carvalho MTDM, Madari BE (2015) Biochar: Pyrogenic carbon for agricultural use - A critical review. Rev Bras Cienc Solo 39:321–344.

Ofomaja AE, Pholosi A, Naidoo EB (2014) Kinetics and competitive modeling of cesium biosorption onto iron(III) hexacyanoferrate modified pine cone powder. Int Biodeterior Biodegrad 92:71–78.

Park JH, Wang JJ, Kim SH, Cho JS, Kang SW, Delaune RD, Han KJ, Seo DC (2017) Recycling of rice straw through pyrolysis and its adsorption behaviors for Cu and Zn ions in aqueous solution. Colloid Surf A 533:330–337.

Peng Q, Zhang F, Zhou Y, Zhang J, Wei J, Mao Q, Huang H, Chen A, Chai L, Luo L (2018) Formation of composite sorbent by *P. chrysogenum* strain F1 and ferrihydrite in water for arsenic removal. Int Biodeterior Biodegrad 132:208–215.

Peng W, Pivato A (2017) Sustainable management of digestate from the organic fraction of municipal solid waste and food waste under the concepts of back to earth alternatives and circular economy. Waste Biomass Valorization 10:465-481.

Petrovic JT, Stojanovic MD, Milojkovic JV, Petrovic MS, Sostaric TD, Lausevic MD, Mihajlovic ML (2016) Alkali modified hydrochar of grape pomace as a perspective adsorbent of Pb^{2+} from aqueous solution. J Environ Manage 182:292–300.

Pituello C, Francioso O, Simonetti G, Pisi A, Torreggiani A, Berti A, Morari F (2014) Characterization of chemical–physical, structural and morphological properties of biochars from biowastes produced at different temperatures. J Soils Sediments 15:792–804.

Plana PV, Noche B (2016) A review of the current digestate distribution models: Storage and transport. WIT Trans Ecol Environ 202:345–357.

Qiu Y, Zheng Z, Zhou Z, Sheng GD (2009) Effectiveness and mechanisms of dye adsorption on a straw-based biochar. Bioresour Technol 100:5348–5351.

Rees F, Simonnot MO, Morel JL (2013) Short-term effects of biochar on soil heavy metal mobility are controlled by intra-particle diffusion and soil pH. Eur J Soil Sci 65:149–161.

Regmi P, Moscoso JLG, Kumar S, Cao X, Mao J, Schafran G (2012) Removal of copper and cadmium from aqueous solution using switchgrass biochar produced via hydrothermal carbonization process. J Environ Manage 109:61–69.

Shen W, Li Z, Liu Y (2008) Surface chemical functional groups modification of porous carbon. Recent Patents Chem Eng 1:27–40.

Shinogi Y, Kanri Y (2003) Pyrolysis of plant, animal and human waste: Physical and chemical characterization of the pyrolytic products. Bioresour Technol 90:241–247.

Singh R, Singh S, Parihar P, Singh VP, Prasad SM (2015) Arsenic contamination, consequences and remediation techniques: A review. Ecotoxicol Environ Saf 112:247–270.

Sizmur T, Fresno T, Akgül G, Frost H, Moreno-Jiménez E (2017) Biochar modification to enhance sorption of inorganics from water. Bioresour Technol 246, 34–47.

Sohi SP, Krull E, Lopez-Capel E, Bol R (2010) A review of biochar and its use and function in soil. Adv Agron 105:47–82.

Tampio E, Salo T, Rintala J (2016) Agronomic characteristics of five different urban waste digestates. J Environ Manage 169:293–302.

Thomas P, Finnie JK, Williams JG (1997) Feasibility of identification and monitoring of arsenic species in soil and sediment samples by coupled high-performance liquid chromatography — Inductively coupled plasma mass spectrometry. J Anal At Spectrom 12:1367–1372.

Tóth G, Hermann T, Silva MRD, Montanarella L (2016) Heavy metals in agricultural soils of the European Union with implications for food safety. Environ Int 88:299–

309.

Tuna AOA, Ozdemir E, Simsek EB, Beker U (2013) Removal of As(V) from aqueous solution by activated carbon-based hybrid adsorbents: Impact of experimental conditions. Chem Eng J 223:116–128.

Velazquez-Peña GC, Solache-Ríos M, Olguin MT, Fall C (2019) As(V) sorption by different natural zeolite frameworks modified with Fe, Zr and FeZr. Microporous Mesoporous Mater. 273:133–141.

Vithanage M, Herath I, Joseph S, Bundschuh J, Bolan N, Ok YS, Kirkham MB, Rinklebe J (2017) Interaction of arsenic with biochar in soil and water: A critical review. Carbon 113:219–230.

Wan J, Pressigout J, Simon S, Deluchat V (2014) Distribution of As trapping along a ZVI/sand bed reactor. Chem Eng J 246:22–327.

Wang C, Gu L, Liu X, Zhang X, Cao L (2016) Sorption behavior of Cr(VI) on pineapple-peel-derived biochar and the influence of coexisting pyrene. Int Biodeterior Biodegrad 111:78–84.

Wang S, Gao B, Li Y, Mosa A, Zimmerman AR, Ma LQ, Harris WG, Migliaccio KW (2015a) Manganese oxide-modified biochars: Preparation, characterization, and sorption of arsenate and lead. Bioresour Technol 181:13–17.

Wang S, Gao B, Zimmerman AR, Li Y, Ma L, Harris WG, Migliaccio KW (2015b) Removal of arsenic by magnetic biochar prepared from pinewood and natural hematite. Bioresour Technol 175:391–395.

Wang Y, Liu R (2018) H_2O_2 treatment enhanced the heavy metals removal by manure biochar in aqueous solutions. Sci Total Environ 628–629:1139–1148.

Wang Z, Liu G, Zheng H, Li F, Ngo HH, Guo W, Liu C, Chen L, Xing B (2015) Investigating the mechanisms of biochar's removal of lead from solution. Bioresour Technol 177:308–317.

Wen T, Wang J, Yu S, Chen ZS (2017) Magnetic porous carbonaceous material produced from tea waste for efficient removal of As(V), Cr(VI), humic acid and dyes. ACS Sustain Chem Eng 5:4371–4380.

Wongrod S, Simon S, Guibaud G, Lens PNL, Pechaud Y, Huguenot D, van Hullebusch ED (2018a) Lead sorption by biochar produced from digestates: Consequences of chemical modification and washing. J Environ Manage 219:277–284.

Wongrod S, Simon S, van Hullebusch ED, Lens PNL, Guibaud G (2018b) Changes of sewage sludge digestate-derived biochar properties after chemical treatments and influence on As(III and V) and Cd(II) sorption. Int Biodeterior Biodegrad 135:96–102.

Wongrod S, Simon S, van Hullebusch ED, Lens PNL, Guibaud G (2019) Assessing arsenic redox state evolution in solution and solid phase during As(III) sorption onto chemically-treated sewage sludge digestate biochars. Bioresour Technol 275:232–238.

Wu C, Huang L, Xue SG, Huang YY, Hartley W, Cui MQ, Wong MH (2017) Arsenic sorption by red mud-modified biochar produced from rice straw. Environ Sci Pollut Res 24:18168–18178.

Wu W, Li J, Lan T, Müller K, Khan N, Chen X, Xu S, Zheng L, Chu Y, Li J, Yuan G, Wang H (2017) Unraveling sorption of lead in aqueous solutions by chemically modified biochar derived from coconut fiber: A microscopic and spectroscopic investigation. Sci Total Environ 576:766–774.

Xu Z, Hu HY, Chen DK, Cao JX, Yao H (2015) Determination of inorganic arsenic speciation in municipal solid waste incineration fly ash by high performance liquid chromatography-hydride generation-atomic fluorescence spectroscopy with phosphoric acid as extracting agent. Chinese J Anal Chem 43:490–494.

Xue Y, Gao B, Yao Y, Inyang M, Zhang M, Zimmerman AR, Ro KS (2012) Hydrogen peroxide modification enhances the ability of biochar (hydrochar) produced from hydrothermal carbonization of peanut hull to remove aqueous heavy metals: Batch and column tests. Chem Eng J 200–202:673–680.

Yoon K, Cho DW, Tsang DCW, Bolan N, Rinklebe J, Song H (2017) Fabrication of engineered biochar from paper mill sludge and its application into removal of arsenic and cadmium in acidic water. Bioresour Technol 246:69–75.

Yuan H, Lu T, Huang H, Zhao D, Kobayashi N, Chen Y (2015) Influence of pyrolysis temperature on physical and chemical properties of biochar made from sewage sludge. J Anal Appl Pyrolysis 112:284–289.

Zama EF, Zhu YG, Reid BJ, Sun GX (2017) The role of biochar properties in influencing the sorption and desorption of Pb(II), Cd(II) and As(III) in aqueous solution. J Clean Prod 148:127–136.

Zhang S, Hua Y, Deng L (2016) Nutrient status and contamination risks from digested pig slurry applied on a vegetable crops field. Int J Environ Res Public Health 13:1–11.

Zhang T, Zhu X, Shi L, Li J, Li S, Lu J, Li Y (2017) Efficient removal of lead from solution by celery-derived biochars rich in alkaline minerals. Bioresour Technol 235:185–192.

Zhao G, Li J, Ren X, Chen C, Wang X (2011) Few-layered graphene oxide nanosheets as superior sorbents for heavy metal ion pollution management. Environ Sci Technol 45:10454–10462.

Zhao L, Xue F, Yu B, Xie J, Zhang X, Wu R, Wang R, Hu Z, Yang ST, Luo J (2015)

TiO_2–graphene sponge for the removal of tetracycline. J Nanopart Res 17:1–9.

Zhao Z, Wu M, Jiang Q, Zhang Y, Chang X, Zhan K (2015) Adsorption and desorption studies of anthocyanins from black peanut skins on macroporous resins. Int J Food Eng 11:841–849.

Zhou Z, Liu Y, Liu S, Liu H, Zeng G, Tan X, Yang C, Ding Y, Yan Z, Cai X (2017) Sorption performance and mechanisms of arsenic(V) removal by magnetic gelatin-modified biochar. Chem Eng J 314:223–231.

Zielińska A, Oleszczuk P, Charmas B, Skubiszewska-Zięba J, Pasieczna-Patkowska S (2015) Effect of sewage sludge properties on the biochar characteristic. J Anal Appl Pyrolysis 112:201–213.

I

Lead sorption by biochar produced from digestates: Consequences of chemical modification and washing

by

Wongrod, S., Simon, S., Guibaud, G., Lens, P.N.L.,
Pechaud, Y., Huguenot, D., van Hullebusch, E.D., 2018.
Journal of Environmental Management 219: 277–284.

Journal of Environmental Management 219 (2018) 277–284

Contents lists available at ScienceDirect

Journal of Environmental Management

journal homepage: www.elsevier.com/locate/jenvman

Research article

Lead sorption by biochar produced from digestates: Consequences of chemical modification and washing

Suchanya Wongrod [a, b, c], Stéphane Simon [c], Gilles Guibaud [c, *], Piet N.L. Lens [b], Yoan Pechaud [a], David Huguenot [a], Eric D. van Hullebusch [a, b]

[a] Université Paris-Est, Laboratoire Géomatériaux et Environnement (EA 4508), UPEM, 77454, Marne-la-Vallée, France
[b] IHE Delft Institute for Water Education, P.O. Box 3015, 2601 DA, Delft, The Netherlands
[c] Université de Limoges, PEIRENE-Groupement de Recherche Eau Sol Environnement (EA 7500), Faculté des Sciences et Techniques, 123 Avenue Albert Thomas, 87060 Limoges, France

ARTICLE INFO

Article history:
Received 6 January 2018
Received in revised form
21 April 2018
Accepted 24 April 2018
Available online 8 May 2018

Keywords:
Biochar
Digestate
Sorption
Organic sludge
Lead

ABSTRACT

The main objectives of this work are to investigate the consequences of different chemical treatments (*i.e.* potassium hydroxide (KOH) and hydrogen peroxide (H_2O_2)) and the effect of biochar washing on the Pb sorption capacity. Biochars derived from sewage sludge digestate and the organic fraction of municipal solid waste digestate were separately modified with 2 M KOH or 10% H_2O_2 followed by semi-continuous or continuous washing with ultrapure water using batch or a column reactor, respectively. The results showed that the Pb adsorption capacity could be enhanced by chemical treatment of sludge-based biochar. Indeed, for municipal solid waste biochar, the Pb maximum sorption capacity was improved from 73 mg g^{-1} for unmodified biochar to 90 mg g^{-1} and 106 mg g^{-1} after H_2O_2 and KOH treatment, respectively. In the case of sewage sludge biochar, it increased from 6.5 mg g^{-1} (unmodified biochar) to 25 mg g^{-1} for H_2O_2 treatment. The sorption capacity was not determined after KOH treatment, since the Langmuir model did not fit the experimental data. The study also highlights that insufficient washing after KOH treatment can strongly hinder Pb sorption due to the release of organic matter from the modified biochar. This organic matter may interact in solution with Pb, resulting in an inhibition of its sorption onto the biochar surface. Continuous column-washing of modified biochars was able to correct this issue, highlighting the importance of implementing a proper treated biochar washing procedure.

1. Introduction

Metal pollution is of very high concerns for human health due to their persistence and toxicity in the environment even in low concentrations. Lead (Pb) has been recognized as one of the most toxic metals in Europe (Tóth et al., 2016). Pb pollution often originates from smelters, mining, industrial discharges, car batteries and Pb-based piping for water supply. Discharge of untreated wastewater from the industry may cause an adverse effect to animals and humans. One study reported a case of severe Pb poisoning of children in Haina (Dominican Republic), attributed to a car battery recycling factory (Kaul et al., 1999). Many conventional treatment methods have been developed to decrease Pb levels in contaminated water, including chemical precipitation, coagulation, ion exchange and adsorption (Inyang et al., 2016).

Lead sorption by activated carbon (Cechinel et al., 2014), agricultural waste-derived biochars (*e.g.* pine wood or rice husk) (Liu and Zhang, 2009), natural zeolite and kaolinite clay (Andrejkovicova et al., 2016; Jiang et al., 2009) have been reported. Recent studies show the potential application of biochar in metal-polluted water treatment due to its high specific surface area and surface properties, *e.g.* surface charge and hydrophobicity (Liu and Zhang, 2009; Zielińska et al., 2015). Indeed, the solid organic by-product generated by anaerobic digestion of sludge from wastewater treatment plants has been considered as an alternative source of raw material to manufacture adsorbents (*i.e.* biochar) for metal removal (Zhang et al., 2013). Biochar is a black solid char derived from the pyrolysis of organic waste materials in a limiting oxygen environment (Inyang et al., 2016). Through the pyrolysis technology, it promotes the recycling of organic waste and supports

* Corresponding author.
E-mail address: gilles.guibaud@unilim.fr (G. Guibaud).

https://doi.org/10.1016/j.jenvman.2018.04.108
0301-4797/

the environmental sustainability for the community. Biochar has been widely used for many purposes in the environment, such as soil conditioner (Saifullah et al., 2018) or filtration medium in wastewater treatment (Mohan et al., 2014). However, there are only few studies on the use of organic by-product sludge biochar to remove metals from water. Biochar produced from organic digested sludge has been used for As(V), Cd(II), Cr(III), Cu(II) and Ni(II) removal from water (Inyang et al., 2012; Jin et al., 2014). A few studies have been dedicated to the Pb sorption by sludge biochars, which can be found in the literature (Table S1).

The main mechanisms involved in Pb sorption onto the biochar are cation exchange, surface complexation, surface precipitation and physical adsorption (Ho et al., 2017; Li et al., 2017). Among these mechanisms, cation exchange of Pb with Ca^{2+} and Mg^{2+} and is the main contributor to Pb sorption by sludge-based biochar, accounting for 40–52%. Exchanges can also occur to a lesser extend with K^+ and Na^+ and (<8.5%) (Li et al., 2017), which is in a good agreement with the study of Lu et al. (2012). The surface complexation between Pb and surface functional groups of biochar (*e.g.* carboxyl and hydroxyl groups) also plays a major role, contributing for about 40% of Pb removal (Li et al., 2017). Surface precipitation can also occur since sludge biochars generally contain high amounts of phosphate (PO_4^{3-}) and carbonate (CO_3^{2-}) on their surface. Finally, the high surface area of biochar may favor physical adsorption of Pb onto biochar active pore sites (Agrafioti et al., 2014). The relative importance of these sorption mechanisms depends on the biochar feedstock.

Compared to activated carbon, the sorption capacity for Pb by biochar is low and thus numerous modification methods have been applied to improve it. The common treatment methods of biochar are physical activation with steam and chemical treatment with acids, oxidizing agents and alkali solutions (Sizmur et al., 2017). The steam activation of biochar is usually performed at high temperature (>800 °C), thus increasing the adsorbent cost which it is not feasible for large scale operation (Wang and Liu, 2018). The chemical modification of biochar is considered as an inexpensive technique since no heat is required during the operation. Treatment of biochar with KOH increases the surface hydroxyl groups and the basicity on the biochar surface (Fan et al., 2016; Li et al., 2014), dissolves ash and condenses organic matter (*e.g.* lignin and celluloses) in the biochar (Lin et al., 2012; Liou and Wu, 2009; Liu et al., 2012). Modification of biochar with H_2O_2 was found to increase O–containing functional groups, particularly carboxyl groups, on the biochar surfaces (Rajapaksha et al., 2016). Such chemical modifications could induce a leaching of organic matter and mineral ash from biochar pore sites. Thus, after the treatment, several batch washing of the biochar with ultrapure water are required until the pH becomes stable or neutral (Huang et al., 2017; Regmi et al., 2012; Wu et al., 2017). Usually, batch washing of biochar is performed without any concerns on the release of organic or inorganic compounds (*e.g.* PO_4^{3-} and CO_3^{2-}) from biochar. Since this can influence the sorption of metals by biochar, the effective elimination of these released compounds should be considered. Unfortunately, there is currently a lack of information on the effect of biochar washing on the elimination of the released compounds from biochar after chemical treatment.

This work aims to study the consequences of chemical treatments of biochar and subsequent washing conditions on the Pb sorption capacity. Two chemical reagents (*i.e.* KOH and H_2O_2) and two washing modes (semi-continuous batch washing as usually performed in the literature and continuous column washing) were applied to raw biochars from sewage sludge and the organic fraction of municipal solid waste. The consequences onto the Pb sorption were evaluated through adsorption kinetic and isotherm studies.

2. Materials and methods

2.1. Feedstocks and biochar preparation

Raw sewage sludge digestate (RSS) and raw organic fraction of municipal solid waste digestate (RMSW) were obtained separately from a wastewater treatment plant and from a solid waste treatment plant located in France. Biochar from RSS was industrially pyrolyzed at 350 °C for 15 min using the Biogreen® technology, while biochar from RMSW was produced at lab scale. Based on the study of Pituello et al. (2014), the RMSW was dried overnight at 65 °C to reduce the initial moisture content to less than 10%. After that, it was crushed and sieved into a particle size of 2 mm to separate impurities such as plastic bags, needles and glasses. The RMSW-derived biochar was produced at 400 °C using porcelain crucibles with lid-cover (Haldenwanger 79 MF, Germany) in a muffle furnace (heating rate 15 °C min^{-1}) for 1 h. The obtained materials were left to cool down at room temperature with the lids cover.

As recommended by Jin et al. (2014), Wu et al. (2017) and Xue et al. (2012), biochars were washed by semi-continuous means with ultrapure water for 3–4 times (*i.e.* 2 g of biochar per 200 mL of ultrapure water per washing) until a stable pH was obtained. The RSS-derived biochar produced at 350 °C and the RMSW-derived biochar produced at 400 °C are named as SS^{sem} and MSW^{sem}, respectively.

2.2. Biochar chemical modification

In this study, KOH and H_2O_2 were selected for the chemical modification of biochar due to the great enhancement of metal sorption (Rajapaksha et al., 2016). To prepare the modified biochar with H_2O_2, 2 g of biochar was placed into 20 mL of a 10% H_2O_2 solution and shaken at 25 (±2) °C for 2 h (modified from Xue et al., 2012). Biochar treated with KOH was prepared by mixing 2 g biochar with 100 mL of 2 M KOH solution and was shaken at 25 (±2) °C for 2 h (modified from Jin et al., 2014). The total mass of biochar used was around 10 g per each chemical treatment. After chemical modification, biochars were all semi-continuously washed with ultrapure water. Some biochars were submitted to a subsequent continuously washing to study the influence of the washing conditions.

For the semi-continuous washing, the chemically modified biochar was washed in batch by stirring 2 g of biochar in 200 mL of ultrapure water at 20 (±2) °C. The batch washing was repeated for 3–4 times until the pH became stable (Jin et al., 2014; Wu et al., 2017; Xue et al., 2012). For the continuous washing, a part of the semi-continuous washed biochar was subsequently washed by continuous circulation of ultrapure water in a glass column (2.8 cm in diameter and 42.5 cm in height). A peristaltic pump (Ismatec Reglo Analog, Model No. ISM827, Ismatec SA Company, Switzerland) was used to maintain the up-flow velocity of 0.77 (±0.01) cm min^{-1}. Glass beads (2 mm size) were used at the bottom of the column to generate the flow distribution. The column was flushed continuously for at least 70 h at 20 (±2) °C with a hydraulic retention time of 6 h.

Once washed, the modified biochars were recovered using VWR filter papers, then dried in an oven at 50 °C overnight and further kept in a desiccator prior to use. The semi-continuously washed H_2O_2 and KOH-treated biochars are labeled as MSW-$H_2O_2^{sem}$, MSW-KOH^{sem}, SS-$H_2O_2^{sem}$ and SS-KOH^{sem} for RMSW and SS based biochar, respectively. The continuously washed H_2O_2 and KOH-treated sewage sludge biochars are labeled as SS-$H_2O_2^{con}$ and SS-KOH^{con}, respectively.

2.3. Biochar characterization

The pH of the biochar was measured using a pH meter (LPH 330T, Tacussel, France). A suspension of 1 g of sample in 20 mL of deionized water was stirred continuously for 5 min and let to suspend for 15 min.

To quantify the total content of metal(loid)s (*i.e.* Al, As, Cd, Cr, Cu, Ni, Pb, Mn, Fe and Zn) and cationic macroelements (*i.e.* Ca, K, Mg and Na) in biochar, an acid digestion was performed using H_2O_2 (30% w/w, Sigma-Aldrich) and concentrated HCl (37% w/w, Merck) and HNO_3 (65% w/w, Merck) according to EPA Method 3050B (EPA, 1996). The digestion was carried out in a heating block at 95 (±5) °C. After filtration with a Whatman grade 1 qualitative filter paper, trace elements were analyzed using inductively coupled plasma optical emission spectroscopy (ICP-OES) (Optima 8300, PerkinElmer, France).

An X-ray powder diffractometer (AXS D8, Bruker, Germany) was used to identify the crystalline structures of the biochars. Fourier transform infrared (FTIR) spectroscopy (IRAffinity-1, Shimadzu, Japan) was used to identify surface functional groups of biochar with a deuterated-triglycine sulfate (DTGS) detector. The details of the sample preparation for XRD and FTIR analysis are described in the Supplementary Information. Brunauer-Emmett-Teller (BET) specific surface area of chemically-modified biochar samples were determined using the N_2 adsorption method at 77 K (3Flex, Micromeritics, USA). Before BET analysis, the biochar samples were dried at 105 °C for 5 h.

2.4. Characterization of solution after column washing of biochar

During continuous washing of SS-KOH^{sem} and SS-$H_2O_2^{sem}$, liquid samples were collected at the outlet of the column over time to measure pH (LPH 330T, Tacussel, France), conductivity (CDM 210 conductivity-meter, Radiometer, Copenhagen, Denmark), dissolved organic carbon (DOC), PO_4^{3-}, CO_3^{2-} and bicarbonate HCO_3^-. Dissolved organic carbon was determined using a TOC Analyzer (multi N/C® 2100S, Analytikjena, Germany) according to the standard method from Afnor (Afnor, 1997a). A colorimetric method (Afnor, 1997b) was used to measure PO_4^{3-} with a spectrophotometer (DR1900, Hach, France) at λ 700 nm. For CO_3^{2-} and HCO_3^-, they were analyzed by a titrimetric method (Afnor, 1996) using 10^{-3} M HCl as a titrant and phenolphthalein and mixed bromocresol green-methyl red as indicators. Microwave Plasma Atomic Emission Spectroscopy (MP-AES) (Agilent 4100, Agilent Technologies Inc., USA) was used to analyze the released concentration of Ca and Mg at λ 422.673 nm and λ 285.213 nm, respectively.

2.5. Sorption experiments

A stock solution of 1000 mg L^{-1} Pb(II) was prepared from $Pb(NO_3)_2$. The solution was diluted in the range from 10 to 1000 mg L^{-1} and the initial solution pH was adjusted to 5.0 (±0.2) by using 0.1 M HNO_3 or 0.1 M NaOH. For all sorption experiments, 100 mg biochar was added to 25 mL of Pb solution and shaken at 20 (±2) °C using an orbital shaker (KS 501 digital, IKA™, USA) at 180 rpm. All experiments were conducted in triplicate and the average values are reported. Additional analyses were performed when variations over 10% were observed. Samples were filtered through Whatman polyethersulfone syringe filters (0.2 μm) and analyzed by MP-AES (Agilent 4100, Agilent Technologies Inc., USA) at λ 405.781 nm to quantify the remaining Pb concentration in solution.

Adsorption kinetic tests for Pb sorption onto raw and chemically-modified biochars from semi-continuous washing conditions (*i.e.* MSW^{sem}, MSW-$H_2O_2^{sem}$, MSW-KOH^{sem}, SS^{sem}, SS-$H_2O_2^{sem}$ and SS-KOH^{sem}) were performed to determine the time required to reach sorption equilibrium and the sorption kinetic constants using pseudo-first-order (PFO) and pseudo-second-order (PSO) models (kinetic equations are presented in Supplementary Information). These experiments were carried out with 100 mg L^{-1} Pb initial concentration, samples being collected after 10 min, 20 min, 30 min, 1 h, 2 h, 5 h, 7 h and 24 h of stirring.

Adsorption isotherms were performed with initial Pb concentrations between 10 and 1000 mg L^{-1}. Two common adsorption isotherm models (Langmuir and Freundlich) were used to fit the experimental data. The details of these adsorption isotherm equations are provided in the Supplementary Information.

3. Results and discussion

3.1. Characterization of raw and chemically modified biochars

The pH of suspensions of the raw and modified biochars is given in Table 1. A higher pH of the biochar compared to the raw feedstock was observed on both the organic fraction of municipal solid waste and sewage sludge digestate samples. The pH of MSW^{sem} and SS^{sem} was 8.9 and 6.5, respectively. This can be due to the presence of alkali compound (*i.e.* calcite) in the organic fraction of municipal solid waste biochar, while this component was not detected in sewage sludge digestate derived biochars (Fig. 1(S)). Chemical modification with KOH induced a significant shift to higher pH values, while a marginal pH variation was observed after H_2O_2 treatment (Table 2).

Table 1 shows the content of Ca, Mg, Na and K contained in the raw organic digestates (*i.e.* RMSW and RSS) and the derived biochars (*i.e.* MSW^{sem} and SS^{sem}). It was noticed that higher cationic macroelements were found in MSW^{sem} compared to SS^{sem}, particularly for Ca which was almost 4–fold higher in the former than in the latter (Table 1). In addition, the chemical characteristics such as ash and metal(loid) composition of RMSW, MSW^{sem}, RSS and SS^{sem} are reported in Table S2. The XRD characterization demonstrates kaolinite, quartz and calcite were present in the biochars (Fig. S1). The presence of these mineral phases on the biochar surface could facilitate the sorption of metals (Al-Degs et al., 2006; Jiang et al., 2009). Additionally, biochar displays the presence of Al, Fe and Mn (Table 1) that could be partially in metal oxide form, *i.e.* Al_2O_3, Fe_2O_3 and MnO. Thus, this could also promote interaction between the metal ions and biochar (Agrafioti et al., 2014; Wang et al., 2015).

FTIR spectra of MSW^{sem} and SS^{sem} show variations of the surface functional groups according to different biochar types (Fig. S2(a)).

Table 1
The pH and concentrations of Ca, K, Mg, Na, Al, Fe and Mn in the raw organic fraction of municipal solid waste digestate (RMSW), its derived biochar (MSW^{sem}) with semi-continuous washing, raw sewage sludge digestate (RSS) and its derived biochar (SS^{sem}) with semi-continuous washing.

Biochar	pH in water	Ca (g kg^{-1})	K (g kg^{-1})	Mg (g kg^{-1})	Na (g kg^{-1})	Al (g kg^{-1})	Fe (g kg^{-1})	Mn (mg kg^{-1})
RMSW	8.0 ± 0.1	89.2 ± 1.4	32.1 ± 0.3	7.3 ± 0.1	32.2 ± 0.2	17.6 ± 0.2	11.4 ± 0.1	322.9 ± 2.7
MSW^{sem}	8.9 ± 0.1	114.9 ± 0.4	21.8 ± 0.2	10.4 ± 0.1	31.9 ± 0.2	14.2 ± 0.1	16.1 ± 0.2	417.4 ± 2.9
RSS	6.0 ± 0.1	20.2 ± 0.3	3.6 ± 0.9	5.3 ± 0.1	4.2 ± 0.5	11.4 ± 0.4	66.0 ± 0.8	476.9 ± 6.3
SS^{sem}	6.5 ± 0.1	29.5 ± 0.4	4.4 ± 0.1	8.0 ± 0.1	4.6 ± 0.1	14.3 ± 0.2	65.7 ± 0.8	769.9 ± 8.0

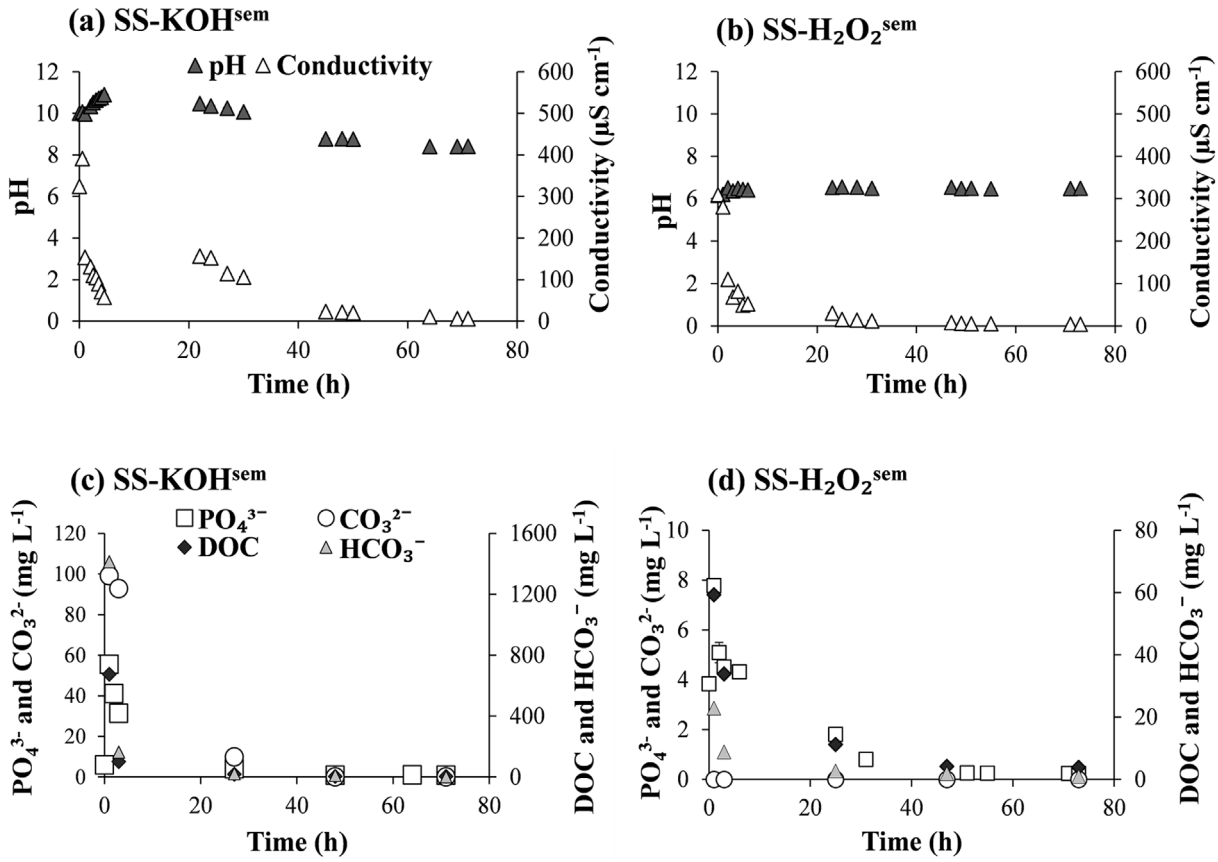

Fig. 1. Evolution of pH and conductivity during continuous washing of SS-KOH^{sem} (a) and SS-$H_2O_2^{sem}$ (b), and concentration profile of phosphate, (bi)carbonate and dissolved organic carbon (DOC) along continuous washing of SS-KOH^{sem} (c) and SS-$H_2O_2^{sem}$ (d).

Table 2
The pH and specific surface area of chemically-modified sewage sludge digestate biochar with semi-continuous washing (SS-$H_2O_2^{sem}$ and SS-KOH^{sem}) and with continuous washing (SS-$H_2O_2^{con}$ and SS-KOH^{con}).

Biochar	pH in water	S_{BET}[a] ($m^2\ g^{-1}$)
SS-$H_2O_2^{sem}$	6.2 ± 0.1	3.6 ± 0.1
SS-KOH^{sem}	10.1 ± 0.1	3.0 ± 0.1
SS-$H_2O_2^{con}$	6.5 ± 0.1	5.7 ± 0.1
SS-KOH^{con}	8.4 ± 0.1	7.9 ± 0.1

[a] S_{BET} refers to Brunauer–Emmett–Teller (BET) surface area of biochar.

After alkali modification, stronger absorbance peaks corresponding to vibration of O–H functional groups (3425 cm^{-1}), $-CH_3$ stretching of long chain aliphatic groups (2924 cm^{-1}) and vibration of the C–C skeleton and C–O stretching (1033 cm^{-1}) were found, especially on SS-KOH^{sem} (Fig. S2(b)). Similar observations were reported by Petrovic et al. (2016) after alkali treatment of biochars. In addition, the FTIR spectra became more intense after H_2O_2 modification, particularly at 1640 cm^{-1} which is assigned to the vibrations of C=O bands (ester) (Fig. S2(b)). Such surface functional groups can take part in the sorption mechanisms for metals (Chen et al., 2011; Pituello et al., 2014).

From Table 2, the BET specific surface areas of SS-$H_2O_2^{sem}$ and SS-KOH^{sem} were 3.7 and 3.0 $m^2\ g^{-1}$, respectively. These values increased after continuous washing with ultrapure water, probably due to the elimination of the ash content or organic matter from biochar pore sites.

3.2. Effect of biochar washing after chemical modification

After several batch-washings (semi-continuous mode) of KOH and H_2O_2–treated sewage sludge biochar, a subsequent column washing (continuous mode) was performed to highlight possible releases of organic or inorganic compounds from the biochar.

Fig. 1(a) and (b) represent the evolution of pH and conductivity of SS-KOH^{sem} and SS-$H_2O_2^{sem}$, respectively, along the column washing time. During the initial stage of washing (0–5 h), increases in pH were noticed for both KOH and H_2O_2–treated sewage sludge biochar. However, after 23 h, the pH of SS-KOH^{sem} started to decrease steadily before it became stable at pH 8.4 (after 64 h). The pH values remained almost unchanged at 6.5 (±0.1) for SS-$H_2O_2^{sem}$ beyond 23 h. On the other hand, decreasing trends of conductivities throughout the manipulation were observed on both chemically-modified biochars (Fig. 1 (a, b)). The values dramatically dropped from 309 to 391 µS cm^{-1} (at the beginning) to 4–6 µS cm^{-1} (at the end of operation), which was comparable to the conductivity of ultrapure water from the inlet flow (~3 µS cm^{-1}).

Fig. 1(c) and (d) show the changes of phosphate, inorganic carbon and dissolved organic matter released from SS-KOH^{sem} and SS-$H_2O_2^{sem}$, respectively, during column washing. The reduction of the PO_4^{3-}, CO_3^{2-}, HCO_3^- and DOC concentrations occurred continuously throughout the period of biochar washing (Fig. 1 (c, d)). Such evolutions are consistent with the conductivity trends (Fig. 1(a, b, c, d)). For instance, the high release of PO_4^{3-} (55 mg L^{-1}), CO_3^{2-} (99 mg L^{-1}) and HCO_3^- (1418 mg L^{-1}) from KOH-treated biochar was related to the high conductivity (391 µS cm^{-1}) (Fig. 1(a, c)) at the initial washing stage. Declining trends of the released compounds were

observed along the lower conductivity level (Fig. 1(a, c)). Similarly, SS-$H_2O_2^{sem}$ showed the same behavior as SS-KOH^{sem}, but with much lower PO_4^{3-}, CO_3^{2-}, HCO_3^- and DOC concentrations (Fig. 1 (b, d)). By comparing KOH and H_2O_2 treatment, it appears that after KOH treatment the biochar released more organic compounds, PO_4^{3-} and HCO_3^-/CO_3^{2-} compared to the H_2O_2 treatment. The DOC released was about 10-fold higher for SS-KOH^{sem} than for SS-$H_2O_2^{sem}$ (at 1 h) (Fig. 1(c and d)). This is likely due to the property of KOH to modify the biochar surface. A similar behavior could be observed on the FTIR spectra, with a significant increase of transmittance for SS biochar treated with KOH (Fig. S2(b, c)).

These results clearly illustrate that a semi-continuous washing of chemically-treated biochar up to a stable pH was not sufficient to prevent the release of organic matter and ions. Indeed, in the batch reactor an equilibrium of released elements was achieved and the pH is usually used as an indicator for biochar washing (Huang et al., 2017; Regmi et al., 2012; Wu et al., 2017). However, to directly control the release of ions such as PO_4^{3-} and HCO_3^-/CO_3^{2-} from the biochar, conductivity is proposed as a more accurate parameter rather than the pH. Therefore, a continuous washing with conductivity monitoring is recommended.

3.3. Adsorption kinetics

Fig. 2 shows the effect of contact time on the Pb removal capacity of MSW^{sem}, MSW-$H_2O_2^{sem}$, MSW-KOH^{sem}, SS^{sem}, SS-$H_2O_2^{sem}$ and SS-KOH^{sem}. The time required to reach the equilibrium state was different for each biochar type (Fig. 2). For sewage sludge based biochars, the equilibrium time was achieved after 5 h for raw SS^{sem}, 7 h for SS-$H_2O_2^{sem}$ and 2 h for SS-KOH^{sem}, while MSW–based biochars showed faster kinetics compared to SS biochars in which the equilibrium time was reached within 5 h for MSW^{sem}, 2 h for MSW-KOH^{sem} and 1 h for MSW-$H_2O_2^{sem}$.

The data of the kinetic experiments were fitted using pseudo-first-order and pseudo-second-order equations. The corresponding kinetic parameters are given in Table S3. The pseudo-second order kinetic model was the most suitable to fit the experimental data for all biochars (Table S3). Considering the parameter k_2, it could be concluded that MSW-$H_2O_2^{sem}$ exhibited the fastest kinetic rate followed by MSW-KOH^{sem}, SS-KOH^{sem}, MSW^{sem}, SS^{sem} and SS-$H_2O_2^{sem}$ (Table S3). In addition, the equilibrium adsorption capacities determined by the second order model (Q_e) were in agreement with the experimental ones ($Q_{e,exp}$) (Table S3).

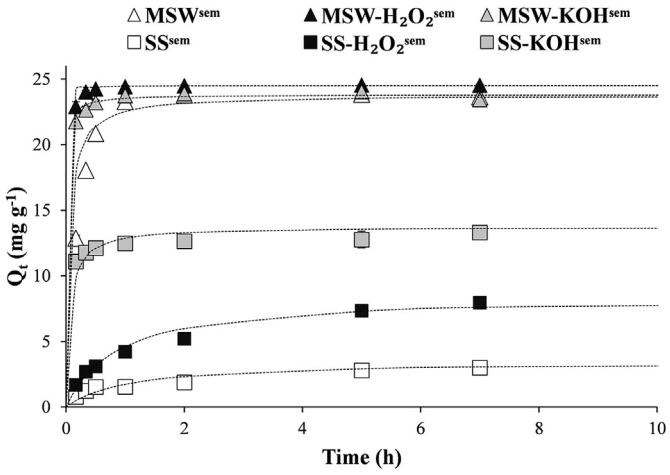

Fig. 2. Adsorption kinetics for Pb by semi-continuous washed MSW^{sem}, MSW-$H_2O_2^{sem}$, MSW-KOH^{sem}, SS^{sem}, SS-$H_2O_2^{sem}$ and SS-KOH^{sem} at different contact times at an initial solution pH of 5 and initial Pb concentration of 100 mg L^{-1} fitted with the pseudo-second order kinetic model.

Comparison of the different chemical modifications for biochar indicated that the alkali treatment (KOH) could induce a faster Pb removal rate, especially for the organic fraction of municipal solid waste (MSW) biochar. This was supported by a previous study from Regmi et al. (2012) on a switchgrass biochar treated with alkali reagent. In contrast, biochar modified with an oxidizing agent (H_2O_2) may not always increase the kinetic rate for Pb sorption. In this case, SS-$H_2O_2^{sem}$ reached equilibrium slightly slower than SS^{sem}.

Different kinetic rates for Pb adsorption were observed when comparing SS^{sem} and MSW^{sem}, the former requiring a longer time to reach sorption equilibrium. This was mainly due to differences in biochar properties resulting from the different origin of these biochars. FTIR spectra show stronger peaks of O–containing functional groups in MSW^{sem} compared to SS^{sem} especially at 1033 cm^{-1} (Fig. S2(a)), which could induce a faster kinetic rate for metals (Bogusz et al., 2017). In addition, MSW^{sem} biochar contained calcite on its surface (Fig. S1(a)) and had higher cationic macroelements (*i.e.* Ca, K, Mg and Na) content than SS^{sem} biochar (Table 1) which could promote cationic metal (*i.e.* Pb) binding onto MSW^{sem} biochar. This is consistent with the study of Zhang et al. (2017) on the use of celery biochars with high amounts of alkaline minerals for cationic metal removal from aqueous solutions. However, the physical properties of biochar like porosity and specific surface area should be also considered as they play a role during the adsorption process.

3.4. Adsorption isotherms

Fig. 3(a) and (b) show the adsorption isotherms for Pb by semi-continuous washed SS^{sem}, SS-$H_2O_2^{sem}$, SS-KOH^{sem} and by MSW^{sem}, MSW-$H_2O_2^{sem}$ and MSW-KOH^{sem}, respectively. Table 3 presents the fitting parameters of the Langmuir and Freundlich isotherm models. All experimental data could be well-described by the Langmuir adsorption isotherms model ($R^2 > 0.98$), except for SS-KOH^{sem}.

The results from Fig. 3(a) demonstrate that chemical treatment of biochar could enhance the Pb sorption capacity from 6.5 mg g^{-1} on SS^{sem} to 25.1 mg g^{-1} on SS-$H_2O_2^{sem}$. However, it was completely different for SS-KOH^{sem} due to unexpected low Pb adsorption capacities at low equilibrium Pb concentration (0–50 mg L^{-1}). As a result, the Langmuir model failed to describe the behavior of this sorption curve. One hypothesis is that a large amount of organic matter released from SS-KOH^{sem} (Fig. 1(c)) inhibits the Pb sorption onto the biochar by forming soluble Pb-ligand complexes, resulting in lower Q_e values at the low C_e range (0–50 mg L^{-1}).

Fig. 3(b) shows that the Pb sorption capability was improved by KOH and H_2O_2 treatment of MSW biochar. It increased from 72.9 mg g^{-1} for MSW^{sem} to 90.0 mg g^{-1} and 106.3 mg g^{-1} for MSW-$H_2O_2^{sem}$ and MSW-KOH^{sem}, respectively. This implies that chemical treatment could be effectively used to promote Pb sorption onto the organic fraction of municipal solid waste-based biochar.

Fig. 4(a) shows the Pb adsorption isotherms on sewage sludge digestate–based biochars fitted with the Langmuir model (except KOH^{sem} due to non-fitting). Fig. 4(b) and (c) compare the adsorption isotherms obtained for two different washing systems: batch semi-continuous versus batch followed by column continuous washing. From Fig. 4(b), a significant enhancement of Pb sorption by KOH^{con} (continuous washed) was observed compared to KOH^{sem} (semi-continuous washed) particularly at low C_e (0–50 mg L^{-1}, highlighting the importance of biochar washing after chemical treatment. These results are consistent with the hypothesis of Pb sorption inhibition due to the formation of soluble complexes with organic matter released by the biochar. Such compounds were removed during the subsequent column washing, leading to a

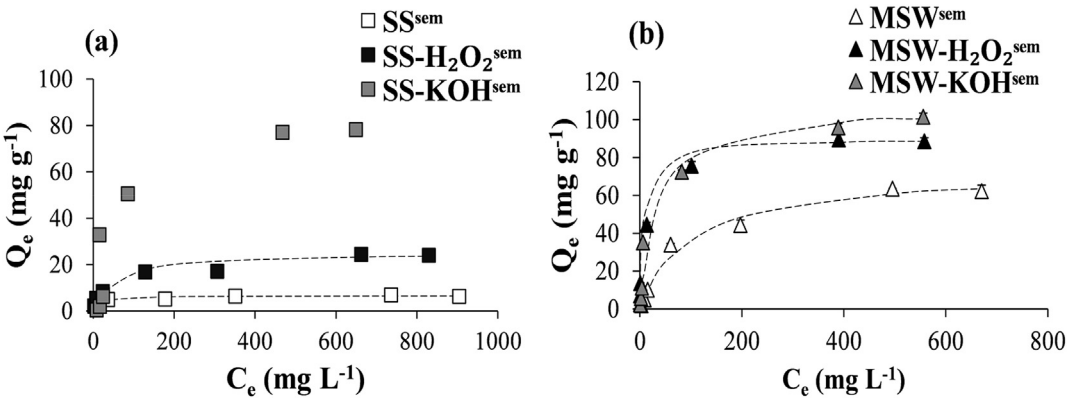

Fig. 3. Adsorption isotherms for Pb by semi-continuous washed SS^{sem}, SS-$H_2O_2^{sem}$ and SS-KOH^{sem} (a) and by MSW^{sem}, MSW-$H_2O_2^{sem}$ and MSW-KOH^{sem} (b) at different equilibrium Pb(II) concentrations at an initial solution pH of 5 fitted with the Langmuir model (except SS-KOH^{sem} due to non-fitting).

Table 3
Effect of biochar modification (H_2O_2 and KOH) and biochar washing (semi-continuous and continuous) on the Pb adsorption capacity.

Biochar	Langmuir isotherm model			Freundlich isotherm model		
	Q_m(mg g^{-1})	K_L (L mg^{-1})	R^2	K_F (mg g^{-1})(L mg^{-1})$^{1/n}$	n	R^2
MSW^{sem}	72.9	0.010	0.992	1.430	1.584	0.940
MSW-$H_2O_2^{sem}$	90.0	0.109	0.999	9.895	2.624	0.894
MSW-KOH^{sem}	106.3	0.030	0.997	4.908	1.888	0.860
SS^{sem}	6.5	0.069	0.994	2.136	5.646	0.782
SS-$H_2O_2^{sem}$	25.1	0.018	0.984	2.117	2.633	0.955
SS-KOH^{sem}	151.5	0.001	0.293	1.201	1.472	0.566
SS-$H_2O_2^{con}$	12.0	0.034	0.993	1.952	3.527	0.967
SS-KOH^{con}	80.6	0.037	0.987	12.406	3.462	0.926

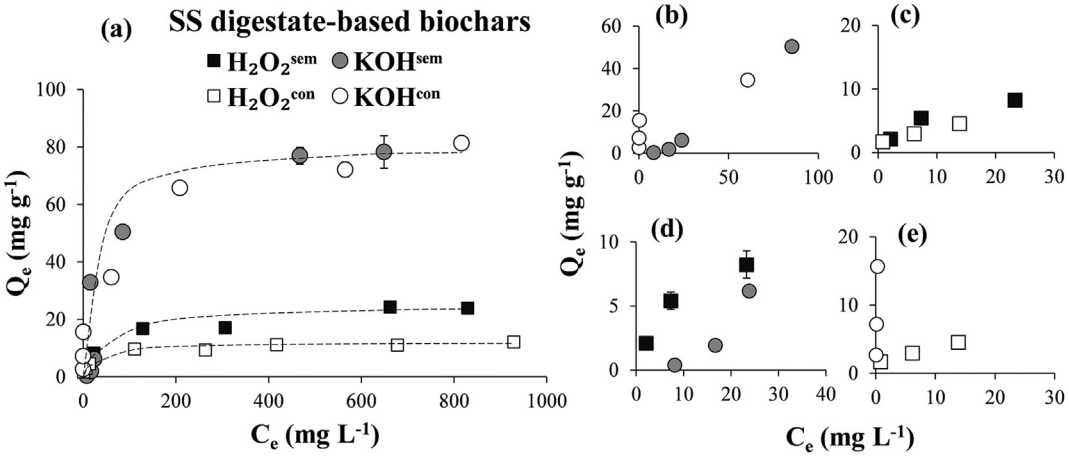

Fig. 4. Comparison of the Pb adsorption isotherms on sewage sludge digestate-based biochars with different washing modes fitted with the Langmuir model (except KOH^{sem} due to non-fitting) (a). Figure (b) to (e) are zooms of C_e at low concentration ranges (<100 mg L^{-1}); semi-continuous washed KOH^{sem} versus continuous washed KOH^{con} (b), $H_2O_2^{sem}$ versus $H_2O_2^{con}$ (c), and with different chemical treatments; KOH^{sem} versus $H_2O_2^{sem}$ (d), and KOH^{con} versus $H_2O_2^{con}$ (e).

higher sorption capacity for KOH^{con} compared to KOH^{sem}, especially at low Pb equilibrium concentrations. In addition, the Langmuir adsorption model was then able to fit with experimental data of KOH^{con} (Table 3). However, no significant differences in Pb sorption capacities between KOH^{sem} and KOH^{con} were observed at higher C_e (400–1000 mg L^{-1}) (Fig. 4(a)). This implies that the presence of organic matter in aqueous solutions significantly affects the Pb sorption onto biochar only at low Pb ion concentrations, especially <50 mg L^{-1}.

In contrast, similar adsorption capacities for Pb by both $H_2O_2^{sem}$ and $H_2O_2^{con}$ were achieved, even at low Pb equilibrium concentrations (0–30 mg L^{-1}, Fig. 4(c)). This is because H_2O_2 treatment induced a small release of inorganic and organic matter from the modified biochar. As a result, batch washing was sufficient and no improvement was obtained with the subsequent column washing.

Fig. 4(d) and (e) compare the adsorption isotherms at low C_e for Pb by H_2O_2 and KOH treated sewage sludge biochars on semi-continuous washing and continuous washing, respectively. The conclusions totally differ according to the washing procedure: the semi-continuous washing indicates that sorption is more important after H_2O_2 (Fig. 4(d)), whereas the continuous washing leads to

the opposite conclusion (Fig. 4(e)). This is the consequence of the uncompleted efficiency of batch washing to remove the released compounds for biochar after KOH treatment.

Considering the maximal sorption capacity (Q_m) of each biochar (Table 3), chemical treatments of biochar with KOH and H_2O_2 show an improved Pb sorption capacity, particularly on sewage sludge digestate biochar. Results show an enhanced Q_m for Pb by almost 2–fold for SS-$H_2O_2^{con}$ and by 12–fold for SS-KOH^{con} with respect to the unmodified SS biochar. The use of KOH for chemical treatment thus appears more efficient than H_2O_2. However, a proper biochar washing procedure after chemical treatment is highly required to prevent the altered isotherm shape.

3.5. Possible Pb sorption mechanisms

Previous studies have illustrated the correlation of sorption for Cu^{2+}, Cd^{2+} and Pb^{2+} with the oxygen-contained functional groups obtained from FTIR analysis (Petrovic et al., 2016; Regmi et al., 2012). The interactions between Pb and available surface functional groups on biochar can occur through surface complexation. In addition, possible cation exchange may take place. This is consistent with the observed release of Ca^{2+} and Mg^{2+} in solution after Pb sorption (Fig. 5).

Fig. 5(a) compares the cations (Ca^{2+} and Mg^{2+}) released by KOH-modified sewage sludge biochars from semi-continuous and continuous washing. The results show that the concentration of Ca^{2+} and Mg^{2+} released from SS-KOH^{sem} was relatively low (<3 mg L^{-1}) at initial Pb concentrations between 0–203 mg L^{-1}. This was in correlation to a low sorption capacity for Pb by SS-KOH^{sem} (see section 3.4). In contrast, a huge release of Ca^{2+} and Mg^{2+} by SS-KOH^{con} was observed at adsorption equilibrium (Fig. 5(a)). The released Ca^{2+} and Mg^{2+} from this biochar was related to the amount of Pb adsorbed onto the biochar surface (on molecular mass basis) (Fig. 5(b)). These findings are in accordance with previous studies of biochars produced from grape pomace and water hyacinth for Pb and Cd removal, respectively (Petrovic et al., 2016; Zhang et al., 2015).

Moreover, the characterization of biochar shows the presence of a mineral phase that could also be involved in Pb sorption (Fig. S1). Nevertheless, previous links between the release of cations from biochar and the Pb sorption capacity show that sorption of Pb by the mineral phase in the biochar is not the main mechanism involved in sorption. In addition, Pb precipitation onto sludge biochar may contribute to the sorption mechanism. The results from the simulation shows that at initial Pb concentrations of 10 and 970 mg L^{-1} (Fig. S3), Pb precipitation onto biochar will likely occur when the final pH values are above 6.0 and above 5.0, respectively. Since the final pH in the solutions of both SS-KOH^{sem} and MSW-KOH^{sem} were above these values, Pb precipitation partly occurred on both biochar types during the sorption experiments.

3.6. Practical implications

The conversion of organic digested sludge obtained from wastewater treatment plants through pyrolysis is considered as a promising approach for sludge management. This corresponds to a huge reduction of the sludge quantity as well as a decrease of metal mobility in the sludge. It also promotes the environmental sustainability strategy due to recycling of the organic wastes and adding more value to the obtained products (*i.e.* biochar).

Chemical modification of biochar has been suggested as an economical technique to improve the sorption performance for Pb. From this study, treatment of biochar with chemical reagents affected the sorption kinetics for Pb. In this case, KOH could induce faster Pb removal rates compared to the unmodified biochars, while it was not systematic for biochars treated with H_2O_2. Furthermore, the chemically-modified biochars reveal a significant Pb sorption enhancement, but with a caution on proper-washed biochar especially with KOH treatment. Indeed, we observed that this treatment led to an inhibition of Pb sorption at low Pb initial concentration linked to the release of complexing compounds (*e.g.* phosphate, (bi)carbonate and organic matter). Thus, a sufficient biochar washing is required to remove these compounds prior to practical applications to ensure an improvement of the Pb sorption features and avoid the contamination of water bodies by the released products. Future research on the effect of biochar washing after chemical treatment is required to better understand the role of released organic compounds and other alkali anion ions on Pb sorption by sludge-based biochar.

4. Conclusions

This study demonstrated the capability of raw digested sludge biochars and chemically-modified biochars in Pb removal from water through adsorption kinetic and isotherm studies. Lead sorption data could be well-described by the Langmuir isotherm model and followed the pseudo-second-order kinetic model. The KOH treatment was found more efficient than the H_2O_2 treatment to improve Pb sorption, with an improvement of both the sorption kinetics and capacity. In the case of sewage sludge biochar, the sorption capacity was about 2–fold and 10–fold higher after H_2O_2 and KOH treatment, respectively. However, special attention should

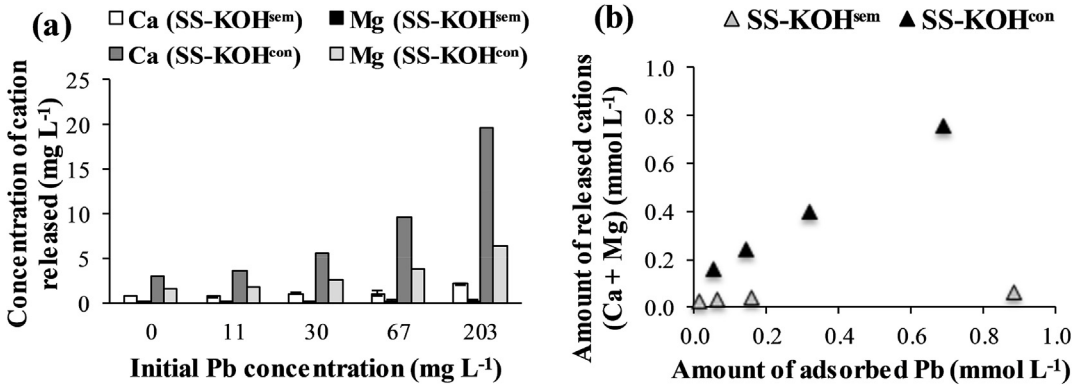

Fig. 5. Comparison of Ca^{2+} and Mg^{2+} released by SS-KOH^{sem} (semi-continuous washed) and SS-KOH^{con} (continuous washed) (a), and the amount of adsorbed Pb versus the summation of the released cations (Ca^{2+} and Mg^{2+}) at Pb adsorption equilibrium (b).

be paid to the washing procedure after chemical modification to avoid an inhibition of metal sorption due to a significant release of soluble compounds from an improperly washed modified biochar.

Acknowledgements

Patrice Fondanèche is acknowledged for technical assistance with the Pb measurement. This research project has received funding from the European Union's Horizon 2020 research and innovation programme under the Marie Sklodowska-Curie grant agreement N° 643071.

Appendix A. Supplementary data

Supplementary data related to this article can be found at https://doi.org/10.1016/j.jenvman.2018.04.108.

References

Afnor, 1997a. Qualité de l'eau. Tome 2. Lignes directrices pour le dosage du carbone organique total (TOC) et carbone organique dissous (COD). Norme EN 1484, sixth ed. France.
Afnor, 1997b. Qualité de l'eau. Tome 3. Dosage du phosphore. Dosage spectrométrique à l'acide du molybdate d'ammonium. Norme EN 1189, sixth ed. France.
Afnor, 1996. Qualité de l'eau. Tome 2. Détermination de l'alcalinité. Norme EN ISO 9963-1, sixth ed. France.
Agrafioti, E., Kalderis, D., Diamadopoulos, E., 2014. Arsenic and chromium removal from water using biochars derived from rice husk, organic solid wastes and sewage sludge. J. Environ. Manage. 133, 309–314.
Al-Degs, Y.S., El-Barghouthi, M.I., Issa, A.A., Khraisheh, M.A., Walker, G.M., 2006. Sorption of Zn(II), Pb(II), and Co(II) using natural sorbents: equilibrium and kinetic studies. Water Res. 40, 2645–2658.
Andrejkovicova, S., Sudagar, A., Rocha, J., Patinha, C., Hajjaji, W., Da Silva, E.F., Velosa, A., Rocha, F., 2016. The effect of natural zeolite on microstructure, mechanical and heavy metals adsorption properties of metakaolin based geopolymers. Appl. Clay Sci. 126, 141–152.
Bogusz, A., Nowak, K., Stefaniuk, M., Dobrowolski, R., Oleszczuk, P., 2017. Synthesis of biochar from residues after biogas production with respect to cadmium and nickel removal from wastewater. J. Environ. Manage. 201, 268–276.
Cechinel, M.A.P., Ulson De Souza, S.M.A.G., Ulson De Souza, A.A., 2014. Study of lead (II) adsorption onto activated carbon originating from cow bone. J. Clean. Prod. 65, 342–349.
Chen, X., Chen, G., Chen, L., Chen, Y., Lehmann, J., McBride, M.B., Hay, A.G., 2011. Adsorption of copper and zinc by biochars produced from pyrolysis of hardwood and corn straw in aqueous solution. Bioresour. Technol. 102, 8877–8884.
EPA, U.S., 1996. Acid digestion of sediments, sludges, and soils, revision, 2, 1–12.
Fan, S., Tang, J., Wang, Y., Li, H., Zhang, H., Tang, J., Wang, Z., Li, X., 2016. Biochar prepared from co-pyrolysis of municipal sewage sludge and tea waste for the adsorption of methylene blue from aqueous solutions: kinetics, isotherm, thermodynamic and mechanism. J. Mol. Liq. 220, 432–441.
Ho, S.H., Chen, Y., Yang, Z., Nagarajan, D., Chang, J.S., Ren, N., 2017. High-efficiency removal of lead from wastewater by biochar derived from anaerobic digestion sludge. Bioresour. Technol. 246, 142–149.
Huang, H., Tang, J., Gao, K., He, R., Zhao, H., Werner, D., 2017. Characterization of KOH modified biochars from different pyrolysis temperatures and enhanced adsorption of antibiotics. RSC Adv. 7, 14640–14648.
Inyang, M., Gao, B., Yao, Y., Xue, Y., Zimmerman, A.R., Pullammanappallil, P., Cao, X., 2012. Removal of heavy metals from aqueous solution by biochars derived from anaerobically digested biomass. Bioresour. Technol. 110, 50–56.
Inyang, M.I., Gao, B., Yao, Y., Xue, Y., Zimmerman, A., Mosa, A., Pullammanappallil, P., Ok, Y.S., Cao, X., 2016. A review of biochar as a low-cost adsorbent for aqueous heavy metal removal. Crit. Rev. Environ. Sci. Technol. 4, 406–433.
Jiang, M., Wang, Q., Jin, X., Chen, Z., 2009. Removal of Pb(II) from aqueous solution using modified and unmodified kaolinite clay. J. Hazard. Mater 170, 332–339.
Jin, H., Capareda, S., Chang, Z., Gao, J., Xu, Y., Zhang, J., 2014. Biochar pyrolytically produced from municipal solid wastes for aqueous As(V) removal: adsorption property and its improvement with KOH activation. Bioresour. Technol. 169, 622–629.
Kaul, B., Sandhu, R.S., Depratt, C., Reyes, F., 1999. Follow-up screening of lead-poisoned children near an auto battery recycling plant, Haina, Dominican Republic. Environ. Health Perspect. 107, 917–920.
Li, H., Dong, X., da Silva, E.B., de Oliveira, L.M., Chen, Y., Ma, L.Q., 2017. Mechanisms of metal sorption by biochars: biochar characteristics and modifications. Chemosphere 178, 466–478.
Li, J., Li, Y., Wu, Y., Zheng, M., 2014. A comparison of biochars from lignin, cellulose and wood as the sorbent to an aromatic pollutant. J. Hazard. Mater 280, 450–457.
Lin, Y., Munroe, P., Joseph, S., Henderson, R., Ziolkowski, A., 2012. Water extractable organic carbon in untreated and chemical treated biochars. Chemosphere 87, 151–157.
Liou, T.H., Wu, S.J., 2009. Characteristics of microporous/mesoporous carbons prepared from rice husk under base- and acid-treated conditions. J. Hazard. Mater 171, 693–703.
Liu, P., Liu, W.J., Jiang, H., Chen, J.J., Li, W.W., Yu, H.Q., 2012. Modification of bio-char derived from fast pyrolysis of biomass and its application in removal of tetracycline from aqueous solution. Bioresour. Technol. 121, 235–240.
Liu, Z., Zhang, F.S., 2009. Removal of lead from water using biochars prepared from hydrothermal liquefaction of biomass. J. Hazard. Mater 167, 933–939.
Lu, H., Zhang, W., Yang, Y., Huang, X., Wang, S., Qiu, R., 2012. Relative distribution of Pb^{2+} sorption mechanisms by sludge-derived biochar. Water Res. 46, 854–862.
Mohan, D., Sarswat, A., Ok, Y.S., Pittman, C.U., 2014. Organic and inorganic contaminants removal from water with biochar, a renewable, low cost and sustainable adsorbent – a critical review. Bioresour. Technol. 160, 191–202.
Petrovic, J.T., Stojanovic, M.D., Milojkovic, J.V., Petrovic, M.S., Sostaric, T.D., Lausevic, M.D., Mihajlovic, M.L., 2016. Alkali modified hydrochar of grape pomace as a perspective adsorbent of Pb^{2+} from aqueous solution. J. Environ. Manage. 182, 292–300.
Pituello, C., Francioso, O., Simonetti, G., Pisi, A., Torreggiani, A., Berti, A., Morari, F., 2014. Characterization of chemical–physical, structural and morphological properties of biochars from biowastes produced at different temperatures. J. Soils Sediment. 15, 792–804.
Rajapaksha, A.U., Chen, S.S., Tsang, D.C.W., Zhang, M., Vithanage, M., Mandal, S., Gao, B., Bolan, N.S., Ok, Y.S., 2016. Engineered/designer biochar for contaminant removal/immobilization from soil and water: potential and implication of biochar modification. Chemosphere 148, 276–291.
Regmi, P., Garcia Moscoso, J.L., Kumar, S., Cao, X., Mao, J., Schafran, G., 2012. Removal of copper and cadmium from aqueous solution using switchgrass biochar produced via hydrothermal carbonization process. J. Environ. Manage. 109, 61–69.
Saifullah, Dahlawi, S., Naeem, A., Rengel, Z., Naidu, R., 2018. Biochar application for the remediation of salt-affected soils: challenges and opportunities. Sci. Total Environ. 625, 320–335.
Sizmur, T., Fresno, T., Akgül, G., Frost, H., Moreno Jiménez, E., 2017. Biochar modification to enhance sorption of inorganics from water. Bioresour. Technol. 246, 34–47.
Tóth, G., Hermann, T., Silva, M.R. Da, Montanarella, L., 2016. Heavy metals in agricultural soils of the European Union with implications for food safety. Environ. Int. 88, 299–309.
Wang, S., Gao, B., Li, Y., Mosa, A., Zimmerman, A.R., Ma, L.Q., Harris, W.G., Migliaccio, K.W., 2015. Manganese oxide-modified biochars: preparation, characterization, and sorption of arsenate and lead. Bioresour. Technol. 181, 13–17.
Wang, Y., Liu, R., 2018. H_2O_2 treatment enhanced the heavy metals removal by manure biochar in aqueous solutions. Sci. Total Environ. 628–629, 1139–1148.
Wu, W., Li, J., Lan, T., Müller, K., Khan, N., Chen, X., Xu, S., Zheng, L., Chu, Y., Li, J., Yuan, G., Wang, H., 2017. Unraveling sorption of lead in aqueous solutions by chemically modified biochar derived from coconut fiber: a microscopic and spectroscopic investigation. Sci. Total Environ. 576, 766–774.
Xue, Y., Gao, B., Yao, Y., Inyang, M., Zhang, M., Zimmerman, A.R., Ro, K.S., 2012. Hydrogen peroxide modification enhances the ability of biochar (hydrochar) produced from hydrothermal carbonization of peanut hull to remove aqueous heavy metals: batch and column tests. Chem. Eng. J. 200–202, 673–680.
Zhang, F., Wang, X., Yin, D., Peng, B., Tan, C., Liu, Y., Tan, X., Wu, S., 2015. Efficiency and mechanisms of Cd removal from aqueous solution by biochar derived from water hyacinth (*Eichornia crassipes*). J. Environ. Manage. 153, 68–73.
Zhang, T., Zhu, X., Shi, L., Li, J., Li, S., Lu, J., Li, Y., 2017. Efficient removal of lead from solution by celery-derived biochars rich in alkaline minerals. Bioresour. Technol. 235, 185–192.
Zhang, W., Mao, S., Chen, H., Huang, L., Qiu, R., 2013. Pb(II) and Cr(VI) sorption by biochars pyrolyzed from the municipal wastewater sludge under different heating conditions. Bioresour. Technol. 147, 545–552.
Zielińska, A., Oleszczuk, P., Charmas, B., Skubiszewska-Zięba, J., Pasieczna-Patkowska, S., 2015. Effect of sewage sludge properties on the biochar characteristic. J. Anal. Appl. Pyrolysis 112, 201–213.

Supplementary Information

Lead sorption by biochar produced from digestates: Consequences of chemical modification and washing

Suchanya Wongrod[a,b,c], Stéphane Simon[c], Gilles Guibaud[c,*], Piet N.L. Lens[b], Yoan Pechaud[a], David Huguenot[a], Eric D. van Hullebusch[a,b]

[a] Université Paris-Est, Laboratoire Géomatériaux et Environnement (EA 4508), UPEM, 77454, Marne-la-Vallée, France

[b] IHE Delft Institute for Water Education, P.O. Box 3015, 2601 DA Delft, The Netherlands

[c] Université de Limoges, PEIRENE-Groupement de Recherche Eau Sol Environnement (EA 7500), Faculté des Sciences et Techniques, 123 avenue Albert Thomas, 87060 Limoges, France

*****Corresponding author: gilles.guibaud@unilim.fr

XRD and FTIR analysis

X-ray diffractometry (XRD) was employed to identify the crystalline structures presented in raw and modified biochars. The samples were grounded to less than 100 µm particle size and were characterized using a powder diffractometer (AXS D8, Bruker, Germany) with Cu Kα radiation at 1.54 Å wavelength, over the 2θ range from 10° to 32°, for 10 seconds per step, at 40 kV voltage and 40 mA current with a Solx (Si-Li) detector. The crystalline compounds present in biochar were identified by search-match software with reference from the American Mineralogist Crystal Structure Database.

Fourier transform infrared spectroscopy (FTIR) were recorded to identify the functional groups present on biochar surfaces. Each sample was mixed with KBr in a ratio of 1 mg sample (particle size 100 µm) per 200 mg KBr and the pellet was prepared by compression under vacuum (Jouraiphy et al., 2005). The analysis was performed using a Shimadzu IRAffinity-1 Spectrometer with a deuterated-triglycine sulfate (DTGS) detector. The number of scans was 12 with a resolution of 16 cm^{-1} and a frequency in a range from 4000 to 800 cm^{-1}.

XRD spectra of biochars

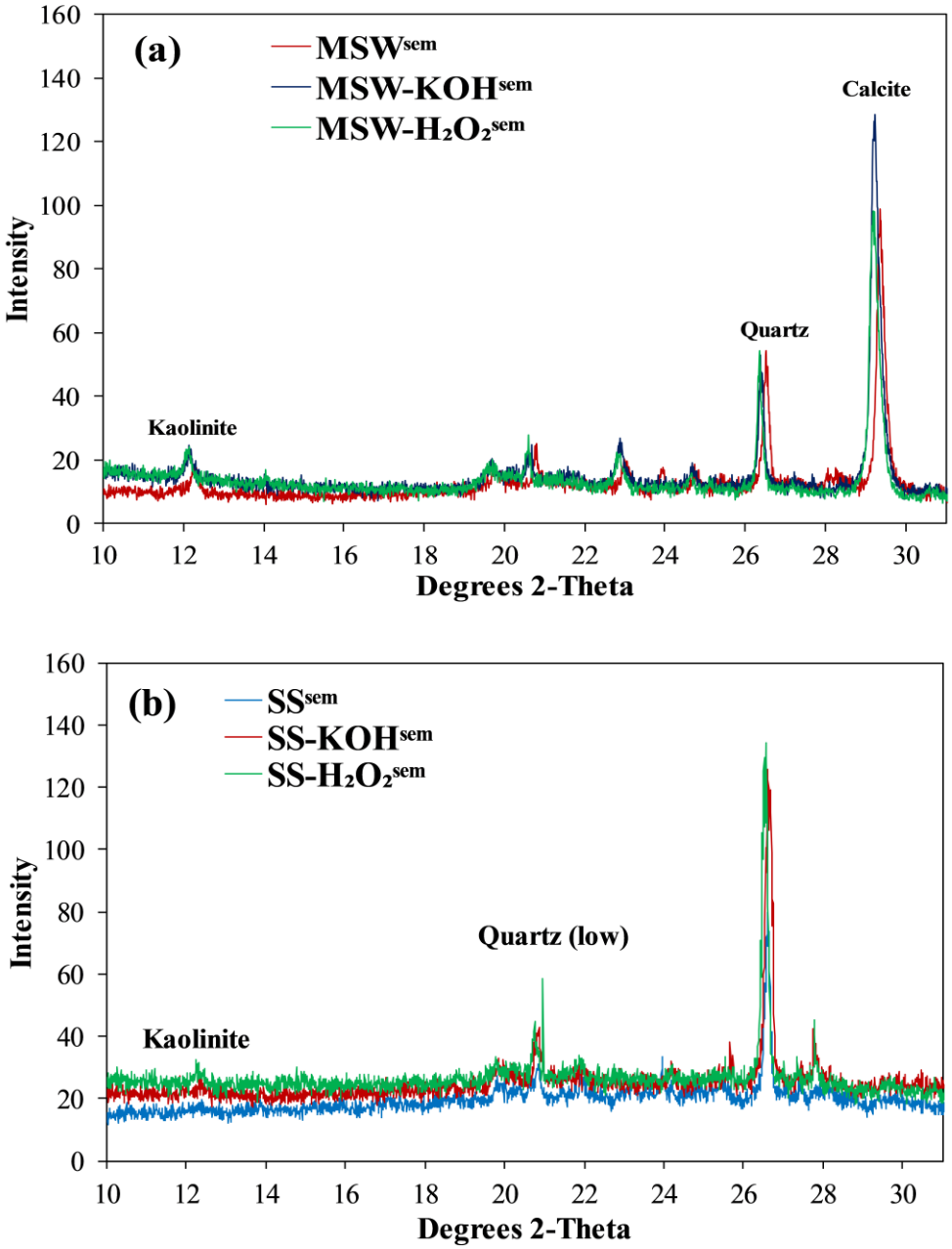

Fig. S1. XRD spectra of semi-continuous washed MSW^{sem}, MSW-KOH^{sem} and MSW-$H_2O_2^{sem}$ (a) and SS^{sem}, SS-KOH^{sem} and SS-$H_2O_2^{sem}$ (b).

XRD analysis showed that MSW^{sem} contained the crystalline structures of kaolinite ($Al_2Si_2O_5(OH)_4$), quartz (SiO_2) and calcite ($CaCO_3$) at 2θ 12.38°, 26.68° and 29.51°, respectively (Fig. S1(a)). Similar trends were also found in its chemically-modified biochar

with slight shifts on the XRD spectra. For instance, the XRD peak of $CaCO_3$ was shifted from 29.36° (MSW^{sem}) to 29.23° ($MSW\text{-}KOH^{sem}$) and 29.20° ($MSW\text{-}H_2O_2{}^{sem}$). On the other hand, only $Al_2Si_2O_5(OH)_4$ and SiO_2 were detected in SS^{sem}, $SS\text{-}KOH^{sem}$ and $SS\text{-}H_2O_2{}^{sem}$ (Fig. S1(b)). The results showed no significant differences of XRD spectra between the raw and chemical treated sewage sludge biochars. Kaolinite and carbonates present in the biochar can be partly involved in adsorption of Pb onto the biochar surface.

FTIR spectra of biochars

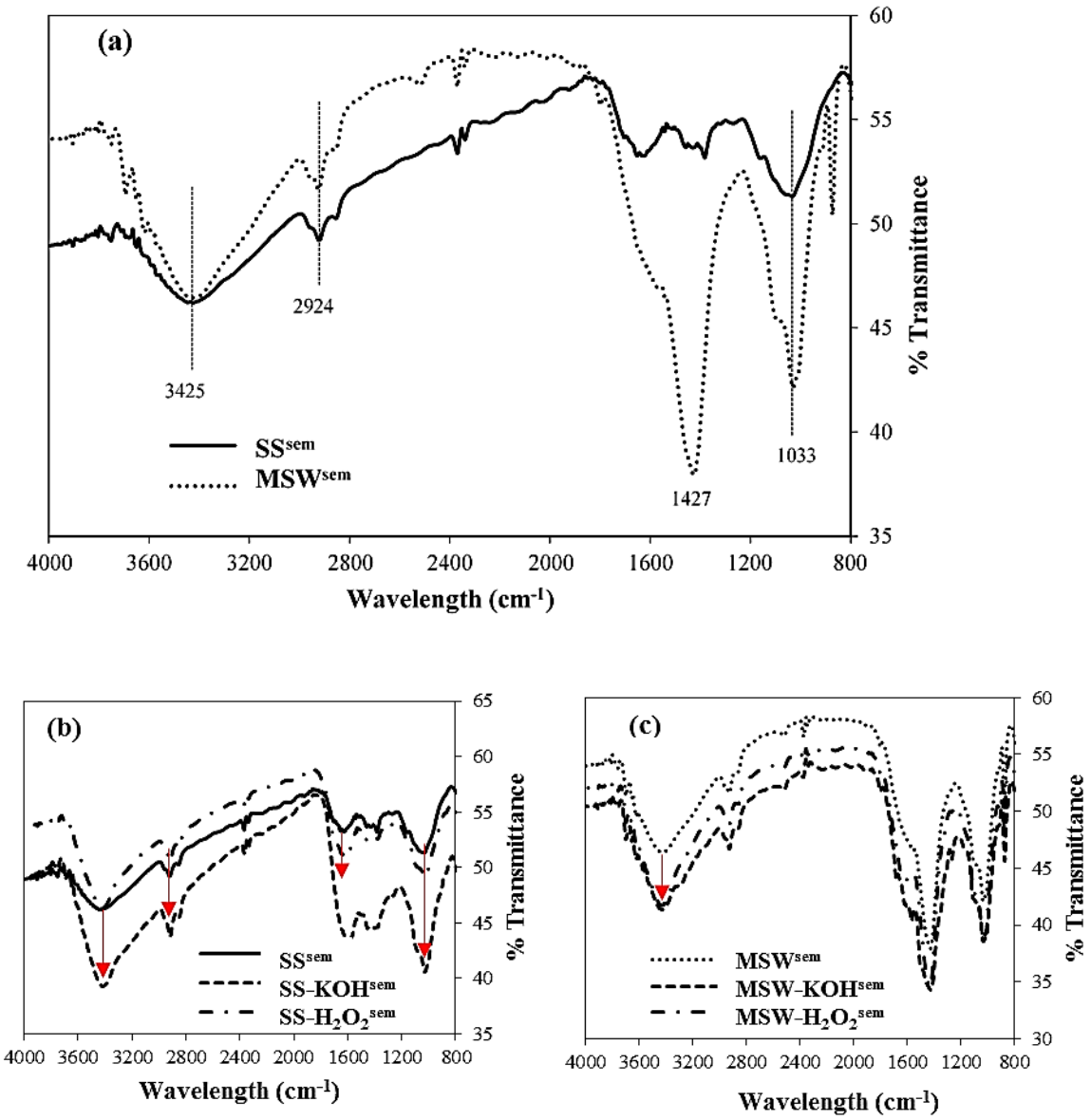

Fig. S2. Comparison of the FTIR spectra of semi-continuous washed SS^{sem} and MSW^{sem} (a), SS^{sem}, SS-KOH^{sem}, SS-$H_2O_2{}^{sem}$ (b), and MSW^{sem}, MSW-KOH^{sem} and MSW-$H_2O_2{}^{sem}$ (c).

The peak band of 3425 cm^{-1} referred to the stretching vibration of O–H functional groups (H-bonded) of alcohols and phenols and was present in all biochars (Fig. S2(a)). The bands at 2924 cm^{-1} was due to the vibration of C–H stretching of long chain aliphatic groups (Chen et al., 2011) and was also found in all biochars (Fig. S2(a)). The bands of 1660–1600

cm^{-1} were assigned to the stretching vibrations of C=C and were observed only in SS^{sem}, SS-KOH^{sem} and SS-$H_2O_2{}^{sem}$ (Fig. S2(b)). Since sewage sludge digestate is generally composed of cellulose, hemicellulose and lignin (Jouraiphy et al., 2005), thus the spectra of the amides band are broad bands of 1690–1640 cm^{-1}. The broad bands between 1442–1384 cm^{-1} was assigned to $–CH_2$ scissoring and were observed in raw and modified biochars from sewage sludge (Fig. S2(b)). A strong intensity of $–CH_2$ scissoring was found at a peak of 1427 cm^{-1} in MSW^{sem}, MSW-KOH^{sem} and MSW-$H_2O_2{}^{sem}$ (Fig. S2(c)). The stretching of carboxylate groups and C–O of alcohols appeared in the sample between 1300 and 1000 cm^{-1}. The peaks at 1033 cm^{-1} were assigned to C–C skeleton vibration and C–O stretching vibration and were found in all biochars (Fig. S2(a, b, c)). The FTIR spectra provide the qualitative information of functional groups present on the surfaces of biochars. The results demonstrated the differences in surface functional groups between MSW^{sem} and SS^{sem} corresponding to different feedstock type and pyrolysis temperature. From Fig. S2(b), it is obvious that there were similar FTIR spectra between SS^{sem}, SS-KOH^{sem}, SS-$H_2O_2{}^{sem}$ with a small shift at 1635 cm^{-1} (SS^{sem}) to 1597 cm^{-1} (SS-KOH^{sem}).

Adsorption kinetics

The simulation of the sorption kinetics for Pb(II) by raw and modified biochars was performed using pseudo-first-order (Eq. 1) and pseudo-second-order (Eq. 2) kinetic models, which are illustrated as followed:

$$\log(Q_e - Q_t) = \log Q_e - \frac{k_1 t}{2.303} \quad (1)$$

$$\frac{t}{Q_t} = \frac{1}{k_2 Q_e^2} + \frac{t}{Q_e} \quad (2)$$

where Q_t and Q_e are Pb(II) adsorption capacity (mg g^{-1}) at time t (h) and equilibrium, k_1 (h^{-1}) and k_2 ($g(mg\ h)^{-1}$) are the rate constants for pseudo-first-order and pseudo-second-order models, respectively (Liu & Zhang, 2009). The pseudo-first-order curves were plotted via $\log(Q_e - Q_t)$ versus time t in which the values of k_1 can be obtained from the slope corresponding to Eq. (1). The pseudo-second-order model was also applied to test the experimental data from the plot of t/Q_t against t, from which Q_e and k_2 values can be calculated from the slope and interception of this plot, respectively.

Adsorption isotherms

Langmuir and Freundlich models are presented in equation (3) and (4), respectively:

$$\frac{C_e}{Q_e} = \frac{1}{K_L Q_m} + \frac{C_e}{Q_m} \quad (3)$$

$$\ln Q_e = \ln K_F + \frac{1}{n} \ln C_e \quad (4)$$

where C_e is the equilibrium Pb solution concentration (mg L^{-1}), Q_e and Q_m are the Pb(II) adsorption capacity at equilibrium and at maximum capacity (mg g^{-1}), n is the Freundlich constant which indicates the favorability of adsorption, and K_L and K_F are the adsorption constants for the Langmuir and Freundlich isotherm models, respectively.

Evolution of pH during Pb adsorption isotherms

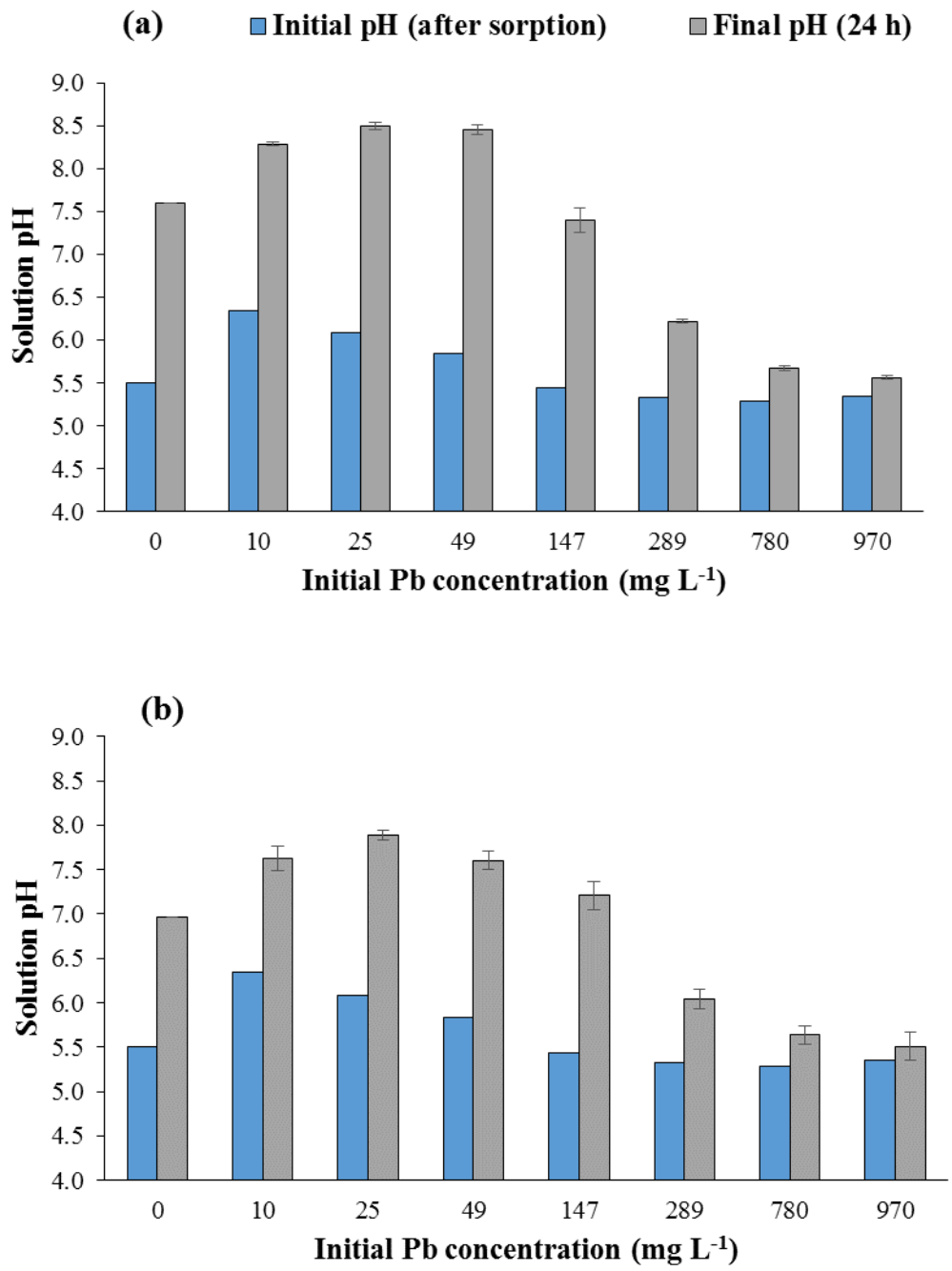

Fig. S3. The evolution of solution pH during Pb adsorption isotherms onto SS-KOH^{sem} (a) and MSW-KOH^{sem} (b).

Table S1.

Comparison of maximum adsorption capacities for lead by biochar produced from different waste materials.

Biochar material	Pyrolysis temperature	Q_m (mg g^{-1})	Isotherm well-fitted model	Expriemental conditions: initial pH, biochar dosage	Reference
Peanut shell	350	52.8	Freundlich, Langmuir	pH 5, 4 g L^{-1}	Wang et al. (2015)
Medicine material residues	350	46.1	Langmuir	pH 5, 4 g L^{-1}	Wang et al. (2015)
Pine wood	300	3.9	Langmuir	pH 5, 4 g L^{-1}	Liu & Zhang (2009)
Rice husk	300	1.8	Langmuir	pH 5, 4 g L^{-1}	Liu & Zhang (2009)
Digested dairy waste	600	51.4	-	2 g L^{-1}	Inyang et al. (2012)
Digested whole sugar beet	600	40.8	Langmuir	2 g L^{-1}	Inyang et al. (2012)
Sewage sludge digestate	350	6.5	Langmuir	pH 5, 4 g L^{-1}	This study
Organic fraction of municipal solid waste digestate	400	72.9	Langmuir	pH 5, 4 g L^{-1}	This study

Table S2.

Chemical characteristics of the organic fraction of municipal solid waste digestate (RMSW), its derived biochar (MSW^{sem}), sewage sludge digestate (RSS) and its derived biochar (SS^{sem}).

Parameters	RMSW	MSW^{sem}	RSS	SS^{sem}
Biochar yield (%wt)	NA[a]	74 ± 1	NA	NA
Ash (%wt)	52 ± 1	68 ± 1	NA	NA
Moisture content (%wt)	81 ± 1	NA	NA	NA
As (mg kg^{-1})[b]	dl[c]	dl	79 ± 3[d]	34 ± 12
Cd (mg kg^{-1})	dl	dl	dl	9 ± 1
Cr (mg kg^{-1})	94 ± 1	100 ± 2	42 ± 1	48 ± 1
Cu (mg kg^{-1})	261 ± 7	436 ± 5	390 ± 10	617 ± 7
Ni (mg kg^{-1})	43 ± 5	38 ± 3	25 ± 1	41 ± 1
Pb (mg kg^{-1})	101 ± 5	130 ± 12	80 ± 9	85 ± 3
Zn (mg kg^{-1})	693 ± 13	888 ± 12	756 ± 10	1017 ± 13

[a] NA refers to not available.
[b] Values reported on dry basis.
[c] dl refers to below detection limit.
[d] Values reported as means (n=3) followed by standard deviation.

Table S2 shows the metal(loid) contents of RMSW, MSW^{sem}, RSS and SS^{sem}. Metals such as Cr, Cu, Pb and Zn were retained in the biochars during pyrolysis, while As (metalloid) was volatilized at the temperature below 400 °C (Table S2), this was also affirmed by previous studies from Duan et al. (2017). As expected, Cu and Zn were the main components in both the solid digestates and biochars (Table S2), which was in correlation to the studies from Pituello et al. (2014). Additionally, no metals exceeded the limit values of metal(loid)s present in the sludge based on the French guidelines (Directive 86/278/EEC).

Table S3.

Parameters of pseudo-first-order and pseudo-second-order kinetics for lead sorption by SS^{sem}, $SS\text{-}H_2O_2{}^{sem}$, $SS\text{-}KOH^{sem}$, MSW^{sem}, $MSW\text{-}H_2O_2{}^{sem}$ and $MSW\text{-}KOH^{sem}$.

Sample		Pseudo-first-order (PFO)			Pseudo-second-order (PSO)		
	$Q_{e,exp}$	Q_e	k_1	R^2	Q_e	k_2	R^2
SS^{sem}	3.4	3.5	0.536	0.146	3.5	0.270	0.997
$SS\text{-}H_2O_2{}^{sem}$	8.2	8.8	0.633	0.653	8.5	0.137	0.999
$SS\text{-}KOH^{sem}$	13.7	13.9	1.780	NF[a]	14.0	1.057	0.999
MSW^{sem}	23.7	24.2	4.287	0.990	23.8	0.735	0.999
$MSW\text{-}H_2O_2{}^{sem}$	24.4	24.5	10.177	0.856	24.5	18.496	1.000
$MSW\text{-}KOH^{sem}$	23.8	24.0	7.766	0.78	23.8	3.528	1.000

[a]NF refers to no satisfactory fit by the model.

References

Chen X, Chen G, Chen L, Chen Y, Lehmann J, McBride MB, Hay AG (2011) Adsorption of copper and zinc by biochars produced from pyrolysis of hardwood and corn straw in aqueous solution. Bioresour Technol 102:8877–8884.

Duan L, Li X, Jiang Y, Lei M, Dong Z, Longhurst P (2017) Arsenic transformation behaviour during thermal decomposition of *P. vittata*, an arsenic hyperaccumulator. J Anal Appl Pyrolysis 124:584–591.

Inyang M, Gao B, Yao Y, Xue Y, Zimmerman AR, Pullammanappallil P, Cao X (2012) Removal of heavy metals from aqueous solution by biochars derived from anaerobically digested biomass. Bioresour Technol 110:50–56.

Jouraiphy A, Amir S, Gharous ME, Revel JC, Hafidi M (2005) Chemical and spectroscopic analysis of organic matter transformation during composting of sewage sludge and green plant waste. Int Biodeterior Biodegrad 56:101–108.

Liu Z, Zhang FS (2009) Removal of lead from water using biochars prepared from hydrothermal liquefaction of biomass. J Hazard Mater 167:933–939.

Pituello C, Francioso O, Simonetti G, Pisi A, Torreggiani A, Berti A, Morari F (2014) Characterization of chemical–physical, structural and morphological properties of biochars from biowastes produced at different temperatures. J Soils Sediments 15:792–804.

Wang Z, Liu G, Zheng H, Li F, Ngo HH, Guo W, Liu C, Chen L, Xing B (2015) Investigating the mechanisms of biochar's removal of lead from solution. Bioresour Technol 177:308–317.

II

Changes of sewage sludge digestate-derived biochar properties after chemical treatments and the influence on As(III and V) and Cd(II) sorption.

by

Wongrod, S., Simon, S., van Hullebusch, E.D.,
Lens, P.N.L., Guibaud, G., 2018.
International Biodeterioration & Biodegradation 135: 96–102.

International Biodeterioration & Biodegradation 135 (2018) 96–102

Contents lists available at ScienceDirect

International Biodeterioration & Biodegradation

journal homepage: www.elsevier.com/locate/ibiod

Changes of sewage sludge digestate-derived biochar properties after chemical treatments and influence on As(III and V) and Cd(II) sorption

Suchanya Wongrod[a,b,c], Stéphane Simon[b,*], Eric D. van Hullebusch[a,c,d], Piet N.L. Lens[c], Gilles Guibaud[b]

[a] Université Paris-Est, Laboratoire Géomatériaux et Environnement (EA 4508), UPEM, 77454, Marne-la-Vallée, France
[b] Université de Limoges, PEIRENE, Equipe Développement d'indicateurs ou prévision de la qualité des eaux, URA IRSTEA, 123 avenue Albert Thomas, 87060, Limoges, France
[c] UNESCO-IHE Institute for Water Education, P.O. Box 3015, 2601 DA, Delft, the Netherlands
[d] Institut de Physique du Globe de Paris, Sorbonne Paris Cité, Université Paris Diderot, UMR 7154, CNRS, F-75005, Paris, France

ARTICLE INFO

Keywords:
Sewage sludge digestate derived biochar
Chemical activation
As(III)
As(V)
Cd(II)
Biochar washing

ABSTRACT

This work seeks to extend the knowledge on the effect of chemical treatment of sewage sludge digestate (SSD)-derived biochar for the As(III and V) and Cd(II) sorption ability using potassium hydroxide (KOH) or hydrogen peroxide (H_2O_2). Results showed the increases of the pH of point of zero charge, the Brunauer-Emmett-Teller (BET) surface area and cation exchange capacity (CEC) after chemical treatment of biochar. The sorption ability was enhanced from 1.6 μmol g^{-1} (As(V)) and 16.1 μmol g^{-1} (Cd(II)) on raw biochar to 8.5 μmol g^{-1} (As(V)) and 318.5 μmol g^{-1} (Cd(II)) on KOH-modified biochar. Furthermore, arsenic redox distribution showed a large oxidation (70%) of As(III) to As(V) in KOH-biochar with batch washing, while a partial oxidation (7%) was observed in KOH-biochar with batch and subsequent column washing. The washing procedures after KOH treatment play an important role on arsenic sorption, due to the release of phosphate (PO_4^{3-}) as well as organic matter from the biochar that may subsequently lead to the oxidation of As(III) to As(V). Our findings highlight the potential influence of biochar on the redox transformation of As(III) to As(V) and therefore requires a careful assessment while investigating the fate of As in aquatic environments.

1. Introduction

Arsenic (As) and cadmium (Cd) contamination in water creates a pressing toxicity towards aquatic organisms. Arsenic is mostly present as two inorganic species, arsenite (As(III)) and arsenate (As(V)), whereas a divalent cadmium ion (Cd(II)) dominantly prevails in water. Due to the toxicity of As and Cd, numerous treatments have been dedicated to removing these elements from polluted water. Among them, sorption is a cost-effective and simple treatment for metal(loid) removal from water (Ding et al., 2016; Ofomaja et al., 2014; Peng et al., 2018; Wang et al., 2016; Zhou et al., 2017). In recent years, biochar, a black solid char obtained from pyrolysis (> 250 °C) of biomass under oxygen-limiting conditions (Ahmad et al., 2014), has been considered as a potential alternative to activate charcoal in sorption treatments. Sewage sludge digestate (SSD) obtained from wastewater treatment plants is currently considered as a promising material to produce a low-cost biochar (Agrafioti et al., 2013; Rajapaksha et al., 2014; Yuan et al., 2015; Zielińska and Oleszczuk, 2015).

During the pyrolysis step of biochar preparation, the organic matter from biomass undergoes structural modifications such as oxidation and conversion of aliphatic forms to aromatic forms (Zama et al., 2017). The resulting biochar generally harbors negative and positives charges on its surface depending on the neighboring pH. Consequently, at circumneutral pH, where negative charges are predominant, it has been applied to sorb cationic metals like lead (Pb), zinc (Zn) and cadmium (Cd) from polluted water (Ding et al., 2016; Ho et al., 2017; Park et al., 2017; Wongrod et al., 2018). Unfortunately, the sorption ability of SSD biochar for metal(loid)s, particularly As oxyanions, is relatively low compared to activated carbon or paper mill sludge biochar (Table S1, supplementary information). Therefore, biochar modifications like physical activation and chemical treatment have been applied to improve its sorption ability (Li et al., 2017; Rajapaksha et al., 2016; Sizmur et al., 2017). Even though there are many studies on the adsorption capacity of raw and modified biochars (Liu et al., 2017; Zuo et al., 2017), an evaluation of the modification of the biochar properties is yet to be done. Indeed, the biochar surface properties are important

* Corresponding author.
E-mail address: stephane.simon@unilim.fr (S. Simon).

https://doi.org/10.1016/j.ibiod.2018.10.001
Received 17 August 2018; Received in revised form 1 October 2018; Accepted 1 October 2018

parameters that influence the behavior of a sorbent to sorb anionic and cationic pollutants.

The present work aimed to study the consequences of chemical treatments of SSD biochar using KOH or H_2O_2 on its arsenic and cadmium sorption capacities. Batch experiments were performed to evaluate the sorption kinetics and capacity of raw and modified biochars for As(III, V) and Cd(II). Several surface properties, such as the pH of point of zero charge (pH_{PZC}), the cation exchange capacity (CEC) and the Brunauer-Emmett-Teller (BET) surface area were determined to access information on, respectively, the net surface charge, cation exchange capacity and available specific surface area of the SSD biochars. These parameters can be used to discuss the sorption characteristics of the biochar. The influence of chemical modifications of the biochar onto sorption of redox-sensitive elements was also investigated through the determination of arsenic redox transformation (*i.e.* As(III) and As(V)) during sorption experiments. Finally, the consequences of biochar washing on all these parameters were considered by comparing the results obtained with a KOH-modified biochar submitted either to only a batch washing or to a subsequent continuous column washing.

2. Materials and methods

2.1. Chemical reagents

Cadmium ($Cd(NO_3)_2.4H_2O$, 99% *w/w*, Merck), arsenate ($Na_2HAsO_4.7H_2O$, 98% *w/w*, Sigma-Aldrich) and arsenite ($AsNaO_2$, 98% *w/w*, Merck) were used to prepare 10 mM of Cd(II), As(V) and As (III) stock solutions, respectively. The ultrapure water (18.2 MΩ, MilliQ Gradient A10, Millipore SAS 67120, Molsheim, France) was used to wash biochars, as well as to prepare and dilute all solutions and samples.

2.2. Biochar preparation and chemical treatment

Pellets of domestic sewage sludge digestate (SSD) were obtained from a wastewater treatment plant (WWTP) located in Limoges, France (size: 285,000 equivalent population). The main treatment processes of the WWTP include activated sludges with anoxic treatment and addition of iron(III) chloride ($FeCl_3$) to, respectively, remove nitrogen(N) and phosphorus (P). Particularly, the SSD sample was collected in the storage tank after dewatering and drying.

The sample was heated at 350 °C for 15 min under slow pyrolysis technology to produce SSD biochar and more information was described in our previous work (Wongrod et al., 2018). The SSD biochar was chemically treated for 2 h with a 10% H_2O_2 solution (100 g: 1 l) or with 2 M KOH solution (100 g: 2.5 l) (Wongrod et al., 2018).

The raw and chemically-modified biochars were subsequently washed as follows: a triple batch washing in a row followed by a continuous column washing (Wongrod et al., 2018). These washing steps were performed to remove competitive ions (*e.g.* PO_4^{3-}, HCO_3^-/CO_3^{2-}, Ca^{2+} and Mg^{2+}) and organic matter released by the biochar during the chemical treatment. These released compounds can react with elements and thus interfere with the biochar-metal(loid) sorption system. In addition, clogging of the biochar pore sites by small particles can be eliminated through these washing steps. To determine if the washing procedure influences the metal(loid) sorption, a KOH-modified biochar was washed only with a batch procedure. The raw SSD biochar, its H_2O_2 and KOH-modified SSD biochar are denoted as, respectively, BSS, BH_2O_2 and BKOH. The KOH-modified biochar washed with only the batch procedure is labeled as $BKOH^{bat}$.

2.3. Biochar characterization

X-ray powder diffraction (XRD) and Fourier transform infrared spectroscopy (FTIR) of the SSD and its derived biochar were analyzed to observe the changes of, respectively, crystalline structures and surface functional groups after biochar production. The total amount of metal and metalloid in the SSD and its derived biochar was determined using acid digestion from the EPA Method 3050B (EPA, 1996). The details of the digestion procedures are described by Wongrod et al. (2018).

The pH (pH-meter LPH 330T, Tacussel, France) and electrical conductivity (EC) (CDM 210 conductivity-meter, Radiometer, Denmark) of the biochar were measured in water. The surface area of biochar was measured using N_2 sorption by the Brunauer-Emmett-Teller (BET) method at 77 K (3Flex, Micromeritics, USA). Pretreatment of biochar was performed by drying at 105 °C for 5 h prior to the BET surface area (S_{BET}) analysis.

The pH of point of zero charge (pH_{PZC}) of the biochar was determined from zetametry by determining the zeta potential at different pH ranges (Mahmood et al., 2011). For the determination of the cation exchange capacity (CEC), 2 g of biochar (dry weight) were mixed with 40 ml of 0.05 N cobalt hexamine trichloride ($[Co(NH_3)_6]Cl_3$) solution (99% *w/w*, Sigma-Aldrich) in polypropylene tubes (Aran et al., 2008). The details of the biochar preparation for pH_{PZC} and CEC measurement are provided in the supplementary information.

2.4. Sorption experiments

In sorption kinetic experiments, 10 µM As(III), As(V) and Cd(II) were prepared separately from stock solutions of 1 mM As(III), As(V) and Cd(II) (as $AsNaO_2$, $NaHAsO_4.7H_2O$ and $Cd(NO_3)_2$, respectively). Raw and modified biochars (600 mg) were added to 150 ml of metal (loid) solution. The initial pH was adjusted to 5 using HNO_3 and NaOH. The solutions were agitated at 20 (± 2) °C at 180 rpm for 24 h using an orbital shaker (KS 501 digital, IKA™, USA). The sorption experiments were performed in duplicate. Samples of solution were collected over time. The total collected volume was less than 5% of the initial volume to prevent any alteration of the sorption equilibrium. Sampled solutions were filtered through Lab Logistics Group (LLG) cellulose acetate syringe filters (0.45 µm) and their As and Cd concentrations were determined by graphite furnace atomic absorption spectrometry (240Z, Agilent Technologies, USA) at λ 193.7 nm and λ 228.8 nm for As and Cd, respectively. The pseudo-first-order (PFO) and the pseudo-second-order (PSO) kinetics models were used to describe the experimental data. The intraparticle diffusion model was also studied to access information on the mechanism of the sorption processes (Zhao et al., 2015a).

Adsorption isotherms were performed with initial concentrations ranging from 10 to 300 µM for As(III, V) and from 10 to 4000 µM for Cd (II). After 24 h of agitation, the residual concentrations of As were determined by graphite furnace atomic absorption spectrometry as detailed previously, whereas the residual concentrations of Cd were determined by Microwave Plasma Atomic Emission Spectroscopy (MP-AES) (Agilent 4100, USA) at λ 228.8 nm. Two common adsorption isotherm models (Langmuir and Freundlich) were used to fit the experimental data. Arsenic speciation was determined by High-Performance Liquid Chromatography (HPLC) coupled to Atomic Fluorescence Spectrometry (AFS) with Hydride Generation (HG) (PS Analytical Millennium Excalibur, P S Analytical, UK). For the chromatographic conditions, a Hamilton PRP-X100 column was used with a phosphate buffer solution as the mobile phase at a rate of 1 ml min^{-1}. Detailed information can be found in Wan et al. (2014).

2.5. Statistical analysis

Results are reported as means ± standard deviation (n = 3) unless otherwise stated. Uncertainties of sorption parameters were obtained by non-linear regression using Statistica software (v6.1, StatSoft). *t*-test with two-tailed distribution at a statistical significance level of $P \leq 0.01$ were used for data comparison.

Table 1
pH, electrical conductivity and surface area of the raw and chemically-modified biochars.

Biochar	pH in water	pH_{pzc}	Electrical conductivity (EC) (μS cm^{-1})	S_{BET}[a] (m^2 g^{-1})	CEC[b] ($cmol^+$ kg^{-1})	Reference
BSS[c]	6.4 ± 0.1	2.7	4.0 ± 0.1	0.4 ± 0.1	2.0 ± 0.1	This study
BH_2O_2[c]	6.5 ± 0.1	2.9	4.1 ± 0.3	5.7 ± 0.1	2.9 ± 0.1	This study
BKOH[c]	8.4 ± 0.1	3.4	6.2 ± 0.5	7.9 ± 0.1	13.4 ± 0.1	This study
$BKOH^{bat}$[c]	10.0 ± 0.1	2.9	324.0 ± 2.4	3.0 ± 0.1	20.8 ± 0.1	This study
Sewage sludge (300 °C)	6.7 ± 0.2	na[d]	7750.0 ± 160.0	14.3 ± 0.2	na	Yuan et al. (2015)
Sewage sludge (300 °C)	na	na	na	4.0	na	Agrafioti et al. (2013)

[a] S_{BET} refers to Brunauer-Emmett-Teller surface area of biochar.
[b] CEC refers to cation exchange capacity of biochar.
[c] BSS: biochar from sewage sludge digestate, BH_2O_2: H_2O_2-modified biochar, BKOH and $BKOH^{bat}$: KOH-modified biochars, respectively, with batch and column washing, and with batch washing.
[d] na refers to not available.

3. Results and discussion

3.1. Influence of chemical treatment on biochar characteristics

The XRD analysis showed that quartz was present in both SSD and BSS with insignificant modification of the surface properties after biochar pyrolysis (Fig. S1). FTIR spectra demonstrated similar binding between atoms of both the SSD and BSS (Fig. S2). The absorbance peaks of hydroxyl (–OH) groups (3425 cm^{-1}), $–CH_3$ stretching of aliphatic groups (2924 cm^{-1}), C = C stretching vibrations (1600 cm^{-1}), and C–C skeleton and C–O stretching (1033 cm^{-1}) were mainly detected on the SSD and BSS (Fig. S2). These functional groups can be involved in the sorption for metal(loid)s (Pituello et al., 2014).

The pH values of the suspensions of the raw and chemically-modified biochars are given in Table 1. The KOH treatment induced a change from 6.4 (± 0.1) for BSS to 8.4 (± 0.1) for BKOH and 10.1 (± 0.1) for $BKOH^{bat}$, whereas no significant difference ($P \leq 0.01$) was observed after H_2O_2 treatment (Table 1). Results also showed no significant changes of the electrical conductivity (EC) among each biochar suspension (*i.e.* BSS, BH_2O_2 and BKOH), except for $BKOH^{bat}$ where a 50-fold higher value 324 (± 2) μS cm^{-1} was observed. The high EC value of $BKOH^{bat}$ is probably due to a significant release of weakly sorbed ions (*e.g.* PO_4^{3-}, HCO_3^-, CO_3^{2-}, Ca^{2+} and Mg^{2+}) from $BKOH^{bat}$ as previously reported by Wongrod et al. (2018). A previous study published by Yuan et al. (2015) is in agreement with our finding, as the authors have reported a very high EC of 7750 μS cm^{-1} in the sewage sludge biochar that was not washed with ultrapure water after pyrolysis (Table 1).

Fig. 1 shows the evolution of the zeta potential according to pH values for BSS, BH_2O_2, BKOH and $BKOH^{bat}$. The corresponding pH_{PZC} are given in Table 1. Results demonstrated similar pH_{PZC} values for both BSS (~2.7) and BH_2O_2 (~2.9) biochars, whereas a slightly higher value was obtained for BKOH (~3.4). Such limited variations of pH_{PZC} (2.7–3.4) are not prone to significantly modify the pH on the As and Cd sorption, except if the manipulations are performed at a pH lower than 5 (*i.e.* pH at sorption experiment, see section 2.4). In contrast, the more negative values of zeta potential observed for BH_2O_2 and $BKOH^{bat}$ (Fig. 1) could indicate higher amounts of negative charges at the surfaces of these two modified biochars, resulting in higher sorption capacities towards cationic metals.

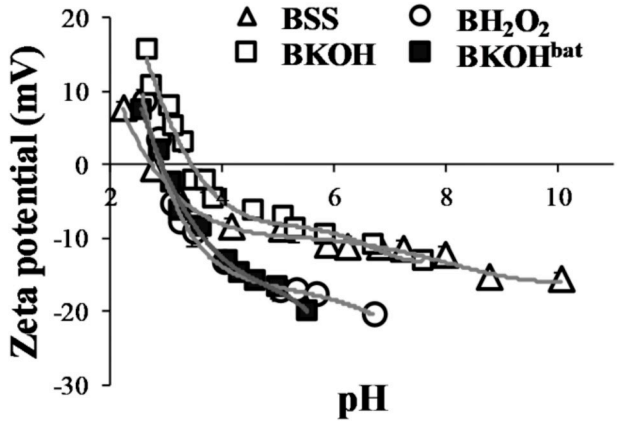

Fig. 1. Evolution of the zeta potential as a function of the pH values.

The pH_{PZC} results showed that all biochars carried net negative charges at neutral pH (Fig. 1). At present, the pH_{PZC} of biochar has been rarely reported in the literature and there is a lack of information to understand its variability among different chemical treatments. However, our results are in agreement with a straw-derived biochar with a pH_{PZC} ~1.9 (Qiu et al., 2009) and a paper mill sludge with pH_{PZC} ranging from 4.0 to 6.0 (Guo et al., 2018).

The BET surface area (S_{BET}) of the raw and modified biochars is given in Table 1. A significant increase of the S_{BET} was observed for BH_2O_2 and BKOH, from 0.4 (± 0.1) to 5.7 (± 0.1) and 7.9 (± 0.1) m^2 g^{-1}, respectively. This increasing S_{BET} is an indicator of higher porosity on the modified biochar and thus a growing chance for metal(loid)s to sorb onto the biochar surface (*e.g.* by complexation) (Mohan et al., 2014). Our findings are similar to those determined for sewage sludge biochars (4.0–14.3 m^2 g^{-1}) (Agrafioti et al., 2013; Yuan et al., 2015) and pineapple-peel-derived biochars (0.7–2.1 m^2 g^{-1}) (Wang et al., 2016). Nevertheless, these values are still far lower than those reported for activated carbons (1215.0–1316.0 m^2 g^{-1}) (Gong et al., 2015).

The CEC values determined for the different biochars are presented in Table 1. Results showed a slight increase of CEC after treating the biochar with H_2O_2 from 1.9 (± 0.1) to 3.0 (± 0.1) $cmol^+$ kg^{-1}, whereas a significantly increase (6 times) after the KOH treatment ($P \leq 0.01$) was reported. This higher CEC of BKOH could induce an enhanced sorption ability towards cationic metals. Previously published data showed variable high ranges of the CEC of the biochars from 45.7 $cmol^+$ kg^{-1} to 483.4 $cmol^+$ kg^{-1} on wood and straw-based biochars, respectively (Ding et al., 2016; Jiang et al., 2014).

The variations in the S_{BET} and CEC after chemical treatments of the biochars suggest that H_2O_2 and KOH-modified biochars provided higher amounts of active pore sites, surface functional groups and exchangeable cations that could enhance the sorption of metallic elements on the biochar surface. For anion sorption, the increase of S_{BET} could influence the arsenic sorption capacity (Table 1).

Concerning the effect of the washing procedures after KOH treatment, the results showed significantly higher values of both pH and conductivity on $BKOH^{bat}$ than BKOH (Table 1), which were attributed to a release of ions such as PO_4^{3-} and HCO_3^-/CO_3^{2-} from the biochar (Wongrod et al., 2018). As discussed previously (Wongrod et al., 2018), the insufficient batch washing after biochar modification led to the release of ions (*e.g.* PO_4^{3-}, HCO_3^-/CO_3^{2-}, Ca^{2+} and Mg^{2+}) and organic compounds from the biochar which interacted with metals and modified the sorption behavior. In the case of As(V), PO_4^{3-} is expected

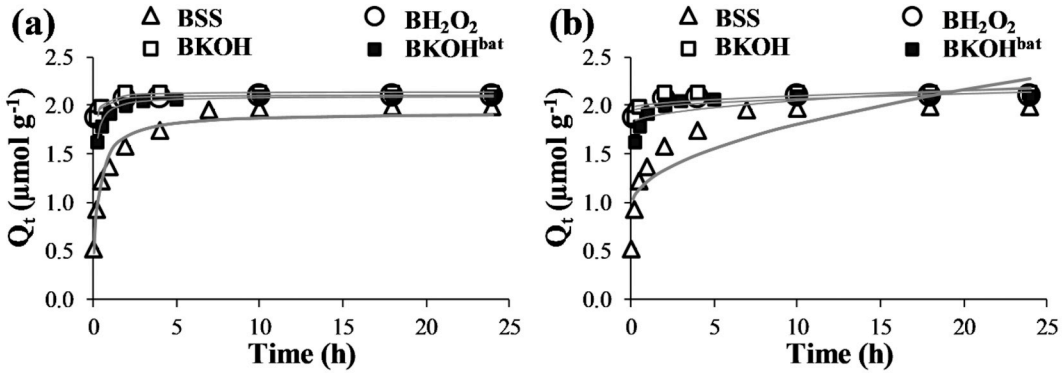

Fig. 2. Effect of chemical treatment and biochar washing on adsorption kinetics for Cd(II) by the raw and chemically-modified biochars fitted with the pseudo-second-order kinetic model (a), and with the intraparticle diffusion model (b) (initial pH = 5, initial concentration: 10 µmol l^{-1}).

to be a strong competitor, reducing its sorption onto the biochar. The pH_{PZC}, S_{BET} and CEC values were also significantly affected by the uncomplete batch washing, resulting in an alteration of the biochar surface properties.

3.2. Effect of chemical treatment and washing on Cd(II) sorption

The results of the kinetic study of the Cd(II) sorption fitted better to the pseudo-second-order (PSO) (Fig. 2a) than intraparticle diffusion (Fig. 2b) models. All values for the kinetic model-fitting can be found in Table 2 and Table S2 (supplementary information). Results showed that the sorption of Cd(II) by all biochars were well-described by the PSO kinetic model (Table 2 and Fig. 2a), literally suggesting that the sorption mainly occurred *via* simple chemical reaction (Nethaji et al., 2013). Both the KOH and H_2O_2-treated SSD biochars showed faster removal kinetics than the raw biochar, reaching the equilibrium in less than 5 h for BH_2O_2 and BKOH, and after 10 h for BSS (Fig. 2a). These results are consistent with a previous study with faster kinetics on the KOH-modified switchgrass biochar than the raw biochar (Regmi et al., 2012). Fig. 2b shows that the plots did not pass through the origin as the C values are not equal to zero (Table 2). This indicates some degree of boundary layer and the intraparticle diffusion was not the only rate controlling step, but other mechanisms like film diffusion and external mass transfer may also play important roles in the sorption (Nethaji et al., 2013).

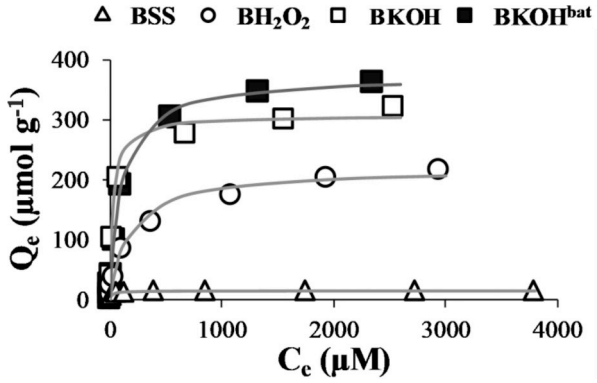

Fig. 3. Effect of chemical treatment and biochar washing on adsorption isotherms for Cd(II) by the raw and chemically-modified biochars (initial pH = 5, 24 h, Langmuir model fitting).

Sorption isotherms are shown in Fig. 3, and the corresponding parameters can be found in Table 3 and Table S3 (supplementary information). Cd sorption was better described by the Langmuir model

Table 2
Constants for adsorption kinetics of As(III), As(V) and Cd(III) by biochars with the pseudo-second-order and intraparticle diffusion models.

Pseudo-second-order model

Biochar	As(III)			As(V)			Cd(II)		
	k_2[a]	Q_e[b]	R^2	k_2	Q_e	R^2	k_2	Q_e	R^2
BSS[c]	–	–	–	0.630 ± 0.098	0.62 ± 0.03	0.985	1.724 ± 0.204	1.93 ± 0.04	0.983
BH_2O_2[c]	–	–	–	0.619 ± 0.092	0.66 ± 0.03	0.985	12.251 ± 0.803	2.09 ± 0.01	9.985
BKOH[c]	0.378 ± 0.067	2.83 ± 0.11	0.961	0.052 ± 0.006	2.35 ± 0.09	0.995	12.907 ± 0.479	2.14 ± 0.01	0.993
$BKOH^{bat}$[c]	0.205 ± 0.042	1.94 ± 0.10	0.975	1.599 ± 0.340	0.27 ± 0.02	0.969	6.298 ± 0.338	2.09 ± 0.10	0.987

Intraparticle diffusion model

Biochar	As(III)			As(V)			Cd(II)		
	k_i[d]	C	R^2	k_i	C	R^2	k_i	C	R^2
BSS	–	–	–	0.115 ± 0.013	0.065 ± 0.035	0.910	0.269 ± 0.039	0.956 ± 0.101	0.852
BH_2O_2	–	–	–	0.121 ± 0.014	0.083 ± 0.036	0.913	0.042 ± 0.010	1.932 ± 0.029	0.787
BKOH	0.429 ± 0.044	0.981 ± 0.113	0.938	0.396 ± 0.012	−0.074 ± 0.030	0.993	0.041 ± 0.013	1.973 ± 0.036	0.699
$BKOH^{bat}$	0.358 ± 0.033	0.219 ± 0.086	0.948	0.050 ± 0.006	0.036 ± 0.015	0.919	0.077 ± 0.018	1.799 ± 0.046	0.749

[a] k_2 unit: g(µmol h)$^{-1}$.
[b] Q_e unit: in µmol g^{-1}.
[c] BSS: biochar from sewage sludge digestate, BH_2O_2: H_2O_2-modified biochar, BKOH and $BKOH^{bat}$: KOH-modified biochars, respectively, with batch and column washing, and with batch washing.
[d] k_i unit: µmol (g $h^{1/2}$)$^{-1}$.

Table 3
Parameters determined from adsorption isotherms for As(III), As(V) and Cd(II) by biochars with the Langmuir model.

Biochar	As(III)			As(V)			Cd(II)		
	K_L[a]	Q_m[b]	R^2	K_L	Q_m	R^2	K_L	Q_m	R^2
BSS[c]	–	–	–	0.015 ± 0.006	1.60 ± 0.23	0.958	0.061 ± 0.009	15.49 ± 0.32	0.992
BH_2O_2[c]	–	–	–	0.012 ± 0.003	7.22 ± 0.67	0.989	0.005 ± 0.001	218.73 ± 6.91	0.990
BKOH[c]	0.103 ± 0.018	8.74 ± 0.33	0.976	0.014 ± 0.003	8.11 ± 0.53	0.994	0.032 ± 0.004	306.09 ± 6.07	0.994
$BKOH^{bat}$[c]	0.088 ± 0.007	7.60 ± 0.12	0.996	0.024 ± 0.008	0.85 ± 0.09	0.965	0.009 ± 0.001	372.49 ± 6.71	0.996

[a] K_L unit: in l μmol^{-1}.
[b] Q_m unit: in μmol g^{-1}.
[c] BSS: biochar from sewage sludge digestate, BH_2O_2: H_2O_2-modified biochar, BKOH and $BKOH^{bat}$: KOH-modified biochars, respectively, with batch and column washing, and with batch washing.

(Table S3), suggesting the possibility of a monolayer sorption of Cd onto the homogeneous biochar surfaces (Zhao et al., 2015b). The Langmuir maximal sorption capacity, Q_m, increased by a 15-fold–20-fold factor after treatment with H_2O_2 and KOH, respectively (Table 3). This can be linked to the previous observation that the chemical treatments not only increase the S_{BET}, but also the CEC, resulting in an increase of the sorption sites and exchangeable cations. The higher Q_m value of BKOH compared to BH_2O_2 is consistent with the more pronounced improvement of both S_{BET} and CEC with the KOH treatment (Table 1).

The effect of the washing procedure applied after KOH treatment on the adsorption kinetics and isotherms are shown in Figs. 2 and 3 and Tables 2 and 3. The sorption kinetic constant for biochar with the KOH treatment was lower without the column washing step, but the value was still higher than that for the raw biochar. This finding could result from the reduction of S_{BET} for the insufficient batch washed $BKOH^{bat}$. A slightly higher Q_m was observed for $BKOH^{bat}$ compared to BKOH, meaning that the sorption of this cationic metal was not strongly affected by the washing procedure. The release of ions and organic compounds from the $BKOH^{bat}$ did not appear to modify the Cd(II) behavior, in contrast to what was observed in a previous study with Pb(II) (Wongrod et al., 2018). This could be due to a higher affinity of Cd(II) for biochar sites (*i.e.* higher K_L values than Pb(II)) and/or weaker interactions between Cd(II) and dissolved compounds in the solutions. For example in our findings, the K_L values of BKOH were 0.032 l μmol^{-1} and 0.007 l μmol^{-1} for Cd(II) and Pb(II), respectively (Wongrod et al., 2018).

3.3. Arsenic sorption

3.3.1. Effect of chemical treatment of biochar on As(V) sorption

Fig. 4a shows the effect of chemical treatments on the adsorption kinetics for As(V) onto BSS, BH_2O_2 and BKOH. All experimental data fitted with a pseudo-second-order kinetic model ($R^2 \geq 0.98$, Table S2, supplementary information) and corresponding parameters are given in Table 2. These results showed that the sorption kinetics were unchanged for BH_2O_2, with a sorption equilibrium reached after 10 h, while it was reached after 24 h for BKOH.

The sorption isotherms for As(V) are shown in Fig. 4b. Similar to Cd, the Langmuir model provided the best fit for As(V) sorption (Table S3, supplementary information). The corresponding sorption parameters are given in Table 3. No significant evolution was observed for the values of K_L, indicating that the chemical treatments did not modify the affinity of the biochar for As(V). In contrast, the sorption capacity was enhanced by both H_2O_2 and KOH-treated biochars (except $BKOH^{bat}$), and the Q_m values being, respectively, about 4 times and 5 times higher than the raw biochar.

These results indicate that H_2O_2 treatment only improved the sorption capacity, whereas KOH treatment improved the sorption capacity but induced slower sorption kinetics for As(V) (Tables 2 and 3). In both cases, the enhanced sorption ability for As(V) by the chemically-modified biochars could be linked to the increase of the S_{BET}, which was slightly higher for BKOH than BH_2O_2 (Table 1). These results are in agreement with previous studies (Ding et al., 2016; Wu et al., 2017), that showed that the surface area plays an important role in the sorption of elements onto biochar. The slightly increased pH_{pzc} of BKOH (Table 1) may result in a little increase of the positive charges at the surface of the biochar, and thus enhance the sorption ability for the anionic As(V).

3.3.2. Comparison of biochar washing

The effect of the washing procedure applied after KOH treatment on the adsorption kinetics and isotherms for arsenic are presented in Fig. 5a-d. The corresponding sorption parameters are given in Tables 2 and 3. The experiments were performed for As(V) and As(III) to determine if the washing procedure affects similarly both arsenic species, taking into account that, in the experimental conditions, As(III) is neutral whereas As(V) is negatively-charged.

It appeared that the washing procedures of KOH-biochars had a low impact on the sorption kinetics for As(III), k_2 values increasing from 0.20 (± 0.05) h^{-1} to 0.38 (± 0.07) h^{-1} with the addition of the subsequent column washing step (Fig. 5a). In contrast, the addition of

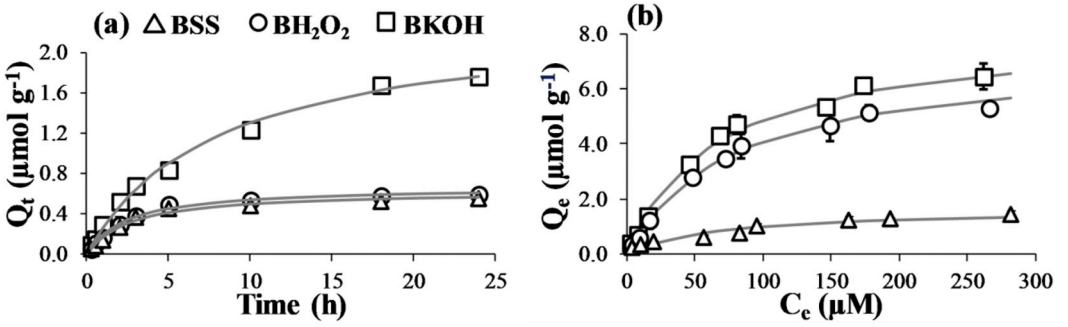

Fig. 4. Effect of chemical treatment on As(V) adsorption kinetics by biochars (a) (initial pH = 5, initial concentration: 10 μmol l^{-1}, pseudo-second-order kinetic model fitting), and As(V) adsorption isotherms by biochars (b) (initial pH = 5, 24 h, Langmuir model fitting).

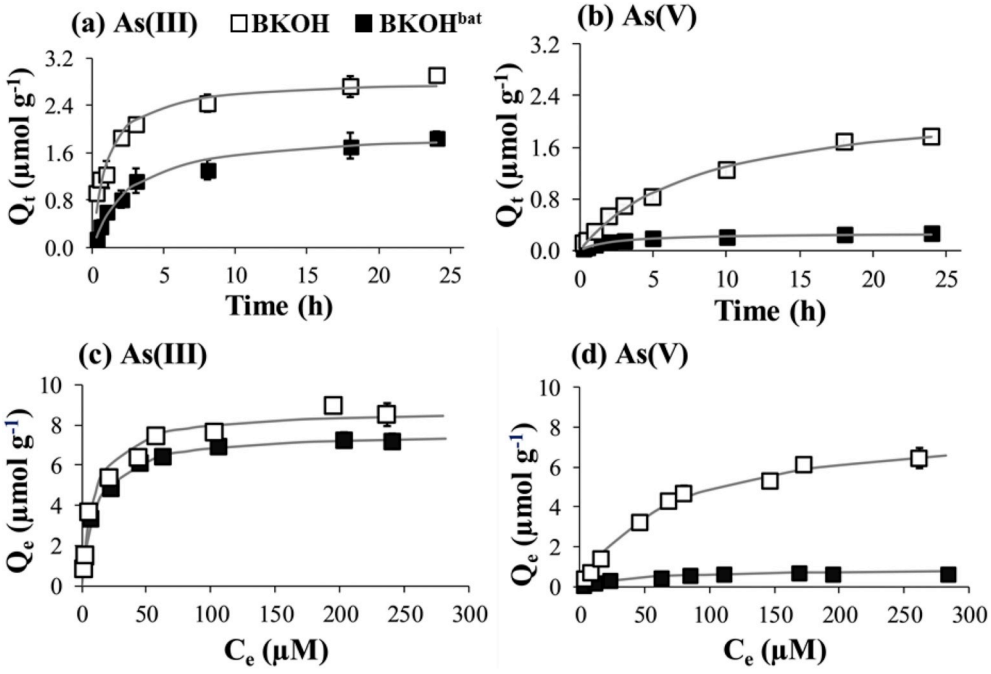

Fig. 5. Influence of biochar washing of KOH-modified biochars on adsorption kinetics for As(III) (a) and As(V) (b) (initial pH = 5, initial concentration: 10 µmol l^{-1}, pseudo-second-order kinetic model fitting), and on adsorption isotherms for As(III) (c) and As(V) (d) (initial pH = 5, 24 h, Langmuir model fitting).

this step strongly affected the sorption kinetics for As(V) (Fig. 5b), inducing a 3-fold decrease of k_2 (Table 2). The sorption isotherms showed an opposite trend: the column washing step only marginally modified the Q_m of the biochar for As(III), but induced an almost 10-fold improvement for As(V). This strong difference of the Q_m values for As(V) can be attributed to the PO_4^{3-} released from $BKOH^{bat}$, as highlighted in a previous study (Wongrod et al., 2018). Indeed, the PO_4^{3-} may strongly compete with As(V) for sorption onto the biochar. It has been previously established that excessive PO_4^{3-} concentrations could mobilize As(V) from the sorbent (Neupane et al., 2014). This is likely due to the similar chemical properties between PO_4^{3-} and As(V) since both chemicals are negatively-charged oxyanions. Moreover, the leaching of dissolved organic carbon (DOC) from the biochar (Wongrod et al., 2018) could accelerate the mobilization of As, as observed in a previous study in a biochar-soil system (Kim et al., 2018). Concerning the sorption constant K_L, there was no significant difference ($P \leq 0.01$) according to the washing procedures for As(V) and As(III), indicating that no evolution in the affinity of biochar for both arsenic species was observed. When comparing K_L values between As(III) and As(V), it appears that the latter has less affinity for BKOH and $BKOH^{bat}$ (Table 3). It could be hypothesized from these results that arsenic species interact differently with the biochar surface or with different types of surface functions.

3.3.3. Evolution of arsenic redox speciation

The arsenic redox speciation in solution was determined during As (III) and As(V) sorption experiments in order to determine whether the biochar was able to induce redox conversions. During the sorption of As (III) onto $BKOH^{bat}$, up to 70% of arsenic in solution was As(V), despite only As(III) was initially added. A partial oxidation (< 10%) was also observed in the presence of BKOH and no As(V) was detected in the controls. In contrast, no reduction of As(V) to As(III) was noticed during As(V) sorption experiments. These results show that biochar is able to modify the arsenic redox state in solution and this could be strongly increased with an insufficient washing. These findings are in agreement with a previous study (Fakour and Lin, 2014) that reported an increased oxidation of As(III) in the presence of organic matter in solution.

4. Conclusions

Chemical treatment of biochar is considered to enhance the sorption performance for both oxyanions and cationic metals. The treatment with KOH or H_2O_2 strongly affects the sorption kinetics for As(III and V) and Cd(II). For As(V), KOH treatment induced a slower kinetic sorption compared to the raw biochar, while no significant variation was noticed for the H_2O_2-modified biochar. In contrast, both treatments showed faster sorption for Cd(II). All treatments induced a strong sorption capacity enhancement, particularly with alkali treatment. This is consistent with the observed evolutions of biochar properties such as CEC, S_{BET} and, to a lesser extent, pH_{ZPC}. Unfortunately, as previously highlighted, without the implementation of a careful washing procedure, this treatment also generated a strong release of inorganic and organic compounds from the biochar that can alter the evaluation of its sorption properties. This issue clearly affected As(V) sorption due to the competition with the released PO_4^{3-}.

When working with a redox-sensitive element, such as arsenic, it was observed that the biochar may also play an important role in the oxidation of As(III) to As(V). This phenomenon was enhanced by the insufficient washing process. The potential chemical transformation of arsenic should be carefully considered in future research in order to better understand the role of chemically modified biochar on the removal of such compounds from contaminated water.

Conflict of Interest

The authors declare no conflict of interest.

Acknowledgments

We thank Patrice Fondanèche (Université de Limoges, France) for technical assistance with the arsenic and cadmium analysis. This work was financially supported by the Marie Sklodowska-Curie European Joint Doctorate Advanced Biological Waste-to-Energy Technologies (ABWET) under the European Union's Horizon 2020 research and innovation programme (grant agreement N° 643071).

Appendix A. Supplementary data

Supplementary data to this article can be found online at https://doi.org/10.1016/j.ibiod.2018.10.001.

References

Agrafioti, E., Bouras, G., Kalderis, D., Diamadopoulos, E., 2013. Biochar production by sewage sludge pyrolysis. J. Anal. Appl. Pyrolysis 101, 72–78.

Ahmad, M., Rajapaksha, A.U., Lim, J.E., Zhang, M., Bolan, N., Mohan, D., Vithanage, M., Lee, S.S., Ok, Y.S., 2014. Biochar as a sorbent for contaminant management in soil and water: a review. Chemosphere 99, 19–23.

Aran, D., Maul, A., Masfaraud, J.F., 2008. A spectrophotometric measurement of soil cation exchange capacity based on cobaltihexamine chloride absorbance. Comptes. Rendus. Geosci. 340, 865–871.

Ding, Z., Hu, X., Wan, Y., Wang, S., Gao, B., 2016. Removal of lead, copper, cadmium, zinc, and nickel from aqueous solutions by alkali-modified biochar: batch and column tests. J. Ind. Eng. Chem. 33, 239–245.

EPA, 1996. Method 3050B: acid digestion of sediments, sludges, and soils. Revision 2, 1–12.

Fakour, H., Lin, T.F., 2014. Effect of humic acid on as redox transformation and kinetic adsorption onto iron oxide based adsorbent (IBA). Int. J. Environ. Res. Publ. Health 11, 10710–10736.

Gong, X.J., Li, W.G., Zhang, D.Y., Fan, W.B., Zhang, X.R., 2015. Adsorption of arsenic from micro-polluted water by an innovative coal-based mesoporous activated carbon in the presence of co-existing ions. Int. Biodeterior. Biodegrad. 102, 256–264.

Guo, K., Gao, B., Yue, Q., Xu, X., Li, R., Shen, X., 2018. Characterization and performance of a novel lignin-based flocculant for the treatment of dye wastewater. Int. Biodeterior. Biodegrad. 133, 99–107.

Ho, S.H., Chen, Y., Yang, Z., Nagarajan, D., Chang, J.S., Ren, N., 2017. High-efficiency removal of lead from wastewater by biochar derived from anaerobic digestion sludge. Bioresour. Technol. 246, 142–149.

Jiang, T., Xu, R., Gu, T., Jiang, J., 2014. Effect of crop-straw derived biochars on Pb(II) adsorption in two variable charge soils. J. Integr. Agric. 13, 507–516.

Kim, H. Bin, Kim, S.H., Jeon, E.K., Kim, D., Tsang, D.C.W., Alessi, D.S., Kwon, E.E., Baek, K., 2018. Effect of dissolved organic carbon from sludge, rice straw and spent coffee ground biochar on the mobility of arsenic in soil. Sci. Total Environ. 636, 1241–1248.

Li, H., Dong, X., da Silva, E.B., de Oliveira, L.M., Chen, Y., Ma, L.Q., 2017. Mechanisms of metal sorption by biochars: biochar characteristics and modifications. Chemosphere 178, 466–478.

Liu, S., Huang, B., Chai, L., Liu, Y., Zeng, G., Wang, X., Zeng, W., Shang, M., Deng, J., Zhou, Z., 2017. Enhancement of As(V) adsorption from aqueous solution by a magnetic chitosan/biochar composite. RSC Adv. 7, 10891–10900.

Mahmood, T., Saddique, M.T., Naeem, A., Westerho, P., Mustafa, S., 2011. Comparison of different methods for the point of zero charge determination of NiO. Ind. Eng. Chem. Res. 50, 10017–10023.

Mohan, D., Sarswat, A., Ok, Y.S., Pittman, C.U., 2014. Organic and inorganic contaminants removal from water with biochar, a renewable, low cost and sustainable adsorbent – a critical review. Bioresour. Technol. 160, 191–202.

Nethaji, S., Sivasamy, A., Mandal, A.B., 2013. Adsorption isotherms, kinetics and mechanism for the adsorption of cationic and anionic dyes onto carbonaceous particles prepared from *Juglans regia* shell biomass. Int. J. Environ. Sci. Technol. 10, 231–242.

Neupane, G., Donahoe, R.J., Arai, Y., 2014. Kinetics of competitive adsorption/desorption of arsenate and phosphate at the ferrihydrite-water interface. Chem. Geol. 368, 31–38.

Ofomaja, A.E., Pholosi, A., Naidoo, E.B., 2014. Kinetics and competitive modeling of cesium biosorption onto iron(III) hexacyanoferrate modified pine cone powder. Int. Biodeterior. Biodegrad. 92, 71–78.

Park, J.H., Wang, J.J., Kim, S.H., Cho, J.S., Kang, S.W., Delaune, R.D., Han, K.J., Seo, D.C., 2017. Recycling of rice straw through pyrolysis and its adsorption behaviors for Cu and Zn ions in aqueous solution. Colloids Surf., A 533, 330–337.

Peng, Q., Zhang, F., Zhou, Y., Zhang, J., Wei, J., Mao, Q., Huang, H., Chen, A., Chai, L., Luo, L., 2018. Formation of composite sorbent by *P. chrysogenum* strain F1 and ferrihydrite in water for arsenic removal. Int. Biodeterior. Biodegrad. 132, 208–215.

Pituello, C., Francioso, O., Simonetti, G., Pisi, A., Torreggiani, A., Berti, A., Morari, F., 2014. Characterization of chemical–physical, structural and morphological properties of biochars from biowastes produced at different temperatures. J. Soils Sediments 15, 792–804.

Qiu, Y., Zheng, Z., Zhou, Z., Sheng, G.D., 2009. Effectiveness and mechanisms of dye adsorption on a straw-based biochar. Bioresour. Technol. 100, 5348–5351.

Rajapaksha, A.U., Chen, S.S., Tsang, D.C.W., Zhang, M., Vithanage, M., Mandal, S., Gao, B., Bolan, N.S., Ok, Y.S., 2016. Engineered/designer biochar for contaminant removal/immobilization from soil and water: potential and implication of biochar modification. Chemosphere 148, 276–291.

Rajapaksha, A.U., Vithanage, M., Zhang, M., Ahmad, M., Mohan, D., Chang, S.X., Ok, Y.S., 2014. Pyrolysis condition affected sulfamethazine sorption by tea waste biochars. Bioresour. Technol. 166, 303–308.

Regmi, P., Garcia Moscoso, J.L., Kumar, S., Cao, X., Mao, J., Schafran, G., 2012. Removal of copper and cadmium from aqueous solution using switchgrass biochar produced via hydrothermal carbonization process. J. Environ. Manag. 109, 61–69.

Sizmur, T., Fresno, T., Akgül, G., Frost, H., Moreno-Jiménez, E., 2017. Biochar modification to enhance sorption of inorganics from water. Bioresour. Technol. 246, 34–47.

Wan, J., Pressigout, J., Simon, S., Deluchat, V., 2014. Distribution of as trapping along a ZVI/sand bed reactor. Chem. Eng. J. 246, 322–327.

Wang, C., Gu, L., Liu, X., Zhang, X., Cao, L., 2016. Sorption behavior of Cr(VI) on pineapple-peel-derived biochar and the influence of coexisting pyrene. Int. Biodeterior. Biodegrad. 111, 78–84.

Wongrod, S., Simon, S., Guibaud, G., Lens, P.N.L., Pechaud, Y., Huguenot, D., van Hullebusch, E.D., 2018. Lead sorption by biochar produced from digestates: consequences of chemical modification and washing. J. Environ. Manag. 219, 277–284.

Wu, W., Li, J., Lan, T., Müller, K., Khan, N., Chen, X., Xu, S., Zheng, L., Chu, Y., Li, J., Yuan, G., Wang, H., 2017. Unraveling sorption of lead in aqueous solutions by chemically modified biochar derived from coconut fiber: a microscopic and spectroscopic investigation. Sci. Total Environ. 576, 766–774.

Yuan, H., Lu, T., Huang, H., Zhao, D., Kobayashi, N., Chen, Y., 2015. Influence of pyrolysis temperature on physical and chemical properties of biochar made from sewage sludge. J. Anal. Appl. Pyrolysis 112, 284–289.

Zama, E.F., Zhu, Y.G., Reid, B.J., Sun, G.X., 2017. The role of biochar properties in influencing the sorption and desorption of Pb(II), Cd(II) and As(III) in aqueous solution. J. Clean. Prod. 148, 127–136.

Zhao, L., Xue, F., Yu, B., Xie, J., Zhang, X., Wu, R., Wang, R., Hu, Z., Yang, S.T., Luo, J., 2015a. TiO_2–graphene sponge for the removal of tetracycline. J. Nanoparticle Res. 17, 1–9.

Zhao, Z., Wu, M., Jiang, Q., Zhang, Y., Chang, X., Zhan, K., 2015b. Adsorption and desorption studies of anthocyanins from black peanut skins on macroporous resins. Int. J. Food Eng. 11, 841–849.

Zhou, Z., Liu, Y., Liu, S., Liu, H., Zeng, G., Tan, X., Yang, C., Ding, Y., Yan, Z., Cai, X., 2017. Sorption performance and mechanisms of arsenic(V) removal by magnetic gelatin-modified biochar. Chem. Eng. J. 314, 223–231.

Zielińska, A., Oleszczuk, P., 2015. The conversion of sewage sludge into biochar reduces polycyclic aromatic hydrocarbon content and ecotoxicity but increases trace metal content. Biomass Bioenergy 75, 235–244.

Zuo, W.Q., Chen, C., Cui, H.J., Fu, M.L., 2017. Enhanced removal of Cd(II) from aqueous solution using $CaCO_3$ nanoparticle modified sewage sludge biochar. RSC Adv. 7, 16238–16243.

Supplementary Information

Changes of sewage sludge digestate-derived biochar properties after chemical treatments and the influence on As(III and V) and Cd(II) sorption

Suchanya Wongrod[a,b,c], Stéphane Simon[b,*], Eric D. van Hullebusch[a,c,d], Piet N.L. Lens[c], Gilles Guibaud[b]

[a] Université Paris-Est, Laboratoire Géomatériaux et Environnement (EA 4508), UPEM, 77454, Marne-la-Vallée, France

[b] Université de Limoges, PEIRENE, Equipe Développement d′indicateurs ou prévision de la qualité des eaux, URA IRSTEA, 123 avenue Albert Thomas, 87060 Limoges, France

[c] UNESCO-IHE Institute for Water Education, P.O. Box 3015, 2601 DA Delft, The Netherlands

[d] Institut de Physique du Globe de Paris, Sorbonne Paris Cité, Université Paris Diderot, UMR 7154, CNRS, F-75005 Paris, France

[*] Corresponding author. Université de Limoges, PEIRENE, Equipe Développement d′indicateurs ou prévision de la qualité des eaux, URA IRSTEA, 123 avenue Albert Thomas, 87060 Limoges, France
Email: stephane.simon@unilim.fr

Measurement of pH of point of zero charge (pH_{PZC}) of biochar

The pH_{PZC} of raw and chemically-modified biochars was determined from zetametry by determining the zeta potential at different pH ranges (Mahmood et al., 2011). Firstly, 40 mL of background electrolyte solution (0.01 M $NaNO_3$) containing 0.2 g of biochar was equilibrated with continuous magnetic stirring at 20 (± 2) °C for 40 min. The pH of the mixture was adjusted in the range of 2.0 – 10.0 by using HNO_3 (0.1, 0.5 and 1 M) and NaOH (0.1, 0.5 and 1 M). After 40 min of stirring, the pH was measured and readjusted to correct the pH value until each solution reached a stable pH. The suspension was then filtered with a 0.45 µm cellulose acetate syringe filter before determining the zeta potential (Zetasizier Nanoseries (Nano-ZS), Malvern, UK). This filtration was performed to prevent the settlement of biochar particles in the measurement cell of the zetameter and to avoid the clogging of big particles in the device. We hypothesize that all biochar particles display the same behavior, neglecting the particle size.

Measurement of the cation exchange capacity (CEC) of biochar

For the determination of the CEC, 2 g of biochar (dry weight) were mixed with 40 mL of 0.05 N cobalt hexamine trichloride ($[Co(NH_3)_6]Cl_3$) solution (99% w/w, Sigma-Aldrich) in polypropylene tubes (Aran et al., 2008). The suspensions were shaken for 1 h using an orbital shaker (KS 501 digital, IKA^{TM}, USA) at 60 rpm, then centrifuged at 7000 g for 10 min (Rotina 420, Hettich, Germany). The supernatant was filtered through Whatman polyethersulfone syringe filters (0.2 µm). The pH (Präzisions-pH-meter E510, Metrohm AG, Switzerland) and absorbency at 472 nm (UV–vis spectrophotometer, Lambda 365, PerkinElmer, USA) of each sample were measured immediately. All experiments were performed in triplicate and the results are reported as mean values. The CEC (meq 100 g^{-1} or $cmol^{+}$ kg^{-1}) can be calculated as follows using Eq. (1) (Aran et al., 2008):

$$CEC = \left[\frac{Abs_{Co} - Abs_{sample}}{Abs_{Co}}\right] \times 50 \times \frac{V}{m} \times 100 \quad (1),$$

where Abs_{Co} and Abs_{sample} refer to the absorbency (at 472 nm) of 0.05 N $[Co(NH_3)_6]Cl_3$ and of sample (supernatant after filtration), respectively. V and m correspond to solution volume in liter and biochar dry mass in gram, respectively.

X-ray powder diffraction (XRD) analysis

X-ray diffractometry (XRD) was employed to identify the crystalline structures presented in raw and modified biochars. The samples were grounded to less than 100 µm particle size and were characterized using a powder diffractometer (AXS D8, Bruker, Germany) with Cu Kα radiation at 1.54 Å wavelength over the 2θ range from 10° to 32°, for 10 seconds per step, at 40 kV voltage

and 40 mA current with a Solx (Si-Li) detector. The crystalline compounds present in biochar were identified using the X'Pert HighScore software for data analysis with the reference from the International Center for Diffraction Data (ICDD).

Fourier-transform infrared spectroscopy (FTIR) analysis

FTIR spectra were recorded to identify the functional groups present on biochar surfaces. Each sample was mixed with KBr in a ratio of 1 mg sample (particle size 100 µm) per 200 mg KBr and the pellet was prepared by compression under vacuum (Jouraiphy et al., 2005). The analysis was performed using a Shimadzu IRAffinity-1 Spectrometer with a deuterated-triglycine sulfate (DTGS) detector. The number of scans was 12 with a resolution of 16 cm^{-1} and a frequency in a range from 4000 to 800 cm^{-1}.

XRD spectra of raw sewage sludge digestate and its derived biochar

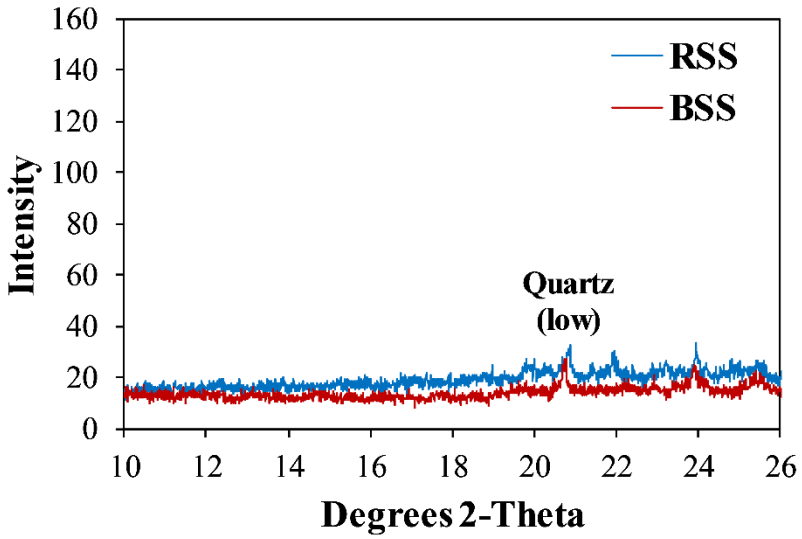

Fig. S1. XRD spectra of raw sewage sludge digestate (RSS) and biochar from sewage sludge digestate (BSS) produced at 350 ℃ under slow pyrolysis.

FTIR spectra of raw sewage sludge digestate and its derived biochar

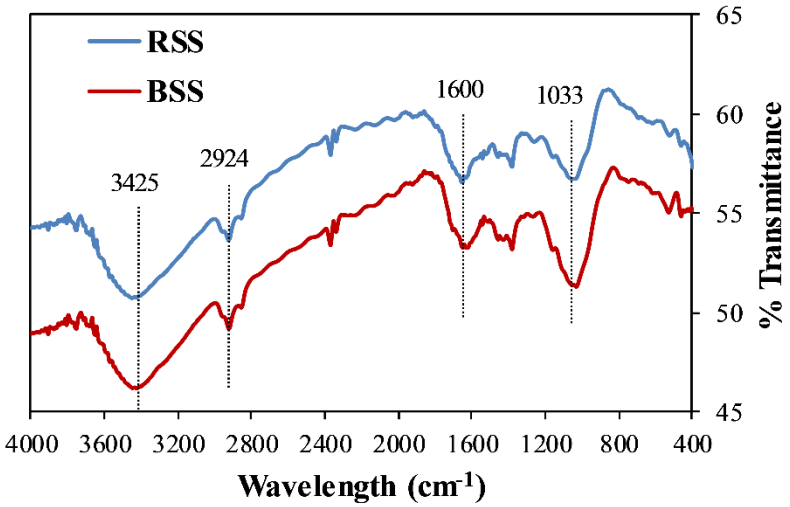

Fig. S2. FTIR spectra of raw sewage sludge digestate (RSS) and biochar from sewage sludge digestate (BSS) produced at 350 °C under slow pyrolysis.

Table S1. Comparison of the sorption performance of As(V) and Cd(II) by different types of biochars.

Adsorbent	Element	Maximum adsorption capacity (μmol g^{-1})	Concentration ranges (μM)	Solution pH	References
BSS[a]	As(V)	1.6	10 – 300	5.0	This study
BH_2O_2[a]	As(V)	7.1	10 – 300	5.0	This study
BKOH[a]	As(V)	8.5	10 – 300	5.0	This study
Fe(II)-loaded activated carbon	As(V)	27	7 – 113	3.0	Özge et al. (2013)
Paper mill sludge biochar	As(V)	303	280 – 2529	6.5	Yoon et al. (2017)
Magnetic carbonaceous tea waste	As(V)	507	10 – 1335	5.0	Wen et al. (2017)
Carbonaceous nanofibers	As(V)	670	100 – 900	5.0	Cheng et al. (2016)
BSS	Cd(II)	16	10 – 4000	5.0	This study
BH_2O_2	Cd(II)	220	10 – 4000	5.0	This study
BKOH	Cd(II)	318	10 – 4000	5.0	This study
Paper mill sludge biochar	Cd(II)	369	187 – 2506	6.5	Yoon et al. (2017)
H_2O_2-treated yak manure biochar	Cd(II)	419	10 – 1779	-	Wang and Liu (2018)
Graphene oxide nanosheets	Cd(II)	945	40 – 450	6.0	Zhao et al. (2011)

[a] BSS, BH_2O_2 and BKOH refer to, respectively, biochar produced from sewage sludge digestate, and its derived biochar with H_2O_2 and KOH treatments.

Table S2. Chemical characteristics of raw sewage sludge digestate (RSS) and its derived biochar produced at 350 °C under slow pyrolysis (BSS).

Parameters	RSS	BSS
pH in water	6.0 ±0.1	6.4 ±0.1
As (mg kg^{-1})	79 ±3[a]	47 ±1
Cd (mg kg^{-1})	dl[b]	9 ±1
Cr (mg kg^{-1})	42 ±1	48 ±1
Cu (mg kg^{-1})	390 ±10	617 ±7
Ni (mg kg^{-1})	25 ±1	41 ±1
Pb (mg kg^{-1})	80 ±9	85 ±3
Zn (mg kg^{-1})	756 ±10	1017 ±13

[a] Values reported as means (n=3) on dry mass basis followed by standard deviation.

[b] dl refers to value below detection limit.

Adsorption kinetics

The sorption kinetic data for arsenic and cadmium by biochars was calculated using the pseudo-first-order (PFO) (Eq. 2), pseudo-second-order (PSO) (Eq. 3) and intraparticle diffusion (Eq. 4) kinetic models, which are illustrated as followed:

$$\log(Q_e - Q_t) = \log Q_e - \frac{k_1 t}{2.303} \quad (2),$$

$$\frac{t}{Q_t} = \frac{1}{k_2 Q_e^2} + \frac{t}{Q_e} \quad (3),$$

$$Q_t = k_i t^{1/2} + C \quad (4),$$

where Q_t and Q_e are arsenic or cadmium adsorption capacity (μmol g^{-1}) at time t (h) and at equilibrium, k_1 (h^{-1}), k_2 ($g(\mu mol\ h)^{-1}$) and k_i ($\mu mol\ (g\ h^{1/2})^{-1}$) are the rate constants for the PFO, PSO and intraparticle diffusion kinetic models, respectively (Liu and Zhang, 2009; Zhao et al., 2015). C is the intraparticle diffusion constant related to the boundary layer diffusion. All uncertainties of sorption kinetic parameters were obtained by non-linear regression using Statistica software (v6.1, StatSoft).

Adsorption isotherms

Langmuir and Freundlich models are presented, respectively, in Eqs. (4) and (5):

$$\frac{C_e}{Q_e} = \frac{1}{K_L Q_m} + \frac{C_e}{Q_m} \quad (5),$$

$$\ln Q_e = \ln K_F + \frac{1}{n} \ln C_e \quad (6),$$

where C_e is the equilibrium arsenic or cadmium solution concentration (μM). Q_e and Q_m are the arsenic or cadmium adsorption capacity at equilibrium and at maximum capacity (μmol g^{-1}), respectively. K_L and K_F are the adsorption constants for the Langmuir and Freundlich isotherm models, and n is the Freundlich constant which indicates the favorability of adsorption, respectively.

Table S3. Constants for the pseudo-first-order (PFO), pseudo-second-order (PSO) and intraparticle diffusion kinetic models for As(III, V) and Cd(II) sorption by different types of biochars (BSS: biochar from sewage sludge digestate, BH_2O_2: H_2O_2-modified biochar, BKOH and $BKOH^{bat}$: KOH-modified biochars, respectively, with batch and column washing and with batch washing).

Biochar	As(III)								
	PFO			PSO			Intraparticle diffusion		
	k_1[a]	Q_e[b]	R^2	k_2[a]	Q_e	R^2	k_i	C	R^2
BSS	-	-	-	-	-	-	-	-	-
BH_2O_2	-	-	-	-	-	-	-	-	-
BKOH	0.128	1.62	0.934	0.378	2.83	0.961	0.429	0.981	0.938
$BKOH^{bat}$	0.134	1.44	0.967	0.205	1.94	0.975	0.358	0.219	0.948
Biochar	As(V)								
	PFO			PSO			Intraparticle diffusion		
	k_1	Q_e	R^2	k_2	Q_e	R^2	k_i	C	R^2
BSS	0.167	0.40	0.918	0.630	0.62	0.985	0.115	0.065	0.910
BH_2O_2	0.188	0.44	0.948	0.619	0.66	0.985	0.121	0.083	0.913
BKOH	0.165	1.84	0.969	0.052	2.35	0.995	0.396	-0.074	0.993
$BKOH^{bat}$	0.139	0.19	0.954	1.599	0.27	0.969	0.050	0.036	0.919
Biochar	Cd(II)								
	PFO			PSO			Intraparticle diffusion		
	k_1	Q_e	R^2	k_2	Q_e	R^2	k_i	C	R^2
BSS	0.184	0.94	0.923	1.724	1.93	0.983	0.269	0.956	0.852
BH_2O_2	0.400	0.14	0.881	12.251	2.09	9.985	0.042	1.932	0.787
BKOH	1.217	0.19	0.763	12.907	2.14	0.993	0.041	1.973	0.699
$BKOH^{bat}$	0.652	0.38	0.942	6.298	2.09	0.987	0.077	1.799	0.749

[a] k_1 and k_2 units: h^{-1} and $g(\mu mol\ h)^{-1}$, respectively.

[b] Q_e unit: in $\mu mol\ g^{-1}$.

Table S4. Constants for the Langmuir and Freundlich isotherms for As(III), As(V) and Cd(II) sorption by different types of biochars (BSS: biochar from sewage sludge digestate, BH_2O_2: H_2O_2-modified biochar, BKOH and $BKOH^{bat}$: KOH-modified biochars, respectively, with batch and column washing and with batch washing).

Biochar	As(III)						As(V)						Cd(II)					
	Langmuir			Freundlich			Langmuir			Freundlich			Langmuir			Freundlich		
	K_L[a]	Q_m[b]	R^2	K_F[c]	n	R^2	K_L	Q_m	R^2	K_F	n	R^2	K_L	Q_m	R^2	K_F	n	R^2
BSS	-	-	-	-	-	-	0.015	1.60	0.958	0.112	2.185	0.986	0.061	15.49	0.992	3.163	4.336	0.796
BH_2O_2	-	-	-	-	-	-	0.012	7.22	0.989	0.156	1.456	0.966	0.005	218.73	0.990	5.893	2.008	0.942
BKOH	0.103	8.74	0.976	1.059	2.299	0.884	0.014	8.11	0.994	0.196	1.473	0.967	0.032	306.09	0.994	23.460	2.570	0.933
$BKOH^{bat}$	0.088	7.60	0.996	1.007	2.420	0.880	0.024	0.85	0.965	0.044	1.867	0.906	0.009	372.49	0.996	9.013	1.849	0.882

[a] K_L unit: in l μmol^{-1}.

[b] Q_m unit: in $\mu mol\ g^{-1}$.

[c] K_F unit: in $(\mu mol\ g^{-1})(l\ \mu mol^{-1})^{1/n}$.

References

Aran D, Maul A, Masfaraud JF (2008) A spectrophotometric measurement of soil cation exchange capacity based on cobaltihexamine chloride absorbance. Comptes Rendus Geosci 340:865–871.

Cheng W, Ding C, Wang X, Wu Z, Sun Y, Yu S, Hayat T, Wang X (2016) Competitive sorption of As(V) and Cr(VI) on carbonaceous nanofibers. Chem Eng J 293:311–318.

Jouraiphy A, Amir S, Gharous ME, Revel JC, Hafidi M (2005) Chemical and spectroscopic analysis of organic matter transformation during composting of sewage sludge and green plant waste. Int Biodeterior Biodegrad 56:101–108.

Liu Z, Zhang FS (2009) Removal of lead from water using biochars prepared from hydrothermal liquefaction of biomass. J Hazard Mater 167:933–939.

Mahmood T, Saddique MT, Naeem A, Westerho P, Mustafa S (2011) Comparison of different methods for the point of zero charge determination of NiO. Ind Eng Chem Res 50:10017–10023.

Tuna AOA, Ozdemir E, Simsek EB, Beker U (2013) Removal of As(V) from aqueous solution by activated carbon-based hybrid adsorbents: Impact of experimental conditions. Chem Eng J 223:116–128.

Wang Y, Liu R (2018) H_2O_2 treatment enhanced the heavy metals removal by manure biochar in aqueous solutions. Sci Total Environ 628–629:1139–1148.

Wen T, Wang J, Yu S, Chen ZS (2017) Magnetic porous carbonaceous material produced from tea waste for efficient removal of As(V), Cr(VI), humic acid and dyes. ACS Sustain Chem Eng 5:4371–4380.

Yoon K, Cho DW, Tsang DCW, Bolan N, Rinklebe J, Song H (2017) Fabrication of engineered biochar from paper mill sludge and its application into removal of arsenic and cadmium in acidic water. Bioresour Technol 246:69–75.

Zhao G, Li J, Ren X, Chen C, Wang X (2011) Few-layered graphene oxide nanosheets as superior sorbents for heavy metal ion pollution management. Environ Sci Technol 45:10454–10462.

Zhao Z, Wu M, Jiang Q, Zhang Y, Chang X, Zhan K (2015) Adsorption and desorption studies of anthocyanins from black peanut skins on macroporous resins. Int J Food Eng 11:841–849.

III

Assessing arsenic redox evolution in solution and solid phase during sorption onto different chemically-treated sewage sludge digestate biochars.

by

Wongrod, S., Simon, S., van Hullebusch, E.D., Lens, P.N.L., Guibaud, G., 2019.
Bioresource Technology 275: 232–238.

Bioresource Technology 275 (2019) 232–238

Contents lists available at ScienceDirect

Bioresource Technology

journal homepage: www.elsevier.com/locate/biortech

Assessing arsenic redox state evolution in solution and solid phase during As (III) sorption onto chemically-treated sewage sludge digestate biochars

Suchanya Wongrod[a,b,c], Stéphane Simon[b,*], Eric D. van Hullebusch[a,c,d], Piet N.L. Lens[c], Gilles Guibaud[b]

[a] Université Paris-Est, Laboratoire Géomatériaux et Environnement (EA 4508), UPEM, 77454 Marne-la-Vallée, France
[b] Université de Limoges, PEIRENE, Équipe Développement d'indicateurs ou prévision de la qualité des eaux, URA IRSTEA, 123 avenue Albert Thomas, 87060 Limoges, France
[c] IHE Delft Institute for Water Education, P.O. Box 3015, 2601 DA Delft, The Netherlands
[d] Institut de Physique du Globe de Paris, Sorbonne Paris Cité, Université Paris Diderot, UMR 7154, CNRS, F-75005 Paris, France

GRAPHICAL ABSTRACT

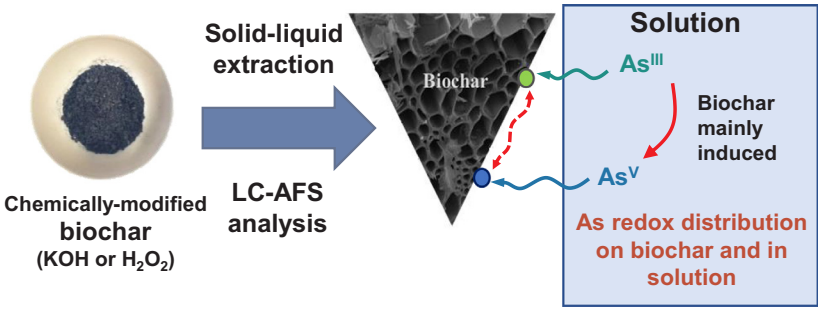

ARTICLE INFO

Keywords:
Sewage sludge digestate biochar
As(III) removal
Arsenic redox distribution
Sorption

ABSTRACT

This work aimed to determine the arsenic redox state distribution during As(III) sorption onto chemically-modified biochars. A solid–liquid extraction protocol using phosphoric (0.3 M) and ascorbic (0.5 M) acids at 80 °C for 20 min was established to ensure a quantitative recovery and stability of As(III) during the extraction. During sorption experiments, the redox conversions of As occurred and As(III) was either stable or partially oxidized in solution. The As distribution strongly varied depending on the biochar chemical treatment performed as well as the selected washing procedures (batch *versus* column washings). As(III) oxidation was favored with the KOH-modified biochar washed in batch mode. This oxidation was mostly induced by the biochar solid compounds rather than by soluble compounds released in solution. The As redox state distribution of As sorbed onto the biochars was successfully assessed using the extraction procedure. Arsenic was predominantly sorbed as As(III) (76–92%) onto the biochars.

1. Introduction

Elevated concentrations of arsenic (As) in water bodies represent a global environmental and health issue because of its toxic features. The increasing threats of As contamination mainly originate from anthropogenic sources, particularly mining, industrial and agricultural activities (Vithanage et al., 2017). Arsenic toxicity in targeted organisms is strongly linked to its chemical speciation, especially its redox state.

* Corresponding author.
E-mail address: stephane.simon@unilim.fr (S. Simon).

https://doi.org/10.1016/j.biortech.2018.12.056
Received 15 October 2018; Received in revised form 10 December 2018; Accepted 16 December 2018
Available online 17 December 2018
0960-8524/

Indeed, organic forms of As such as monomethylarsonic acid (MMA) and dimethylarsinic acid (DMA) present intermediate toxicity, whereas inorganic As species, *i.e.* arsenite (As(III)) and arsenate (As(V)), are known as the most toxic ones (Hughes et al., 2011).

Regarding the acute toxicity of As, efforts have been made to efficiently remove As from polluted water streams by using several treatment techniques such as oxidation, coagulation-flocculation, ion exchange, phytoremediation, membrane separation and adsorption (Jadhav et al., 2015; Jain and Singh, 2012; Singh et al., 2015). Among these methods, sorption is well known as a cost effective approach to remediating metal(loid)s polluted water (Ahmad et al., 2014). Biochar is a type of charcoal obtained from pyrolysis of biowaste materials in an oxygen-limited environment (Novotny et al., 2015). Because of the low-cost and the great abundance of biowaste feedstocks (*e.g.* sewage sludge digestate obtained from wastewater treatment), biochars are considered as alternatively potential sorbents for metal(loid)s removal from water (Mohan et al., 2014). Most of the sewage sludge biochars were used to sorb cationic metals like lead (Pb(II)) and chromium (Cr(VI)) (Ifthikar et al., 2017; Lu et al., 2012; Zhang et al., 2013), and to a lesser extent to metalloids like arsenic (As) and antimony (Sb). Thus, the development of sewage sludge biochar with chemical modification to improve As sorption (Sizmur et al., 2017) as well as the investigation of As speciation is of great interest. To date, As redox species repartition during the adsorption process onto biochar, and the role of biochar on redox modifications of As are not known. Hence, it is worthwhile to investigate the redox transformation of As(III) during its sorption onto biochars, since As(III) is more toxic and weakly bound to solid material than As(V) (Manning et al., 2002). Therefore, the As(III) oxidation induced by biochars is an important reaction that can possibly decrease As toxicity in As polluted water bodies.

Arsenic speciation in solid-phase samples can be accessed via X-ray absorption near edge structure (XANES) spectroscopy (Niazi et al., 2018a, 2018b). However, the use of this technique is limited due to the very high operation cost and the accessibility to synchrotron facilities. Solid-liquid extraction followed by separation techniques, for instance, liquid chromatography (LC) coupled to spectrometric detection techniques such as atomic fluorescence spectroscopy (AFS) or inductively coupled plasma mass spectrometry (ICP-MS), could be an effective and more accessible technique to determine the As species sorbed onto the solid-phase samples.

The present study focused on the determination of the inorganic As redox distribution in raw sewage sludge digestate (SSD) biochar and the H_2O_2 and KOH modified biochars before and after As(III) sorption using an analytical approach based on a solid–liquid extraction. At present, no study has reported on the implementation of an extraction method to recover As(III) and As(V) from the solid-phase of biochar. An extraction method using phosphoric and ascorbic acids as extracting agents was thus investigated before studying the possibility of redox transformations of As(III) during sorption experiments onto the biochar. The main objectives of this work were to: (1) validate the extraction procedure for As(III) and As(V) speciation in the biochars; (2) investigate the sorption ability for As(III) by the raw and chemically-modified biochars; and (3) report on the redox conversions of arsenic during the sorption experiments.

2. Material and methods

2.1. Biochar production and chemical modification

Sewage sludge digestate (SSD) was collected from a wastewater treatment plant (WWTP) located in Limoges (France), after its dewatering and drying processes. Biochar was produced from the SSD sample under slow pyrolysis conditions (at 350 °C for 15 min) (Wongrod et al., 2018a). The SSD biochar (100 g) was then modified with a 1 L of 10% H_2O_2 solution (modified from Xue et al., 2012) or with a 2.5 L of 2 M KOH solution (modified from Jin et al., 2014). For each biochar modification, the mixed biochar-solution was continuously stirred at room temperature for 2 h.

Raw and modified biochars were further washed with ultrapure water (18.2 MΩ, MilliQ Gradient A10, Millipore SAS 67120, Molsheim, France) in a batch system (triplicate in a row) followed by a continuous column washing (Wongrod et al., 2018a). These washing steps were performed to eliminate releasable organic compounds and inorganic ions (*i.e.* PO_4^{3-}, HCO_3^-, CO_3^{2-}, Ca^{2+} and Mg^{2+}) from the prepared biochars, particularly after chemical modification. The KOH modified biochar was also submitted to only a triple batch washing (Huang et al., 2017; Regmi et al., 2012; Wongrod et al., 2018a; Wu et al., 2017) to study the influence of washing steps onto As sorption and redox transformations.

The raw, H_2O_2 and KOH modified SSD biochars are labeled as BSS, BH_2O_2 and BKOH, respectively. The KOH modified SSD biochar with only batch washing is denoted as $BKOH^{bat}$.

2.2. Biochar characterization

The pH of the biochar was measured using a pH-meter (LPH 330 T, Tacussel, France) after stirring 1 g biochar in 20 mL deionized water for 5 min and allowed it to settle for 15 min. The electrical conductivity (EC) of biochar was measured using a conductivity meter at 20 °C (CDM 210, Radiometer, Denmark).

The Brunauer-Emmett-Teller surface area (S_{BET}) of biochar was measured using N_2 sorption at 77 K (3Flex, Micromeritics, USA) after pretreatment of biochar by drying at 105 °C for 5 h. The pH of point of zero charge (pH_{PZC}) of the biochar was determined from the zeta potential at different pH ranges (Mahmood et al., 2011). The cation exchange capacity (CEC) of the biochar was determined by using a cobalt hexamine trichloride solution (99% *w/w*, Sigma-Aldrich) (Aran et al., 2008).

2.3. Sorption experiments

A 13.33 mM stock solution of arsenite (As(III)) was prepared from $AsNaO_2$ (98% *w/w*, Merck) and was diluted to 50 µM prior to As(III) sorption and arsenic speciation (*i.e.* As(III) and As(V)) experiments. Biochar (0.15 g) was separately added to 37.5 mL of As(III) solution in a polyethylene tube to obtain an initial 146 µg of As(III) in the solution. The initial pH was adjusted to 5.0 (± 0.5) by adding 0.01 M HNO_3 or NaOH. The sorption experiments were performed in triplicate at 20 (± 2) °C at 180 rpm for 24 h using an orbital shaker (KS 501 digital, IKA™, USA).

The significant presence in solution of releasable dissolved compounds (RDC) from $BKOH^{bat}$ (Wongrod et al., 2018a) could affect arsenic speciation. To determine whether the arsenic oxidation was mainly induced by the biochar itself or by these RDC, a control experiment was carried out. For this purpose, 1 g $BKOH^{bat}$ in 250 mL ultrapure water was stirred at 180 rpm for 24 h at room temperature (20 °C). The resulting solution was filtered with a 0.2 µm polyethersulfone (PES) membrane filter to remove the solid biochar. The resulting solution thus only contains the RDC. A control experiment was then performed by replacing the $BKOH^{bat}$ by this solution of RDC during sorption kinetics experiments.

In all these experiments, samples were collected at 1, 3, 7, 16 and 24 h. The total sampled volume was less than 5% of the initial volume to avoid any disturbance on the sorption equilibrium. Solutions were filtered through a 0.2 µm PES syringe filter and stored in a dark cold room at 4 °C until analysis.

2.4. Arsenic redox state distribution in biochars

Total As and its redox state distribution in raw and chemically-modified biochars before and after As(III) sorption experiments were determined through solution analysis, extraction and acid digestion as

described in the following subsections.

2.4.1. Arsenic analysis in solution and deduction of sorbed arsenic

Total arsenic analysis was performed using graphite furnace atomic absorption spectrometry (GF-AAS) (240Z, Agilent Technologies, USA) at λ 193.7 nm. The standard calibrations of As were prepared in the ranges of 10–50 μg L^{-1}. The detection limit was estimated from the mean of the blank and standard deviation, and the analyte solution was measured to produce a signal of at least 3 times higher signal than the noise level.

The arsenic redox distribution was assessed by liquid chromatography coupled to atomic fluorescence spectroscopy (LC-AFS) with hydride generation (HG) (PS Analytical Millennium Excalibur, PS Analytical, UK). The chromatographic separation was performed using a Hamilton PRP-X100 column with a phosphate buffer solution as the mobile phase at pH 6.9 and at a flow rate of 1 mL min^{-1}. The details of the experimental conditions for speciation analysis can be found in a previous study reported by Wan et al. (2014). To avoid any transformation between As(III) and As(V), arsenic speciation on both liquid and extracted solutions was performed within 5 h after sample recovery.

The amount of As sorbed onto the biochar was calculated from differences between initial and final concentrations of arsenic during sorption experiments. The sorbed As onto biochar can be calculated following Eq. (1):

$$Q_{sol.} = (C_i - C_f) \times V \quad (1)$$

where $Q_{sol.}$ is the amount of arsenic sorbed onto biochar (μg) (based on 0.15 g of biochar in this study), C_i and C_f are, respectively, initial and final equilibrium concentrations of arsenic in the solution (μg L^{-1}), and V is the total volume of the solution (L).

2.4.2. Extraction of As(III) and As(V) from biochar

Due to the lack of a soft extraction procedure for arsenic from biochar in the literature, this study designed one extraction method based on the extraction procedures described by Thomas et al. (1997), Montperrus et al. (2002) and Zhang et al. (2015). The extractant was prepared from 0.3 M phosphoric acid (H_3PO_4, 85% *w/w*, Carlo ERBA) with or without the addition of 0.5 M ascorbic acid (99.5% *w/w*, Fluka). Ascorbic acid was used to prevent the oxidation of As(III) in the solution during the extraction (Xu et al., 2015).

After the sorption experiments, 0.15 g of biochar was quickly rinsed 3 times with ultrapure water and transferred into a Teflon digestion tube with 25 mL of the extracting solution. The extraction was operated using microwave assistance (Multiwave GO, Anton Paar, France) by heating at 80 °C for 20 min. The resulting solution was then centrifuged (Multifuge X3 FR, Thermo Fisher Scientific) at 3400 rpm for 20 min. The supernatant was collected and filtered through a 0.2 μm PES syringe filter and diluted to a constant volume of 50 mL. Samples were analyzed for As speciation using LC-AFS as mentioned in Section 2.4.1.

2.4.3. Biochar acid digestion for total arsenic measurements

After the sorption experiments, the biochar (about 0.15 g) was rinsed with ultrapure water and transferred into a digestion tube (Teflon). Concentrated nitric acid (HNO_3, 69.5% *w/w*, Panreac ITW) (6 mL) was added to the digestion tube. Hydrogen peroxide (H_2O_2, 30% *w/w*, Carlo ERBA) (6 mL) was then slowly added into the digestion tube with a caution regarding its strong oxidizing property. The digestion tube was left overnight (12 h) to oxidize and digest organic matter in biochar prior to a microwave acid digestion (in order to avoid overpressure due to the high initial release of CO_2). Finally, 3 mL of concentrated hydrochloric acid (HCl, 37% *w/w*, VWR) were added before starting the digestion that was operated at 180 °C for 4 h (4 cycles) using a microwave digestion (1 cycle per 1 h) to sufficiently digest all biochar particles. After digestion, the resulting solution was recovered and the dilution in a 50 mL volume was made with ultrapure water. It was filtered through a 0.2 μm PES syringe filter before analysis. Total arsenic content was analyzed by GF-AAS as previously mentioned in Section 2.4.1. Regarding the analysis of total arsenic in the biochars, the As content that is already present in each biochar (before sorption) was deduced from the sorbed As after the As(III) sorption experiments. This deduction was made to avoid errors in the experimental results.

2.5. Statistical analysis

The biochar characteristics and As(III) sorption experiments were carried out in triplicate. Results are reported as the mean value followed by standard deviation. Constants for sorption parameters were obtained by the non-linear regression using Statistica software (v6.1, StatSoft). Statistical analysis of the experimental data was performed by the *t*-test with two-tailed distribution at a statistical significance level of $p \leq 0.01$.

3. Results and discussion

3.1. Characterization of raw and chemically-modified biochars

The total As content in the raw and chemically-modified biochars is given in Table 1. Results show a significant ($p \leq 0.01$) decrease of the As content after treating the raw biochar with H_2O_2 or KOH from 47 (± 1) μg g^{-1} for BSS to 29 (± 1) and 13 (± 1) μg g^{-1}, respectively, for BH_2O_2 and BKOH. These reductions can be due to the ability of KOH to dissolve ash contents (Lin et al., 2012; Liou and Wu, 2009; Liu et al., 2012) and H_2O_2 to oxidize organic matter present in the solid phase of the biochars (Xue et al., 2012). As a result, the As bound to the biochar matrix could be chemically altered and thus the As contents were lower in the chemically-modified biochars compared to the raw biochar (Table 1).

Considering BKOH and $BKOH^{bat}$, an almost 2 times decrease of As, from 23 (± 2) μg g^{-1} for $BKOH^{bat}$ to 13 (± 1) μg g^{-1} for BKOH, was found after the subsequent continuous column washing.

The pH values of all biochar suspensions are also provided in Table 1. The pH of BSS (6.4 ± 0.1) increased to 8.4 (± 0.1) and 10.1 (± 0.1) for BKOH and $BKOH^{bat}$, respectively, whereas H_2O_2 induced no significant change ($p \leq 0.01$) on the pH suspension of biochar. The electrical conductivity (EC) of biochar suspensions remained in similar ranges from 4.0 (± 0.1) to 4.1 (± 0.3) and 6.2 (± 0.5) μS cm^{-1} for

Table 1
pH, electrical conductivity and surface area of the raw and chemically-modified biochars.

Biochar	Total As (μg g^{-1})	pH in water	pH_{pzc}	Zeta potential at pH 5 (mV)	Electrical conductivity (at 20 °C) (μS cm^{-1})	S_{BET}[a] (m^2 g^{-1})	CEC[b] (cmol$^+$ kg^{-1})
BSS	47 ± 1	6.4 ± 0.1	2.7	−9.8	4.0 ± 0.1	0.4 ± 0.1	2.0 ± 0.1
BH_2O_2	29 ± 1	6.5 ± 0.1	2.9	−16.5	4.1 ± 0.3	5.7 ± 0.1	2.9 ± 0.1
BKOH	13 ± 1	8.4 ± 0.1	3.4	−8.1	6.2 ± 0.5	7.9 ± 0.1	13.4 ± 0.1
$BKOH^{bat}$	23 ± 2	10.0 ± 0.1	2.9	−17.1	324.0 ± 2.4	3.0 ± 0.1	20.8 ± 0.1

Note: all values reported are mean of triplicate followed by standard deviation, except pH_{PZC} and zeta potential.
[a] S_{BET} refers to Brunauer-Emmett-Teller surface area of biochar.
[b] CEC refers to cation exchange capacity of biochar.

BSS, BH_2O_2 and BKOH, respectively. However, a significantly higher EC value (324 ± 2 μS cm^{-1}) for BKOH^{bat} was found, compared to BKOH (Table 1). This highlights the ability of BKOH^{bat} to release a relatively high amount of dissolved ions as previously reported by Wongrod et al. (2018a).

The pH_{PZC} and zeta potential (at pH 5) values of the raw and chemically-modified biochars are given in Table 1. Results showed similar pH_{PZC} ranges (2.7–3.4) among the raw and modified biochars. Currently, there is still a lack of information regarding pH_{PZC} of biochars reported in the literature. Nevertheless, these findings are consistent with previous studies from Qiu et al. (2009) who reported a pH_{PZC} of 1.9 on straw biochar and Petrovic et al. (2016) with pH_{PZC} values of 4.5 and 6.0, respectively, on grape pomace biochar and its KOH modified biochar. Moreover, the negative zeta potential values of the biochars implied that all biochars carried net negative charges at pH 5, particularly for the BH_2O_2 (−16.5 mV) and BKOH^{bat} (−17.1 mV). These negatively charges may hinder the sorption ability for arsenic oxyanions at pH 5.

The BET surface area (S_{BET}) of all biochars is reported in Table 1. The S_{BET} was significantly improved by 7–20 times after H_2O_2 or KOH modification of the biochar compared to the non-treated biochar. In this case, the S_{BET} increased from 0.4 (± 0.1) (the raw biochar) to 5.7 (± 0.1) and 7.9 (± 0.1) m^2 g^{-1} for BH_2O_2 and BKOH, respectively. This implies that H_2O_2 and KOH induced higher porosity on the modified biochars, thus As sorption can be enhanced for these biochars (Mohan et al., 2014). These S_{BET} results are in agreement with those reported for sewage sludge biochars (4.0–14.3 m^2 g^{-1}) (Agrafioti et al., 2013; Yuan et al., 2015), but lower than biochar made from wood (475 m^2 g^{-1}) (Niazi et al., 2018b). Nevertheless, they remain very low compared to activated carbon which displays specific surface area beyond 1000 m^2 g^{-1} in most cases (Gonzalez-Garcia, 2018) (*e.g.* 1215.0–1316.0 m^2 g^{-1} for activated carbon prepared from coal) (Gong et al., 2015).

The CEC values for all biochars are also given in Table 1. Results demonstrate a similar CEC of the biochar after H_2O_2 modification, *i.e.* from 2.0 (± 0.1) to 3.0 (± 0.1) cmol$^+$ kg^{-1}, whereas the CEC values were much higher (7–10 times) for BKOH (13.4 ± 0.1 cmol$^+$ kg^{-1}) and BKOH^{bat} (20.8 ± 0.1 cmol$^+$ kg^{-1}) (Table 1). Nevertheless, in the literature much higher CEC values are reported for wood and straw derived biochars, ranging from 45.7 to 483.4 cmol$^+$ kg^{-1} (Ding et al., 2016; Jiang et al., 2014).

The biochar properties reported in Table 1 highlight that the total As content, zeta potential and S_{BET} are the key indicators that were significantly affected by the biochar treatment. Due to its lower negative charge and its higher S_{BET}, BKOH can potentially sorb more As compared to other biochars. Furthermore, the biochar washing procedure is an important parameter to be considered after the chemical treatment, since the biochar properties significantly change between BKOH and BKOH^{bat}.

3.2. As redox state evolution during sorption kinetics by BKOH^{bat} and its dissolved solutions

Fig. 1a shows the As redox state distribution in the solution during adsorption experiments for As(III) onto BKOH^{bat}. The results demonstrate that while As was gradually sorbed onto BKOH^{bat} (corresponding to the decrease of total As over time), the oxidation of As(III) to As(V) occurred continuously. To elucidate whether this oxidation was promoted by compounds released from the biochar into the solution or by the biochar itself, a control experiment was performed by replacing the biochar by a solution of released dissolved compounds (RDC) from BKOH^{bat}. The experimental data and corresponding results are shown in Fig. 1b. From the results, a slight oxidation of As(III) with a final proportion of 9% As(V) in the RDC solution was found, compared to 43% oxidation with the presence of biochar. This demonstrates that the oxidation of As(III) to As(V) was mainly induced by the biochar material itself and to a lesser extent by the dissolved compounds being released from the BKOH^{bat}. At present, there is still a lack of information on the role of biochars and the released dissolved compounds towards the As(III) oxidation. Nevertheless, the findings are supported by Niazi et al. (2018a, 2018b) who found the oxidation of As(III) sorbed onto biochars prepared from Japanese oak wood and perilla leaf. However, Dong et al. (2014) showed the high potential oxidation of As (III) (up to 25%) induced by the dissolved organic matter from sugar beet tailing and Brazilian pepper derived biochars.

3.3. Extraction procedure for As redox state distribution in biochars

In order to assess the redox state distribution of As sorbed onto biochar by LC-AFS, it was first necessary to validate an extraction procedure that allows a quantitative As recovery without any conversion of As species, especially As(III) being oxidized to As(V).

The importance of adding ascorbic acid in the extraction solution to stabilize As(III) was assessed by applying the extraction procedure to a biochar sample with and without spiking with a known amount of As (III) just before performing the extraction step. In this study, the BKOH^{bat} was selected due to its release of dissolved compounds and its ability to oxidize As(III) as previously reported by Wongrod et al. (2018a, 2018b).

Table 2 shows the recoveries of the arsenic species and total As after the extraction using H_3PO_4 with or without addition of ascorbic acid onto the BKOH^{bat} sample, and with and without As(III) spiking just before the extraction. Results show that all spiked arsenic was recovered by the extraction procedure. The results also highlight that when using only 0.3 M H_3PO_4, a significant amount of spiked As(III) was oxidized. Indeed, the addition of 12.5 μg of As(III) to the biochar before performing the extraction step resulted in an increase of 8.8 (± 0.7) μg and 3.5 (± 0.3) μg for As(III) and As(V), respectively. Thus, 29% of spiked As(III) was converted into As(V). In contrast, no oxidation of As(III) was observed during extraction with H_3PO_4 and ascorbic acid: the difference between the As(III) amount before and after spiking is 12.6 (± 0.7) μg, which is in agreement with the amount of As(III) added (12.5 μg). Therefore, the addition of ascorbic acid is essential to ensure As(III) stability during the extraction step. The findings are also in agreement with the study of Xu et al. (2015) who reported the efficiency of using both phosphoric and ascorbic acids as extracting agents to quantitatively recover As(III) and As(V) from fly ash.

To estimate the extraction yield of As sorbed onto the biochar after the As(III) sorption experiments, the biochars were recovered and submitted to both acid digestion and extraction procedures (see Section 2.4). The corresponding results are presented in Table 3. For BSS and BH_2O_2, the amount of total sorbed As was too low to allow an accurate determination after the acid digestion and/or extraction. As a result, no extraction yield was calculated. For BKOH^{bat}, the total amount of sorbed As was quantitatively recovered by the extraction procedure. In the case of BKOH, most of the sorbed As was recovered but about one fourth could not be extracted under the applied conditions. This difference in the extraction efficiency may result from different sorption mechanisms of As from one biochar type to the other. Nevertheless, the majority of As could be extracted from the biochars and thus the identification of the As species in the extracted solutions gives the main As species sorbed onto the biochars.

3.4. Determination of As(III) and As(V) sorbed onto biochars

Different types of biochars were exposed in the solution containing an initial As(III) amount of 146 μg. After 24 h of As(III) sorption, the biochars were recovered and the exposure solutions were analyzed to determine the remaining amount of As and to assess its distribution between As(III) and As(V). The biochars were separately submitted to acid digestion for the determination of the total quantity of sorbed As and to the extraction for the assessment of the redox distribution of

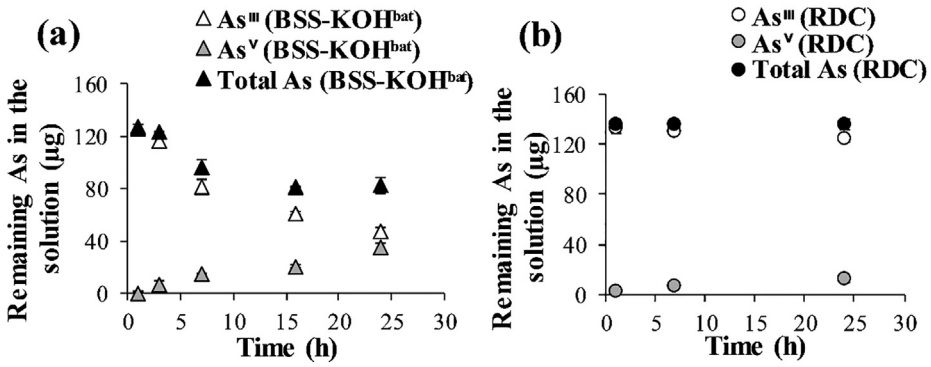

Fig. 1. Arsenic redox distribution in solution during adsorption kinetics for As(III) by BKOH^{bat} (a) and for the control with only released dissolved compounds (RDC) from BKOH^{bat} (b).

sorbed As. The amounts of As(III), As(V) and total As in the exposure solutions and sorbed onto the biochars (determined after acid digestion and extraction steps) are shown in Table 4.

Results showed that the total As (*i.e.* As(III) + As(V)) remaining in the final exposure solutions of BSS and BH_2O_2 were not significantly different from the initial As(III), indicating that no As was sorbed onto these biochars. In contrast, As was removed from the exposure solutions by both BKOH and BKOH^{bat}, corresponding to an As sorption efficiency of 67% and 50%, respectively. These results are in agreement with the sorption yield estimated with the amount of As quantified in the digestate-based biochars (Table 4).

The arsenic redox distribution in the final exposure solution shows almost no As(III) oxidation for both BSS and BH_2O_2 as the final amount of As(III) remained the same as the initial As(III) amount (Table 4). For the KOH treated biochars, the assessment of the redox distribution only concerned the unsorbed As. In the case of BKOH, no significant oxidation of As(III) was observed, whereas for BKOH^{bat} about 28% of the remaining As was oxidized to As(V) (Table 4). These findings are in agreement with a previous study from Wongrod et al. (2018b) with a large oxidation of As(III) in BKOH^{bat} and a partial oxidation in BKOH during As(III) sorption. As previously discussed (Fig. 1a and 1b), the majority of As(III) oxidation was induced by the biochar solid compounds.

Considering As(III) and As(V) extracted from the biochars after the sorption experiment, a similar distribution of the As species was found for BKOH and BKOH^{bat} (Table 4). Arsenic was mainly sorbed as As(III) (90–92%) and only 8–10% was sorbed as As(V) onto the KOH biochars. In the case of BKOH, the redox distribution of As sorbed onto the biochar is quite similar to the distribution observed in the final exposure solution. However, for BKOH^{bat}, the evolution of the As species in solution and on the biochar was different: As(V) represents only 8% of the sorbed arsenic whereas it corresponds to 28% of the dissolved As(V) (Table 4). This suggests that the As(III) sorption onto the KOH biochar was favored compared to As(V) sorption. This finding is consistent with results previously reported by Wongrod et al. (2018b) when comparing As(III) and As(V) sorption onto such biochars. Another possible explanation would be that As(V) could be reduced into As(III) during the sorption process, as observed by Niazi et al. (2018a, 2018b) who studied the speciation of As onto wood and leaf derived biochars using the solid-phase XANES technique. Depending on the nature and chemical treatment applied to the biochar, it could also contain chemical functions that act as electron donors to facilitate the As reduction (Choppala et al., 2016).

Table 3
Comparison of total amount of sorbed arsenic determined after acid digestion or extraction procedure.

Biochar	Total arsenic (µg)		Recovery from extraction (%)
	Extraction	Acid digestion	
BSS	0.2 ± 1	1 ± 1	na[a]
BH_2O_2	3 ± 1	6 ± 1	na
BKOH	70 ± 3	93 ± 3	75 ± 4
BKOH^{bat}	63 ± 4	60 ± 3	105 ± 9

[a] na refers to not available due to very low values detected by liquid chromatography coupled to atomic fluorescence spectroscopy (LC-AFS) and/or graphite furnace atomic absorption spectrometry (GF-AAS).

Comparison of the two KOH biochars showed that the adsorption capabilities for As(III) were quite similar for both the BKOH (410 µg g^{-1}) and BKOH^{bat} (385 µg g^{-1}) at As(III) concentration ranges of 0–4000 µM (or 0–54 µg L^{-1}) and the initial solution pH at 5.0. Nevertheless, a much higher As(III) sorption was observed onto the Japanese oak wood derived biochar (3,890 µg g^{-1}) (concentrations of 27–144 µg L^{-1} and at pH 7.0 ± 0.1) (Niazi et al., 2018b). This is probably due to different biochar properties between the SSD-based biochars and the Japanese oak wood biochar. For instance, the specific surface area was substantially lower with the KOH modified biochars from SSD (3.0–7.9 m^2 g^{-1}) (Table 1) compared to the oak wood biochar (475 m^2 g^{-1}) (Niazi et al., 2018b).

In the case of BH_2O_2, the amount of sorbed As being low, the results of the As redox distribution were less accurate and should thus be taken with caution. The percentage of As(V) sorbed onto the H_2O_2-modified

Table 2
Arsenic speciation stability using H_3PO_4 with or without ascorbic acid (BKOH^{bat} sample, with and without As(III) spiking just before extraction).

Extraction method		Extracted arsenic (µg)		Spiking recovery[a] (%)	
		As(III)	As(V)	As(III)	Total As
No ascorbic acid	Before As(III) spiking	0.3[b] ± 0.1	1.1 ± 0.1	–	–
	After As(III) spiking (12.5 µg)	9.1 ± 0.7	4.6 ± 0.3	71	99
With ascorbic acid	Before As(III) spiking	0.4[b] ± 0.1	0.8[b] ± 0.1	–	–
	After As(III) spiking (12.5 µg)	13.0 ± 0.7	0.8[b] ± 0.1	101	101

[a] Recovery: amount of spiked As(III) recovered by extraction either as As(III) or total arsenic (*i.e.* As(III) + As(V)).
[b] Value close to limit of quantification.

Table 4
Comparison of As speciation and total As in exposure solutions and sorbed onto biochars (initial As(III) amount in exposure solution: 146 µg).

Biochar	Exposure solution				Sorbed As onto biochar				
	Initial	Final			Acid digestion		Extraction		
	As(III) (µg)	As(III) + As(V) (µg)	As(III) (%)	As(V) (%)	Total As (µg)	Sorption yield (%)	As(III) + As(V) (µg)	As(III) (%)	As(V) (%)
BSS	146	145 ± 2	99	1	1 ± 1	< 1	0.2 ± 0.3	na[a]	na
BH_2O_2	146	143 ± 3	96	4	6 ± 1	4	3 ± 1	76	24
BKOH	146	48 ± 3	98	2	93 ± 3	64	70 ± 3	90	10
$BKOH^{bat}$	146	72 ± 5	72	28	60 ± 3	41	63 ± 4	92	8

[a] na refers to not available due a value close to limit of quantification.

biochar appears to be higher than into solution, highlighting a potential oxidation of As(III) during sorption. This phenomenon was also observed by Niazi et al. (2018a, 2018b), who suggested that redox active species present at the biochar surface such as NO_3^- or FeO(OH) could induce As(III) oxidation. Therefore, the presence of iron (Fe) (65 g kg^{-1}) and manganese (Mn) (769 mg kg^{-1}) on the SSD biochar, that could be partially in metal oxide forms (Wongrod et al., 2018a), could promote the redox transformation of As(III) to As(V) on metal oxides associated onto the biochars (Vithanage et al., 2017). Such a phenomenon is also reported by several studies (Han et al., 2011; Manning et al., 2002; Wang et al., 2015).

4. Conclusions

The extraction using phosphoric and ascorbic acids allowed recovering sorbed arsenic, while preserving As(III) oxidation state. Arsenic redox distribution could thus be assessed in both solid and liquid phases. Arsenic was mainly sorbed onto biochar as As(III) but during sorption, As(III) oxidation may occur over time. This oxidation, mainly induced by biochar solid compounds rather than by soluble compounds released from biochar, can strongly vary depending on the chemical treatment and efficiency of washing procedures applied to biochar after chemical treatment. The KOH modification efficiently improves the biochar sorption capacity but also promotes As(III) oxidation, especially with an incomplete washing.

Acknowledgments

Patrice Fondanèche (Université de Limoges, France) is acknowledged for technical assistance with arsenic analysis. This research work was economically supported by the Marie Sklodowska-Curie European Joint Doctorate in Advanced Biological Waste-to-Energy (ABWET) under the European Union's Horizon 2020 framework [grant agreement N° 643071].

Conflict of interest

The authors declare no conflict of interest.

References

Agrafioti, E., Bouras, G., Kalderis, D., Diamadopoulos, E., 2013. Biochar production by sewage sludge pyrolysis. J. Anal. Appl. Pyrol. 101, 72–78.
Ahmad, M., Rajapaksha, A.U., Lim, J.E., Zhang, M., Bolan, N., Mohan, D., Vithanage, M., Lee, S.S., Ok, Y.S., 2014. Biochar as a sorbent for contaminant management in soil and water: a review. Chemosphere 99, 19–23.
Aran, D., Maul, A., Masfaraud, J.F., 2008. A spectrophotometric measurement of soil cation exchange capacity based on cobaltihexamine chloride absorbance. C. R. Geosci. 340, 865–871.
Choppala, G., Bolan, N., Kunhikrishnan, A., Bush, R., 2016. Differential effect of biochar upon reduction-induced mobility and bioavailability of arsenate and chromate. Chemosphere 144, 374–381.
Ding, Z., Hu, X., Wan, Y., Wang, S., Gao, B., 2016. Removal of lead, copper, cadmium, zinc, and nickel from aqueous solutions by alkali-modified biochar: batch and column tests. J. Ind. Eng. Chem. 33, 239–245.
Dong, X., Ma, L.Q., Gress, J., Harris, W., Li, Y., 2014. Enhanced Cr(VI) reduction and As(III) oxidation in ice phase: important role of dissolved organic matter from biochar. J. Hazard. Mater. 267, 62–70.
Gong, X.J., Li, W.G., Zhang, D.Y., Fan, W.B., Zhang, X.R., 2015. Adsorption of arsenic from micro-polluted water by an innovative coal-based mesoporous activated carbon in the presence of co-existing ions. Int. Biodeterior. Biodegrad. 102, 256–264.
Gonzalez-Garcia, P., 2018. Activated carbon from lignocellulosics precursors: a review of the synthesis methods, characterization techniques and applications. Renew. Sustain. Energ. Rev. 82, 1393–1414.
Han, X., Li, Y.L., Gu, J.D., 2011. Oxidation of As(III) by MnO_2 in the absence and presence of Fe(II) under acidic conditions. Geochim. Cosmochim. Acta 75, 368–379.
Huang, H., Tang, J., Gao, K., He, R., Zhao, H., Werner, D., 2017. Characterization of KOH modified biochars from different pyrolysis temperatures and enhanced adsorption of antibiotics. RSC Adv. 7, 14640–14648.
Hughes, M.F., Beck, B.D., Chen, Y., Lewis, A.S., Thomas, D.J., 2011. Arsenic exposure and toxicology: a historical perspective. Toxicol. Sci. 123, 305–332.
Ifthikar, J., Wang, J., Wang, Q., Wang, T., Wang, H., Khan, A., Jawad, A., Sun, T., Jiao, X., Chen, Z., 2017. Highly efficient lead distribution by magnetic sewage sludge biochar: sorption mechanisms and bench applications. Bioresour. Technol. 238, 399–406.
Jadhav, S.V., Bringas, E., Yadav, G.D., Rathod, V.K., Ortiz, I., Marathe, K.V., 2015. Arsenic and fluoride contaminated groundwaters: a review of current technologies for contaminants removal. J. Environ. Manage. 162, 306–325.
Jain, C.K., Singh, R.D., 2012. Technological options for the removal of arsenic with special reference to South East Asia. J. Environ. Manage. 107, 1–18.
Jiang, T., Xu, R., Gu, T., Jiang, J., 2014. Effect of crop-straw derived biochars on Pb(II) adsorption in two variable charge soils. J. Integr. Agric. 13, 507–516.
Jin, H., Capareda, S., Chang, Z., Gao, J., Xu, Y., Zhang, J., 2014. Biochar pyrolytically produced from municipal solid wastes for aqueous As(V) removal: adsorption property and its improvement with KOH activation. Bioresour. Technol. 169, 622–629.
Lin, Y., Munroe, P., Joseph, S., Henderson, R., Ziolkowski, A., 2012. Water extractable organic carbon in untreated and chemical treated biochars. Chemosphere 87, 151–157.
Liou, T.H., Wu, S.J., 2009. Characteristics of microporous/mesoporous carbons prepared from rice husk under base- and acid-treated conditions. J. Hazard. Mater. 171, 693–703.
Liu, P., Liu, W.J., Jiang, H., Chen, J.J., Li, W.W., Yu, H.Q., 2012. Modification of bio-char derived from fast pyrolysis of biomass and its application in removal of tetracycline from aqueous solution. Bioresour. Technol. 121, 235–240.
Lu, H., Zhang, W., Yang, Y., Huang, X., Wang, S., Qiu, R., 2012. Relative distribution of Pb^{2+} sorption mechanisms by sludge-derived biochar. Water Res. 46, 854–862.
Mahmood, T., Saddique, M.T., Naeem, A., Westerho, P., Mustafa, S., 2011. Comparison of different methods for the point of zero charge determination of NiO. Ind. Eng. Chem. Res. 50, 10017–10023.
Manning, B.A., Fendorf, S.E., Bostick, B., Suarez, D.L., 2002. Arsenic(III) oxidation and arsenic(V) adsorption reactions on synthetic birnessite. Environ. Sci. Technol. 36, 976–981.
Mohan, D., Sarswat, A., Ok, Y.S., Pittman, C.U., 2014. Organic and inorganic contaminants removal from water with biochar, a renewable, low cost and sustainable adsorbent – a critical review. Bioresour. Technol. 160, 191–202.
Montperrus, M., Bohari, Y., Bueno, M., Astruc, A., Astruc, M., 2002. Comparison of extraction procedures for arsenic speciation in environmental solid reference materials by high-performance liquid chromatography-hydride generation-atomic fluorescence spectroscopy. Appl. Organomet. Chem. 16, 347–354.
Niazi, N.K., Bibi, I., Shahid, M., Ok, Y.S., Burton, E.D., Wang, H., Shaheen, S.M., Rinklebe, J., Lüttge, A., 2018a. Arsenic removal by perilla leaf biochar in aqueous solutions and groundwater: an integrated spectroscopic and microscopic examination. Environ. Pollut. 232, 31–41.
Niazi, N.K., Bibi, I., Shahid, M., Ok, Y.S., Shaheen, S.M., Rinklebe, J., Wang, H., Murtaza, B., Islam, E., Farrakh Nawaz, M., Lüttge, A., 2018b. Arsenic removal by Japanese oak wood biochar in aqueous solutions and well water: investigating arsenic fate using integrated spectroscopic and microscopic techniques. Sci. Total Environ. 621, 1642–1651.
Novotny, E.H., Maia, C.M.B.D.F., Carvalho, M.T.D.M., Madari, B.E., 2015. Biochar: pyrogenic carbon for agricultural use – a critical review. Rev. Bras. Cienc. Solo 39, 321–344.
Petrovic, J.T., Stojanovic, M.D., Milojkovic, J.V., Petrovic, M.S., Sostaric, T.D., Lausevic, M.D., Mihajlovic, M.L., 2016. Alkali modified hydrochar of grape pomace as a perspective adsorbent of Pb^{2+} from aqueous solution. J. Environ. Manage. 182, 292–300.

Qiu, Y., Zheng, Z., Zhou, Z., Sheng, G.D., 2009. Effectiveness and mechanisms of dye adsorption on a straw-based biochar. Bioresour. Technol. 100, 5348–5351.
Regmi, P., Moscoso, J.L.G., Kumar, S., Cao, X., Mao, J., Schafran, G., 2012. Removal of copper and cadmium from aqueous solution using switchgrass biochar produced via hydrothermal carbonization process. J. Environ. Manage. 109, 61–69.
Singh, R., Singh, S., Parihar, P., Singh, V.P., Prasad, S.M., 2015. Arsenic contamination, consequences and remediation techniques: a review. Ecotoxicol. Environ. Saf. 112, 247–270.
Sizmur, T., Fresno, T., Akgül, G., Frost, H., Moreno-Jiménez, E., 2017. Biochar modification to enhance sorption of inorganics from water. Bioresour. Technol. 246, 34–47.
Thomas, P., Finnie, J.K., Williams, J.G., 1997. Feasibility of identification and monitoring of arsenic species in soil and sediment samples by coupled high-performance liquid chromatography – inductively coupled plasma mass spectrometry. J. Anal. At. Spectrom. 12, 1367–1372.
Vithanage, M., Herath, I., Joseph, S., Bundschuh, J., Bolan, N., Ok, Y.S., Kirkham, M.B., Rinklebe, J., 2017. Interaction of arsenic with biochar in soil and water: a critical review. Carbon 113, 219–230.
Wan, J., Pressigout, J., Simon, S., Deluchat, V., 2014. Distribution of As trapping along a ZVI/sand bed reactor. Chem. Eng. J. 246, 322–327.
Wang, S., Gao, B., Li, Y., Mosa, A., Zimmerman, A.R., Ma, L.Q., Harris, W.G., Migliaccio, K.W., 2015. Manganese oxide-modified biochars: preparation, characterization, and sorption of arsenate and lead. Bioresour. Technol. 181, 13–17.
Wongrod, S., Simon, S., Guibaud, G., Lens, P.N.L., Pechaud, Y., Huguenot, D., van Hullebusch, E.D., 2018a. Lead sorption by biochar produced from digestates: consequences of chemical modification and washing. J. Environ. Manage. 219, 277–284.
Wongrod, S., Simon, S., van Hullebusch, E.D., Lens, P.N.L., Guibaud, G., 2018b. Changes of sewage sludge digestate-derived biochar properties after chemical treatments and the influence on As(III and V) and Cd(II) sorption. Int. Biodeterior. Biodegrad. 36, 96–102.
Wu, W., Li, J., Lan, T., Müller, K., Khan, N., Chen, X., Xu, S., Zheng, L., Chu, Y., Li, J., Yuan, G., Wang, H., 2017. Unraveling sorption of lead in aqueous solutions by chemically modified biochar derived from coconut fiber: a microscopic and spectroscopic investigation. Sci. Total Environ. 576, 766–774.
Xu, Z., Hu, H.Y., Chen, D.K., Cao, J.X., Yao, H., 2015. Determination of inorganic arsenic speciation in municipal solid waste incineration fly ash by high performance liquid chromatography-hydride generation-atomic fluorescence spectroscopy with phosphoric acid as extracting agent. Chinese J. Anal. Chem. 43, 490–494.
Xue, Y., Gao, B., Yao, Y., Inyang, M., Zhang, M., Zimmerman, A.R., Ro, K.S., 2012. Hydrogen peroxide modification enhances the ability of biochar (hydrochar) produced from hydrothermal carbonization of peanut hull to remove aqueous heavy metals: batch and column tests. Chem. Eng. J. 200–202, 673–680.
Yuan, H., Lu, T., Huang, H., Zhao, D., Kobayashi, N., Chen, Y., 2015. Influence of pyrolysis temperature on physical and chemical properties of biochar made from sewage sludge. J. Anal. Appl. Pyrolysis 112, 284–289.
Zhang, W., Mao, S., Chen, H., Huang, L., Qiu, R., 2013. Pb(II) and Cr(VI) sorption by biochars pyrolyzed from the municipal wastewater sludge under different heating conditions. Bioresour. Technol. 147, 545–552.